GEORGIA INSTITUTE OF TECHNOLOGY
OFFICE OF CONTRACT ADMINISTRATION

NOTICE OF PROJECT CLOSEOUT

Closeout Notice Date 05/16/90

oject No. E-18-625 Center No. R6169-0A0

roject Director SAXENA A School/Lab MAT ENG

ponsor US DEPT OF ENERGY/DOE OAK RIDGE - TN

ntract/Grant No. DE-FG05-86ER45257 Contract Entity GTRC

rime Contract No.

:le A STUDY OF MECHANISMS OF TIME-DEPENDENT CRACK GROWTH AT ELEVATED TEMPERAT

'ective Completion Date 890831 (Performance) 891130 (Reports)

›seout Actions Required:	Y/N	Date Submitted
Final Invoice or Copy of Final Invoice	Y	900221
Final Report of Inventions and/or Subcontracts	N	
Government Property Inventory & Related Certificate	Y	891013
Classified Material Certificate	N	
Release and Assignment	Y	900221
Other	N	

Comments

›project Under Main Project No.

:tinues Project No.

tribution Required:

Project Director	Y
Administrative Network Representative	Y
GTRI Accounting/Grants and Contracts	Y
Procurement/Supply Services	Y
Research Property Managment	Y
Research Security Services	N
Reports Coordinator (OCA)	Y
GTRC	Y
Project File	Y
Other	N
	N

GEORGIA INSTITUTE OF TECHNOLOGY — OFFICE OF CONTRACT ADMINISTRATION

PROJECT ADMINISTRATION DATA SHEET

[X] ORIGINAL [ ] REVISION NO. _____

Project No. E-18-625 (R6169-0A0) GTRC/~~GTX~~ DATE 7 /24 / 86

Project Director: Dr. Ashok Saxena School/~~XXX~~ Materials Engineering

Sponsor: U.S. Department of Energy
Oak Ridge, TN

Type Agreement: Grant # DE-FG05-86ER45257

Award Period: From 7/1/86 To 6/30/89 (Performance) 9/30/89 (Reports)

Sponsor Amount:	This Change	Total to Date
Estimated:	$ 104,179	$ 341,439
Funded:	$ 104,179	$ 104,179 (through 6/30/87)

Cost Sharing Amount: $ None Cost Sharing No: _____

Title: A Study of Mechanisms of Time-Dependent Crack Growth at Elevated Temperatures.

ADMINISTRATIVE DATA OCA Contact Brian J. Lindberg X-4820

1) Sponsor Technical Contact:

Dr. Joseph B. Darby, Jr.
Office of Basic Energy Sciences, ER-131
U.S. Department of Energy
19901 Germantown Road
Germantown, Md. 20874
(301) 353-3428

2) Sponsor Admin/Contractual Matters:

Marlena Clark, Contract Specialist
Contract Management Branch
Procurement & Contracts Division
U.S. Department of Energy,
Oak Ridge Operations, P.O. Box E
Oak Ridge, TN 37831 (615) 576-7599

Defense Priority Rating: N/A Military Security Classification: N/A
(or) Company/Industrial Proprietary: N/A

RESTRICTIONS

See Attached N/A Supplemental Information Sheet for Additional Requirements.

Travel: Foreign travel must have prior approval – Contact OCA in each case. Domestic travel requires sponsor approval where total will exceed greater of $500 or 125% of approved proposal budget category.

Equipment: Title vests with Grantee. However, expenditures for equipment having a unit cost of $500 or more require prior approval of Sponsor with one exception. For special purpose equipment, prior approval is required only when cost is $1,000 or more.

COMMENTS:

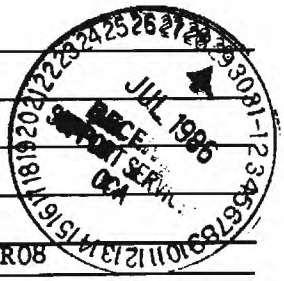

COPIES TO: SPONSOR'S I. D. NO. 02.141.002.86.R08

Project Director	Procurement/EES Supply Services	GTRC
Research Administrative Network	Research Security Services	Library
Research Property Management	~~Reports Coordinator~~ (OCA)	Project File
Accounting	Research Communications (2)	Other A. Jones

FORM OCA 65:285

DOE/ER/45257-1

Progress Report on

A STUDY OF MECHANISMS OF TIME-DEPENDENT CRACK GROWTH AT ELEVATED TEMPERATURE

DOE Grant # DE-FG05-86ER-45257

Period Covered - July '86 to June '87

Date of Submission: 2/28/87

Ashok Saxena
S. R. Stock
Brian Gieseke
J. T. Staley

Approved:

Ashok Saxena
Project Director

S. D. Antolovich, Director
Fracture & Fatigue Research Lab

W. M. Sangster, Dean
College of Engineering

1. PROGRAM OBJECTIVES AND SUMMARY

The prediction of design and remaining life of several heavy section components which are subjected to elevated temperatures in energy conversion machinery require accurate methods for predicting crack growth behavior in the presence of time-dependent creep strains. Significant progress has recently been made in extending the linear-elastic and elastic-plastic fracture mechanics concepts into the creep regime. Thus, the use of fracture mechanics for predicting the crack growth life of elevated temperature components is a viable approach. However, serious deficiencies exist in the understanding of the damage mechanisms that lead to time-dependent crack growth. Specifically, the interactions between creep and fatigue damage mechanisms for slow frequency cyclic loading are not well understood. Therefore, cumulative damage laws for creep-fatigue loading based on physical damage mechanisms are non-existent.

The objective of this study is to conduct creep and creep-fatigue crack growth tests and to characterize the crack tip damage mechanisms in a model material which is known to cavitate at the grain boundaries under creep deformation. The above data and observations will be used to develop mechanistic models for cumulative crack tip damage under complex loading conditions at elevated temperature. The application of these models will also be extended to situations involving non-periodic loading. The results of this program will be integrated into an Electric Power Research Institute (EPRI) sponsored study (also to be conducted

at Georgia Tech under the direction of Dr. A. Saxena) for characterizing the creep-fatigue crack growth behavior of Cr-Mo-V steels. The techniques to be used for detection of crack tip damage include electron metallography, x-ray and electron radiography and small angle neutron scattering (SANS).

The proposed program is being conducted over a period of thirty six months in four distinct tasks listed below:

Task I Material Selection and Characterization

Task II Creep and Creep-Fatigue Crack Growth Testing

Task III Characterization of the Influence of Loading Transients

Task IV Crack Tip Damage Characterization

The program was initiated on 7/1/86. During the period of 7/1/86 to 2/15/87, the model test material was selected and a heat of the material was produced and processed. Considerable progress has been made in Task I and some progress has also been made on Tasks II and IV. This progress is summarized in Section 2 of this report.

2. TECHNICAL PROGRESS

2.1. Material Selection and Procurement

The model test material selected was copper with 1 weight percent antimony as indicated in the original proposal. The segregation of antimony to the grain boundaries embrittles the material considerably at room temperature and causes the fracture to occur exclusively at the grain boundaries. This will allow the precise determination of the grain boundary damage due to prior creep or creep-fatigue loading.

Specifications were developed for producing a special 200 lb. heat of antimony-copper for testing in this project. After detailed discussion with several vendors, a contract was placed (through the DOE field office) with the Metal Processing Theory and Practice Group of the Oak Ridge National Laboratory, Martin Marietta Energy Systems to produce the test material.

Oxygen free copper (99.99 percent) and pure antimony (99.999 percent) were melted in a vacuum induction furnace and cast into a 5 inch diameter billet. The billet was homogenized at 950 C for five hours and then extruded into a rectangular bar of 2 3/4" x 2" at a temperature 700 C. The bar was ultrasonically tested for defects. The areas giving rise to defect indications were marked to avoid taking test samples from those regions. The defective regions were a very small portion of the material, and sufficient material is available for conducting the test program.

2.2. Material Characterization

2.2.1 Microstructure and Auger Results

Due to the high extrusion temperatures the microstructure after extrusion consisted of annealed equiaxed grains. Pieces of this material were annealed at 500 C to determine if further annealing of any residual cold work from the extrusion process was necessary. Even several hours at 500 C did not change the grain size or hardness of the material significantly. Figure 1 shows the as extruded microstructure of the material. The average grain diameter was approximately 90 μm.

The average antimony content analysis was performed by x-ray fluorescence. This analysis showed an antimony content of 0.98 percent by weight which was well within our specifications. A more detailed analysis including contents of the trace elements is being performed by ORNL and will be reported in later reports.

Since the extrusion temperature was high enough to permit segregation of antimony to the grain boundary, it was suspected that the material would be quite embrittled in the as extruded conditions. Small Charpy-type specimens were machined from the material and were fractured by impact loading. Figure 2 shows a SEM micrograph of the fracture surface. The fracture was 100 percent inter-granular.

In order to assure that the segregation of antimony was nearly complete in the as extruded material, the following experiments were conducted. A small piece of the test material was heat treated at 675 C for twenty four hours in an inert

environment. Subsequently, small cylindrical specimens with notches for Auger analyses were prepared from this piece and also from the as extruded material. Figures 3a and b show the results of the Auger analysis of the heat treated and as extruded pieces, respectively. The intensity of the antimony peaks are comparable in both materials. The grain boundary concentration of antimony was approximately nine wt. percent and dropped to two percent after sputtering in both cases. From these results, it was concluded that no further segregation treatments were required for this material.

2.2.2. Tensile Properties

The short-term tensile properties of the test material were obtained by testing standard cylindrical specimens which were 6.25 mm diameter at test temperatures of 400, 425 and 452 C. These data are reported in Table I. Comparison is also made with previous results from oxygen saturated (OS) and oxygen free (OF) copper (1). Addition of one percent antimony considerably alters the tensile stress-strain response of copper. The 0.2% yield strength increases significantly and the percentage elongation decreases significantly with the addition of antimony. This result is particularly encouraging from the stand-point of the goals of the project. Small-scale-yielding (SSY) and small-scale-creep (SSC) conditions can be produced in 50 mm wide compact type (CT) specimens. By using smaller size specimens large scale yielding and extensive creep conditions can be

obtained. Thus, the damage distribution ahead of the crack tip under these very different conditions can be compared for creep and creep-fatigue conditions.

2.2.3. Creep Deformation Behavior of the Test Material

Figure 4 shows the minimum creep deformation rate as a function of stress for the test material for two test temperatures. These tests were conducted to primarily select the test temperature for the remainder of our studies. The creep behavior is also compared with similar data on copper and antimony-copper available in the literature (2,3).

The creep deformation rates are sensitive to the grain size in copper and antimony-copper. The smaller grain size accelerates the creep rate due to increased grain boundary sliding and also to the presence of more grain boundary facets on which cavities can nucleate and grow. The creep rates measured on our test material appear to be somewhat faster than those observed by Tipler and McLean (2). The difference could be rationalized by the differences in grain diameter which was 280 μm for their material as compared to 90 μm for our material. We will be conducting our future tests at 400 C. Two tests are already in progress and more creep deformation data will be available shortly.

2.3 Damage Characterization Studies

Feasibility studies were made on potential techniques for

damage characterization: small angle neutron scattering (SANS), electron radiography (ER), synchrotron x-ray micro-radiography (SXMR) and fractography using SEM. The SANS experiments and the electron radiography were performed at ORNL (National Center for Small Angle Scattering Research and High Voltage Electron Microscopy Facility) in collaboration with Drs. Stephen Spooner and Joachim Schneibel, respectively. Crept copper specimens, described below, were examined with SANS and ER in the early stages of our program, when the copper-antimony material was not available: testing conditions were chosen to produce cavities similar to what we would expect for the Cu-Sb material (4,5). The Cu-Sb specimens have been studied with SXMR and surface fractography. Our experience indicates that SXMR and fractography, along with computed microtomography (described in the continuation proposal), will be the optimum techniques for damage characterization.

Conventional SANS as well as high resolution, double crystal SANS (pre-specimen collimator and post specimen analyzer) were used to study two polycrystalline copper specimens crept at 405 C and under applied stresses of 4174 and 4505 psi for 10.8 and 23.8 hrs., respectively. The specimens were right cylinders with 5mm thickness and 10mm diameters. Linear Guinier plots could not be obtained, indicating that a significant fraction of the cavities were too large (>1μm) for an average cavity size to be determined with small angle scattering (Fig. 5). Linear Porod plots could be obtained, however, so that the surface to volume ratios are

known (Fig. 6). Without knowing the average scatterer size and the number of scatterers, normally provided by the analysis of linear Guinier plots, little progress can be made. High precision densitometry can be used to furnish some additional information (4), but this approach involves making significant assumptions.

The evaluation of ER was with our JEOL 100C TEM and with the ORNL HVEM. Specimens were mechanically polished to thicknesses of about 35 μm using a final polish of 0.05 μm diamond paste. Occasional voids could be observed within specimens with both microscopes, but their images were weak and extremely difficult to record. Figure 7 shows a typical image recorded at 5000X magnification.

X-ray imaging methods appear to be very promising, based on our work to date. Synchrotron microradiography using white radiation was performed at the Stanford Synchrotron Research Laboratory (SSRL) on a cracked, Cu-Sb compact tension specimen. The specimen had been pre-cracked in fatigue and was crept at 400 C under 532 pounds load for 41.2 hrs. Subsequently a 1mm section was cut from near the center of the specimen and was mechanically polished to a final thickness of 250 μm. Radiographs were recorded with the beam at normal incidence and at +10 and -20 deg. from normal incidence (Fig. 8). Exposure times were about 0.1 sec. We note that considerably thicker specimens can be examined. The images do not reveal any cavities greater than 5 μm in diameter, which is in agreement with the results of

fractography described in the following paragraph. For these test conditions rapid crack growth was obtained, yielding little opportunity for cavitation. The transition from the room temperature pre-crack to the creep crack is evident in the radiographs (labeled by T). The different projections show the three-dimensional nature of the crack. We are currently developing computer programs which will allow the (x,y,z) coordinates of discrete features to be obtained from the (x',y') coordinates from different projection directions.

SEM fractography was performed on the creep crack growth specimen and on a creep deformation specimen. The average creep crack growth rate of the compact type specimen was on the order of 10^{-3} in/hr. which is considered too fast for cavitation type damage to develop. The SEM analysis of the fracture surface confirmed this suspicion. Few cavities were formed on the feature surface. In the future, tests will be conducted at lower creep crack growth rates to allow sufficient time for cavitation damage to develop ahead of the crack tip.

Figure 9 shows the SEM fractograph of a creep deformation specimen. The specimen was strained to 2.2 percent creep strain at 410 C and a stress level of 2000 psi. A sharp notch was cut in the gage length of the specimen with a saw and it was fractured by impact loading. This picture showed three large cavities and several small cavity like features on the grain boundary facets. The small, cavity-like features have not been definitely identified yet. Transmission electron microscopy

(TEM) is planned to determine if these features are due to oxides or if they are in fact small cavities of a critical nucleus size.

3. REFERENCES

1. T.G. Nieh, "The Influence of Grain Boundary Segregation and Cavity Formation on High-Temperature Fracture of Silver and Copper," Ph.D. Thesis, Stanford University, 1980.

2. H.R. Tipler and D. McLean, Journal of Materials Science, vol. 4, 1970, p. 103.

3. P. Feltham and J.D. Meakin, Acta Metallurgica, vol. 7, 1959, p. 614.

4. M.S. Yang, J.R. Weertman and M. Roth, Scripta Metallurgica, vol. 18, 1984, p. 543.

5. J.C. Earthman, J.C. Gibeling and W.D. Nix, Acta Metallurgica, vol. 33, 1985, p. 805.

Table 1 - Short Term High-Temperature Tensile Results

Material	Temperature (C)	0.2% Y.S. (psi)	Tensile Strength (psi)	% Elong. in 1"	$n^{(5)}$	$K^{(5)}$
OS-Cu[1]	400	4700[2]	6200	3	-	-
"	425	4600[2]	-	2.5	-	-
"	450	4400[2]	-	2.5	-	-
OF-Cu[1]	400	2200[2]	8300	18	-	-
"	425	2250[2]	-	16-17	-	-
"	450	2300[2]	-	15	-	-
Cu-Sb	400	9300	14,900	7	.21	27,900
"	425	8100	13,400	-	.20	24,700
"	452	6700	12,800	8	.22	24,300

Notes:
(1) From the work of Nieh (1).
(2) These are estimates from Nieh's graphs.
(3) $\dot{\varepsilon}$ = .60%/min. for tests by Nieh.
(4) $\dot{\varepsilon}$ = .50%/min. in present study.
(5) K and n represent constants in the equation is $\sigma = K \varepsilon^n$.
(6) Initial hardness of OS-Cu was 27 HRF, and it was 56 HRF for Cu-Sb.

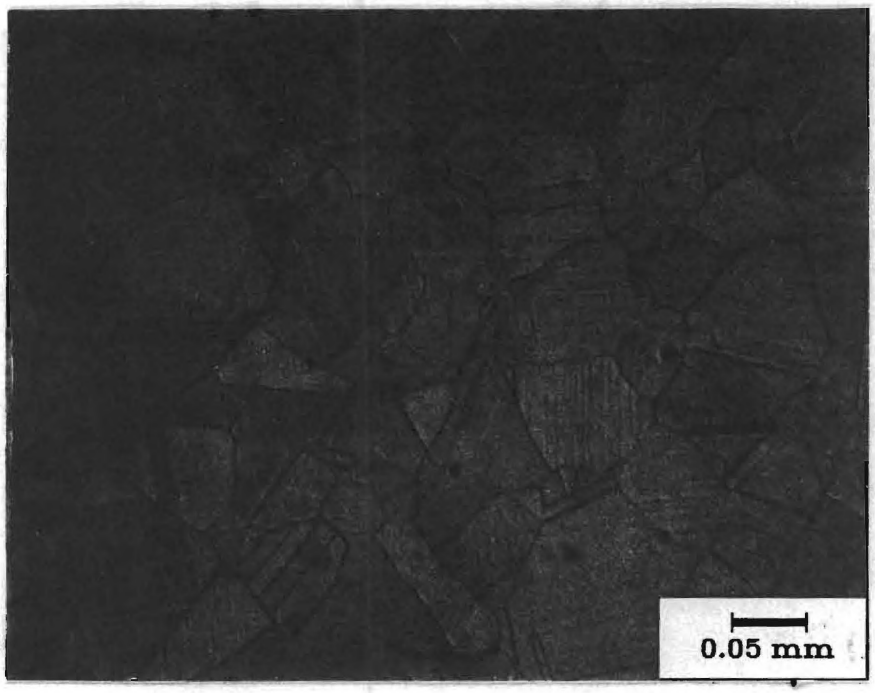

Fig. 1 - Microstructure of the as extruded antimony-copper alloy.

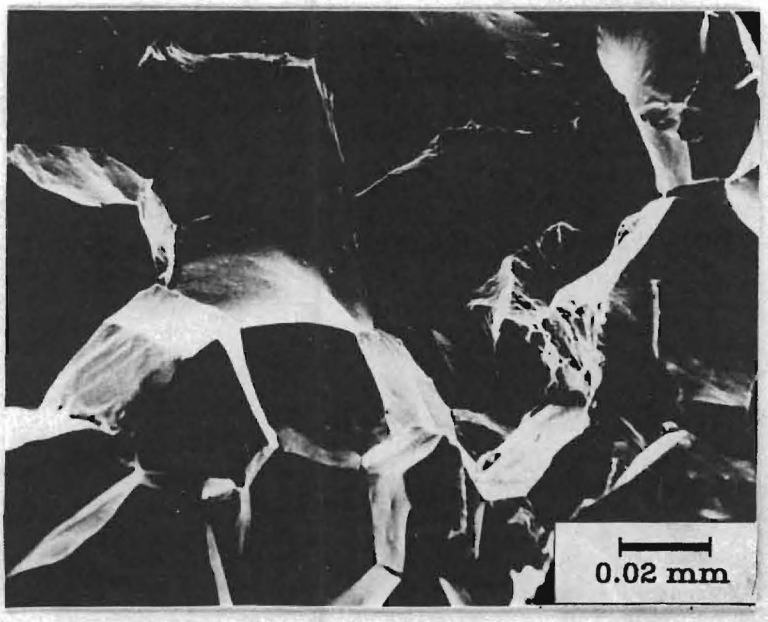

Fig. 2 - SEM photomicrograph of the fracture produced at room temperature in the antimony-copper material.

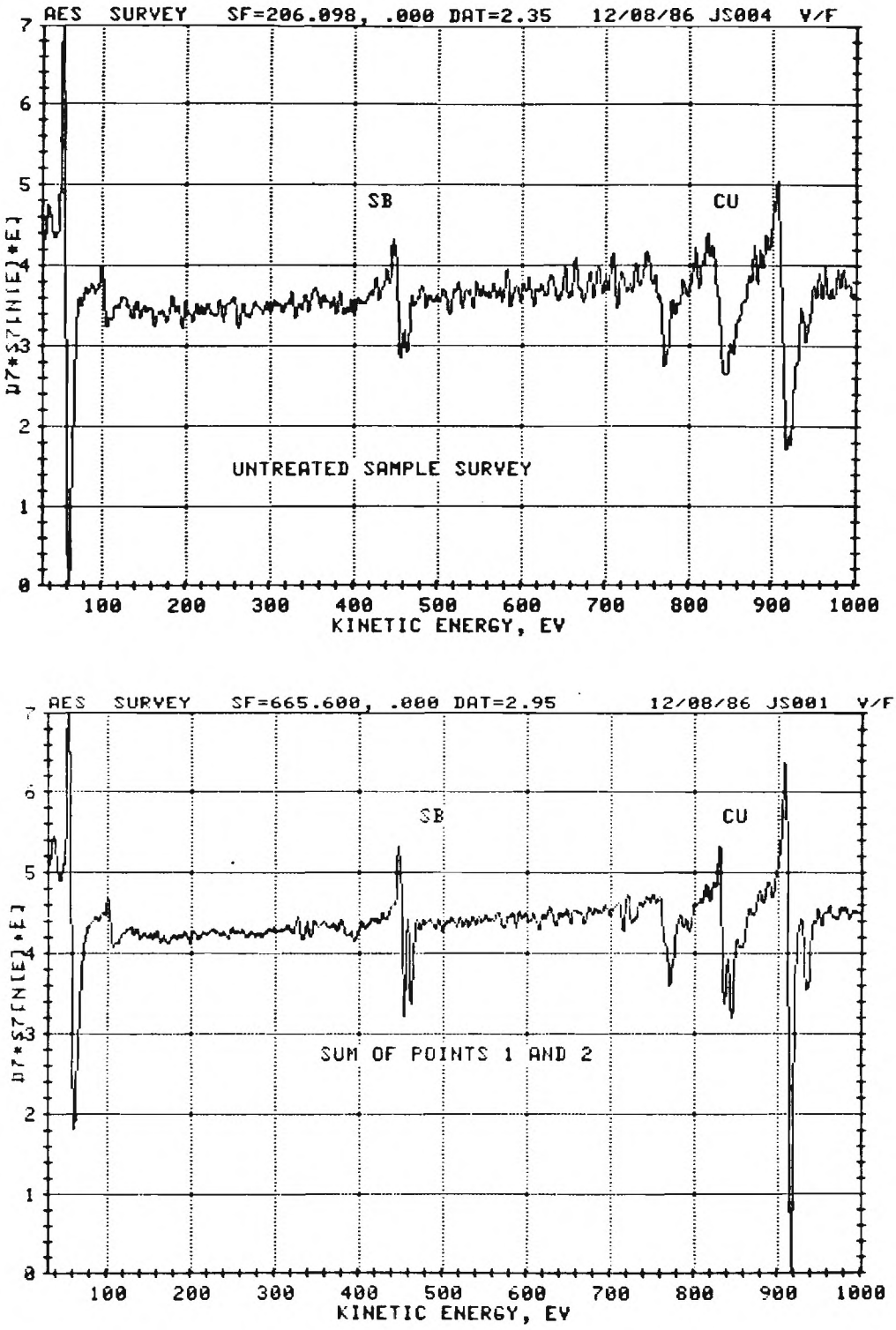

Fig. 3 - Auger Spectrum of the (a) as-extruded and (b) as-extruded plus 24 hours at 675 C specimens of Sb-Cu.

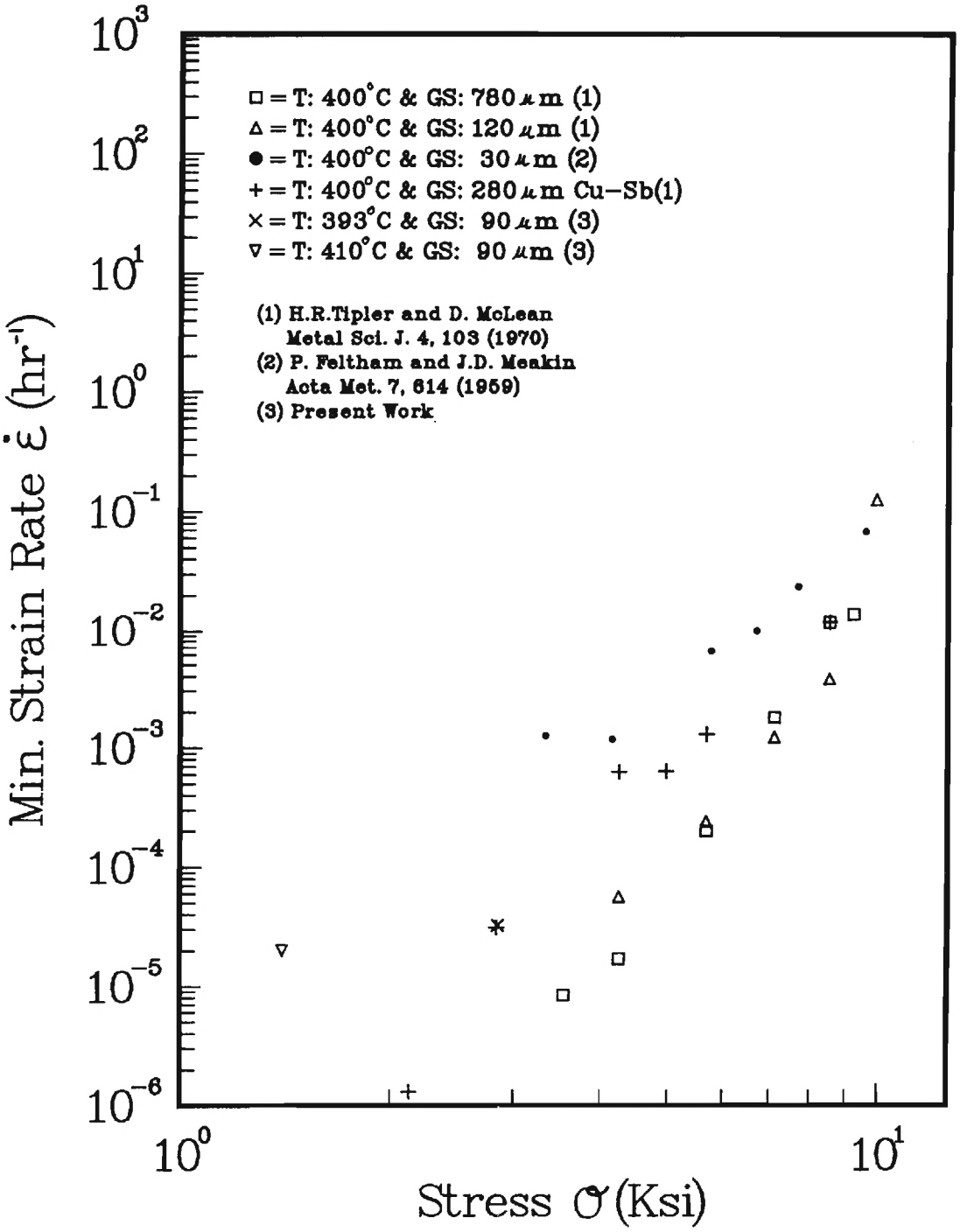

Fig. 4 - Minimum creep rate as a function of applied stress at 400 C for copper and antimony-copper.

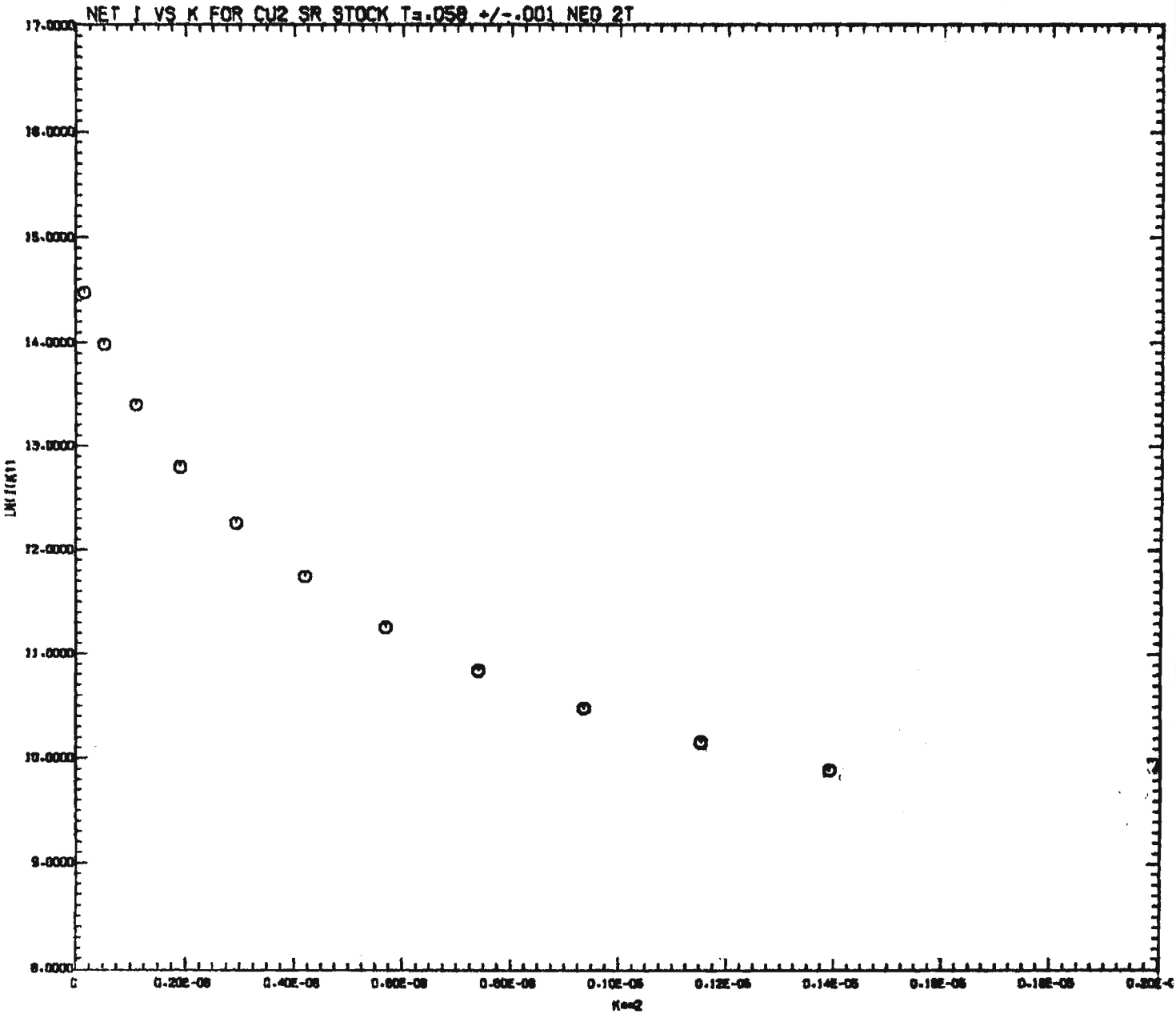

Figure 5 - Guinier Plot of neutron scattering from copper crept at 405 C. This data was obtained using a double crystal small angle scattering apparatus. The plot of ln I as a function K^2 is not linear even at the smallest values of K.

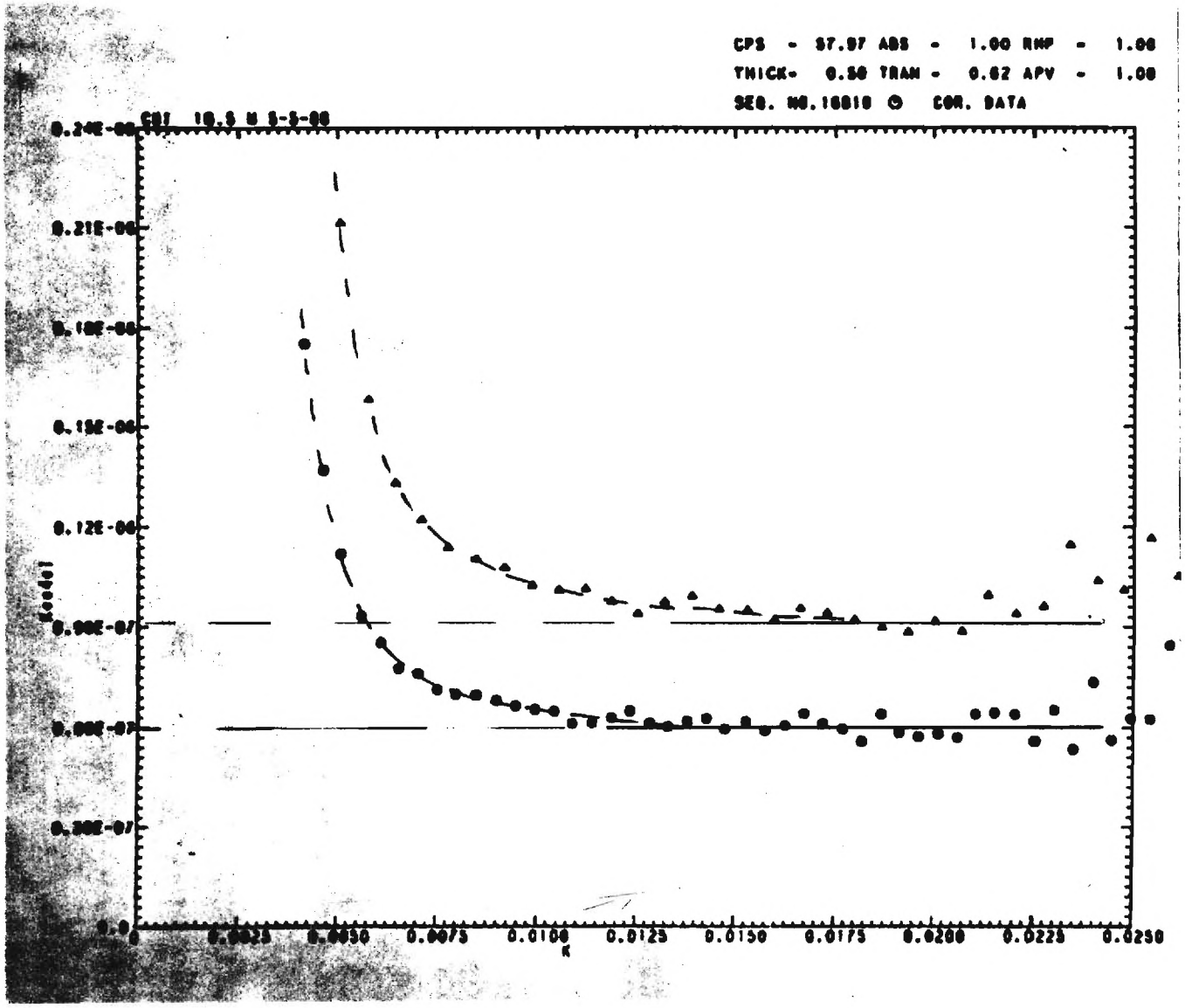

Figure 6 - Plot of intensity multiplied by K^4 as a function of K. The horizontal portion of the curve defines the Porod constant.

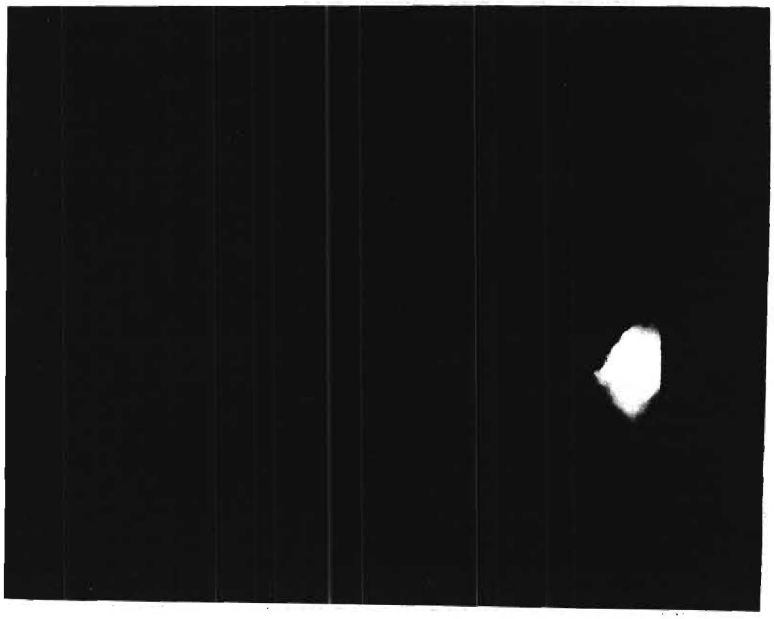

Figure 7 - Electron radiography of a creep cavity in copper. The magnificaiton is 5000X.

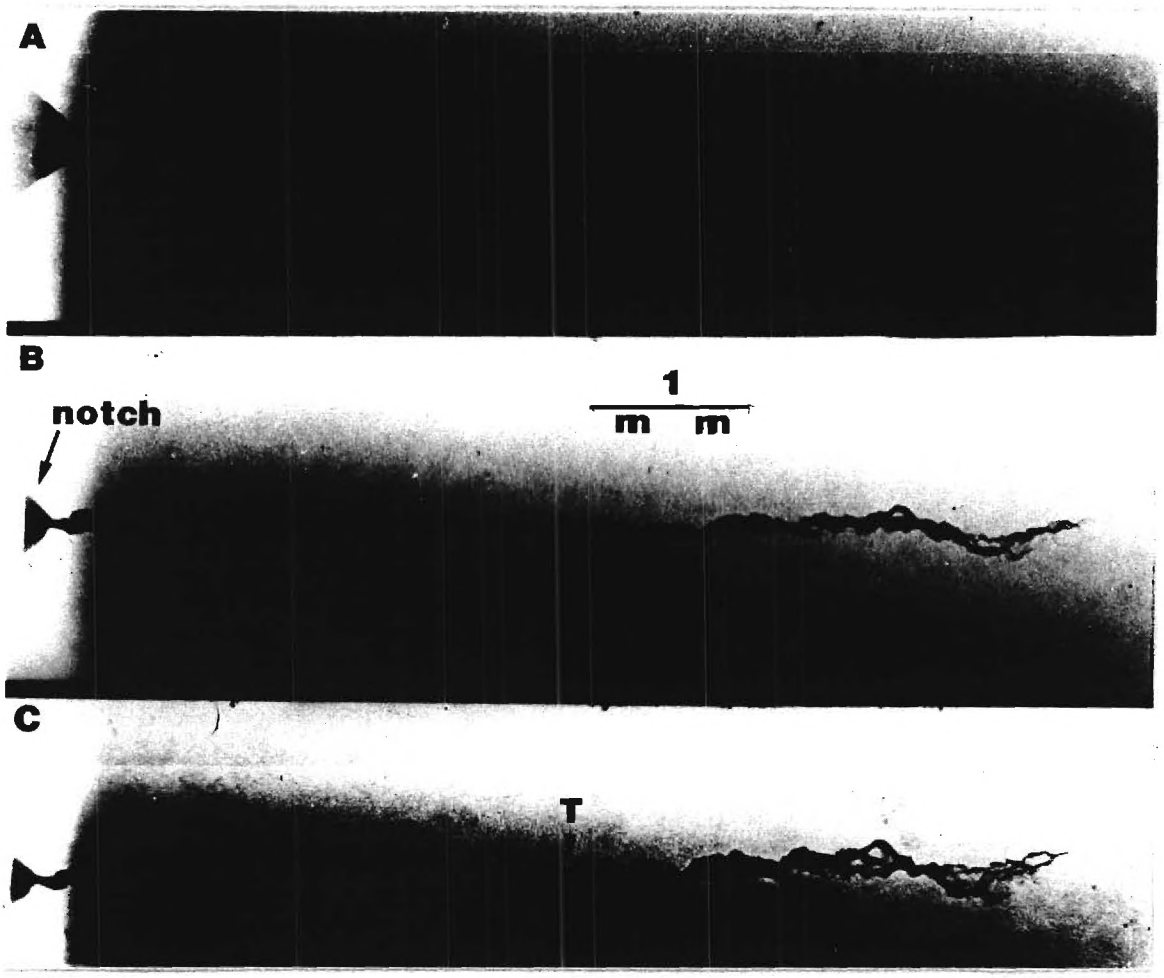

Figure 8 - Synchrotron microradiographs of a cracked Cu-Sb specimen. The 250 μm thick specimen was cut from the center of the specimen perpendicular to the plane of the crack. Radiographs recorded at different orientations of the specimen relative to the beam are shown: a) beam normal to specimen, b) beam at +10° angle of incidence and c) beam at -20° angle of incidence.

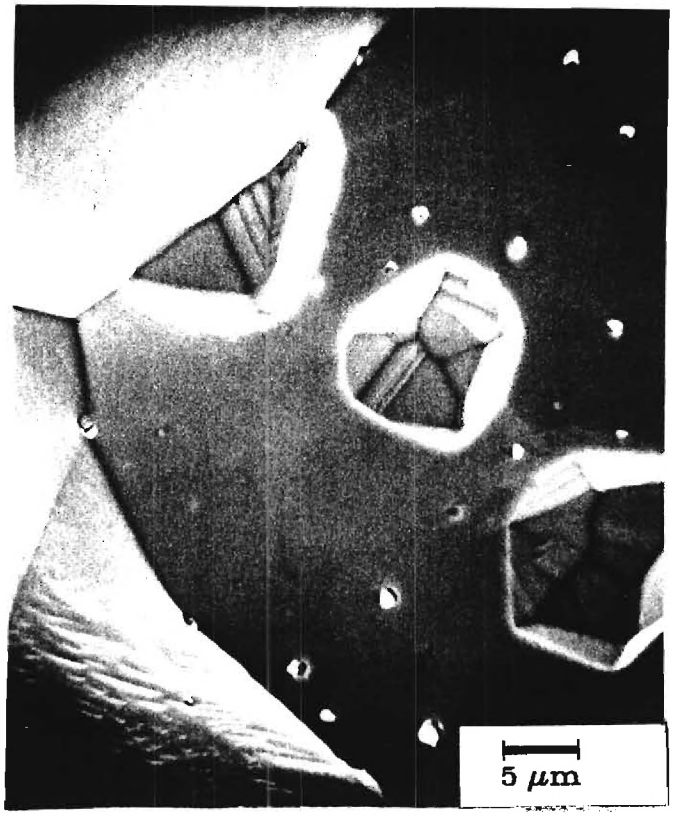

Fig. 9 - Photomicrograph of grain boundary cavities in a creep deformation specimen tested at 400 C and a stress level of 13.8 MPa.

DOE F 1332.16 (10-84)
(Formerly RA-427)

OMB Approval
No. 1910-1400

U. S. DEPARTMENT OF ENERGY

UNIVERSITY CONTRACTOR, GRANTEE, AND COOPERATIVE AGREEMENT RECOMMENDATIONS FOR ANNOUNCEMENT AND DISTRIBUTION OF DOCUMENTS

See Instructions on Reverse Side

1. DOE Report No. DOE/ER/45257-1

2. DOE Contract No. DE-FG05-86ER-45257

3. Title First Annual Progress Report on a Study of Mechanisms of Time-Dependent Crack Growth at Elevated Temperature

4. Type of Document ("x" one)
   - [X] a. Scientific and technical report
   - [ ] b. Conference paper:
     - Title of conference _____
     - Date of conference _____
     - Exact location of conference _____
     - Sponsoring organization _____
   - [ ] c. Other (Specify) _____

5. Recommended Announcement and Distribution ("x" one)
   - [X] a. Unrestricted unlimited distribution.
   - [ ] b. Make available only within DOE and to DOE contractors and other U. S. Government agencies and their contractors.
   - [ ] c. Other (Specify) _____

6. Reason for Recommended Restrictions

7. Patent and Copyright Information:
   Does this information product disclose any new equipment, process, or material? [X] No [ ] Yes If so, identify page nos. _____
   Has an invention disclosure been submitted to DOE covering any aspect of this information product? [ ] No [ ] Yes
   If so, identify the DOE (or other) disclosure number and to whom the disclosure was submitted.
   Are there any patent-related objections to the release of this information product? [X] No [ ] Yes If so, state these objections.
   Does this information product contain copyrighted material? [X] No [ ] Yes
   If so, identify the page numbers _____ and attach the license or other authority for the government to reproduce.

8. Submitted by A. Saxena
   Name and Position (Please print or type) Professor, Materials Engineering
   Organization Fracture and Fatigue Research Laboratory, Georgia Tech.
   Signature
   Phone (404) 894-2888
   Date 2-28-87

FOR DOE OR OTHER AUTHORIZED USE ONLY

9. Patent Clearance ("x" one)
   - [ ] a. DOE patent clearance has been granted by responsible DOE patent group.
   - [ ] b. Report has been sent to responsible DOE patent group for clearance.

Georgia Institute of Technology
School of Materials Engineering
Atlanta, Georgia 30332-0245
(404) 894-2888

July 16, 1986

MEMORANDUM

TO: Brian Lindberg, OCA

FROM: A. Saxena

Subject: DOE Grant Project # E-18-625

Attached is a completed form DOE538 for transmittal to DOE which they require within thirty days of award of a new grant. Please check the details and fill blanks where I could not find the necessary information to fill.

U.S. DEPARTMENT OF ENERGY

NOTICE OF ENERGY RD&D PROJECT

OMB Approval No 1901-021

MOVED FOR USE BY SMITHSONIAN SCIENCE INFORMATION EXCHANGE

Descriptive title of work: A study of Mechanisms of Time-Dependent Crack Growth at Elevated Temperature

Performing organization control number:

Work status: ☒ New ☐ Continuing ☐ Terminated

3. Contract or grant number: DE-FG05-86ER45257

Contractor's principal investigator/project manager and address where work is performed

A. Name (Last, First, MI): Saxena, Ashok B. Phone: FTS- (404) 894-2888

C. Research organization business address: Street: School of Materials Engineering Com.-

City: Atlanta State: GA Zip: 30332

4A. Name of performing organization: Georgia Institute of Tech (Organization) School of Materials Eng. (Department)

B. Mailing address (If different from 4C)

C. Circle only one code for TYPE OF ORGANIZATION PERFORMING R&D (See instructions):

CU FF IN NP ST TA US XX EG

D. Location where the work is being performed

E. Country sponsoring research

Supporting organization

A. Program division or office (Full name): Office of Basic Energy Sciences, Materials Science Div. Department of Energy

B. Technical monitor (Last, First, MI): Darby, Joseph B. C. Phone: FTS- 301-353-3428

D. Address (If different from DOE Hqs.): Office of Basic Energy Sciences ER-131, U.S. Department of Energy, Germantown, MD 20874 Com.-

E. Administrative monitor (Last, First, MI): Clark, Marlena

Project schedule

A. Start date: 7-86 (Month) (Year) B. Expected completion date: 6 - 89 (Month) (Year)

Funding in thousands of dollars (Funds represent budget obligations for operating and capital equipment)

Funding organization(s)	Current FY	Next FY 88
Basic Energy Sciences, DOE	104,179	109,537

For DOE projects, enter budgeting and reporting classification code

Interagency agreement (Specify funding agency)

Agency in-house effort (Check if applicable) ☐

EPA "pass-thru" funding (Check if applicable) ☐

Note: Funding Section utilization is optional on Federal Financial Assistance Programs: grants, direct payments, cooperative agreements, loan guarantees, and other related programs.

Descriptive summary of work (Limit to 200 words. Include objective, approach, results to date and their significance, and expected product. Quantify where possible).

The objective of this research is to study the mechanisms of time-dependent crack growth antimony-copper subjected to creep and creep-fatigue loading. The influence of loading waveform will also be characterized. Models for growth of grain boundary cavities under the action of crack tip stress fields will be developed. These microscopic models will used to develop engineering models for predicting the influence of cyclic waveform and frequency on the fatigue crack growth behavior at elevated temperature. The results this program will be applied to predict the behavior of Cr-Mo-V steels for which creep-fatigue data will be available from a separate study.

9. List the most descriptive publications in the last year that are available to the public which have resulted from the project (give a complete bibliographic citation. Use additional sheets if necessary).

NEW PROJECT, NO PUBLICATIONS

11. General technology categories (Enter applicable code of codes from instructions).

A 1 | A 2 | A 3 | E 3 | | | | | | | | | |

12. Type of research activity (Check applicable activities)

A. [X] Basic research
B. [X] Applied research
C. [ ] Laboratory scale R&D
D. [ ] Technology development
E. [ ] Field study
F. [ ] Pilot plant scale R&D
G. [ ] Full scale demonstration
H. [X] Mathematical model development
I. [X] Data analysis/assessments
J. [ ] Information systems management
K. [ ] Policy analysis
L. [ ] Socioeconomic
M. [ ] Other (Specify)_____
N. [ ] Not applicable

13. Keywords (Please list 5 keywords).

copper, creep, Fatigue, crack, cavitation

14. Is this research project solely an ANALYTICAL/PAPER STUDY? (Non-experimental, paper and pencil, computer analysis, etc.) YES _____ NO X

Respondent's Name: A. Saxena Phone No.: (404) 894-2888 Date: 7/14/86

Street: School of Materials Engineering
Georgia Institute of Technology
City: Atlanta State: GA Zip: 30332

DOE F 1332.16 (10-84)
(Formerly RA-427)

OMB Approval
No. 1910-1400

U. S. DEPARTMENT OF ENERGY

UNIVERSITY CONTRACTOR, GRANTEE, AND COOPERATIVE AGREEMENT RECOMMENDATIONS FOR ANNOUNCEMENT AND DISTRIBUTION OF DOCUMENTS

See Instructions on Reverse Side

1. DOE Report No. DOE/ER/45257-2

2. DOE Contract No. DE-Fg05-86ER45257

3. Title Second Annual Progress Report on a Study of Mechanisms of Time-Dependent Crack Growth at Elevated Temperature

4. Type of Document ("x" one)
   - ☒a. Scientific and technical report
   - ☐b. Conference paper:
     - Title of conference _____
     - Date of conference _____
     - Exact location of conference _____
     - Sponsoring organization _____
   - ☐c. Other (Specify) _____

5. Recommended Announcement and Distribution ("x" one)
   - ☒a. Unrestricted unlimited distribution.
   - ☐b. Make available only within DOE and to DOE contractors and other U. S. Government agencies and their contractors.
   - ☐c. Other (Specify) _____

6. Reason for Recommended Restrictions

7. Patent and Copyright Information:
   Does this information product disclose any new equipment, process, or material? ☒ No ☐ Yes If so, identify page nos. _____
   Has an invention disclosure been submitted to DOE covering any aspect of this information product? ☐ No ☐ Yes
   If so, identify the DOE (or other) disclosure number and to whom the disclosure was submitted.
   Are there any patent-related objections to the release of this information product? ☒ No ☐ Yes If so, state these objections.
   Does this information product contain copyrighted material? ☒ No ☐ Yes
   If so, identify the page numbers _____ and attach the license or other authority for the government to reproduce.

8. Submitted by A. Saxena
   Name and Position (Please print or type) Professor, Materials Engineering
   Organization Fracture and Fatigue Research Laboratory, Georgia Tech.
   Signature
   Phone (404) 894-2888
   Date 2-27-88

FOR DOE OR OTHER AUTHORIZED USE ONLY

9. Patent Clearance ("x" one)
   - ☐a. DOE patent clearance has been granted by responsible DOE patent group.
   - ☐b. Report has been sent to responsible DOE patent group for clearance.

Second Annual Progress Report on a Study of Mechanisms of Time-Dependent Crack Growth at Elevated Temperature

Submitted to

U.S. Department of Energy
Basic Energy Science-Division of Materials Science
Washington, D.C.

by

A. Saxena, S. R. Stock, B. Gieseke, K. Banerji
Mechanical Properties Research Laboratory
Georgia Institute of Technology
Atlanta, Ga 30332-0245
Period Covered: 2/16/87 to 2/15/88

Approved:

S. D. Antolovich, Director
Mechanical Properties Research Lab

W. M. Sangster, Dean
College of Engineering

February 25, 1988

1. PROGRAM OBJECTIVES AND SUMMARY

The prediction of design and remaining life of several heavy section components which are subjected to elevated temperatures in energy conversion machinery require accurate methods for predicting crack growth behavior in the presence of time-dependent creep strains. Significant progress has recently been made in extending the linear-elastic and elastic-plastic fracture mechanics concepts into the creep regime. Thus, the use of fracture mechanics for predicting the crack growth life of elevated temperature components is a viable approach. However, serious deficiencies exist in the understanding of the damage mechanisms that lead to time-dependent crack growth. Specifically, the interactions between creep and fatigue damage mechanisms for slow frequency cyclic loading are not well understood. Therefore, cumulative damage laws for creep-fatigue loading based on physical damage mechanisms are non-existent.

The objective of this study is to conduct creep and creep-fatigue crack growth tests and to characterize the crack tip damage mechanisms in a model material (copper with 1 wt percent antimony) which is known to cavitate at the grain boundaries under creep deformation. The above data and observations will be used to develop mechanistic models for cumulative crack tip damage under complex loading conditions at elevated temperatures. The application of these models will also be extended to situations involving non-periodic loading. The results of this program will be integrated into an Electric Power Research Institute (EPRI) sponsored study (also being conducted at Georgia

Tech under the direction of Dr. A. Saxena) for characterizing the creep-fatigue crack growth behavior of Cr-Mo-V steels. The techniques being used for detection of crack tip damage include optical metallography, scanning electron microscopy, x-ray radiography computed tomography and small angle neutron and x-ray scattering (SANS and SAXS).

The proposed program is being conducted over a period of thirty six months in four distinct tasks listed below:

Task I Material Selection and Characterization
Task II Creep and Creep-Fatigue Crack Growth Testing
Task III Characterization of the Influence of Loading Transients
Task IV Crack Tip Damage Characterization

The program began on 7/1/86. The progress for the period 7/1/86 to 2/15/87 was reported previously [1]. During the period of 2/16/87 to 2/15/88, considerable progress was made on all four tasks which is described in detail in the remainder of the report.

Briefly, Task I was completed by finishing the creep deformation and rupture tests. Four creep crack growth tests were performed and extensive characterization of the crack tip damage was conducted using optical, scanning electron microscopy and x-ray radiography. It was shown that the volume fraction of cavitation damage at the crack tip is uniquely related to the applied magnitude of C_t during creep crack growth. Unconstrained cavitation damage at the crack tip leads to crack branching, and

the creep crack growth rates then no longer correlate with C_t. Several creep-fatigue crack growth tests were completed at different loading frequencies and waveforms. These tests were conducted in ultra-high-purity nitrogen environment in a chamber specially designed and fabricated for these tests. Both loading waveform and frequency were shown to have a significant effect on the crack growth rate and the damage developed in the crack tip region.

The program is now at its mid-point and significant results and papers have already been produced (3 papers and 5 conference presentations). In the next few months we will be concentrating on reporting the latest results in leading journals. One student who was entirely supported on this program received his M.S. degree and is currently working in the Aerospace industry.

2. TECHNICAL PROGRESS

2.1 Material Characterization

The model test material selected was copper with 1 weight percent antimony as mentioned before. The segregation of antimony to the grain boundaries embrittles the material considerably at room temperature and causes the fracture to occur exclusively at the grain boundaries. This allows precise determination of the grain boundary damage due to creep or creep-fatigue loading.

The details of the processing and microstructural analysis of the material were included in a previous report [1]. Briefly, oxygen free copper (99.99 percent) and pure antimony (99.999 percent) were melted in a vacuum induction furnace and cast into a 5 inch diameter billet. The billet was homogenized at 950 C for five hours and then extruded into a rectangular bar of 2-3/4" x 2" at 700°C. The bar was ultrasonically tested for defects. The areas producing to defect indications were marked to avoid taking test samples from those regions. The defective regions were a very small portion of the material, and sufficient material is available for conducting the test program.

The results of the Auger analysis for characterizing antimony segregation chemical analysis, will not be repeated here and can be found in last year's report and also in Ref [2]. Instead, this section contains results from tests performed during this reporting period which include the creep deformation and rupture tests.

All mechanical testing in this program was conducted at 400°C. Figure 1 shows a plot of the minimum creep rate as a function of applied stress for the test material. Data from previous studies on creep of copper are provided for comparison. The pre-exponent constant, A and the exponent n, were determined from this data. The full creep curves revealed that tertiary creep was important and that little or no primary creep was observed in these tests. Constitutive equations were derived from the data to include contributions from tertiary creep as well. The complete test results are reported in a recent M.S. thesis [2]. All tested specimens were subjected to a detailed damage characterization. Those results will be briefly summarized later in this report. A few creep tests were interrupted at various percentages of life to determine creep cavity growth rates during various stages.

Figure 2 shows a typical creep curve along with the cavity sizes observed at various life fractions during the test. The test conditions and the cavity sizes and spacings are labelled on the figure. Even at one percent of creep life, micron-size cavities are present in this material. The onset of tertiary creep appears to coincide with coalescence of cavities and occurs at approximately 60 percent of life. Rice's model [3] predicts the cavity growth rate during steady-state creep to within five percent of the measured rates (see [2] for details). These results are used in evaluating models for describing the creep crack growth process.

2.2 Creep and Creep-Fatigue Crack Growth Testing

Four compact type specimens were tested at different load levels to characterize the creep crack growth behavior of this material. The crack growth rate as a function of C_t parameter is shown in Figs. 3 and 4. In Fig. 3, all measured creep crack growth rates are reported and it appears that a poor correlation is observed between da/dt and C_t. To investigate this further, all tested specimens were subjected to a thorough metallographic examination at the crack tip. In two of the four specimens, considerable crack branching was observed, Fig. 5. The cavitation during crack branching was unconstrained. On the other hand, when a single dominant crack was present, the cavitation at the crack tip was constrained and was also localized in the crack tip region. Figure 4 shows the da/dt versus C_t relationship which include only those data points which were obtained during the period in which the cavity growth was constrained. There now appears to be a reasonable relationship between da/dt and C_t among these data points. More work is currently being conducted to investigate this further. These tests will be on specimens which are redesigned to promote constrained damage at the crack tip and also be conducted in a non-oxidizing environment to protect the crack growth surface for examination.

One of the objectives of the creep crack growth experiments was to produce two specimens with comparable C_t values with one undergoing small scale creep and the other undergoing extensive creep. By characterizing damage ahead of the crack tip in these

specimens, we could attempt to understand why C_t is able to normalize creep crack growth data under a wide range of creep conditions. There is considerable evidence in the literature that C_t does normalize creep crack growth rates for conditions ranging from small scale creep to extensive creep [3-5].

It was experimentally difficult to produce two specimens with identical C_t values. However, we managed to achieve that goal approximately. Specimen CT-2 shown in Figs. 3 and 4 was in extensive creep condition and had a C_t value of 0.0162 in lbs/in^2 hr. Specimen CT-5 was in small scale creep condition and had a C_t value of 0.0105 in lbs/in^2 hr. Figures 6 and 7 show the cavity diameter and area density, respectively as a function of the distance from the crack tip. The ratio of the total cavity volume in the crack tip region to the total volume of the damaged region of the specimen (described in the damage characterizaiton section) was calculated for CT-2 and CT-5. The ratio of these values of accumulated damage for specimen CT-2/CT-5 was 1.5 which compared well with the value of 1.54 for the ratio of the two C_t values. Hence, C_t can be understood as a parameter which assures similitude conditions with respect to constrained crack tip damage. This is one of the significant findings of this study.

Figure 8 shows the results of seven creep-fatigue crack growth tests which have been completed to date. All tests were conducted at 400°C. Two initial tests conducted in air at 1.0 Hertz showed that the oxide thickness in the wake of the crack was large and was causing high crack closure loads. Also, the fracture surface was coated with a thick oxide and no

fractography of the failed specimens was possible. To alleviate these problems, major effort was spent in designing and fabricating a test chamber to conduct subsequent tests in a nonoxidizing environment (ultra-high-purity nitrogen). The test chamber fabrication was completed six months ago and we have now also completed several tests as seen in Fig. 8.

In high temperature fatigue crack growth testing in air, thick layers of oxide are often formed on the fracture surface which wedge open the crack during unloading considerably decreasing the applied driving force. To assess the influence of oxide induced crack closure, the results of the 1Hz test in air can be compared with the 10Hz data in N_2. It appears that the oxide induced crack closure at 1.0 Hz played a significant role by decreasing effective ΔK and thereby the crack growth rate. It is also seen that the crack growth rates increase with increasing cycle time. There also seems to be a significant influence of the loading waveform. These effects are rationalized by time-dependent damage accumulation at the crack tip under the varying loading conditions.

The time-dependent damage during creep-fatigue is clearly grain boundary cavitation as shown in Fig. 9. The damage ahead of the crack tip for various loading frequencies and waveforms was quantified by determining the average diameter of cavities, cavity density and percent grain boundary area cavitated. Typical results of these measurements are shown in Figs. 10 to 12. In general, the percent area cavitated and the cavity density increase as the crack tip is approached. Also, the over

all cavitation damage increases with increase in cycle time (decreasing frequency). From the present data, no consistent trends with loading waveforms are apparent. This may change as more data become available.

In Fig. 12, the average cavity diameter as a function of distance from the crack tip is compared for pure creep and creep-fatigue loading. Although, the magnitude of the crack driving forces are quite different in these loadings, some trends are obvious and interesting. For example, the cavity diameter rises sharply as the crack tip is approached. On the other hand, cavity sizes decay at a much smaller rate as a function of crack tip distance indicating that considerable cavity growth occurs in the elastic field outside the creep zone. This observation has interesting implications on the waveform effect during creep-fatigue. This will be explored more fully during subsequent testing and damage evaluation studies.

2.3 Influence of Loading and Crack Growth Transients

When creep crack growth tests are initiated, the growth rate goes through a transient region within which no unique relationship between da/dt and a crack driving force parameter such as C_t or C^* exists. A schematic of such behavior is shown in Fig. 13. The initial crack growth rates are dependent on the starting value of C^*. The period during which the crack growth is retarded is often called the incubation period and is related to the establishment of damage at the crack tip from an initially undamaged state. We will soon begin experiments on the model

material to experimentally characterize these transients. Understanding of these transients may also hold the clue to understanding creep-fatigue interactions as explained below. Figure 14 shows the da/dt versus C_t behavior of creep-fatigue tests under a trapezoidal waveform [6]. Only contribution due to time-dependent crack growth during hold time is included. For comparison, creep crack growth data under static load are also plotted. The influence of unloading is to retard the crack growth rate in this material. this retardation may be due to a fresh incubation period following each unloading. A detailed understanding of this phenomenon is necessary for building accurate models for predicting the crack growth behavior under creep-fatigue conditions and will be the focus of future work on this project.

2.4 Damage Characterization

Optical and scanning electron microscopy (OM and SEM, respectively) were the principal techniques used for damage characterization. Sections parallel to the stress axis and through the center of the cylindrical creep specimens were polished and examined with OM to study gradients of cavitation damage normal to the rupture surface. Creep, creep crack growth and fatigue crack growth specimens were fractured at room temperature, and the exposed, damaged grain boundaries were studied subsequently with SEM. Volume fraction, areal fraction and average diameter of cavities were determined using standard stereological point and linear probes.

Sections with thicknesses between 0.4 and 1.0 mm were cut from the center of the creep and creep crack growth samples for microradiographic study. Synchrotron white radiation from the Stanford storage ring and from the Daresbury storage ring were used to study specimens 1A and 3C (creep) and CT2, CT4[2] and CT5 (creep crack growth). Samples with cross-sectional areas of 1 mm^2 or less have been cut from the creep specimens 1A and 3C (normal to the rupture plane) for microtomographic characterization. Preliminary scans will be completed in the next several months and should allow evaluation of this nondestructive examination technique for cavitation damage studies. Digital radiography using a 10 μm diameter beam and electronic detector (the term "microradiography" is used to denote film methods) is a second novel approach to damage characterization, and its feasibility is currently being assessed by studies of sample CT5.

Creep Deformation Results

Results from stereological or quantitative microscopy are shown in Figure 15 for samples tested at 3.5, 5, 6 and 8 ksi (sample numbers 1A, 4D, 2B and 3C, respectively). A substantial gradient in volume fraction of cavities (V_v) is evident, and with the exception of the 5 ksi sample, increasing stress led to decreased damage. It is interesting to note that V_v for the 3.5, 6 and 8 ksi specimens appeared to approach an asymptotic value at different distances from the rupture surface. This value was on

---

[2]. This sample was studied using laboratory x-radiation.

the order of that reached at 60% of lifetime at 6 ksi (interrupted test 3I).

The results suggest that the gradients in V_v are due to necking or plastic instability. It is clearly inappropriate to take the damage level near the rupture surface as representative of the state of "100 percent damage." A superior measure of 100 percent damage would be that level necessary to induce macroscopic instability in the creep specimen. For 6 ksi this value is 4 volume percent, and for 8 and 3.5 ksi it appears to be somewhat lower and higher, respectively.

As noted above the 5 ksi test results were anomalous; a second creep specimen is being tested under identical conditions. The microstructure and testing records are also being examined to determine the origin of the observed behavior.

Radiographs of samples crept at 3.5 and 8.0 ksi are shown in Figure 16. The damage gradient from the rupture surface is clearly evident as is the difference in the level of damage in each specimen. A significant amount of labor is involved in converting the analog record (film) into numerical form. However, OM with stereological analysis provides the same information on a more practical basis. The major advantage of radiography is its examination of a much greater volume of material. High resolution computed tomography and digital radiography are being examined to combine this advantage with that of direct numerical data acquisition.

Grain boundary cavity dimensions were observed subsequent to room temperature fracture by SEM, and Figure 2 shows micrographs

from specimens tested at 3.5 ksi to 1 percent and 100 percent of life and at 6.0 ksi to 60 percent of life. The average cavitiy diameter and areal density of cavities were 3.2 μm and 2.07 x 10^3 mm^{-2} and 12.1 μm and 1.72 x 10^3 mm^{-2} for the 1 and 60 percent of lifetime specimens, respectively, and could not be determined for the 100 percent specimen. When testing on the other interrupted creep deformation specimens is completed, further cavity measurements will be made.

Creep Crack Growth Results

Metallographic examination showed intergranular, planar crack growth for specimens CT2 and CT5 and considerable crack branching for CT3 and CT4. The average cavity diameter and number density were computed from a 1.0 μm diameter area directly ahead of the crack tip and were 23.3 μm and 8.8 x 10^1 mm^{-2} and 19 μm and 1.19 x 10^2 mm^{-2} for CT2 and CT5, respectively. These quantities were measured above and below the average crack plane for sample CT4 because the crack tip was not well-defined. Before the crack branched the average diameter was 25.2 μm and after branching it was 37 μm; the corresponding number densities were 7.6 x 10^1 and 1.03 x 10^2 mm^{-2}, respectively. The crack branching in samples CT3 and CT4 appeared to be due to microcracking resulting from coalescence of large cavities ahead of the crack tip.

Fracture of samples CT2 and CT5 at room temperature (after testing was complete) allowed grain boundary cavity diameters and number densities to be measured as a function of distance ahead

of the crack tip (Figs. 6 and 7). Cavity diameter and number density decreased for both samples as distance increased, and the values were comparable. Average cavity diameters were larger for CT2 than for CT5, but the opposite was true for number density. As indicated above, the final values of C_t were also comparable, lending credence to the view that C_t is linked to the total damage accumulated within the specimen.

Comparison of the C_t values requires calculation of the diffential volume fraction of cavities for each volume element in the sample and summation of these contributions over the entire volume damaged. The local volume fraction is proportional to the average cavity density multiplied by the square of the average cavity diameter. Data from Figs. 6 and 7 are used to form the ratio of crack tip damage for CT2 to that of CT5; this value is 1.5. The ratio of C_t for CT2 to that of CT5 is 1.54 which is in excellent agreement with the damage measurements. Thus C_t appears to be uniquely related to the damage distribution ahead of the crack tip--even under the very different conditions of transient and steady state creep. Crack tip creep damage may be assesed, therefore, by measuring C_t, and this may be the most important reason for the success of C_t in characterizing creep crack growth data under a wide range of conditions ranging from small-scale to extensive (e.g. steady state) creep.

Considerable effort has also been devoted to the development of x-ray techniques for quantitative damage assessment. Sections perpendicular to the crack plane and parallel to the sample face were cut from the center of CT2, CT4 and CT5. Thicknesses were

less than 0.6 mm, and cavities with diameters greater than 10 or 20 μm should be visible in radiographs recorded with synchrotron radiation. The radiographs of the crack growth specimens showed the cracks clearly, but individual cavities could not be resolved. This is not surprising since little cavity coalescence is expected away from the immediate vicinity of the crack tip and the largest cavity dimensions observed on the grain boundaries are at the limits of detection. The cavities are also lens-shaped so that no sharp changes in contrast are expected. Assesment of novel techniques for damage quantification, digital radiography and high resolution computed tomography are currently underway.

Fatigue crack growth results

Characterization in this part of the project has centered on the evolution of time-dependent damage in the presence of the crack. The simple measures of cavitation damage, average cavity diameter, areal density and area fraction, have been applied to specimen surfaces exposed by room temperature fracture of the cracked specimens. Figure 9 shows typical grain boundary cavities produced by fatigue crack propagation.

Figure 10 shows the percentage of cross-sectional area cavitated as a function of distance from the crack tip. With increasing cycle time the cavitated area fraction increases. This is expected because cavity nucleation and growth are diffusion controlled. The observed crack growth rates follow the same trend: increasing cycle times increase crack propagation

rates. Crack growth rates for the slow-fast and fast-slow tests were inversely proportional to the area fraction of boundaries cavitated. Therefore, increasing cavity area fraction does not always correlate with increased crack propagation rate.

The density of cavities versus distance from the crack tip is shown in Figure 11. No trends are apparent with differences in cycle time and/or waveform. The increase in cavity density as the crack tip is approached indicates that nucleation is a continuous process in the damage zone. This increase is less than an order of magnitude: therefore, cavity nucleation is not a rate limiting step and cavity growth is the primary factor which must be considered in modeling.

Figure 12 plots the average cavity diameter as a function of distance from the crack tip. Increasing cycle times produce larger cavity sizes. The resulting longer test times for the slower cycle experiments is expected, therefore, to produce significant cavity growth.

Characterization during the remainder of the current year will focus on how damage evolves in the presence of the crack and on how cavitation damage interacts with the crack to produce higher crack growth rates. Damage evolution studies will center on determining distributions of cavity sizes and spacings at fixed distances from the crack tip (not merely the average quantities). Significant effort will also be expended in the study of the region immemdiately behind the advancing crack tip. The rate of crack propagation is known for the time during which this volume of material was ahead of the crack tip; and this

should lead to an understanding of how damage ahead of the crack tip accelerates the rate of propagation.

2.5 References

1. A. Saxena, S. R. Stock, B. Gieseke and J. T. Staley, Jr., "First Annual Progress Report on a Study of Mechanisms of Time-Dependent Crack Growth at Elevated Temperature", DOE Report DOE/ER/45257-1, Feb. 1987.

2. J. T. Staley, Jr., "Mechanisms of Creep Crack Growth in a Cu-1wt % Sb Alloy", M.S. Thesis, Georgia Institute of Technology, 1988.

3. A. Saxena, "Creep Crack Growth Under Non Steady-state Conditions", in Fracture Mechanics: Seventeenth Conference, ASTM STP905, 1986 pp. 185-201.

4. J. Bassani, D. E. Hawk and A. Saxena, "Evaluation of C_t Parameter for Creep Crack Growth Under Transient Conditions", Third International Symposium on Nonlinear Fracture Mechanics", to appear in ASTM STP.

5. A. Saxena, "Mechanics and Mechanisms of Creep Crack Growth", ASM Seminar on Mechanics and Micromechanisms of Creep Fracture, Oct. 9-10, 1987, Cincinnati, Ohio (in press).

6. A. Saxena and B. Gieseke, "Transients in Elevated Temperature Crack Growth", International Seminar on Mechanics and Mechanisms of Fracture at Elevated Temperature, Dourdan France, Oct. 1987, pp. III/19-III/36.

3. PUBLICATIONS AND PRESENTATIONS

The following papers and thesis were written from the work performed on the subject DOE grant.

List of Papers

1. A. Saxena, "Creep Crack Growth Under Transient Conditions", Materials Science and Engineering (in press).

2. A. Saxena and B. Gieseke, "Transients in Elevated Temperature Crack Growth", in Proceedings of MECAMAT-International Seminar on High Temperature Fracture Mechanisms and Mechanics", Oct. 1987, pp. III/19 - III/36.

3. A. Saxena "Mechanics and Mechanisms of Creep Crack Growth", to appear as book chapter in ASM book entitled "Fracture Mechanics, Microstructure and Mechanisms" (in press).

Thesis Completed

1. J. T. Staley Jr., "Mechanisms of Creep Crack Growth in a Cu-1 wt% Sb Alloy", M.S. Thesis, Georgia Institute of Technology, January 1988.

Presentations

1. A. Saxena, "Crack Growth at Elevated Temperature", ASME Applied Mechanics Meeting, June 15-16, 1987, Cincinnati, Ohio (invited).

2. A. Saxena, "Creep Crack Growth Under Transient conditons," in DOE Workshop on Mechanics and Physics of Crack Growth and Application to Life Prediction", August 4-7, 1987, Keystone, Colo (invited).

3. A. Saxena and S. D. Antolovich, "Mechanics and Mechanisms of Creep Crack Growth", ASM weekend seminar on Fracture Mechanics, Microstructure and Mechanisms, Oct. 9-10, 1987, Cincinnati, Ohio (invited).

4. A. Saxena and B. Gieseke, "Transients in Elevated Temperature Crack Growth", International Seminar on Mechanics and Mechanisms of High Temperature Fracture", Oct. 13-15, Dourdan, France (invited).

5. B. Gieseke and A. Saxena, "Mechanisms of Creep-Fatigue Crack Growth Interactions in 1wt % Sb-copper", TMS-AIME Meeting, Phoenix Arizona, Jan. 26-28, 1988.

Papers in Preparation

1. J. T. Staley, A. Saxena, K. Banerji and B. Gieseke, "Mechanisms of Creep Crack Growth in 1 wt % Antimony Copper" to be submitted to Acta Metallurgica.

2. S. R. Stock, R. Lee, J. T. Staley and A. Saxena, "Quantitative Characterization of Damage During Creep Crack Growth", to be submitted to Acta Metallurgica.

3. B. Gieseke and A. Saxena, "Crack Growth Under Creep-Fatigue Conditions", Seventh International Congress on Fracture, ICF-7, Houston 1989 (invited).

4. A. Saxena and K. Banerji, "Recent Progress in Elevated Growth Models for Remaining Life Prediction", invited keynote paper for the Seventh International Congress on Fracture, ICF-7, Houston 1989.

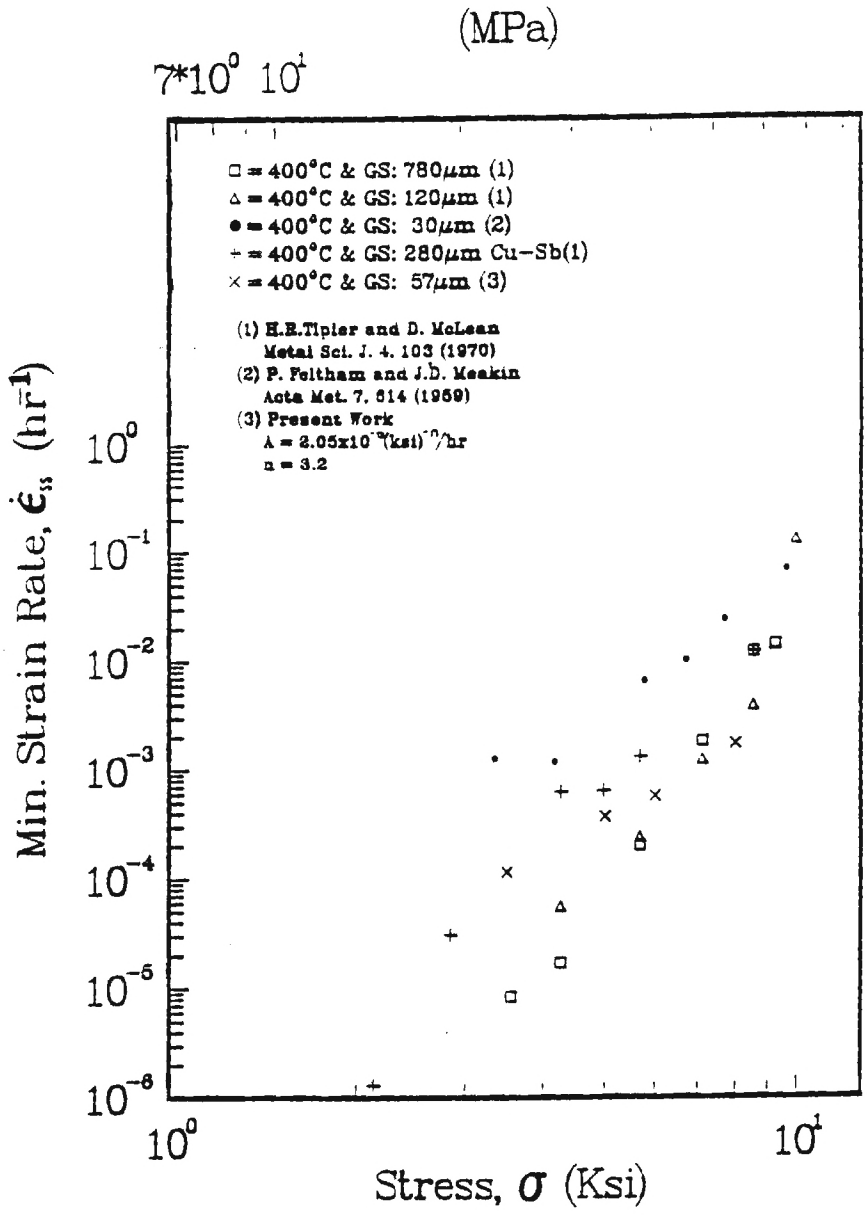

Fig. 1 Minimum (or steady-state) strain rate vs. stress compared with other data on Cu and Cu-Sb.

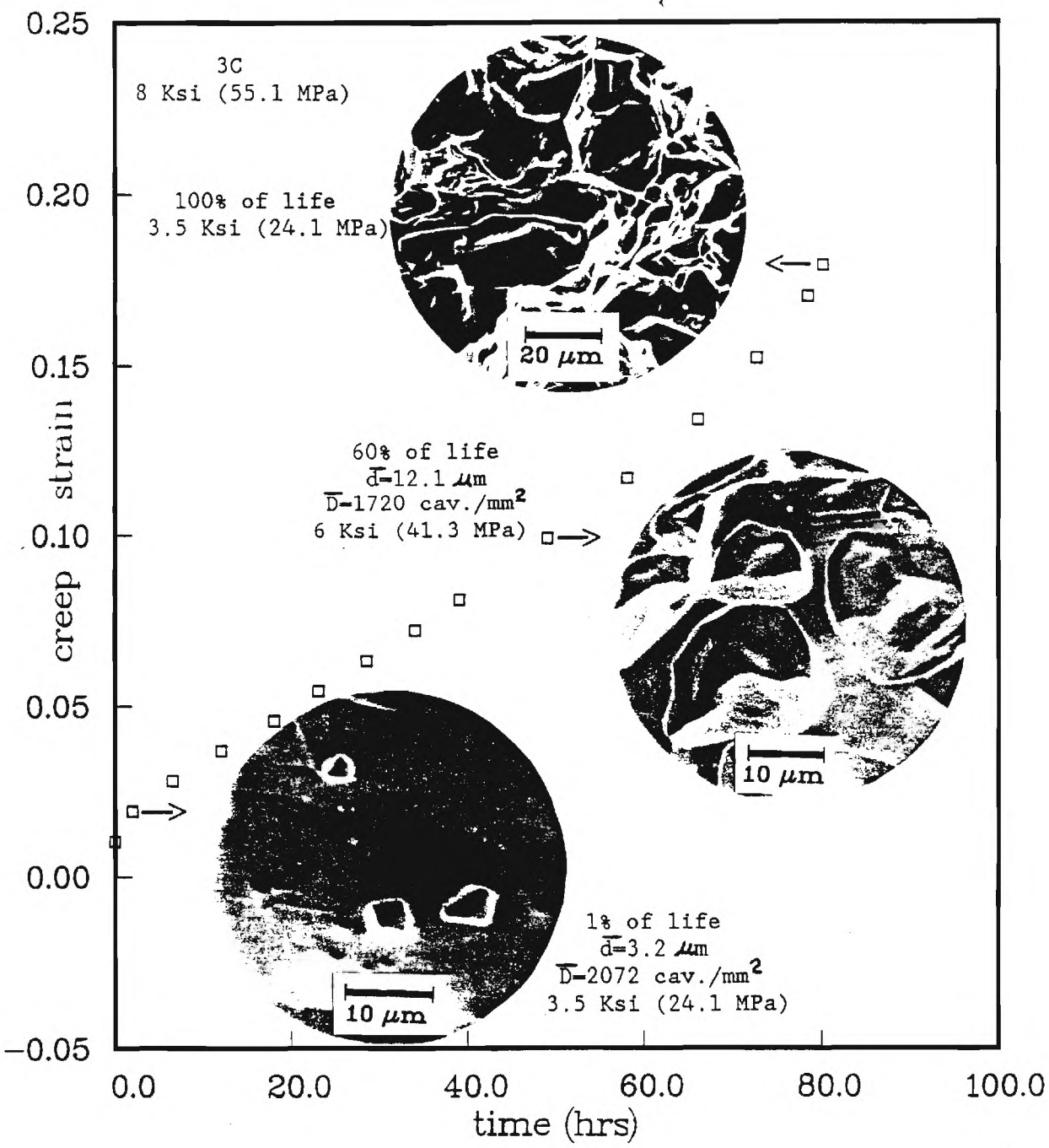

Figure 2 : A representation of cavity growth history in the Cu-1wt.% Sb alloy. $\bar{d}$ is the average cavity diameter and $\bar{D}$ is the average number of cavities per grain boundary facet area.

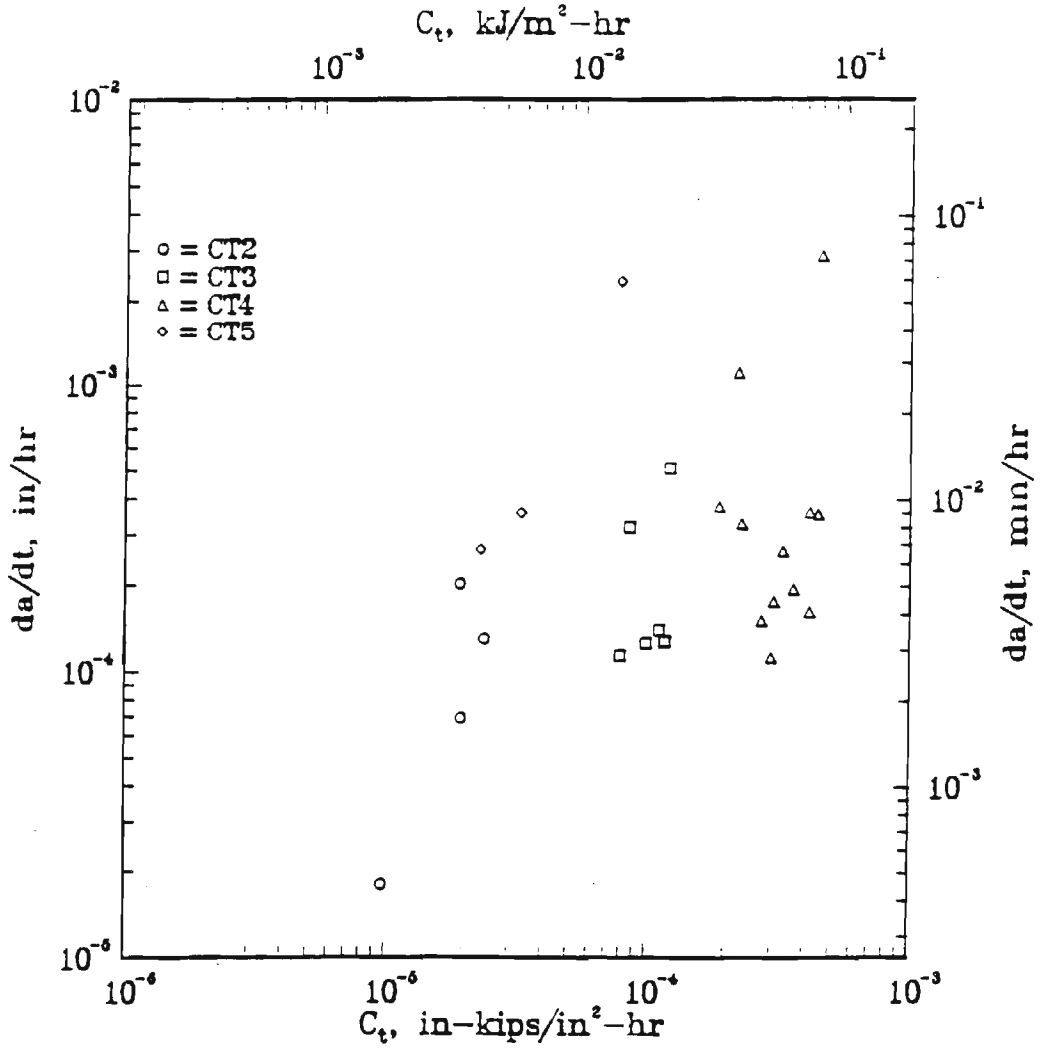

Fig. 3 Creep crack growth behavior of specimens CT2-5.

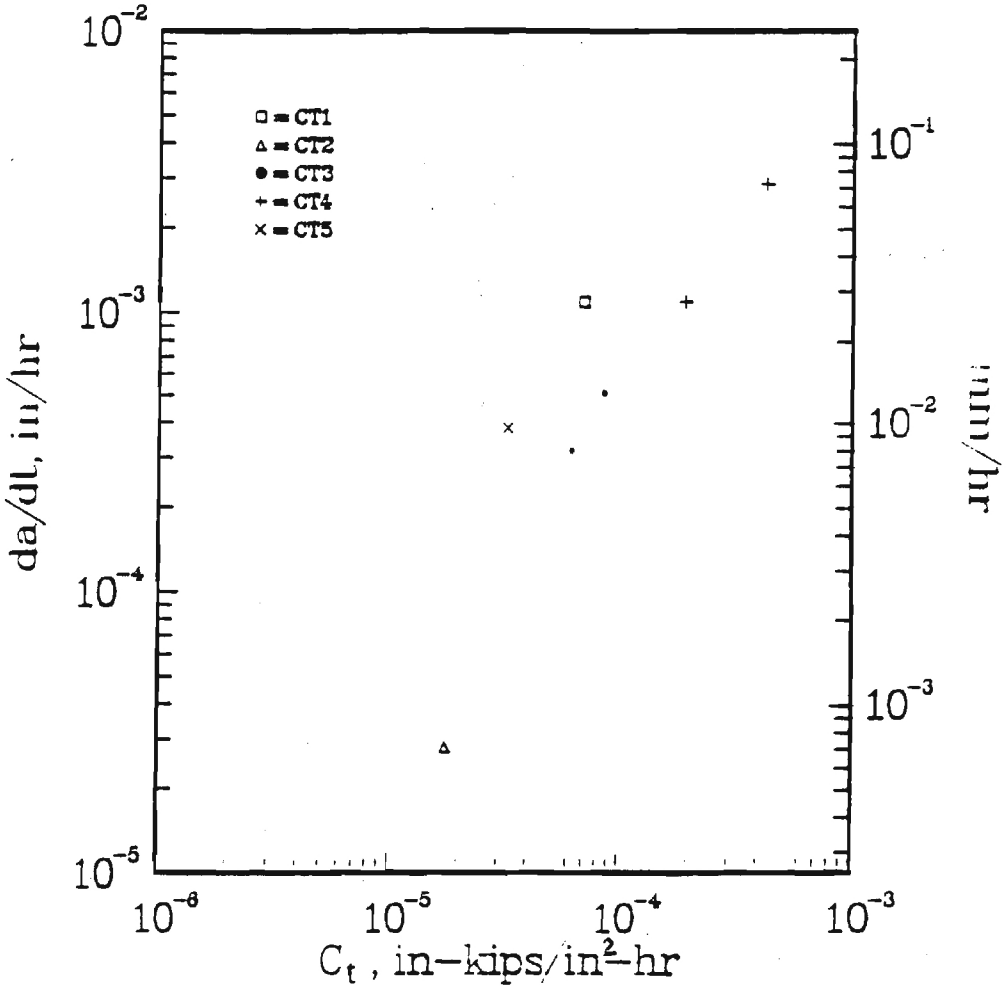

Fig. 4 Plot of da/dt vs. C_t containing only appropriate, reliable data.

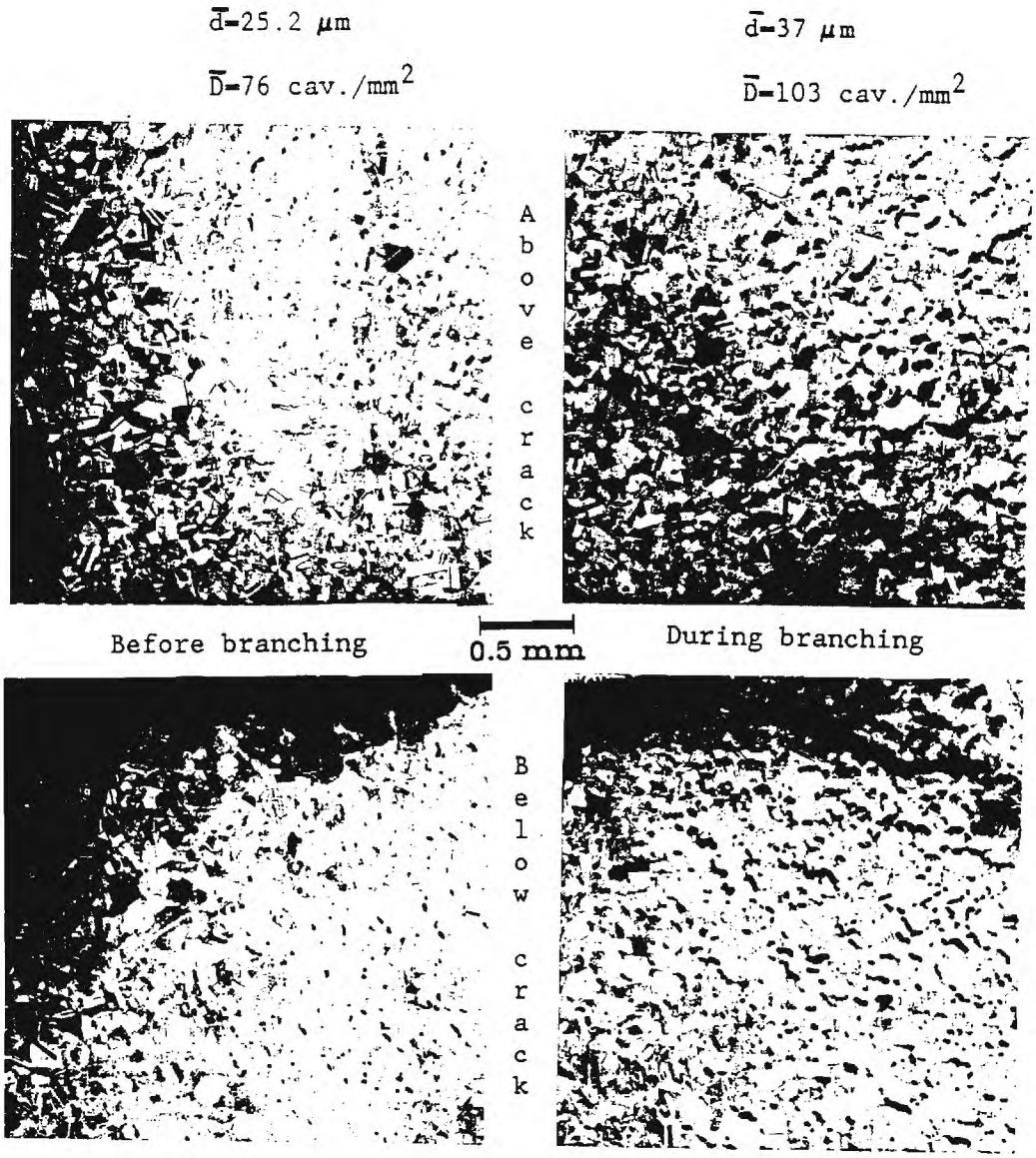

Figure 5 : Comparison of crack area cavitation prior to and during crack branching.

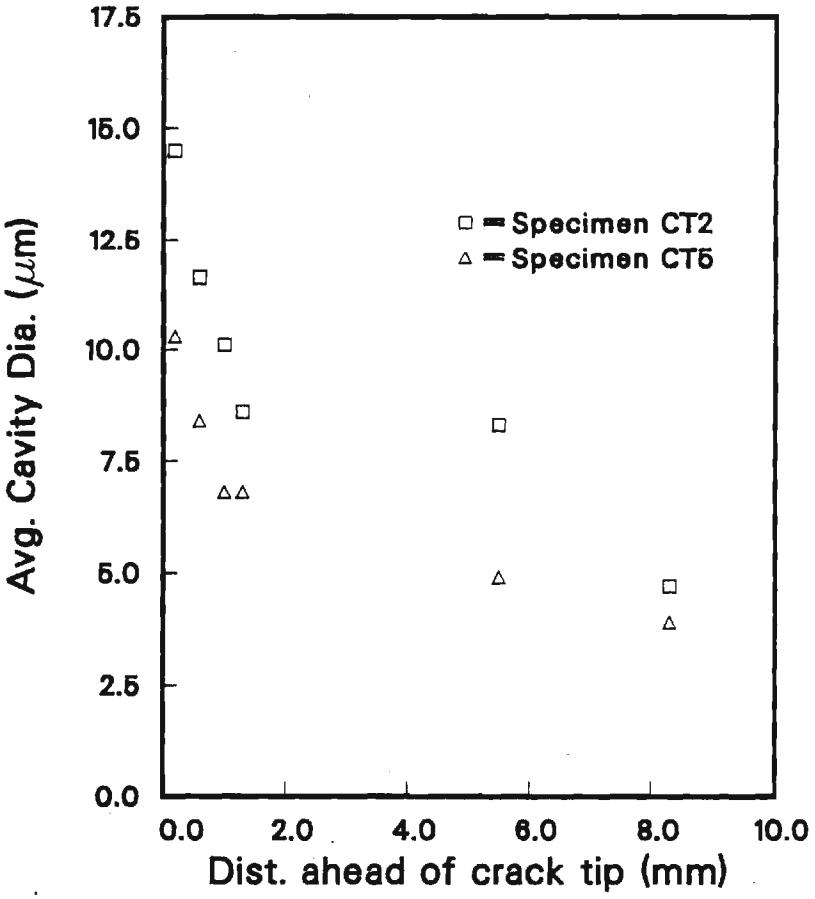

Fig. 6 Average cavity diameter vs. distance ahead of the crack tip in CT2 and CT5.

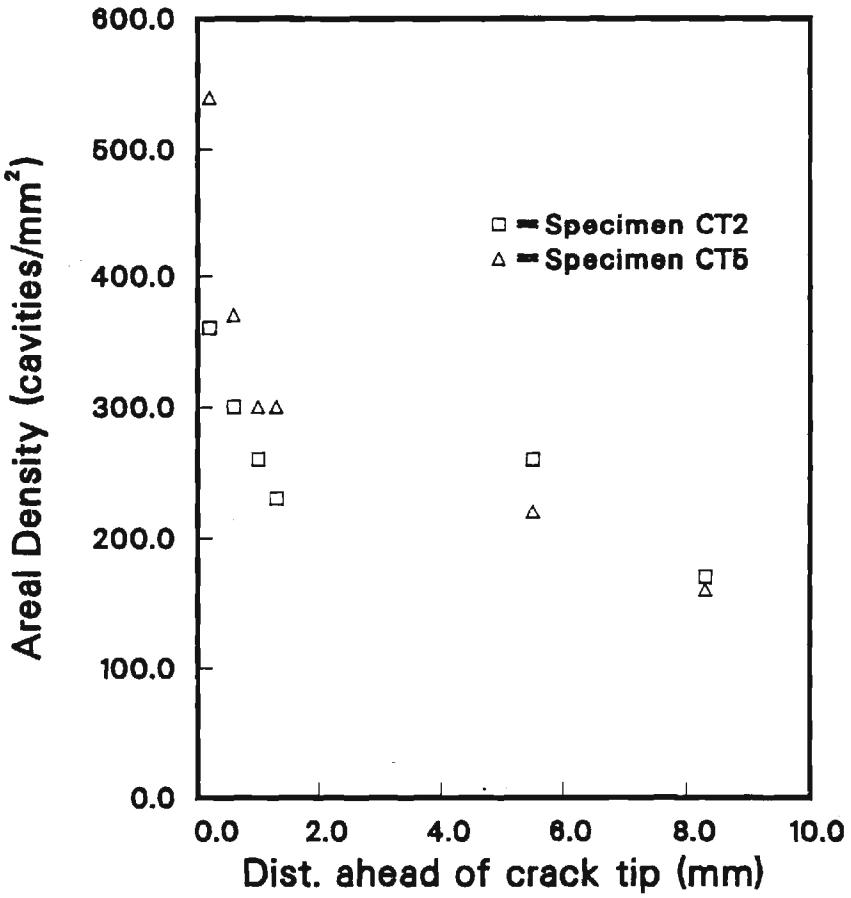

Fig. 7 Average cavity density vs. distance ahead of the crack tip in CT2 and CT5.

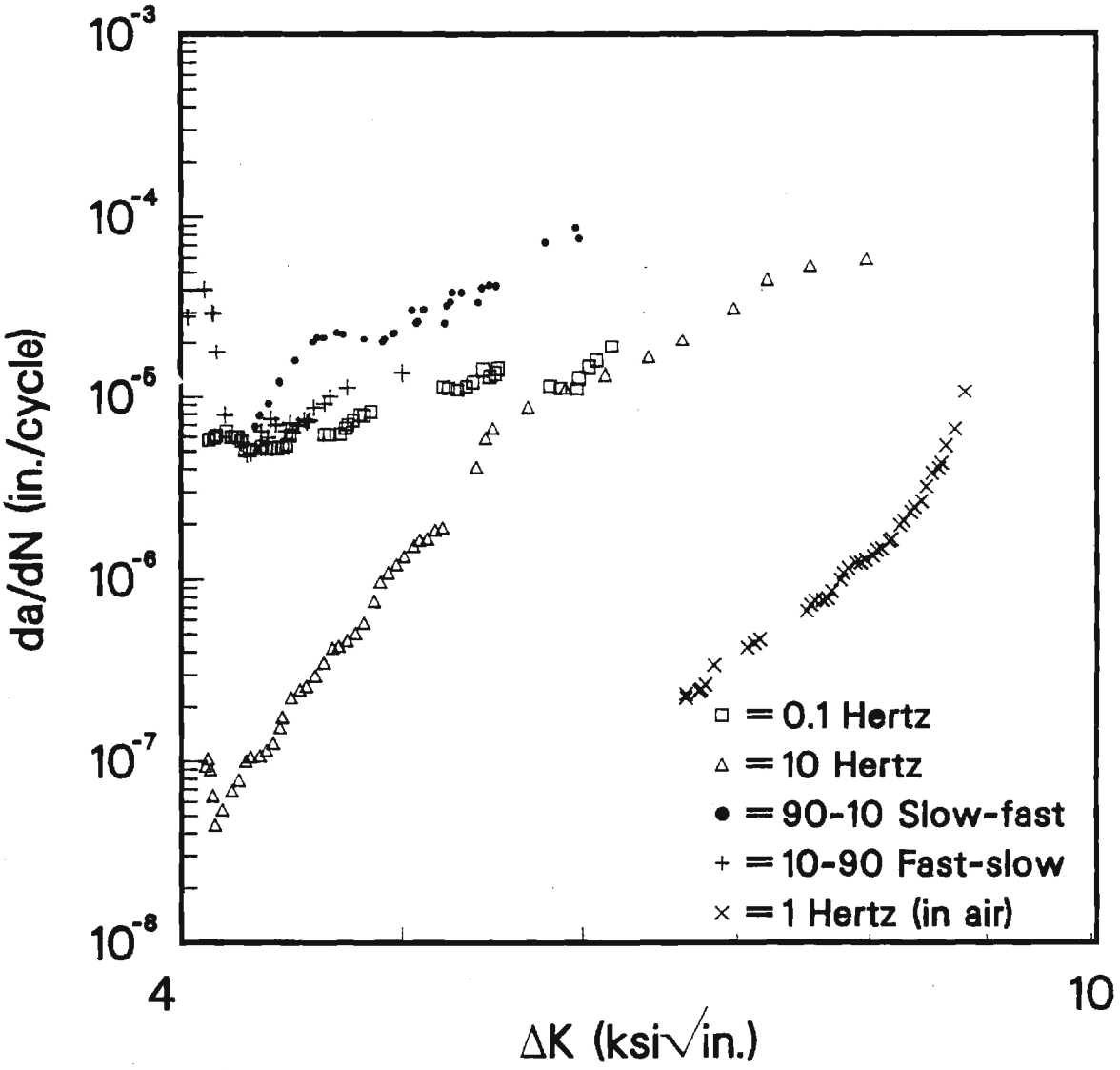

Fig. 8 Fatigue crack growth rate in 1 wt% Sb-Cu at 400°C.

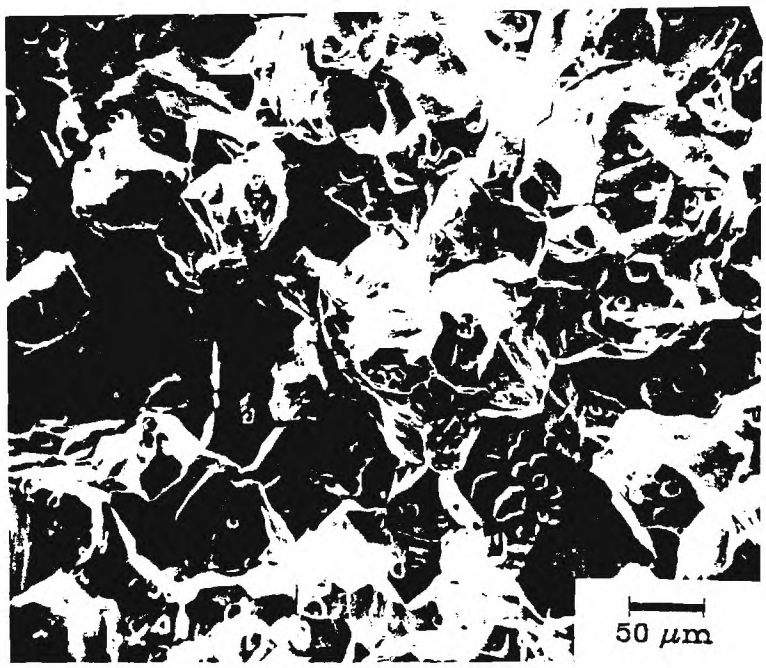

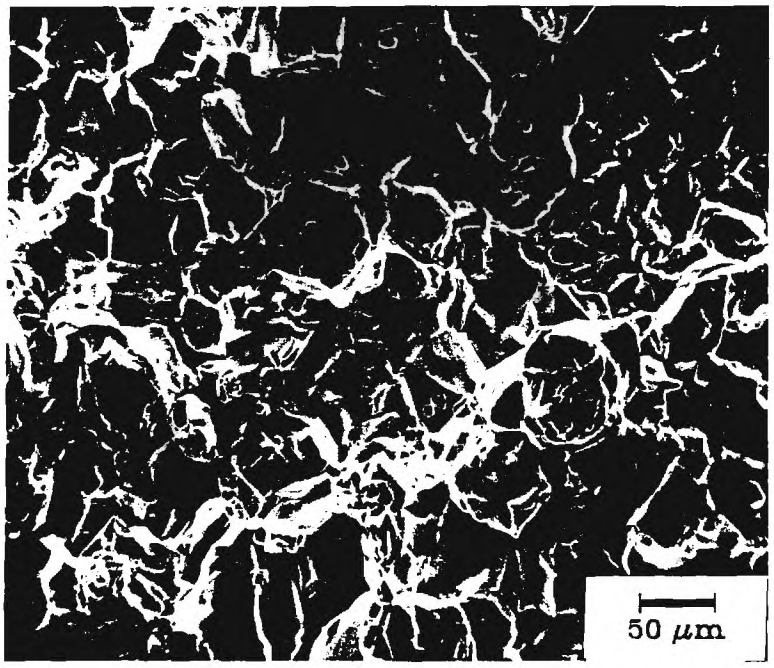

Fig. 9 Cavities 2.5mm ahead of the crack tip in specimens subjected to unbalanced triangular waveform (a) fas-slow and (b) slow-fast.

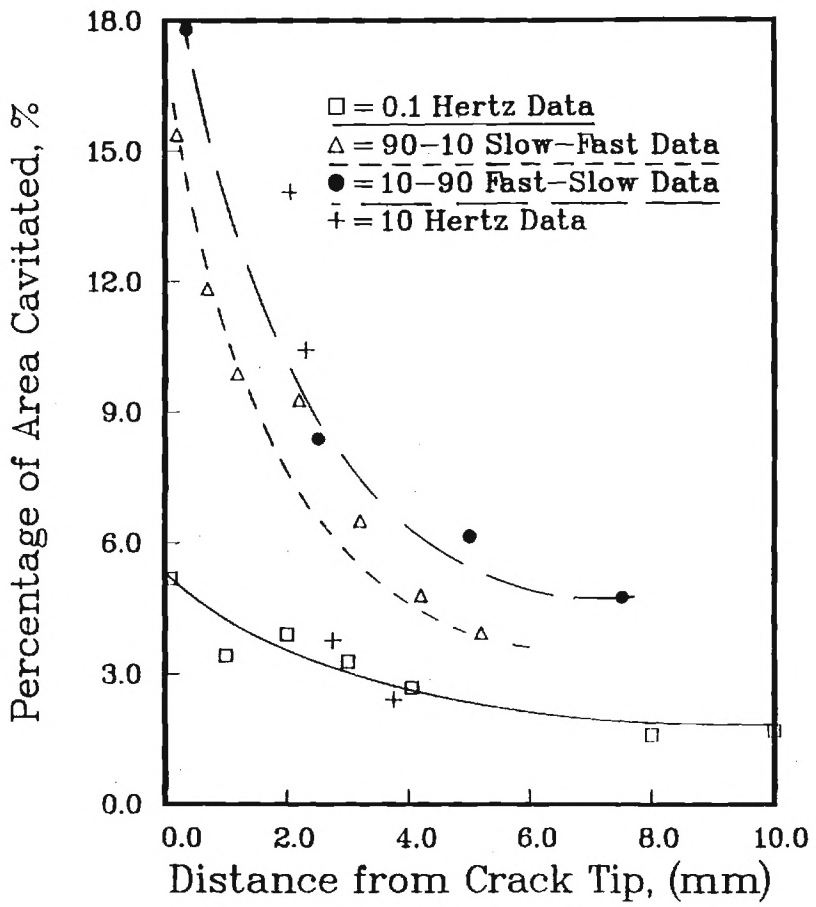

Fig. 10 Percent area cavitated as a function of distance from crack tip for various loading waveforms for 1 wt% Sb-Cu alloy at 400°C.

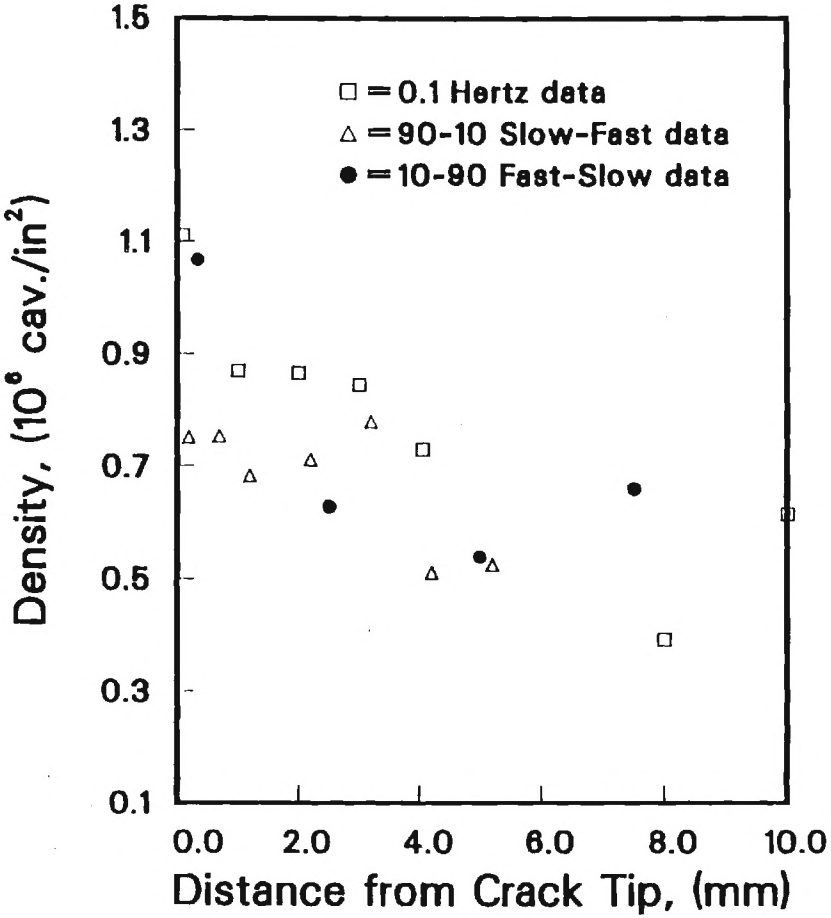

Fig. 11 Cavity density as a function of distance from the crack tip for various loading waveforms.

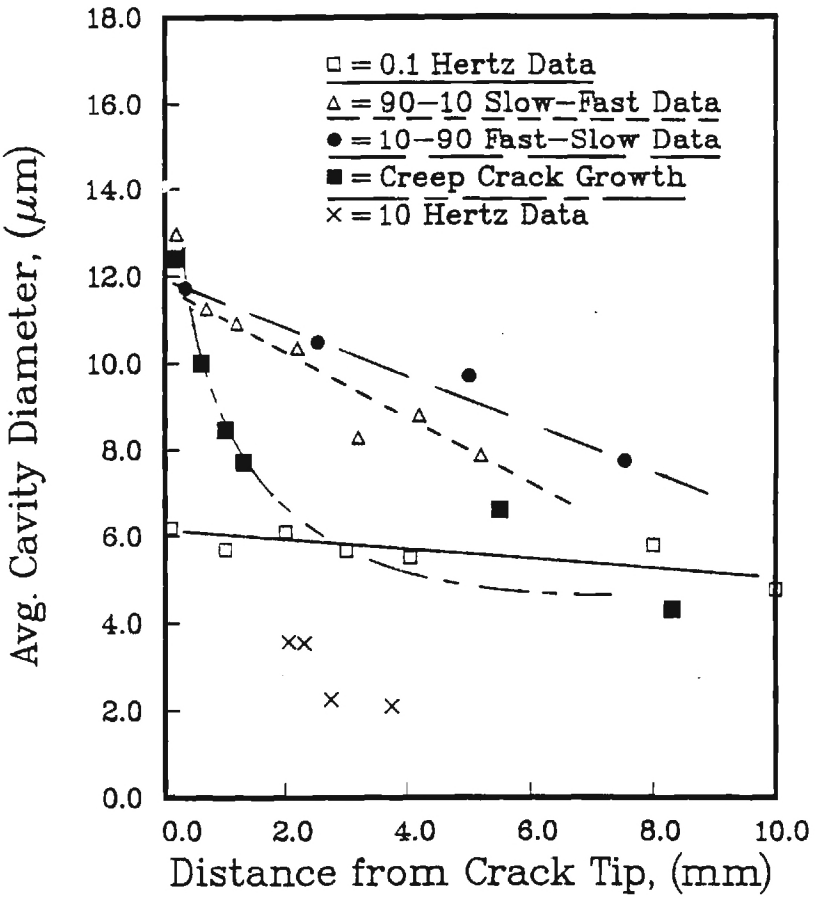

Figure 12 Cavity size as a function of distance from the crack tip for various loading waveforms for 1wt% Sb-Cu alloy at 400°C.

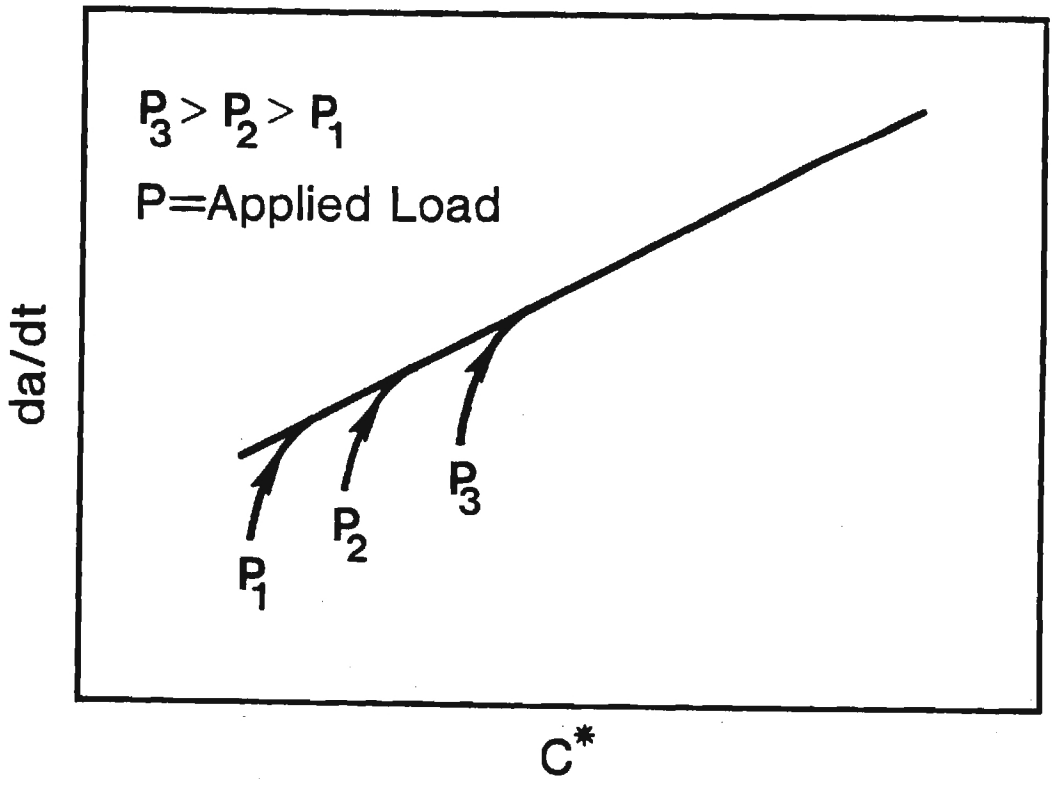

Fig. 13 Schematic illustration of the crack growth transients during the early portion of creep crack growth test.

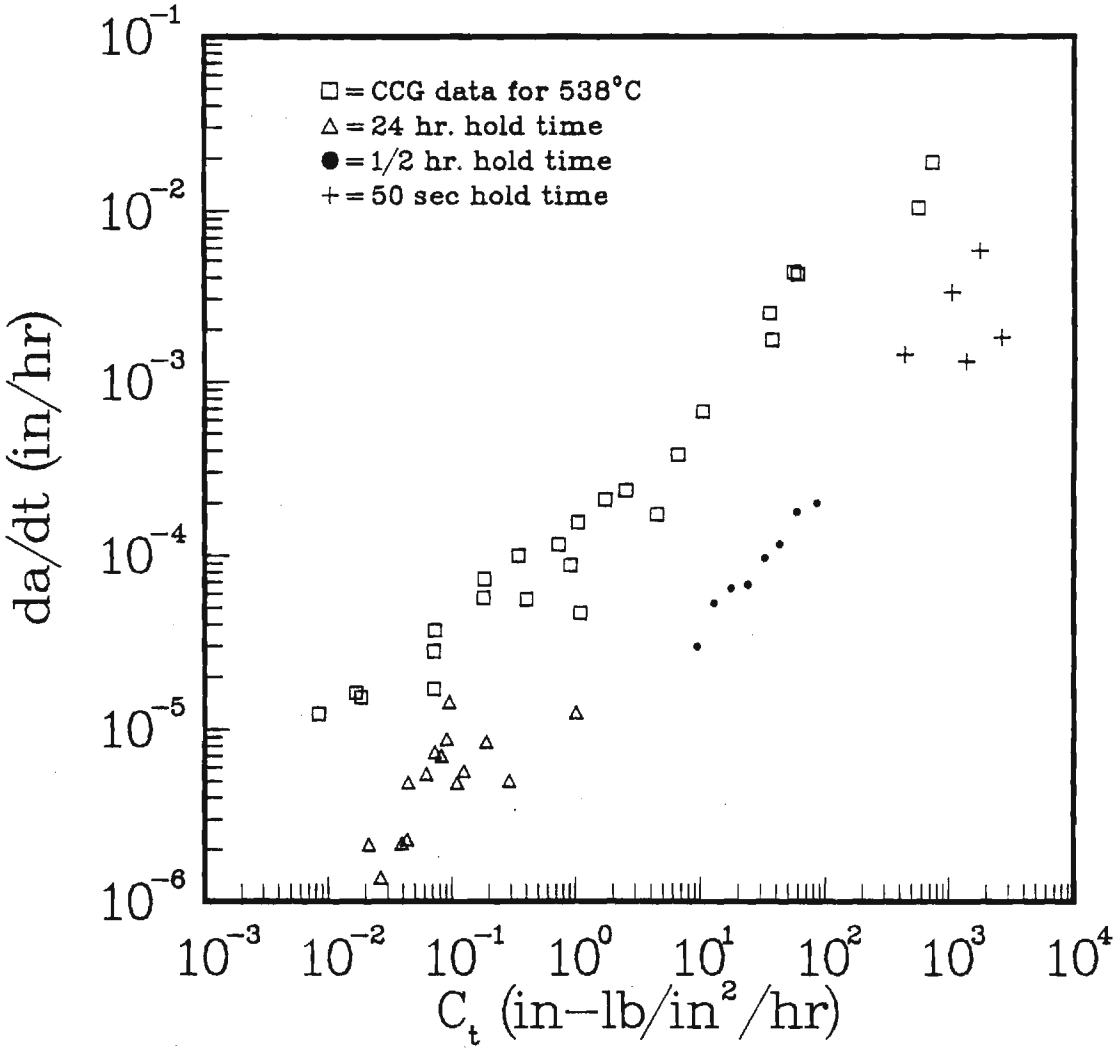

Fig. 14 Creep and creep-fatigue (trapezoidal waveforms) crack growth rates as correlated with C_t parameter.

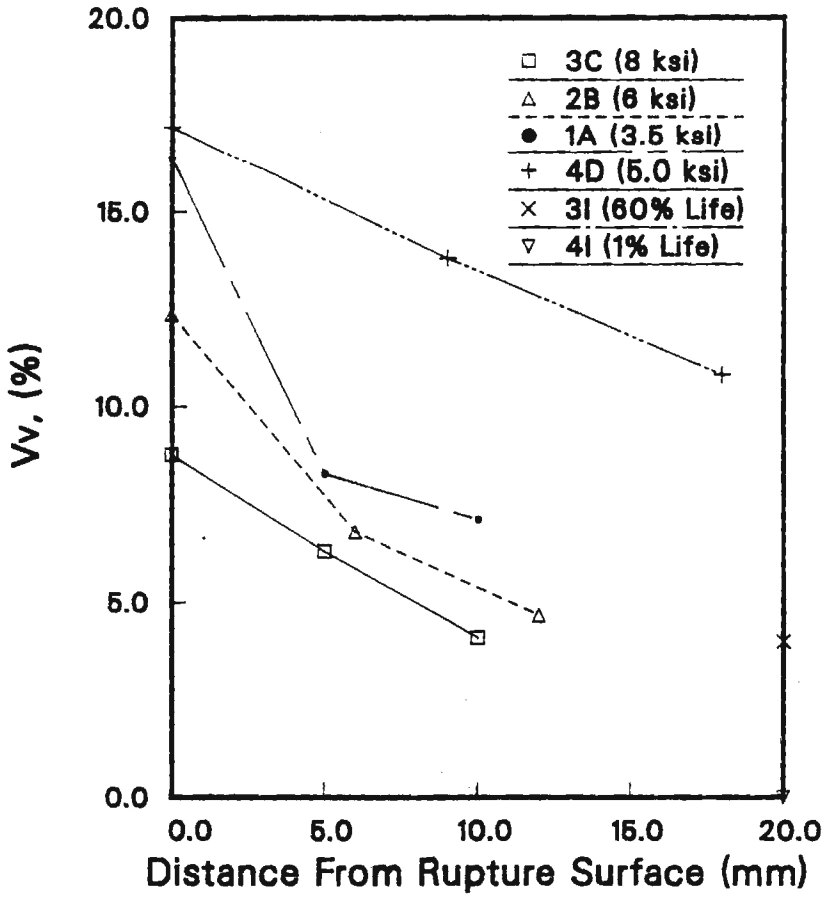

Fig. 15 Volume fraction of damage as a function of distance from rupture surface for various creep specimens tested.

SAMPLE 3C TENSILE CREEP TO RUPTURE, AT 8.0 KSI

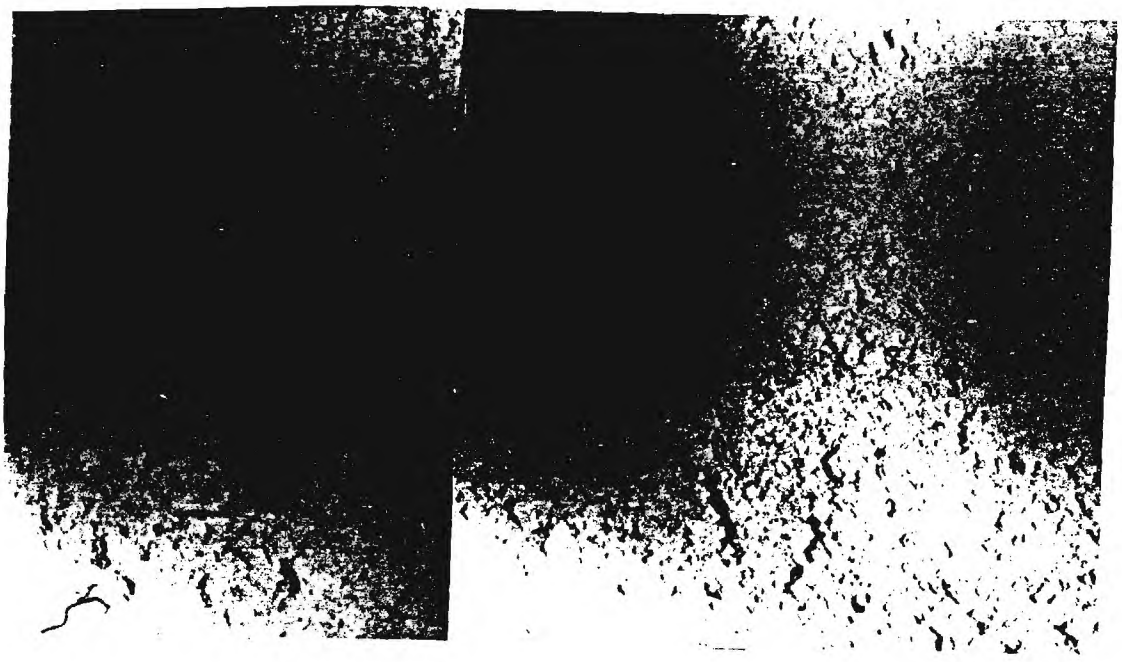

0.4 mm nominal sample thickness
(radiograph #3C-2)

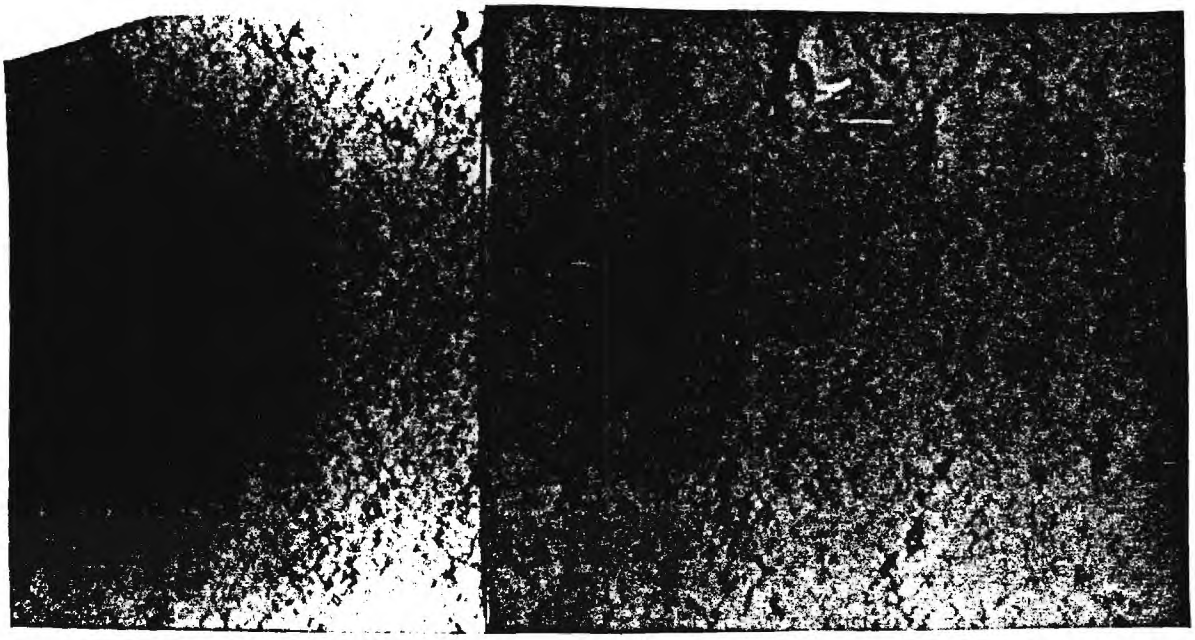

1.0 mm nomial sample thickness
(radiograph #3C-8)

Fig. 16 Radiographs of tested creep specimens

Georgia Tech

Office of Grants and Contracts Accounting

Georgia Institute of Technology
Hinman Building
Atlanta, Georgia 30332-0259
404•894•4624; 2629
Fax: 404•894•5519

February 14, 1990

Ms. Melissa Y. Johnson, Contract Specialist
U. S. Department of Energy-Oak Ridge Operations
Procurement and Contracts Division
P. O. Box 2001
Oak Ridge, TN 37831-8758

REFERENCE: Grant #DE-FG05-86ER45257

Dear Ms. Johnson,

Enclosed in triplicate is the Financial Status Report (SF-269) for Grant No. DE-FG05-86ER45257 covering the period July 1, 1988 through August 31, 1989.

If you should have questions or need additional information, please contact Geraldine Reese of this office or me at (404) 894-2629.

Sincerely,

David V. Welch
Director

DVW/GMR/djt

Enclosures

cc: Dr. S. D. Antolovich, Materials Eng 0245
Dr. Ashok Saxena, Materials Eng 0245
Ms. Mary Wolfe, OCA/CSD 0420
File E-18-625/R6169-0A0

FINANCIAL STATUS REPORT

(Short Form)

(Follow instructions on the back)

1. Federal Agency and Organizational Element to Which Report is Submitted	2. Federal Grant or Other Identifying Number Assigned By Federal Agency	OMB Approval No.	Page	of
U. S. Department of Energy	DE-FG05-86ER45257	0348-0039	1	1 pages

3. Recipient Organization (Name and complete address, including ZIP code)

GEORGIA TECH RESEARCH CORPORATION
P. O. BOX 100117
ATLANTA, GA 30384

4. Employer Identification Number	5. Recipient Account Number or Identifying Number	6. Final Report	7. Basis
58-0603136	E-18-625/R6169-0A0	☐ Yes ☒ No	☒ Cash ☐ Accrual

8. Funding/Grant Period (See Instructions) From: (Month, Day, Year)	To: (Month, Day, Year)	9. Period Covered by this Report From: (Month, Day, Year)	To: (Month, Day, Year)
July 1, 1986	August 31, 1989	July 1, 1988	August 31, 1989

10. Transactions:	I Previously Reported	II This Period	III Cumulative
a. Total outlays	206,763.70	128,135.30	334,899.00
b. Recipient share of outlays	-0-	-0-	-0-
c. Federal share of outlays	206,763.70	128,135.30	334,899.00
d. Total unliquidated obligations			-0-
e. Recipient share of unliquidated obligations			-0-
f. Federal share of unliquidated obligations			334,899.00
g. Total Federal share *(Sum of lines c and f)*			334,899.00
h. Total Federal funds authorized for this funding period			334,899.00
i. Unobligated balance of Federal funds *(Line h minus line g)*			-0-

11. Indirect Expense

a. Type of Rate *(Place "X" in appropriate box)* ☐ Provisional ☐ Predetermined ☐ Final ☒ Fixed

b. Rate	c. Base	d. Total Amount	e. Federal Share
SEE BELOW	MTDC	$47,590.65	$47,590.65

12. *Remarks: Attach any explanations deemed necessary or information required by Federal sponsoring agency in compliance with governing legislation.*

GEORGIA TECH FISCAL YEAR ENDS JUNE 30

Questions pertaining to this report should be directed to: Geraldine Reese (404) 894-2629

13. Certification: **I certify to the best of my knowledge and belief that this report is correct and complete and that all outlays and unliquidated obligations are for the purposes set forth in the award documents.**

Typed or Printed Name and Title	Telephone (Area code, number and extension)
David V. Welch, Director, Grants and Contracts Accounting	(404) 894-2629
Signature of Authorized Certifying Official	**Date Report Submitted**
	February 14, 1990

Previous Editions not Usable	Direct Costs	Indirect Costs
FY'87 @ 63.5%	$60,548.25	$38,448.13
FY'88 @ 60.0%	68,202.95	40,921.75
FY'89 @ 60.0%	76,055.61	45,633.36
FY'90 @ 62.5%	3,131.66	1,957.29

Standard Form 269A (REV 4-88)
Prescribed by OMB Circulars A-102 and A-110

FORM DOE 538
(Rev. 10-80)

U.S. DEPARTMENT OF ENERGY

NOTICE OF ENERGY RD&D PROJECT

APPROVED FOR USE BY
SMITHSONIAN SCIENCE INFORMATION EXCHANGE

OMB Approval
No. 1901-0021

1. Descriptive title of work: A study of Mechanisms of Time Dependent Crack Growth at Elevated Temperature

2. Performing organization control number: _____
Work status: ☐ New ☒ Continuing ☐ Terminated

3. Contract or grant number: DE-FG05-86ER45257

4. Contractor's principal investigator/project manager and address where work is performed
A. Name (Last, First, MI): Saxena, Ashok
B. Phone: FTS- (404) 894-2888
C. Research organization business address: Street: School of Materials Eng. (0245) Com.-
City: Atlanta State: GA Zip: 30332

5. A. Name of performing organization: Georgia Institute of Technology (Organization) School of Materials Eng. (Department)

B. Mailing address (If different from 4C)

C. Circle only one code for TYPE OF ORGANIZATION PERFORMING R&D (See instructions):
(CU) FF IN NP ST TA US XX EG

D. Location where the work is being performed
Georgia Institute of Technology

E. Country sponsoring research
USA

6. Supporting organization
A. Program division or office (Full name): Office of Basic Energy Sciences, Materials Div. Department of Energy
B. Technical monitor (Last, First, MI): Darby, Joseph B. C. Phone: FTS- (301) 353-3428
D. Address (If different from DOE Hqs.) ER-131, U.S. Department of Energy Germantown, MD 20874 Com.-
E. Administrative monitor (Last, First, MI): Clark, Marlena

7. Project schedule
A. Start date: 7-86 (Month) (Year) B. Expected completion date: 6-89 (Month) (Year)

8. Funding in thousands of dollars (Funds represent budget obligations for operating and capital equipment)

	Funding organization(s)	Current FY 88	Next FY 89
A.	Basic Energy Sciences, DOE	$109, 537	$127,723
B.			
C.			

D. For DOE projects, enter budgeting and reporting classification code: _____
E. Interagency agreement (Specify funding agency): _____
F. Agency in-house effort (Check if applicable) ☐ _____
G. EPA "pass-thru" funding (Check if applicable) ☐ _____

Note: Funding Section utilization is optional on Federal Financial Assistance Programs: grants, direct payments, cooperative agreements, loan guarantees, and other related programs.

9. Descriptive summary of work (Limit to 200 words. Include objective, approach, results to date and their significance, and expected product. Quantify where possible).

The objective of this study is to conduct creep and creep fatigue crack growth tests and to characterize the crack tip damage mechanisms in a model material (1 percent sb-copper) which is known to cavitate at the grain boundaries under creep deformation. These data will be used to develop mechainstic models for cumulative crack tip damage under complex loading conditions at elevated temperature. Characterization of creep damage in the crack tip region will be done by scanning electron microscope and advanced radiography techniques such as synchrotron radiation.

10. List the five most descriptive publications in the last year that are available to the public which have resulted from the project (Please give a complete bibliographic citation. Use additional sheets if necessary).

1. A Saxena and B. Gieseke, "Transients in Elevated Temperature Crack Growth", International Seminar on HIgh Temperature Fracture Mechanisms and Mechanics (Conference Proceedings), Oct. 13-15, 1987, Dourdan, France

2. A. Saxena, "Creep Crack Growth Under Transient Conditions", in press, Journal of Materials Science and Engineering

11. General technology categories (Enter applicable code of codes from instructions).

A 1	A 2	A 3	E 3									

12. Type of research activity (Check applicable activities)

A. [x]	Basic research	H. [x]	Mathematical model development
B. [x]	Applied research	I. [x]	Data analysis/assessments
C. [ ]	Laboratory scale R&D	J. [ ]	Information systems management
D. [ ]	Technology development	K. [ ]	Policy analysis
E. [ ]	Field study	L. [ ]	Socioeconomic
F. [ ]	Pilot plant scale R&D	M. [ ]	Other (Specify)_____
G. [ ]	Full scale demonstration	N. [ ]	Not applicable

13. keywords (Please list 5 keywords). cooper, creep, fatigue, crack, cavitation

14. Is this research project solely an ANALYTICAL/PAPER STUDY? (Non-experimental, paper and pencil, computer analysis, etc.) YES _____ NO x

15. Respondent's Name: A. Saxena Phone No.: (404) 894-288 Date: 8/28/87

Street: School of Materials Engineering
Georgia Institute of Tech.
City: Atlanta State: GA Zip: 30332

FRACTURE AND FATIGUE RESEARCH LABORATORY
Georgia Institute of Technology
A UNIT OF THE UNIVERSITY SYSTEM OF GEORGIA
ATLANTA, GEORGIA 30332-0102
404/894-2888

June 2, 1987

Ms. Marlena Clark
Contracts Management Branch
U.S. Department of Energy
Oak Ridge Operations
P.O. Box E
Oak Ridge, TN 37831

Subject: DOE Grant No. DE/FG05-86ER-45257

Dear Ms. Clark:

Enclosed are three copes of a conference paper prepared for submission to the International Seminar on High Temperature Fracture Mechanisms and Mechanics for your approval.

Sincerely,

Ashok Saxena
Professor of Materials Engineering

AS/ptl

cc: Dr. J.B. Darby
Office of Basic Energy Sciences

DOE F 1332.16 (10-84)
(Formerly RA-427)

OMB Approval
No. 1910-1400

U. S. DEPARTMENT OF ENERGY

UNIVERSITY CONTRACTOR, GRANTEE, AND COOPERATIVE AGREEMENT RECOMMENDATIONS FOR ANNOUNCEMENT AND DISTRIBUTION OF DOCUMENTS

See Instructions on Reverse Side

1. DOE Report No. DOE/ER/45257-2

2. DOE Contract No. DE-FG05-86ER-45257

3. Title: Transients in Elevated Temperature Crack Growth

4. Type of Document ("x" one)
- ☐ a. Scientific and technical report
- ☒ b. Conference paper:
  - Title of conference: International Seminar on High Temperature Fracture Mechanisms and Mechanics
  - Date of conference: October 13-15, 1987
  - Exact location of conference: Dourdan, France
  - Sponsoring organization: CNRS-GRECO and Atomic Energy Commission, France
- ☐ c. Other (Specify) _____

5. Recommended Announcement and Distribution ("x" one)
- ☒ a. Unrestricted unlimited distribution.
- ☐ b. Make available only within DOE and to DOE contractors and other U. S. Government agencies and their contractors.
- ☐ c. Other (Specify) _____

6. Reason for Recommended Restrictions

7. Patent and Copyright Information:
Does this information product disclose any new equipment, process, or material? ☒ No ☐ Yes If so, identify page nos. _____
Has an invention disclosure been submitted to DOE covering any aspect of this information product? ☐ No ☐ Yes
If so, identify the DOE (or other) disclosure number and to whom the disclosure was submitted.
Are there any patent-related objections to the release of this information product? ☐ No ☐ Yes If so, state these objections.
Does this information product contain copyrighted material? ☐ No ☐ Yes
If so, identify the page numbers _____ and attach the license or other authority for the government to reproduce.

8. Submitted by — Name and Position (Please print or type)
A. Saxena, Professor of Materials Engineering

Organization
Georgia Institute of Technology

Signature	Phone	Date
	(404) 894-2888	5/28/87

FOR DOE OR OTHER AUTHORIZED USE ONLY

9. Patent Clearance ("x" one)
- ☐ a. DOE patent clearance has been granted by responsible DOE patent group.
- ☐ b. Report has been sent to responsible DOE patent group for clearance.

TRANSIENTS IN ELEVATED TEMPERATURE CRACK GROWTH

Ashok Saxena and Brian Gieseke

Fracture and Fatigue Research Laboratory
School of Materials Engineering
Georgia Institute of Technology
Atlanta, GA 30332-0245

Sponsor:

Basic Energy Sciences
Department of Energy
Grant No. DE/FG05-86ER-45257

DOE Report No. DOE/ER/45257-2, May 1987

Paper to be presented at the "International Seminar on High Temperature Fracture Mechanisms and Mechanics," Dourdan, France, Oct. 13-15, 1987.

Final Report
Proj. # E-18-625

A. Saxena
Mat. Eng.

Mechanisms of Time-Dependent Crack Growth at Elevated Temperature

Final Project Report

Submitted to
Basic Energy Sciences Division
Department of Energy

DOE Grant No: DE-FG05-86ER45257
Period Covered: 7/1/86 to 8/31/89

Submitted by:

Ashok Saxena, Professor

Stuart R. Stock, Associate Professor

Contributors:
J.T. Staley, R.H. Norris, B. Gieseke, A. Guvenilir

School of Materials Engineering
Georgia Institute of Technology
Atlanta, Georgia 30332-0245

April 15, 1990

1. INTRODUCTION AND SUMMARY

The prediction of design life of components subjected to elevated temperatures in energy conversion machinery require accurate methods for predicting crack growth behavior in the presence of time-dependent creep strains. Significant progress has been made in extending the linear-elastic and elastic fracture mechanics concepts into the creep regime. Thus, the use of fracture mechanics for predicting the crack growth life of elevated temperature components is a viable approach [1,2]. However, serious deficiencies exist in the understanding of the damage mechanisms that lead to time-dependent crack growth. Specifically, the interactions between creep and fatigue damage mechanisms for slow frequency cyclic loading are not well understood. Therefore, cumulative damage laws for creep-fatigue loading based on physical damage mechanisms are non-existent.

The objective of this three year study was to conduct creep and creep-fatigue crack growth experiments and to characterize the crack tip damage mechanisms in a model material (1% Sb-Cu) which is known to cavitate at the grain boundaries under creep deformation. These data and observations were to be used to develop mechanistic models for predicting crack tip damage and the resultant crack growth rates under complex loading conditions at elevated temperatures. The results of this program were to be integrated into Electric Power Research Institute (EPRI) sponsored studies at Georgia Tech. for characterizing the creep-fatigue crack growth behavior of Cr-Mo-V steels. Various new and established

techniques for detecting crack tip cavitation damage including electron metallography, synchrotron x-ray tomography, digital microradiography and small angle neutron scattering (SANS) were also evaluated. The study led to the following important conclusions.

- In the presence of large scale cavitation damage and crack branching, time rate of creep crack growth (da/dt) does not correlate with C_t or with C^*. On the other hand, when the cavitation damage is constrained, da/dt is uniquely characterized by C_t.
- Area fraction of grain boundary cavitated, A_c, appears to be the single damage parameter for characterizing the extent of cavitation damage ahead of crack tips. The distribution of A_c ahead of the crack tip is a complex function of loading wave form and cycle time.
- The use of C_t-parameter was extended for characterizing the creep-fatigue crack growth behavior. It was shown that C_t is suitable for characterizing crack growth rate in the presence of different types of deformation transients.
- It was observed that in materials which are prone to rapid cavity nucleation, the creep cracks grow faster initially and then reach a steady-state during which their growth rate is uniquely characterized by C_t.
- The percent creep life exhausted was shown to correlate with the average cavity diameter and also with fraction

of grain boundary area occupied by cavities.

- Synchrotron x-ray tomographic microscopy (XTM) was successfully demonstrated for imaging individual cavities in the 1 percent Sb-Cu material.
- The above concepts have been incorporated in methodologies for remaining life prediction of elevated temperature power-plant components. Specifically, $(C_t)_{avg}$ has been used to correlate creep-fatigue crack growth behavior in Cr-Mo and Cr-Mo-V steel and in weldments.

In Section 2 of this report, the important results from the program are presented. Section 3 of the report contains a list of the publications and presentations from the work performed under the grant and the status of the various students funded under this grant.

2. HIGHLIGHTS OF ACCOMPLISHMENTS

The creep and creep-fatigue crack growth experiments were conducted on a copper alloy containing 1 weight-percent antimony. The segregation of antimony to the grain boundaries embrittles the boundaries. Therefore, the room temperature fracture in this material is one hundred percent intergrannular revealing the cavitation damage on the grain boundary facets. Thus, this alloy was ideally suited for studying the time-dependent damage accumulation at crack tips subjected to creep and creep-fatigue loading. The model alloy was specially produced at the Oak Ridge

National Laboratory and was supplied to Georgia Tech in the form of an extruded rectangular bar which was 2-3/4 in x 2 in cross-section. The chemical composition and the tensile and creep behavior of the material is summarized in reference [3] attached in the Appendix. The highlights of the various aspects of the work are summarized in the following sections.

2.1 Mechanisms of Creep Crack Growth

The creep crack growth data developed in air as a part of this study clearly showed that, in the presence of large scale cavitation damage ahead of the crack tip and crack branching, da/dt does not correlate with C_t (Fig.1). On the other hand , when the damage in the crack tip region is not extensive (or constrained), da/dt is uniquely characterized by C_t after steady-state damage conditions are reached (Fig. 2).

The extensive quantitative damage analysis of the specimens revealed that continuous nucleation and growth of cavities occurs near the crack tip. The fraction of grain boundary area cavitated, A_c, was found to best represent the state of damage at a point ahead of the crack tip. A steep gradient in the extent of cavitation damage as a function of distance from the crack tip was obtained in all creep crack growth specimens which showed constrained cavitation, Fig. 3. A governing equation for damage evolution was proposed (See Ref.3).

In order to promote constrained cavitation during subsequent creep crack growth testing, all specimens were sidegrooved. Also,

to protect the fracture surface from oxidizing, the subsequent testing was performed in ultra-high-purity nitrogen. Fig. 4 shows the creep crack growth rate behavior as a function of C_t from these tests. Transient crack growth rates characterized by non-unique da/dt versus C_t relationship were observed for a substantial portion of the tests. The crack growth rates were high initially and they decreased with subsequent crack extension. Similar transient crack growth behavior has been observed previously [4] in ductile steels but the one observed here is peculiar in two ways. First, the crack growth rates in the transient regime are higher than those at equivalent C_t values in the steady-state crack growth regime. Second, the duration of the crack growth transients in terms of the crack extension required to achieve steady-state was significantly higher in antimony-copper than observed in ductile steels. The transient crack growth rate behavior was examined in great depth through further testing. It was concluded that the transient behavior occurs due to (1) damage done during precracking prior to creep crack growth testing and (2) damage done during initial loading when the crack tip stresses are the highest. A very detailed discussion of this phenomena is contained in a forthcoming M.S. thesis of Mr. Richard Norris. The completed thesis will be mailed to DOE when available.

2.2 Damage and Life Fraction Correlations in Creep Rupture Specimens

Although studying the creep rupture behavior of antimony-copper was not the main objectives of this study, some rupture

testing was necessary to develop the creep constants for crack growth data analysis. Also, the tested specimens were needed to evaluate the nondestructive damage characterization techniques used in this project.

Large gradients in the volume fraction of cavities V_v were observed as a function of distance from the rupture surface of crept specimens (Fig. 5). Optical microscopy and synchrotron microradiography both showed that lower stresses lead to considerably higher damage levels and to more extensive zones of enhanced damage (e.g. much higher than the uniform damage levels elsewhere in the specimens). Each of the curves in Fig. 6 approaches the same asymptotic value of V_v at large distances from the rupture surface, which suggest that a critical level of damage in creep of Cu-1% Sb must be attained to initiate necking leading to fracture.

Both A_c and $\bar{D}$, the average cavity diameter, were determined as a function of lifetime expended for two applied loads (Fig. 6).

Both quantities are linear functions of expended life, and there appears to be little dependence on applied stress. Apparently, failure by ductile rupture is imminent when about 0.45 of the grain boundaries are covered by cavities, regardless of the stress level. This conclusion is consistent with the observation of V_v values far from the rupture surface.

2.3 Crack Growth Mechanisms During Creep-Fatigue Loading

The mechanism of crack advance in Cu-1% Sb is a function of the crack-tip stresses. Below a critical stress, crack growth occurs by coalescence of creep cavities with the crack front. Above this same critical stress, crack growth occurs by a combination of cavity coalescence and grain boundary peeling. The dendritic growth of the crack front, or peeling process occurs when the normal stresses on the boundaries exceed a critical value, and is thus sensitive to grain orientation with respect to the remotely applied stress.

The process of crack growth by cavity coalescence is controlled by the smaller crack-tip cavitation. The size and density distribution of these cavities are functions of loading waveform and cycle time. Any grain boundary area not previously failed by the growth of the large, remote cavities fails by the coalescence of the smaller voids. The widespread, larger cavities have only a secondary effect on the growth rates.

The average rate of crack growth during hold times in trapezoidal loading waveforms, $(\dot{a})_{avg}$ can be uniquely correlated with the average, measured value of the C_t parameter, $(C_t)_{avg}$ (Fig. 7). The $(\dot{a})_{avg}$ vs. $(C_t)_{avg}$ relationship for hold times of ½ hour and longer is identical to that obtained for creep crack growth conditions. This implies, that for hold times larger than ½ hour, creep-fatigue crack growth rates are correlated uniquely by $(C_t)_{avg}$. The creep-fatigue interaction during elevated temperature crack growth may be the result of a change in crack growth mechanism

during the hold times. In the initial portion of each hold time, peeling may occur, and as the stresses relax, crack extension may revert back to a process by cavity coalescence. Thus, shorter hold times maintain higher average crack-tip stresses and have a higher probability for the peeling mechanism to operate. Since peeling occurs at higher stress levels, it is expected to result in higher crack growth rates, and shorter hold times would be expected to have unexpectedly higher crack growth rates.

2.4 Development and Assessment of Advanced Damage Characterization Techniques

Electron radiography and small angle scattering were examined during the very early stages of this three-year study as possible alternatives to optical and scanning electron metallography for damage assessment. Neither was found to be suitable for this study as discussed in earlier progress reports [5]. On the other hand, industrial computed tomography (CT) and high-resolution variants termed x-ray tomographic microscopy (XTM) were found to be very useful for damage characterization; digital microradiography and synchrotron microradiography were also applied successfully to damage characterization in Cu-1%Sb. These novel techniques and results obtained with them as described below.

2.4.1 Microradiography

Synchrotron microradiographs were recorded at the Stanford Synchrotron Radiation Laboratory (SSRL) using white radiation. The nearly parallel, high flux beam makes synchrotron radiation an

ideal source for contact radiography. Optical densitometry tracings of the microradiographs were recorded along a direction normal to the rupture surface and yielded curves such as that shown in Figure 10. Standards of the appropriate thickness and containing no cavitation damage were not run, however, and absolute magnitudes of damage cannot be easily calculated.

Comparison of the relative optical densities with the relative cavity volume fractions for both 3.5 and 6.0 ksi samples (tested to failure) should show quantitative agreement; this is not observed. We suspect that local film saturation occurs at positions where distinct cavity images are seen. This is being checked with further densitometry. During the next experimental period we will also repeat the synchrotron microradiography. We will use undamaged and damaged samples of the same thickness.

Digital microradiography eliminates the photographic emulsion and directly measures the transmitted intensity with electronic x-ray detectors. High resolution can be obtained by using a multiple detector array with very small elements or by using a pinhole collimator and scanning the sample across the beam. The variation of x-ray absorption around a creep crack in the Cu-Sb material was quantified using the latter approach, Ag Kα radiation and a 15 μm diameter beam. The sample studied was CT5 which was crept at 400C and 1.5 ksi$(in.)^{0.5}$. The sample was mechanically polished to about 0.3 mm thickness, and this was adequate to transmit nearly 30% of the incident beam in the vicinity of the crack. A square array of points with spacing of 0.5 mm was used to cover a 3 mm x 5 mm area

around the crack. Counting times were 10 sec per point, and a minimum of 3 x 10^5 counts were obtained at each point, well under one percent standard error in counting statistics. We note that these measurements were performed at London Hospital Medical College in collaboration with Dr. J.C. Elliott's group in the Dept. of Child Dental Health.

Figure 11 shows the two dimensional distribution of transmitted intensity around the creep crack. Note that absorption is reduced as far as 1 mm from the crack. The decrease in absorption could be due to preferential thinning near the crack, i.e. near the center of the sample, and this unlikely source of increased transmissivity is presently being checked by precision metrology. Conversion of the data into volume fraction of cavities will follow shortly.

2.4.2 Industrial Computed Tomography

Industrial computed tomography offers considerable promise for characterizing damage in samples with macroscopic dimensions-- as long as high spatial resolution (< 60 or 70μm) is not required. The compact tension samples crept and fatigued as part of this study are a good example of where use of industrial CT would be very advantageous. Large, long-range gradients in cavitation damage have been observed around the crack (see Sections 2.1 and 2.2) in sample CT2 (tested at 1.5 ksi(in.)$^{0.5}$ for 1250 hrs. and at 1.65 ksi(in.)$^{0.5}$ for times greater than 1250 hrs.). We have not yet reproduced the slices from our imaging terminal.

The adjacent slices surrounding the nominal crack plane for sample CT2 were obtained in collaboration with Dr. R. Isaacs of General Electric Corporation and had 62.5 μm pixels and 0.25 mm slice thicknesses. In these first experiments, the entire sample cross-sectional area (approximately 0.6 in. x 1.5 in.) was studied. Considerable beam hardening is evident which precludes quantitative analysis of the data until it is corrected. This correction is currently underway using a wedge-shaped reference sample from undamaged Cu-1% Sb.

The series of slices viewed on our terminal shows that the crack wandered from a single plane and that the crack extension was greater in the middle of the sample than at its edges. The crack tip structure is clearly evident even without correcting for beam hardening. Progress thus far indicates that prospects are excellent for quantitative measurements of the density variation ahead of creep cracks.

2.4.3. X-ray Tomographic Microscopy

A preliminary XTM scan was run of a small, rectangular prism of material taken from a sample which failed under creep loading at 400C. The XTM experiments were performed at SSRL in collaboration with Dr. J.H. Kinney's group at Lawrence Livermore National Laboratory. The creep test was run at 8 ksi, and one end of the centimeter-long prism was from the exposed fracture surface. Approximately 90 slices were recorded using 35 keV x-rays, and every ninth slice from the fracture surface is shown in Fig. 12.

The minimum dimension of this sample was 0.4 mm. Figure 13 shows enlargements of two of the slices. A few small cavities are visible in the interior of one of the slices, and their diameters of 10-20 μm are consistent with those measured from other volumes of the same sample by conventional techniques. Unfortunately, there were significant penetration problems at 35 keV, and higher energies could not available at SSRL. We intend to use the PEP ring at Stanford with higher x-ray energies to continue this investigation; we should be scheduled during the next PEP run. We have also approached CHESS (Cornell synchrotron) about obtaining time for these experiments. While the XTM sample clearly pushed the limits of what was then available, these results are very exciting: enough so that we will continue this aspect of the research even though the project has concluded.

3. LIST OF PAPERS PUBLISHED, CONFERENCE PRESENTATIONS AND STUDENTS SUPPORTED

In this Section, the published papers and the names of students and Research Associates who received support from the grant are listed.

3.1 Papers Published Acknowledging DOE Support

1. A. Saxena, "Creep Crack Growth Under Transient Conditions", Materials Science and Eng., vol. A(103), 1988, pp. 125-129.
2. A. Saxena and B. Gieseke, "Transients in Elevated Temperature Crack Growth", in High Temperature Fracture

Mechanisms and Mechanics, P. Bensussan Editor, Mech. Eng. Publication, 1990.

3. A. Saxena, "Mechanics and Mechanism of Creep Crack Growth", Invited Book Chapter in Fracture Mechanics: Microstructure and Mechanisms, S.V. Nair et. al. editors ASM International, 1989, pp. 283-334.

4. J.T. Staley, Jr. and A. Saxena, "Mechanisms of Creep Crack Growth in 1 wt-percent Antimony-Copper: Implications for Fracture Parameters", Acta Metallurgica, 1990 (in press).

5. B. Gieseke and A. Saxena, "Correlation of Creep-Fatigue Crack Growth Rates Using Crack Tip Parameters", Advances in Fracture Research, Proceedings of the Seventh International Conference on Fracture, Houston, March 1989, pp. 189-196.

6. A. Saxena, "Recent Advances in Elevated Temperature Crack Growth and Models for Life Prediction", (Keynote Paper), Proceedings of the Seventh International Conference on Fracture, Houston, March 1989, pp. 1675-1688.

3.2 Manuscripts in Preparation

1. S.R. Stock, A. Guvenilir, R. Norris, Y.H. Lee, J.T. Staley, Jr., Z.U. Rek and A. Saxena, "Development of Damage During Creep of Cu-1% Sb at 400 C", to be submitted to Acta Metallurgica.

2. B. Gieseke and A. Saxena, "Mechanisms of Crack Growth in Cu-1% Sb During Hold Time Fatigue", to be submitted to Acta Metallurgica.

3. R.H. Norris and A. Saxena, "A Transients and the Resulting Conditions During Elevated Temperature Crack Growth in an Antimony-Copper Alloy," ASTM STP from the ASTM 22nd. National Symposium on Fracture Mechanics.

3.3 Conference Presentations

1. A. Saxena, "Crack Growth at Elevated Temperature". ASME Applied Mechanics Meeting, June 15-16, 1987, Cincinnati, Ohio (invited).

2. A. Saxena, "Creep Crack Growth Under Transient Conditions", in DOE Workshop on Mechanics and Physics of Crack Growth and Application to Life Prediction", August 4-7, 1987, Keystone, Colorado (invited).

3. A. Saxena and S.D. Antolovich, "Mechanics and Mechanisms of Creep Crack Growth", ASM weekend seminar on Fracture Mechanics, Microstructure and Mechanisms, Oct. 9-10, 1987, Cincinnati, Ohio (invited).

4. A. Saxena and B. Gieseke, "Transients in Elevated Temperature Crack Growth", International Seminar on Mechanics and Mechanisms of High Temperature Fracture", Oct. 13-15, Dourdan, France (invited).

5. B. Gieseke and A. Saxena, "Mechanisms of Creep-Fatigue Crack Growth Interactions in 1wt % Sb-copper", TMS-AIME

Meeting, Phoenix Arizona, Jan. 26-28, 1988.

6. A. Saxena, "Crack Tip Parameters for Correlating Creep Crack Growth Data", (invited) VAMAS meeting, June 18-19, 1988, Freiburg, W. Germany.
7. B. Gieseke and A. Saxena, "Correlation of Creep-Fatigue Crack Growth Rates using Crack Tip Parameters", Seventh International Conference on Fracture, Houston, Texas, March 1989.
8. A. Saxena, "Recent Advances in Elevated Temperature Crack Growth and Models for Life Prediction", (Keynote paper), Seventh International Conference on Fracture, March 1989.

3.4 Students and Research Associates Acknowledging DOE Support

Students

1. James T. Staley, Jr. M.S. 1988, Rockedyne Division, Rockwell International, Canoga Park, CA.
2. Brian Gieseke, Ph.D March 1990, Metals and Ceramics Division, Oak Ridge National Laboratory Oak Ridge, TN.
3. Richard H. Norris, M.S. (expected June 1990 and to continue Ph.D. at Georgia Tech).
4. Abbas Guvenilir, Ph.D (expected December 1991)

Research Associates

1. Dr. K. Banerji (Jan 1987-Dec 1988) currently employed with Motorolla Co., W. Palm Beach, Fla.

2. Dr. Y.H. Lee, Visiting Scientist from Korea Dec 86- Dec 87.

3. Dr. C.P. Leung (Jan 1989 - June 1989) currently employed at Southwest Research Institute, San Antonio, Texas.

4. REFERENCES

1. H. Riedel, Fracture at High Temperatures, Springer-Verlag, 1987.

2. A. Saxena, "Mechanics and Mechanism of Creep Crack Growth", in Fracture Mechanics: Microstructure and Micromechanisms, S.V. Nair et al. editors, ASM International, 1989, pp. 283-334.

3. J.T. Staley, Jr. and A. Saxena, "Mechanisms of Creep Crack Growth in 1 wt % Antimony-Copper: Implications for Fracture Parameters", Acta Metallurgica, 1990 (in press).

4. A. Saxena and B. Gieseke, "Transients in Elevated Temperature Crack Growth", in High Temperature Fracture Mechanisms and Mechanics, P. Bensussan Editor, Mech. Eng. Publications, 1990 (in press)

5. A. Saxena, S.R. Stock, J.T. Staley and B. Gieseke, "Mechanisms of Time-Dependent Crack Growth at Elevated Temperature," First Annual Project Report, DOE Project DE-FG05-86ER 45257, Feb 1987.

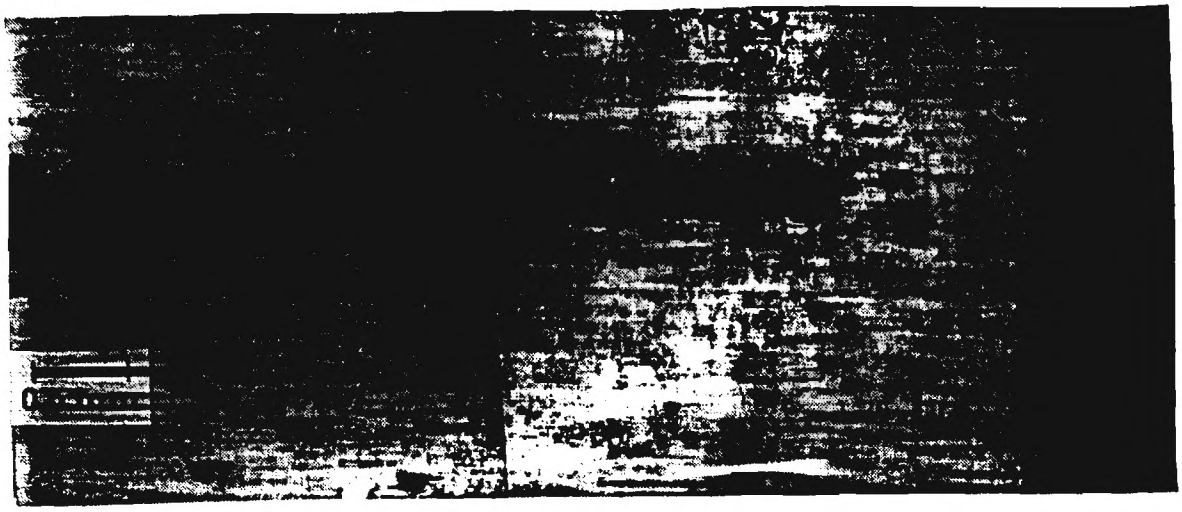

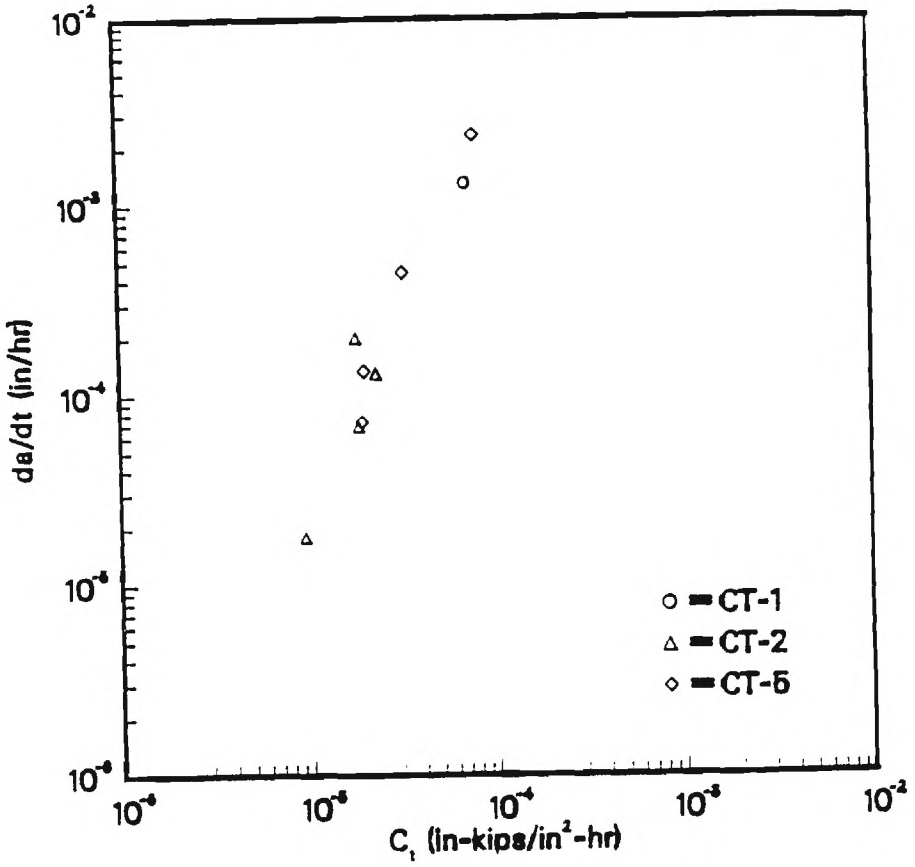

Fig.1 (Top) Unconstrained cavitation at the tip of growing creep crack leading to extensive crack branching; (Bottom) the lack of correlation between da/dt versus C_t when data from specimens which exhibited this behavior were included in the correlation (Staley and Saxena, 1989).

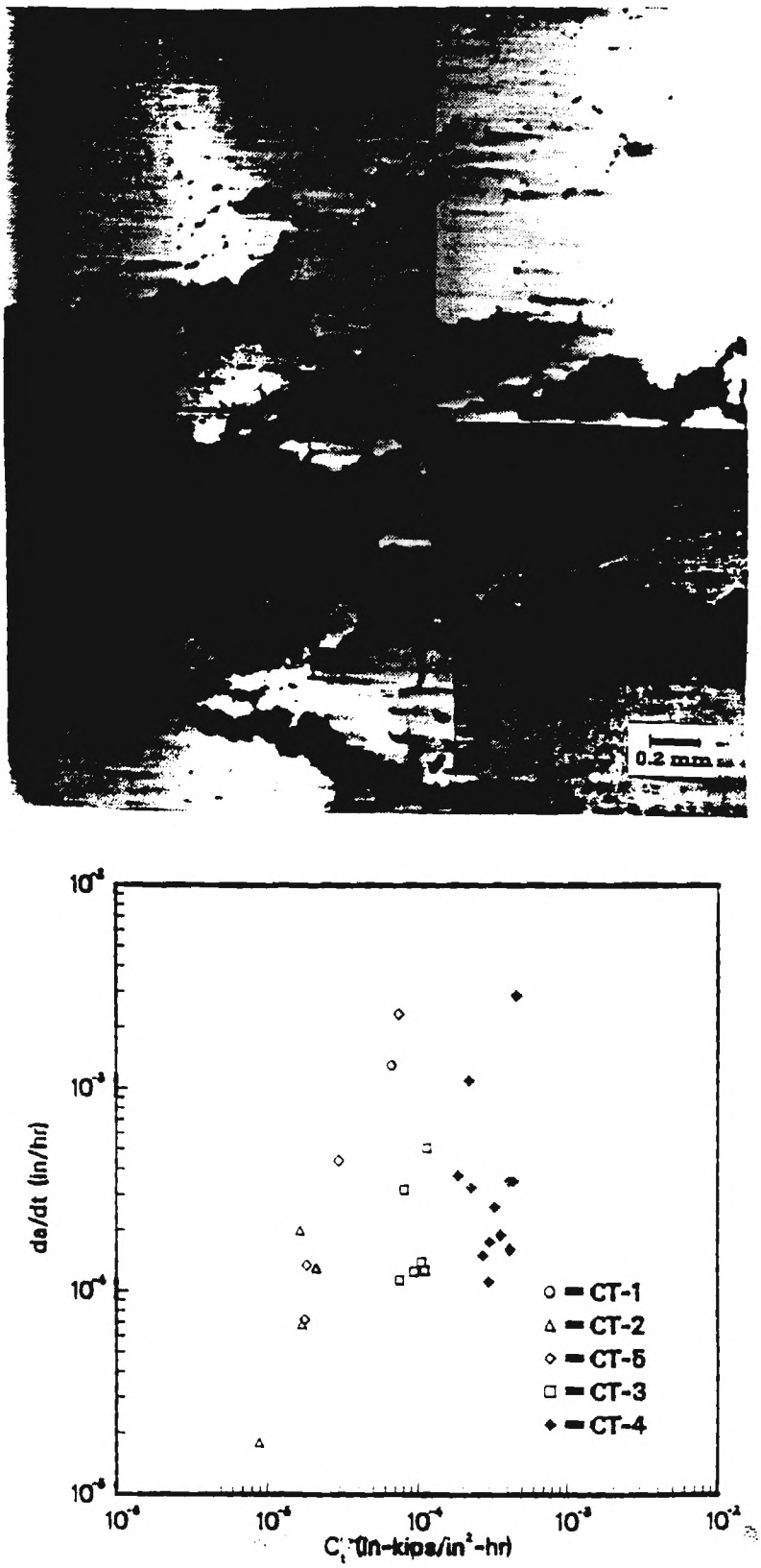

Fig. 2 (Top) Constrained cavitation damage at the tip of a growing creep crack in 1 wt percent antimony-copper; (bottom) the creep crack growth rate as a function of C_t in specimens which exhibited constrained cavitation (Staley and Saxena, 1989).

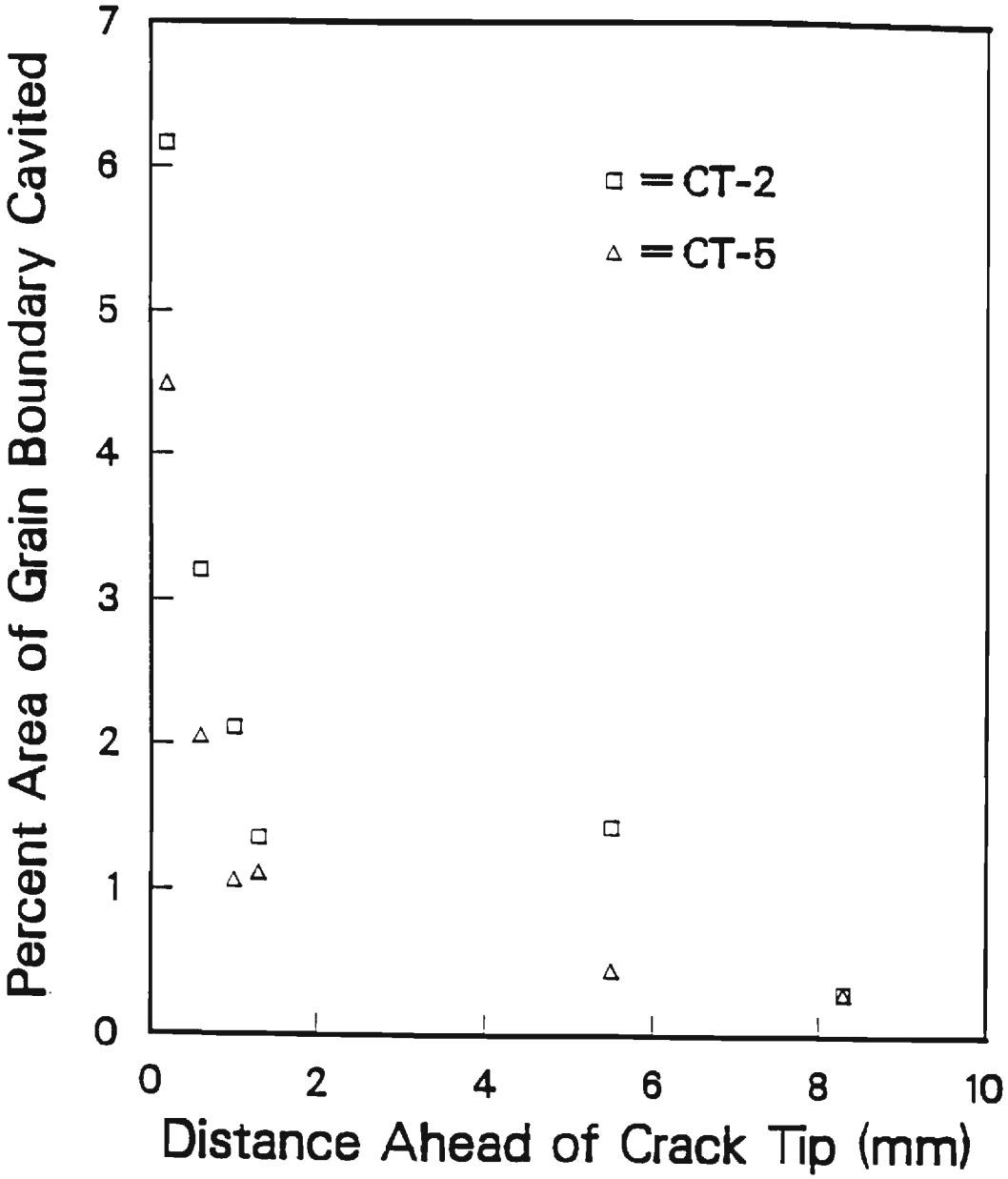

Fig. 3 - Fraction of grain boundary area cavitated as a function of distance from the crack tip for specimens CT-2 and CT-5.

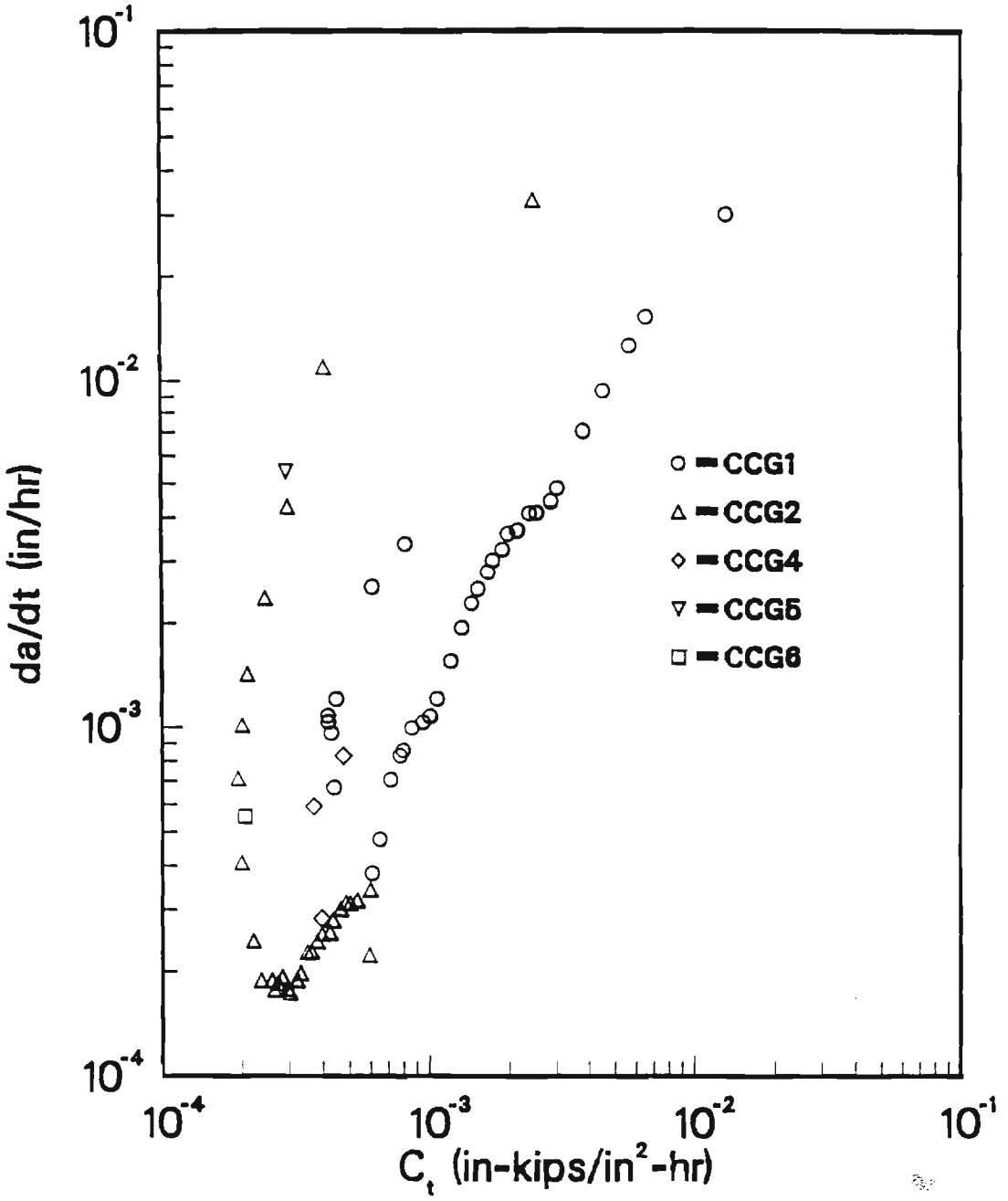

Fig. 4 - Creep crack growth rate of 1 wt percent Sb - Copper in ultra-high purity N_2.

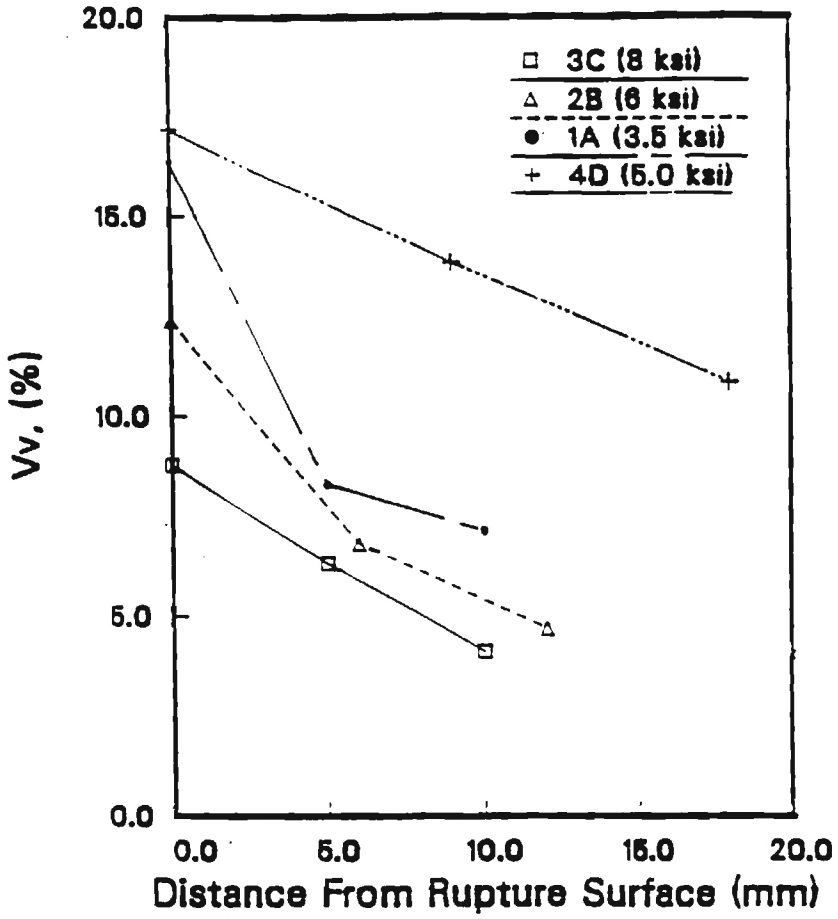

Fig. 5 - Volume fraction V_v of cavities as a function of distance from the rupture surface of samples of Cu - 1 wt. % Sb tested at 400 C. The measurements were made with optical microscopy on a polished section of each sample.

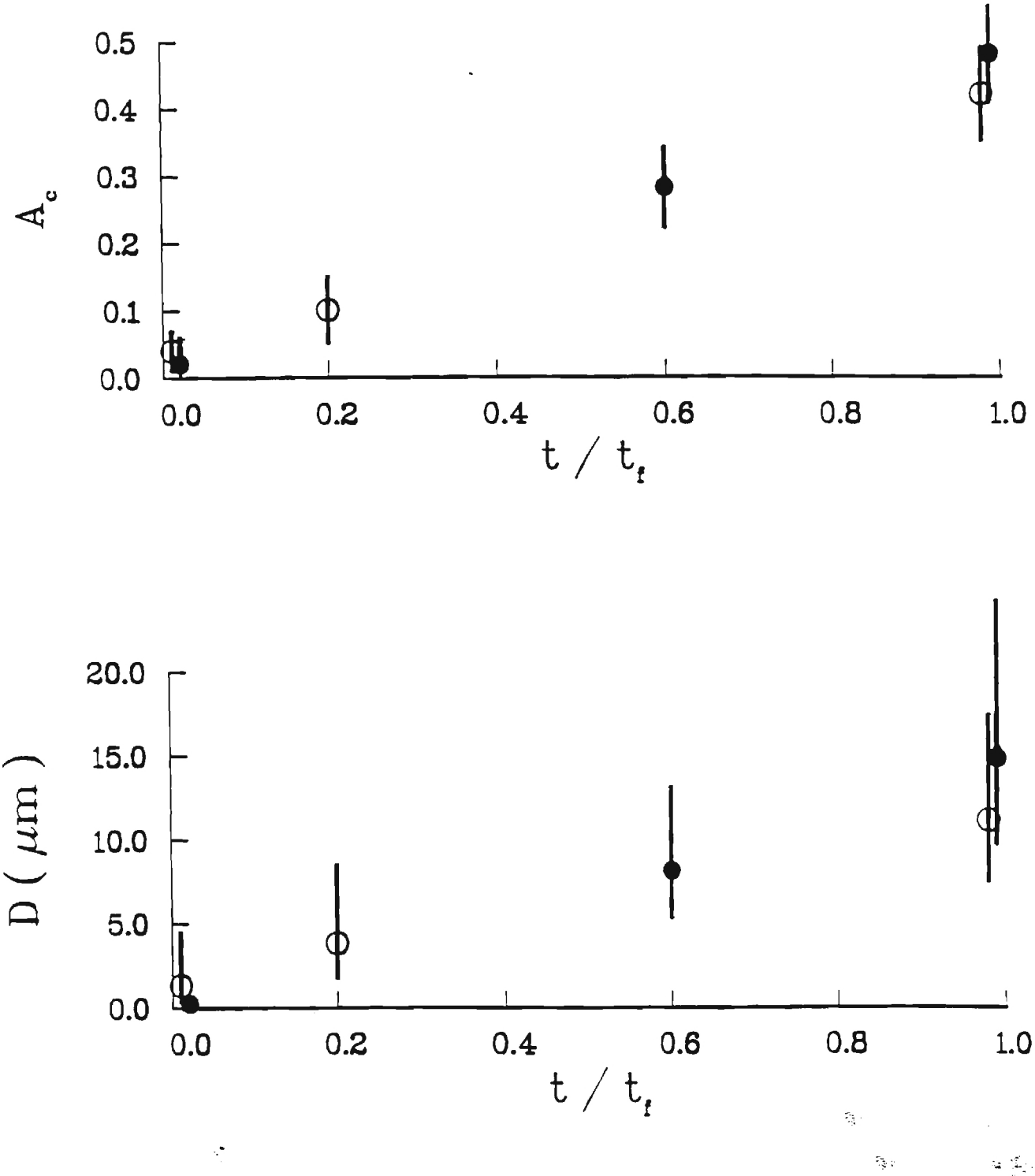

Fig. 6 - a. Fraction of grain boundary area A_c and b. Average cavity diameter D as functions of fraction of elapsed life-time t/t_f. The solid and open circles are for samples tested under 6.0 and 3.5 ksi loads, respectively.

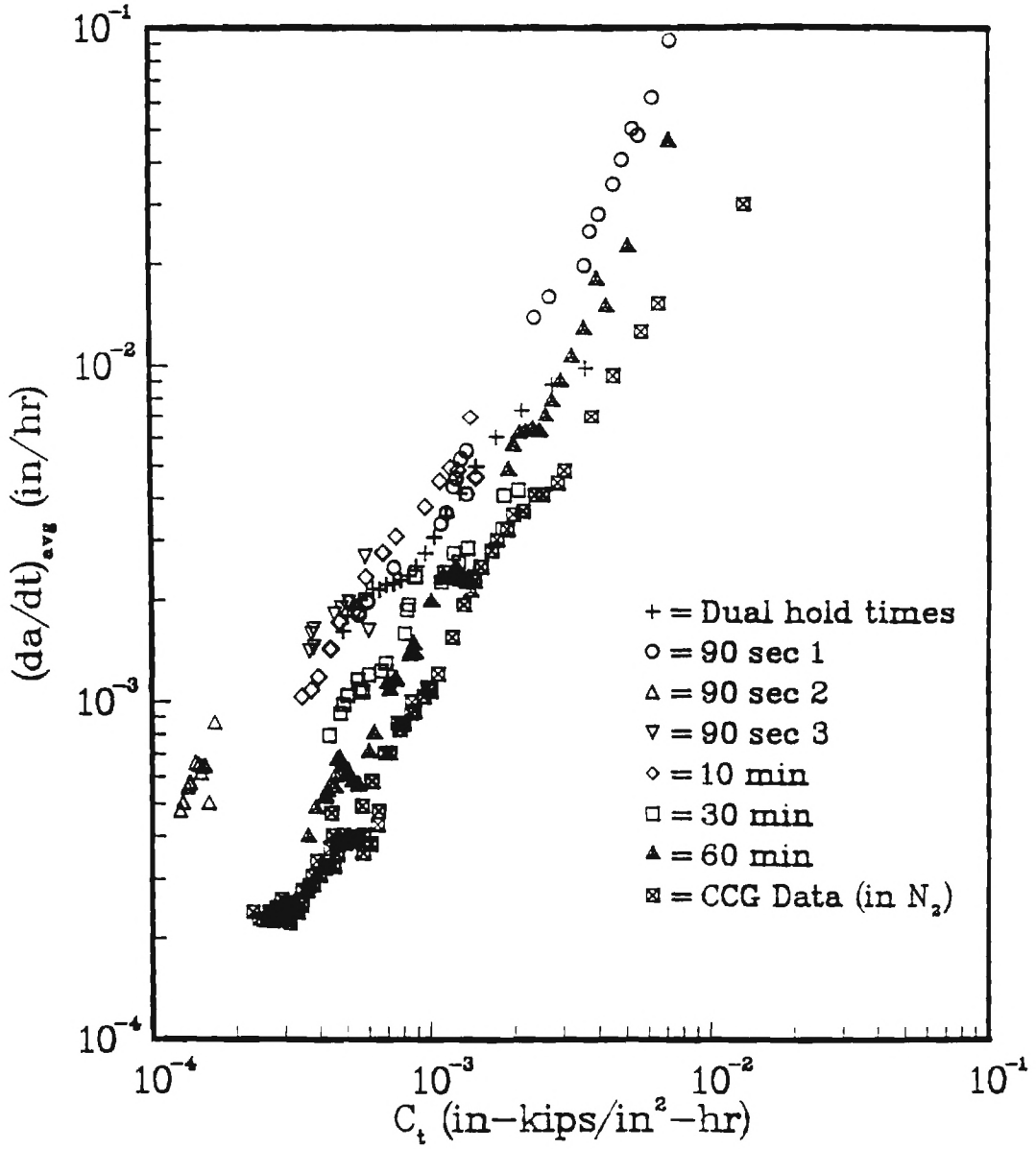

Fig. 7 - The average da/dt during hold time as a function of the $(C_t)_{avg}$ parameter and comparison with creep crack growth rate for a one percent antimony-alloy at 400°C (Gieseke and Saxena, 1989).

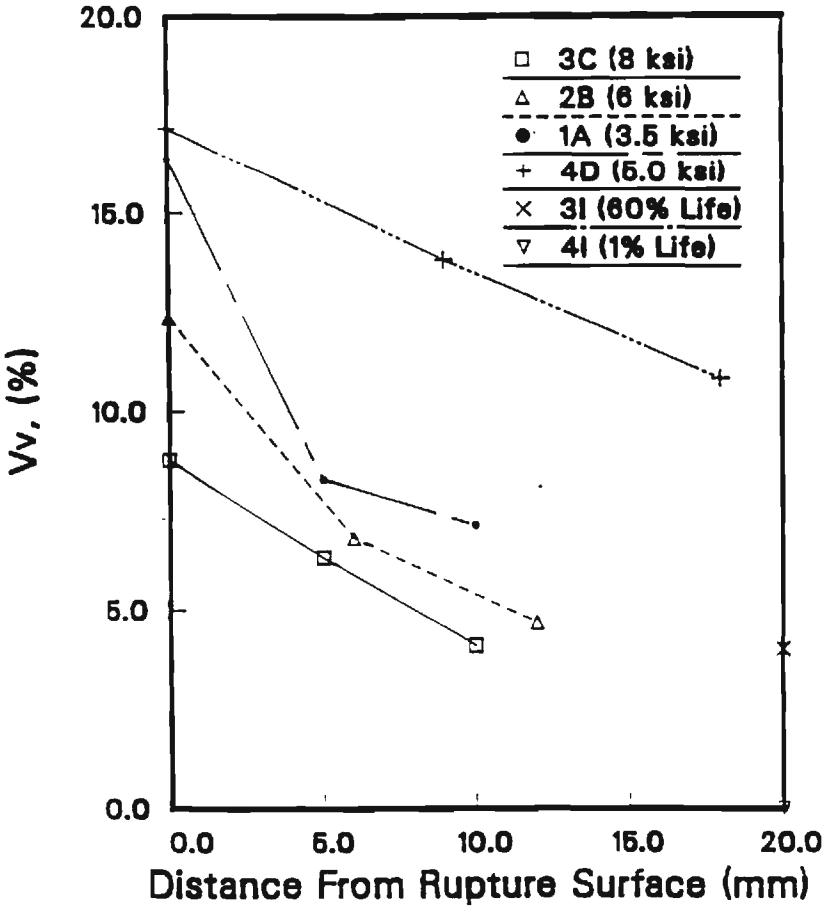

Figure 8. Volume fraction of cavities as a function of distance from the fracture surface of specimens deformed in creep.

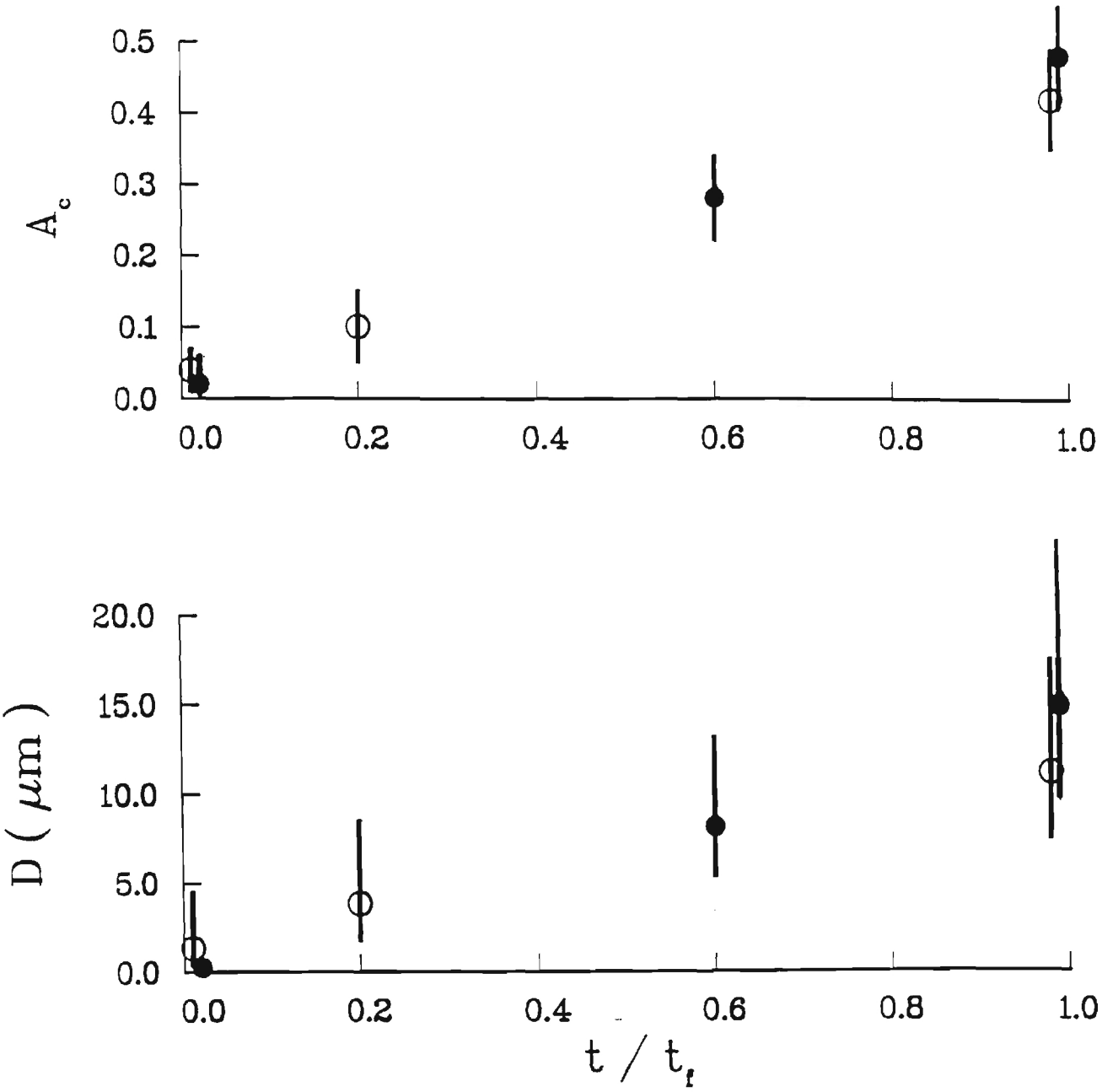

Figure 9. Area fraction A_c and average cavity diameter D for samples tested at 3.5 ksi (open circles) and 6 ksi (closed circles).

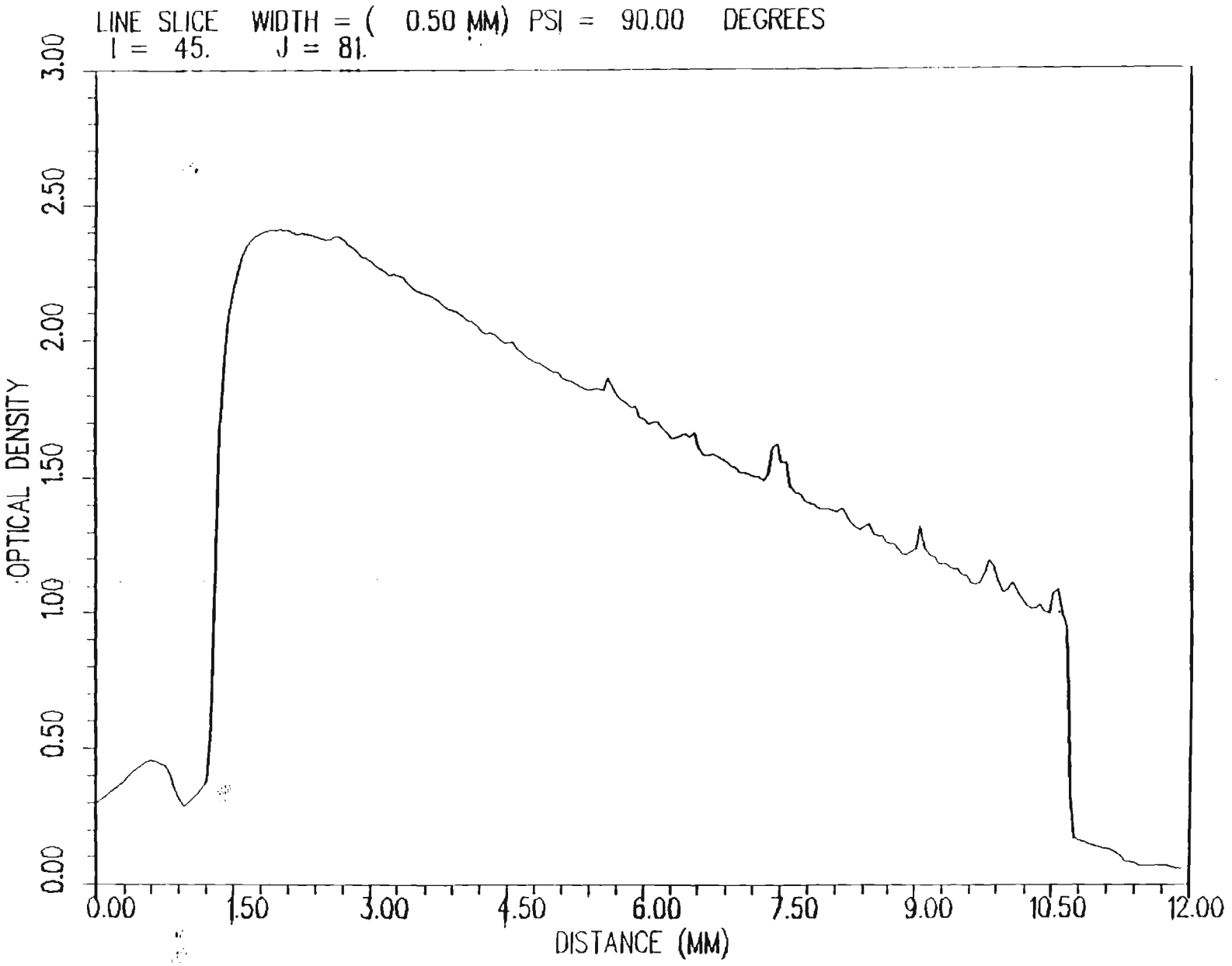

Figure 10. Densitometry trace showing gradient of damage in synchrotron microradiographs of sample 3C.

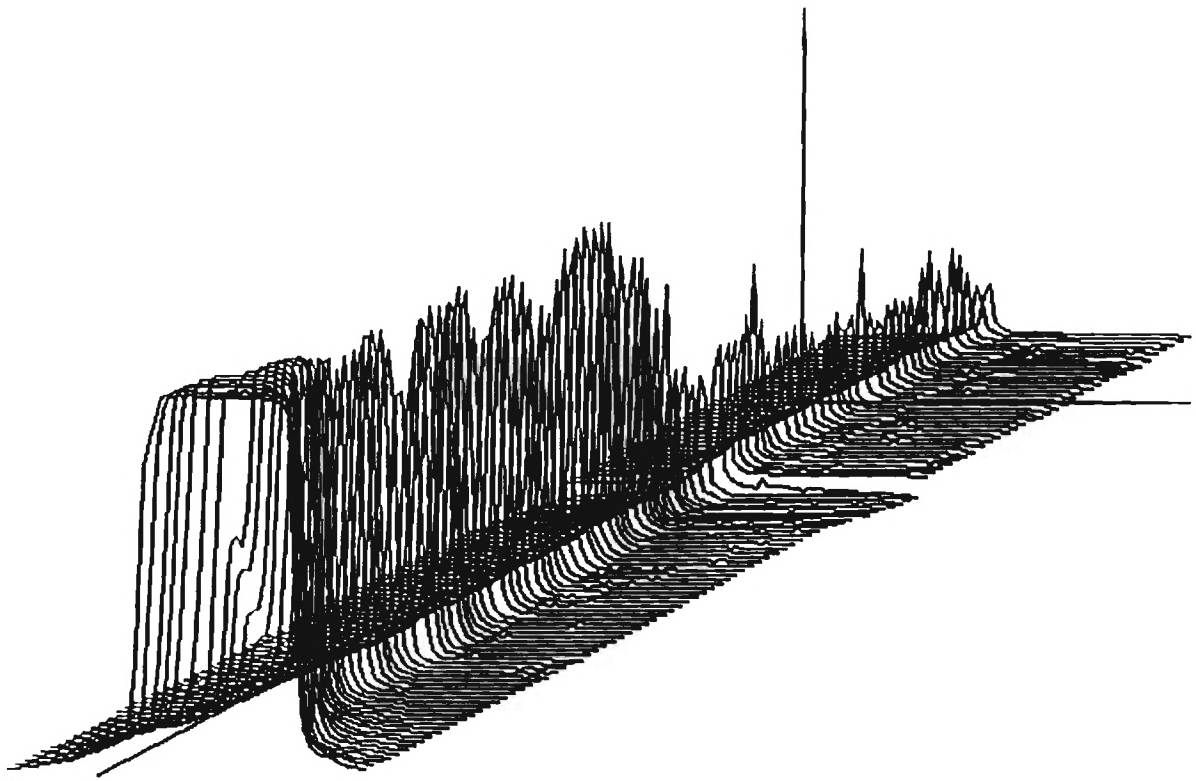

Figure 11. Two-dimensional distribution of transmitted intensity around a creep crack. The vertical axis is transmitted intensity.

Figure 13. Slices recorded with synchrotron XTM parallel to the rupture surface of a Cu- 1 wt. % Sb sample. The sample failed under creep, and the irregularities of the slices shown the jagged rupture surface. The small, dark images, indicated by arrows, appear to be grain boundary cavities.

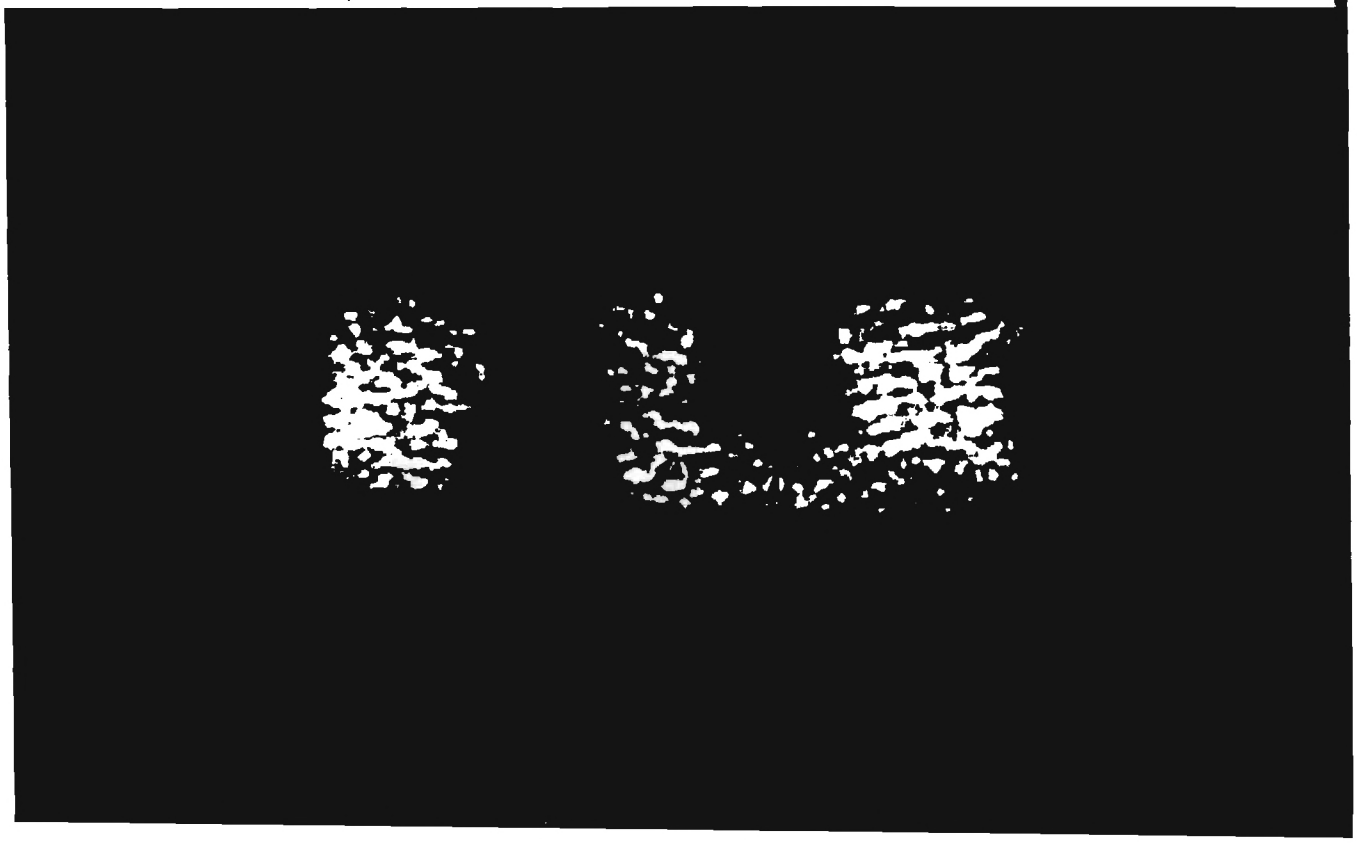

APPENDIX

Copies of papers published on the Grant.

Materials Science and Engineering, A103 (1988) 125–129

Creep Crack Growth under Transient Conditions*

ASHOK SAXENA

Fracture and Fatigue Research Laboratory, School of Materials Engineering, Georgia Institute of Technology, Atlanta, GA 30332-0245 (U.S.A.)

(Received August 1987)

Abstract

The recent advances in time-dependent fracture mechanics concepts for characterizing creep crack growth rate under transient conditions are reviewed. At elevated temperatures, transients in the crack tip stress fields occur owing to stress relaxation during constrained creep due to primary and tertiary creep deformation, cyclic loading and crack growth. A unified crack tip parameter C_t which is formulated to account for all types of transient is described and evaluated. The currently available creep crack growth data support the validity of C_t. Under steady state conditions, C_t reduces to the familiar C^* integral.

1. Introduction

The field of time-dependent fracture mechanics for characterizing crack growth at elevated temperatures has progressed considerably in the recent years. It is now generally accepted that the C^* integral is a good correlating parameter for creep crack growth behavior under steady state conditions in creeping materials [1–7]. Steady state conditions exist in a cracked body when widespread creep deformation characterized by power law creep occurs. Under these conditions, C^* becomes path independent, it equals the stress power (or energy rate) release rate and it also represents the strength of the crack tip stress singularity [1, 3, 4, 7].

Despite the strong mechanics basis, the application of C^* is limited because of the restriction of steady state creep. Most elevated temperature components are designed to resist widespread creep deformation. As a result, the creep strains are expected to be in the primary creep regime for a significant portion of the life. Because of the stress and temperature gradients and periodic start-up and shut-downs in thick section components, there is also a good likelihood of the presence of the small-scale creep conditions during most of the service life. The condition of small-scale creep has been analyzed by several researchers [7–13]. As will be discussed later in the paper, the presence of crack growth also promotes transient stress conditions near the crack tip [12, 13] and so does the occurrence of tertiary creep [14]. Thus, in several practical situations, the consideration of transient stress field is important and, for these applications, C^* is no longer a valid crack tip parameter.

This paper focuses on a crack tip parameter C_t [8] which is general enough to correlate creep crack growth behavior under all types of transient conditions and it reduces to C^* when steady state conditions prevail. Provided that the correct material constitutive laws are used, C_t can be calculated by finite element analysis for components [15, 16]. It can be accurately measured at the loading pins of a specimen [8]. Also, closed-form solutions for estimating C_t are currently available for materials which deform by elastic power law creep [8, 9, 14]. The use of C_t under cyclic loading conditions will also be briefly discussed [17].

2. Formulation of the C_t parameter

The initial formulation of the C_t parameter is made with the assumption that the crack is stationary. Following Saxena [8], let us consider several identical pairs of cracked specimens. For each pair, one specimen has a crack length a and the other has a crack length of $a + \Delta a$. The specimens of each pair are loaded to various constant load levels $P_1, P_2, \ldots, P_i$ at elevated temperatures. As creep deformation progresses in the various specimens, additional deflections V_c accumulate at the load lines owing to growth of the creep zones, as shown in Fig. 1(a). This deflection is

*Paper presented at the Workshop on the Mechanics and Physics of Crack Growth: Application to Life Prediction, Keystone, CO, U.S.A., August 4–7, 1987.

0921-5093/88/$3.50

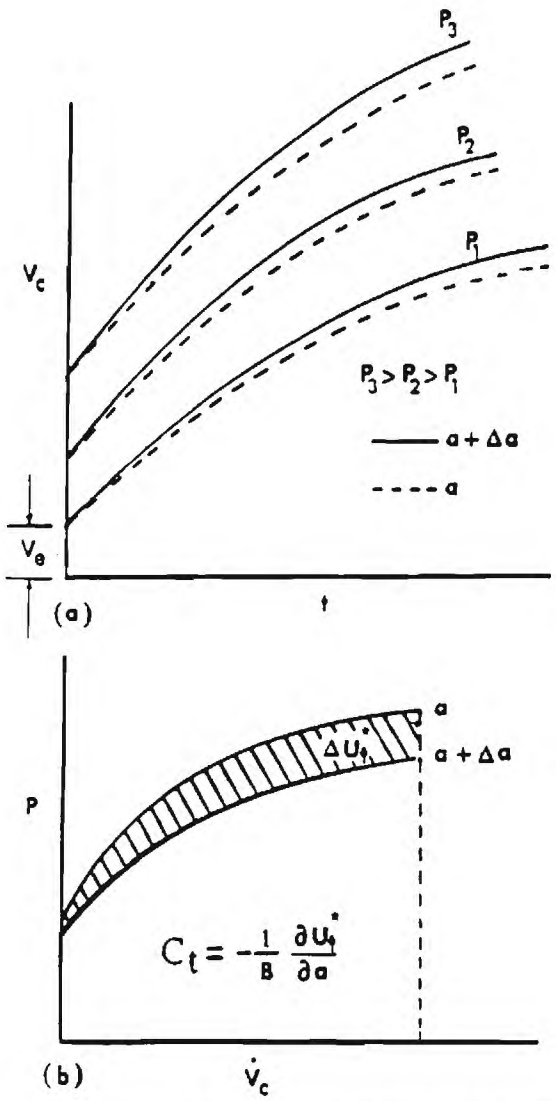

Fig. 1. (a) Load-line deflection V_c as a function of time for bodies of crack lengths a and $a+\Delta a$ at various load levels; (b) the definition of the C_t parameter [8].

attributed to primary and secondary creep in the crack tip region and also to change in elastic strain due to stress relaxation within the body. Under small-scale creep it has been shown [8, 15] that the load-line deflection rate $\dot{V}_c$ is directly proportional to the rate $\dot{r}_c$ of expansion of the creep zone size.

In Fig. 1(b) the instantaneous value of $\dot{V}_c$ is plotted at time t as a function of load P for specimens with crack length a and for specimens with crack length $a+\Delta a$. For other times, similar plots of P *vs.* $\dot{V}_c$ can be constructed. The area between the curves corresponding to crack lengths a and $a+\Delta a$ is designated ΔU_t^*. The subscript t denotes the value for a fixed time. C_t is then defined as

$$C_t = \lim_{\Delta a \to 0}\left(-\frac{1}{B}\frac{\Delta U_t^*}{\Delta a}\right) = -\frac{1}{B}\frac{\partial U_t^*}{\partial a} \qquad (1)$$

where B is the specimen thickness. Under extensive creep conditions where power law creep dominates, $C_t \equiv C^*$ by definition because ΔU_t^* assumes a steady state value ΔU^*. Under extensive creep conditions where primary creep effects are still significant, it follows from Reidel's [14] definition of C_h^* that $C_t \equiv C_h^*/(1+p)t^{p/(1+p)}$ where p is a constant related to the primary creep property of the material. Therefore, in the regime of extensive creep, C_t characterizes the amplitude of the Hutchinson [18], Rice and Rosengren [19] (HRR) crack tip stress fields by virtue of its relationship of C^* and C_h^*.

Under small-scale creep conditions, the amplitude of the HRR field has been derived by several investigators [7, 10, 11, 20] for materials that deform by elastic power law creep. It is given by the following simple equation [20]:

$$C(t) = \frac{K^2}{E(n+1)t} + C^* \qquad (2)$$

Equation (2) is valid for very short to long times [15, 16, 20]. It is important to point out that under small-scale creep conditions $(C_t)_{SSC} \neq C(t)$. In contrast, $(C_t)_{SSC}$ is related uniquely to the rate of expansion of the creep zone size by the following equation [8, 15]:

$$(C_t)_{SSC} = 2(1-\nu^2)\beta\left(\frac{F'}{F}\right)\frac{K^2\dot{r}_c}{EW} \qquad (3)$$

From the relationship between $\dot{r}_c$ and $\dot{V}_c$, the following expression can be derived which is convenient for measuring C_t at the loading pins [8]:

$$(C_t)_{SSC} = \frac{P\dot{V}_c}{BW}\frac{F'}{F} \qquad (4)$$

where the K calibration factor $F = (K/P)BW^{1/2}$ and $F' = dF/d(a/W)$. In eqns. (3) and (4), no assumptions have been made about the constitutive behavior of the material. Hence these equations hold for any constitutive law.* A most general expression for C_t which is valid for primary, secondary and tertiary creep as well as for conditions ranging from small-scale creep to extensive creep is given by the following equation:

*In the original work [8], eqn. (4) was derived for materials obeying elastic power law creep. However, it can be shown easily that this equation is also valid for any more general creeping law.

$$C_t = (C_t)_{SSC} + C_h^*/(1+p)t^{p/(1+p)} \quad (5)$$

If we make the assumption of elastic power law creep, an analytical expression for estimating C_t is derived and given in earlier papers [8, 15].

Figure 2 shows the creep crack growth behavior of Cr-Mo and Cr-Mo-V steels [8, 21], demonstrating the excellent correlation between creep crack growth rates da/dt and C_t obtained over a wide range of growth rates. In these correlations, specimens tested at different load levels are involved and, to a limited extent, specimens of different geometries are also included. In Fig. 3 the average da/dt during the hold period of a fatigue cycle with trapezoidal waveform is also correlated with C_t. The hold times in this study [17] ranged from 50 s to 24 h, and the data appear to correlate with C_t. However, in comparison with the da/dt values under static loading, the crack growth rates during the hold time are much lower. This may be due to the influence of reversed plasticity during unloading in the previous fatigue cycle. For details of these correlations, readers are referred to earlier papers [17]. The presence of cyclic loading promotes transient conditions at the crack tip; hence, the correlation between da/dt and C_t under these conditions is important in establishing C_t as a unifying crack tip parameter which can account for different types of transient.

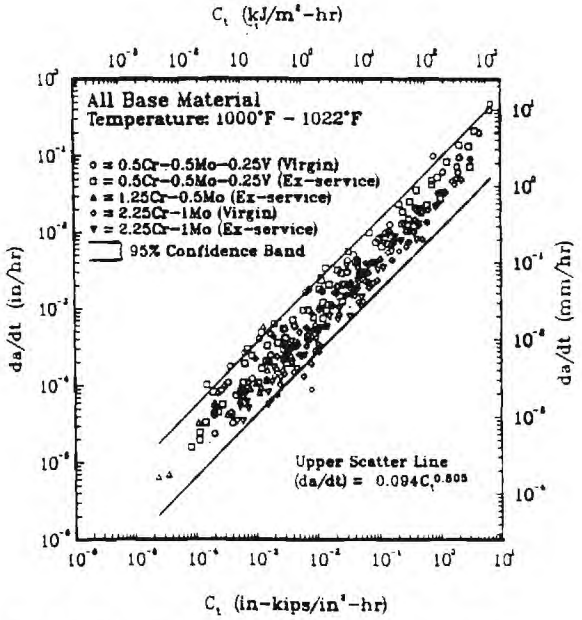

Fig. 2. Creep crack growth behavior of Cr-Mo and Cr-Mo-V steels [21].

3. Considerations due to crack growth

Under extensive creep conditions, the region of influence of crack growth on the crack tip stress fields is small in comparison with the zone of HRR field dominance [22]. In contrast, under small-scale creep conditions the presence of crack growth will significantly alter the crack tip stress fields [12, 13]. The extent of this effect depends on the crack growth rate and the rate at which creep is spreading in the component or specimen. Thus, it is important to discuss the influence of crack growth and its implications on the validity of C_t under small-scale creep conditions.

The consideration of crack growth can be divided into two regimes. The first regime is one of slow crack growth in which the crack tip stress fields are perturbed owing to elastic unloading associated with crack extension near the crack tip. Hence, $\dot{r}_c$ for a growing crack is different from the $\dot{r}_c$ estimated for a stationary crack. We define slow crack growth as a condition under which $\dot{r}_c > 0$; so the crack tip always extends beyond the creep zone boundary. Under such conditions, C_t obtained from eqn. (3) with $\dot{r}_c$ correctly calculated is expected to represent the crack driving force. Also, if C_t is estimated from a measured deflection rate substituted in eqn. (4), the effects on the transient stress field associated with crack growth are included in the estimate of C_t.

The other condition is that of a high crack growth rate under which $\dot{r}_c < 0$. This condition

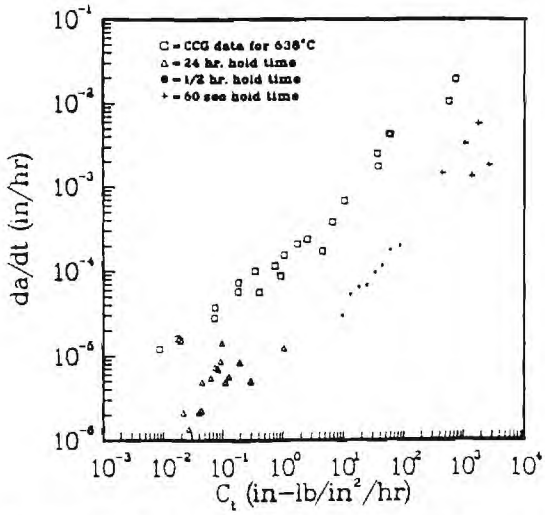

Fig. 3. Creep and creep-fatigue crack growth rate data correlated with the C_t parameter for 1wt.%Cr-1wt.%Mo-0.25wt.%V steel [17].

will only occur if another cracking mechanism such as one dominated by environment or stable crack growth due to ductile tearing is involved. Under such conditions, the characterizing crack tip parameter is expected to change gradually from C_t to J (or K) [23–25]. In between, there can be a regime where neither C_t nor J will characterize the crack growth rate. However, this regime is expected to occur only at very high crack growth rates ($da/dt > 0.1$ mm h^{-1}) and perhaps does not contribute significantly to life.

A very special situation arises when $\dot{r}_c = 0$. This condition implies that the creep zone size remains constant. The mechanism of crack growth will still be creep with the crack tip and the creep zone boundary moving at equal rates. This will lead to a time-independent stress field with respect to a moving crack tip and is therefore a case of steady state. da/dt under such circumstances will correlate with J (or K). The creep-brittle materials such as ceramics or embrittled ferritic steels may exhibit such trends. In general, $\dot{r}_c \leq 0$ should lead to a K-controlled crack growth rate and $\dot{r}_c > 0$ should lead to a C_t-controlled crack growth rate. In an experiment, the condition of a C_t- or K-controlled crack growth rate can be identified through the use of deflection rate partitioning analysis [24, 25]. However, much work remains to be done in the area of how transition from C_t-controlled to J-controlled (or K-controlled) crack growth occurs in creeping materials after ductile tearing begins.

4. Summary and conclusions

Significant progress has occurred in the development of concepts for characterizing crack growth behavior at elevated temperatures where time-dependent creep deformation occurs. The current state of these developments is summarized as follows.

(1) The C^* integral is widely accepted as being the correct crack tip parameter for characterizing creep crack growth behavior under steady state conditions.

(2) Under transient crack tip stress conditions, C_t appears to be promising for characterizing the creep crack growth behavior. There are no inherent limitations in the use of C_t for transients resulting from stress relaxation, primary and tertiary creep deformation, cyclic loading and crack growth.

(3) Expressions for measuring C_t for various specimen geometries are currently available. The validity of these expressions includes situations involving all types of transient deformation. Much work remains to be done in developing accurate expressions to estimating C_t in components in the presence of primary creep deformation and crack growth. Analytical expressions for calculating C_t in components which deform by elastic power law creep are currently available.

Acknowledgments

The author wishes to acknowledge the financial support of the Office of Basic Energy Sciences, U.S. Department of Energy, under Grant DE-FG05-86ER-45257 (Dr. J. B. Darby, Project Manager) for supporting this work.

References

1 J. D. Landes and J. A. Begley, in *Mechanics of Crack Growth, ASTM Spec. Tech. Publ. 590*, 1976, pp. 128–148.
2 K. M. Nikkin, G. A. Webster and C. E. Turner, *Proc. 9th Conf. on Cracks and Fracture*, in *ASTM Spec. Tech. Publ. 601*, 1967, pp. 47–62.
3 A. Saxena, *Proc. 12th Natl. Symp. on Fracture Mechanics*, in *ASTM Spec. Tech. Publ. 700*, 1980, pp. 131–151.
4 N. L. Goldman and J. W. Hutchinson, *Int. J. Solids Struct., 11* (1975) 575–579.
5 S. Taira, R. Ohtani and T. Komastsu, *J. Eng. Mater. Technol. 101* (1979) 162–167.
6 H. Riedel, in R. Raj (ed.), *Flow and Fracture at Elevated Temperatures*, American Society for Metals, Metals Park, OH, 1983, pp. 149–177.
7 H. Riedel and J. R. Rice, *Proc. 12th Natl. Symp. on Fracture Mechanics*, in *ASTM Spec. Tech. Publ. 700*, 1980, pp. 112–130.
8 A. Saxena, in J. H. Underwood, R. Chait, C. W. Smith, D. P. Wilhelm, W. A. Andrews and J. C. Newman (eds.), *Proc. 17th Natl. Symp. on Fracture Mechanics* in *ASTM Spec. Tech. Publ. 905*, 1986, 185–201.
9 A. Saxena and P. K. Liaw, Remaining-life estimation of boiler pressure pars – crack growth studies, *Rep. EPRI CS-4688*, July 1986 (Electric Power Research Institute).
10 J. L. Bassani and F. A. McClintock, *Int. J. Solids Struct., 17* (1981) 479–492.
11 K. Ohji, K. Ogura and S. Kubo, *JSME Rep. 790-13*, 1978, pp 18–20 (Japan Society of Mechanical Engineers) (in Japanese).
12 C. Y. Hui and H. Riedel, *Int. J. Fract., 17* (4) (1981) 409–425.
13 D. E. Hawk and J. L. Bassani, *J. Mech. Phys. Solids, 34* (1986) 191–212.
14 H. Riedel, *J. Mech. Phys. Solids, 29* (1981) 35–49.
15 J. L. Bassani, D. E. Hawk and A. Saxena, Evaluation of C_t parameter for characterizing creep crack growth rate in the transient regime, *Proc. 3rd ASTM Int. Symp. on Nonlinear Fracture Mechanics, 1986*, in *ASTM Spec. Tech. Publ.*, to be published.
16 C. Leung, D. L. McDowell and A. Saxena, A numerical study of nonsteady-state creep at stationary crack tips,

Proc. 3rd ASTM Int. Symp. on Nonlinear Fracture Mechanics, 1986, in *ASTM Spec. Tech. Publ.*, to be published.

17 A. Saxena and B. Gieseke, Transients in elevated temperature crack growth, *Proc. Int. Semin. High Temperature Fracture Mechanisms and Mechanics, Dourdan, October 13–15, 1987*, Mecamat, Cramayel.

18 J. W. Hutchinson, *J. Mech. Phys. Solids, 16* (1968) 13–31.

19 J. R. Rice and G. F. Rosengren, *J. Mech. Phys. Solids, 16* (1968) 1–12.

20 R. Ehlers and H. Riedel, in D. François (ed.), *Advances in Fracture Research, Proc. 5th Int. Conf. on Fracture, Cannes, March 29–April 3, 1981*, Vol. 2, Pergamon, Oxford, 1981, pp. 691–698.

21 A. Saxena, J. Han and K. Banerji, Creep crack growth behavior in power plant materials, submitted to *J. Press. Vessel Technol.*

22 A. Saxena, T. T. Shih and H. A. Ernst, *Proc. 15th Natl. Symp. on Fracture Mechanics*, in *ASTM Spec. Tech. Publ. 833*, 1984, pp. 516–531.

23 C. Y. Hui, *Proc. 2nd Symp. on Elastic–Plastic Fracture*, Vol. I, *Inelastic Crack Analysis*, in *ASTM Spec. Tech. Publ. 803*, 1983, pp. I-573–I-593.

24 A. Saxena, J. D. Landes and H. A. Ernst, *Int. J. Fract., 23* (1983) 245–257.

25 A. Saxena and J. D. Landes, in S. R. Vallari, D. M. Taplin, P. Rama Rao, J. F. Knott and R. Dukey (eds.), *Advances in Fracture Research, Proc. 6th Int. Conf. on Fracture, New Delhi, December 4–10, 1984*, Pergamon, Oxford, 1985, pp. 3977–3988.

(19)

6K-54596T/—MEPL—/HITEMP/1R7017

A. Saxena and B. Gieseke**

Transients in Elevated Temperature Crack Growth

REFERENCE Saxena, A. and Gieseke, B., **Transients in elevated temperature crack growth.** ***High Temperature Fracture Mechanisms and Mechanics,*** EGF6 (Edited by P. Bensussan) 1990, Mechanical Engineering Publications, London, pp. 000–000.

ABSTRACT Transients which affect the crack growth behaviour of metals at elevated temperature under cyclic and static loading are classified as: (1) deformation transients which are present due to the relaxing crack tip stress fields during small scale creep, and (2) damage or crack growth transients which are present during the period in which a steady-state damage state evolves at the crack tip starting from an initially undamaged state.

It is shown using extensive creep and creep–fatigue crack growth data on 1Cr–1Mo–0.25V steel that deformation transients under static as well as cyclic loading are completely normalized by the C_t parameter. It is also shown that the other crack tip parameters such as K, C^*, and $C(t)$ are unable to normalize the influence of deformation transients. However, C_t fails to uniquely characterize the crack growth rate during the damage or crack growth transient.

Introduction and background

Recently, considerable progress has been made in the understanding of micromechanics of damage development in the vicinity of crack tips subjected to creep deformation (1)–(5). Also, experimental studies have been conducted to evaluate crack tip parameters for characterizing creep crack growth behaviour under steady-state and under transient conditions (6)(7). The objective of this paper is to evaluate the suitability of the different crack tip parameters for characterizing the crack growth behaviour under two primary types of transient conditions. These include: (1) deformation transients due to the relaxing stress fields under small-scale creep (SSC) resulting in an expanding crack tip creep zone, and (2) crack growth transients associated with the initial portions of the test during which a steady-state damage pattern develops.

Considerable crack growth data are assembled from previous experimental studies to document the presence of the above transients and to also identify some possible approaches to predict crack growth behaviour in their presence. The nature of the various transients is first discussed in detail. We will be restricting our primary discussion to sharp, Mode I (Fig. 1) cracks in materials which deform elastically and by power-law creep. The uniaxial version of the material constitutive law is as follows

$$\dot{\varepsilon} = \dot{\sigma}/E + A\sigma^n \qquad (1)$$

* Fracture and Fatigue Research Laboratory, School of Materials Engineering, Georgia Institute of Technology, Atlanta, GA 30332-0245, USA.

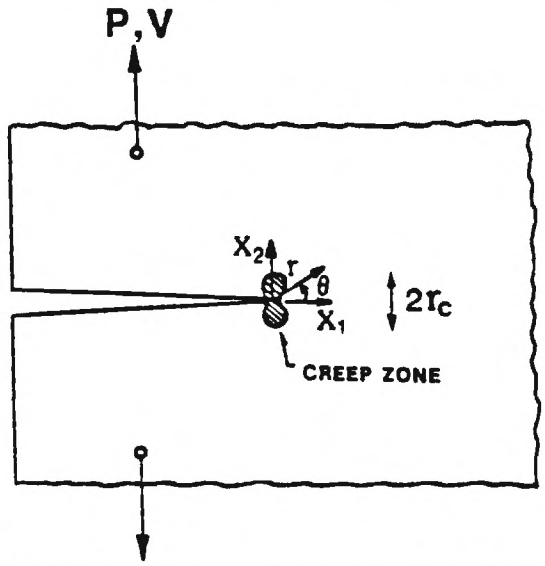

Fig. 1. Mode I crack subjected to load at elevated temperature

where, $\dot{\varepsilon}$ is strain rate, E = elastic modulus, σ = applied stress, and A and n are the power-law creep constants.

Deformation transients

The plane strain Mode I stationary crack subject to a constant load has been investigated by Ohji *et al.* (8), by Riedel and Rice (9), and by Bassani and McClintock (10). The instantaneous response is elastic and the crack tip stress field ($r \to 0$) is completely specified by the stress intensity parameter, K. As time elapses, a time-dependent crack tip stress field which resembles the HRR fields in elastic–plastic fracture mechanics (11)(12) evolves. The crack tip stress is then given by the following equation

$$\sigma_{ij} = \left[\frac{C(t)}{AI_n r}\right]^{1/(n+1)} \tilde{\sigma}_{ij}(\theta, n) \tag{2}$$

where, $\tilde{\sigma}_{ij}(\theta, n)$ and I_n are the HRR field quantities listed in tabular form in reference (13). $C(t)$ is an amplitude factor which is given by the following equation (14)

$$C(t) = \frac{(1-\nu^2)K^2}{(n+1)Et} + C^* \tag{3}$$

where, ν = Poisson's ratio, t = elapsed time, and C^* is a path-independent integral defined in several papers (15). C^* also represents the steady-state value of $C(t)$ when power-law creep dominates the entire specimen (or component). At short times, $C(t)$ is dominated by the first term on the right hand side of

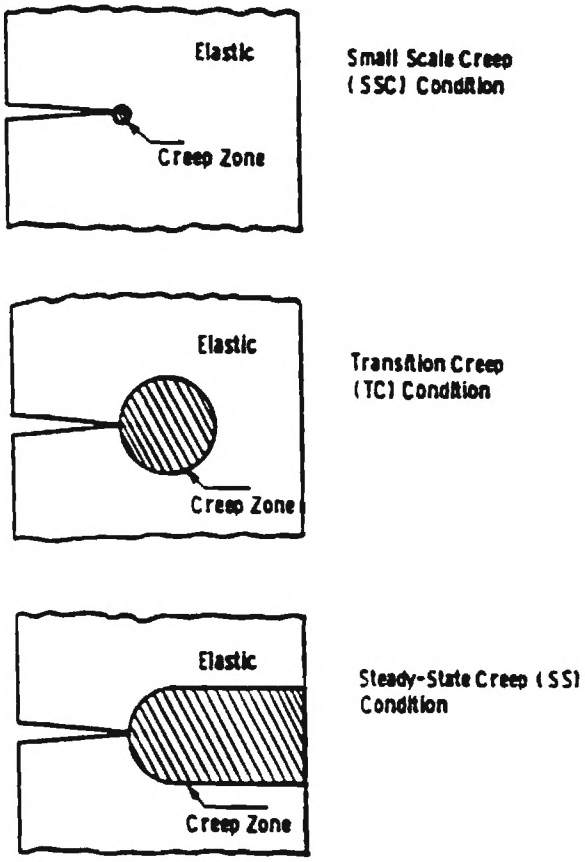

Fig. 2. Schematic representations of the levels of creep deformation under which creep crack growth can occur

equation (3) and small-scale-creep (SSC) conditions prevail. Figure 2 schematically shows the three regimes, namely, the SSC, the transition creep (TC) regime, and the steady-state (SS) regime of extensive creep. The creep zone size $r_c(\theta, t)$ under SSC conditions is given by (9) equation (4)

$$r_c(\theta, t) = \frac{1}{2\pi} K^2 \left\{ (EAt) \frac{I_n(n+1)}{2\pi(1-\nu^2)} \right\}^{2/(n-1)} \tilde{r}_c(\theta) \tag{4}$$

where, $\tilde{r}_c(\theta)$ is an angular function and is described in reference (9).

Under SSC and TC conditions, the crack tip creep zone size as well has the crack tip stress field are continuously changing with time giving rise to a transient condition, labelled deformation transient. If slow crack growth is occurring such that the rate of crack growth, $\dot{a}$, is much smaller than the rate of expansion of the creep zone size, $\dot{r}_c$, it can be argued that the crack tip driving force decreases with time for a constant, K. It is then interesting to

determine if $\dot{a}$ correlates uniquely with any crack tip parameter under such transient conditions. A candidate crack tip driving force parameter can be $C(t)$ which is a measure of the instantaneous amplitude of the crack tip stress field. Further, the parameter $C(t)$ is a local crack tip parameter which cannot be measured at the loading pins in a specimen; it's value can be calculated from equation (3) only.

Saxena (7) has proposed an alternate crack tip parameter, C_t, which is based on the stress–power release rate and can be measured at the loading pins. This parameter converges to C^* by definition when steady-state conditions prevail much like $C(t)$. C_t is defined as follows

$$C_t = -\frac{1}{B}\frac{\partial U_t^*}{\partial a} \tag{5}$$

where, U^* is the instantaneous stress–power release rate and B = thickness of the body. The following expression can be used to estimate C_t from the measured load, P, and the load-line deflection rate due to creep, $\dot{V}_c$.

$$C_t = \frac{P\dot{V}_c}{BW} F'/F - C^*\left(\frac{F'/F}{\eta} - 1\right) \tag{6}$$

where, W = width of the body, F is the K-calibration factor given by $F = (K/P)\, BW^{1/2}$, $F' = \mathrm{d}F/\mathrm{d}(a/W)$, and η is a geometry and crack size dependent parameter used in the calculation of C^* (16)

$$C^* = \frac{P\dot{V}_{ss}}{BW}\eta \tag{7}$$

where, $\dot{V}_{ss}$ = steady-state deflection rate. For details of C_t estimation, the readers are referred to earlier papers (7)(17). C_t has recently shown (17)(18) to be uniquely related to the rate of expansion of the creep zone under SSC conditions by the following relationship

$$(C_t)_{ssc} = 2(1 - \nu^2)\frac{K^2}{EW} F'/F \cdot \beta \dot{r}_c \tag{8}$$

where, β = scaling factor which can be determined numerically. Recent finite element calculations (17)(18) for compact type and centre crack tension geometries have confirmed the relationship between $(C_t)_{ssc}$ and $\dot{r}_c$ beyond reasonable doubt. This relationship makes C_t a unique parameter which can be both measured at the loading pins and also be related to the rate of expansion of the crack tip creep zone size.

Combining equations (4) and (8), an analytical expression for estimating C_t can be derived for elastic, power-law creep as follows

$$C_t = \frac{4\alpha\beta\bar{r}_c(\theta)}{E(n-1)}(1 - \nu^2)K^4 \frac{F'}{WF}(EA)^{2/(n-1)} - t^{(n-3)/(n-1)} + C^* \tag{9}$$

In summary, there are two candidate crack tip parameters, $C(t)$ and C_t for correlating creep crack growth behaviour in the presence of deformation transients. $C(t)$ is based on the instantaneous amplitude of the crack tip stress field and C_t relates to the rate of expansion of the creep zone. Both parameters collapse to C^* when steady-state conditions are reached. C_t can be measured at the loading pins while $C(t)$ can only be calculated. In a later section, both parameters will be evaluated using the same set of creep crack growth data.

Damage or crack growth transients

Several analytical studies have modelled creep crack growth as a process governed by nucleation, growth, and coalescence of grain boundary cavities **(1)(2)(4)**. These studies have focused mostly in the steady-state creep regime where crack growth rate has been shown to be governed by C^*. The experimental evidence supports such a mechanism for slow crack growth **(5)**. In this discussion, we will first focus on steady-state conditions with regard to deformation transients by assuming that the extensive creep conditions dominated by C^* prevail. Under these conditions it is intuitively appealing to think that a unique relationship between $\dot{a}$ and C^* can only be achieved if the state of creep damage in the form of cavitation within the process zone ahead of the crack tip is a characteristic of the applied C^* level. In other words, at any given time, the size, spacing, and the number of cavities ahead of the crack tip are only a function of C^*, and as the crack tip advances, the state of damage moves with it in a self-similar manner. However, it takes a certain amount of crack extension in order to achieve a steady-state level of crack tip damage, as explained below.

When the crack tip is first subjected to creep deformation at the beginning of the test, the cavity closest to the crack tip grows from its nucleation size to the coalescence size. This situation is compared with one following a substantial amount of crack extension in which the cavities grow significantly past their nucleation size before reaching the position of the cavity nearest to the crack tip. Hence, the time needed to grow this cavity to the coalescence size is expected to be smaller than the time required to grow the former. Thus, during the transient period of crack extension, a steady-state relationship between $\dot{a}$ and C^* is not expected. The existing experimental data tend to show this behaviour which is schematically illustrated in Fig. 3. In this figure, it is shown that tests begun at different C^* values have a non-unique $\dot{a}$ vs C^* relationship until the crack extends a certain distance. After some crack extension has occurred, the results from the three tests fall on the same trend. Actual data supporting such trends is shown later in the paper.

Transients during cyclic loading

Both deformation and crack growth transients can exist during cyclic loading at elevated temperature. For simplicity, a trapezoidal loading waveform with a

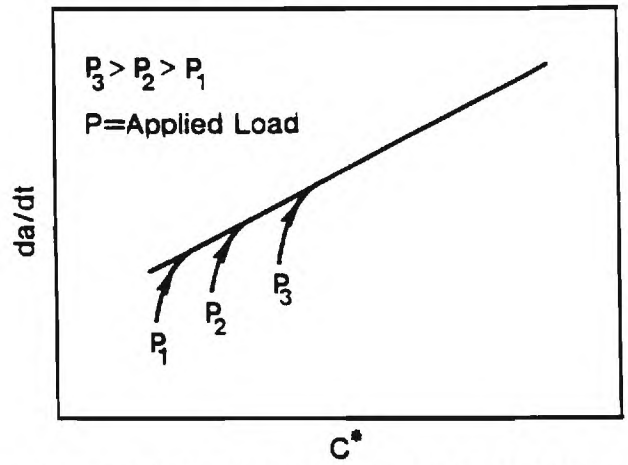

Fig. 3. Schematic illustration of the crack growth transients during the early portion of creep crack growth test

fast loading/unloading segment and a hold time in between will be considered. This is equivalent to a situation in which a static load is periodically interrupted by a unloading event. The unloading and reloading is accomplished in a time much smaller than the time between successive interruptions, also called the hold time, t_h. Also, t_h is much smaller than the transition time, t_T, from SSC to SS conditions given by the following relationship (9)

$$t_T = \frac{K^2}{E(n+1)C^*} \tag{10}$$

Thus, we will be restricting the discussion here to SSC conditions and also to situations where no creep deformation is occurring during the loading/unloading portions of the cycle.

Figure 4(a) schematically shows the various deformation zones in the vicinity of the crack tip, and Fig. 4(b) shows the expected stress–strain behaviour within the various deformation zones. If both small-scale-yielding (SSY) as well as small-scale-creep (SSC) are assumed, the stress–strain behaviour in Region 1 is linear-elastic. In Region 2 (the monotonic plastic zone), monotonic plasticity occurs during the first loading cycle, but no reversed plastic deformation occurs. In Region 3 (cyclic plastic zone), reversed plasticity occurs but no substantial creep deformation during the hold period occurs. In Region 4 (creep zone), substantial creep deformation occurs during the hold time, which is reversed during the unloading portion of the cycle via plastic deformation. The extents of creep, cyclic, and monotonic plastic zones depend on the applied K level, the rate of creep deformation, and the hold time. It is by no means implied in Fig. 4 that the creep zone is always contained in the cyclic zone, which in turn is contained in the monotonic zone. Region 4 can be larger than Region 2 for sufficiently large hold times. However, for short hold times

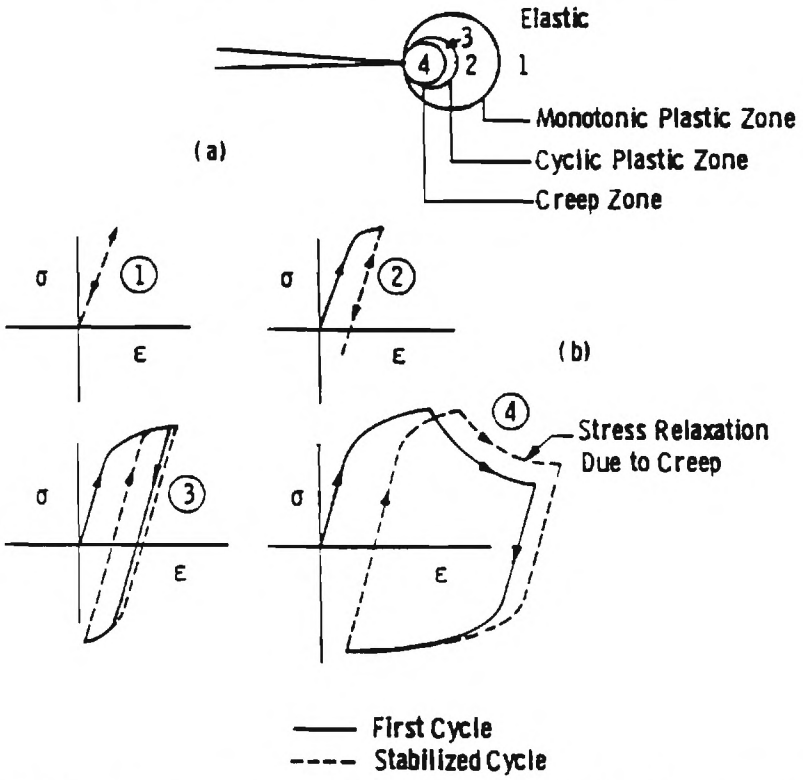

Fig. 4. (a) The various deformation zones in the crack tip region during fatigue at elevated temperature.
(b) The schematic stress–strain behaviour of material elements located within the various zones in the crack tip region under dominantly elastic conditions subjected to the square waveform

the creep zone will be contained within the cyclic plastic zone, which will always be within the monotonic plastic zone. During the period in which the creep zone (Region 4) grows through the cyclic plastic zone (Region 3), a creep–fatigue interaction can be expected to occur. This will give rise to crack growth as well as deformation transients, because the fatigue loading will influence the creep deformation rates as well as the rate of damage accumulation.

Analysis of crack growth data

All data analyzed in this paper was obtained on a single heat of 1Cr–1Mo–0.25V steel manufactured in accordance with the ASTM *Specification for Vacuum-Treated Carbon and Alloy Steel Forgings for Turbine Rotors and Shafts (A 470, Class 8)*. The tensile and steady state creep properties have been extensively characterized at 427, 482, and 538°C in previous papers (7)–

(9). The pertinent creep constants, equation (1), were taken as 5.18×10^{-31} $(\text{MPa})^{-n}\ \text{hr}^{-1}$, $n = 10.5$, with Young's modulus taken as 1.62×10^5 MPa. For additional data, the reader is referred to the earlier papers.

Analysis of creep crack growth test data

Creep crack growth tests were conducted at 538°C on eight, standard 25.4 mm (1 in) thick compact-type (1T-CT) specimens subjected to dead weight loading in lever-type creep machines. The load-line deflection was recorded periodically during all the tests. In two of the tests, the crack length was monitored using the electric potential drop method (20). The crack growth rates during these tests were calculated using the secant method. In other tests, the cracks were grown only a short distance and the crack extension was measured directly from the fracture surfaces. The crack growth rates, da/dt were calculated by dividing the crack extension by the test time. The da/dt data were correlated with crack tip parameters, K, C^*, $C(t)$, and C_t. The results of these correlations will be discussed in the next section. In the following discussion, the procedure used for calculating the crack tip parameters are described.

K was calculated using the standard expression given by Srawley (21).

For calculating C^* using equation (7), a steady-state deflection rate, $\dot{V}_{ss}$, is required but it cannot be measured unless the test itself is under steady-state conditions. Since none of our tests were entirely under steady-state conditions, an expression was used to calculate C^* in which the steady-state deflection rate was analytically estimated. That expression is given as follows for CT specimens (6)(22)

$$C^* = \frac{AW}{(1 - a/W)^n} h_1 \left(\frac{P}{1.455\ \alpha_1 B} \right)^{n+1} \tag{9}$$

In this equation, A and n represent the steady-state creep constants, W = the specimen width, B = the specimen thickness, and P = the applied load. The factor α_1 is given by the equation

$$\alpha_1 = [\{2a/(W - a)\}^2 + 4a/(W - a) + 2]^{1/2} - \{2a/(W - a) + 1\} \tag{10}$$

and $h_1\ (a/W, n)$ is a dimensionless calibration function given in (22).

The crack tip parameter $C(t)$ was calculated using equation (3). To obtain an average value of $C(t)$ during a time interval, equation (3) was integrated with respect to time and divided by the time interval. The values of K and C^* were considered as constant within the small crack length interval and were calculated at the average crack length for the interval. Thus, the average $C(t)$ during the interval $t_i \leqslant t \leqslant t_{i+1}$ is given by the following equation

$$C(t) = \frac{1}{t_{i+1} - t_i} \frac{K^2}{E(n + 1)} \ln \left(\frac{t_{i+1}}{t_i} \right) + C^* \tag{11}$$

In cases where t_i was zero it was assumed to be 1 second to avoid the singularity.

The average value of C_t over an interval $t_i \leqslant t \leqslant t_{i+1}$ was calculated using equation (6). F'/F, C^*, and η were calculated for the average a/W over the interval. The deflection rates were calculated as follows

$$\dot{V}_i = (V_{i+1} - V_i)/(t_{i+1} - t_i) \tag{12}$$

The deflection rate due to creep was estimated by using the expression (23)(24)

$$\dot{V}_c = \dot{V} - \frac{\dot{a}B}{P}(2K^2/E) \tag{13}$$

Analysis of fatigue crack growth data with hold times

Fatigue crack growth rate behaviour of the Cr–Mo–V steel was characterized at 538°C for loading waveforms which included hold times of 0 s, 50 s, 0.5 h, and 24 h (25)(26).

The tests with 0 and 50 second hold times were conducted on 1T-CT specimens in servo-hydraulic test machines. The crack length was monitored by the electric potential drop method. The 0.5 and 24 hour hold time tests were conducted on creep machines in which the tests were periodically cycled by unloading followed by reloading. The unloading and reloading times during all the hold time testing was on the order of 0.5 seconds. The 0.5 hour hold time test was conducted on a 1T-CT specimen. The twenty-four hour hold time tests were conducted on multiple-edge-crack (MEC) specimens. The MEC specimens contained five shallow edge cracks of different sizes. These specimens were cycled constant load amplitude for periods of six months to a year and then the specimens were broken open at the various crack locations to determine the crack extension. Thus, five crack growth rate data points were obtained from each test. The overall cyclic crack growth rate da/dN, was correlated with ΔK in earlier studies (25)(26). The time rate of crack growth during the hold time were correlated with the average value of the C_t parameter during the hold time as a part of this study.

The above cyclic tests were conducted in a dominantly small-scale creep regime. The longest hold time of 24 hours was much smaller than the smallest transition time, t_T (equation (10)) which was at least 585 hours. Hence, the transient term in equation (9) will dominate the magnitude of C_t and the C^* term can be neglected. Thus, the average C_t is given by the following equation

$$C_t|_{avg} = \frac{1}{t_h}\int_0^{t_h} C_t \, dt \tag{14}$$

In order to estimate C_t, it was necessary to determine the values of F'/F for the MEC specimens. Since the cracks were small, the F'/F values for single-edge-notch (SEN) specimens were used. Finite element analysis was performed on the specimens (27) to assure that virtually no interaction occurred between the various cracks. Thus, the use of SEN K-calibration expressions is justified.

The average crack growth rate during the hold time was calculated as follows

$$da/dt\,|_{avg} = \left\{\frac{da}{dN} - \left(\frac{da}{dN}\right)_0\right\} \cdot \frac{1}{t_h} \qquad (17)$$

where $da/dt\,|_{avg}$ is the average da/dt value during the hold time and $(da/dN)_0$ is the crack growth rate per cycle for zero hold time. Therefore, the fatigue contribution to the overall cyclic crack growth rate was subtracted in order to estimate the average da/dt during the hold time.

Results and discussion

In this section, the results of the crack growth rate correlations with the various crack tip parameters are presented and subsequently discussed in light of the three types of transients described in Section 1. First, the creep crack growth rate data are discussed and then the results of the fatigue with hold time tests will be discussed.

Creep crack growth data

Correlation between da/dt and K

The correlation between creep crack growth rate, da/dt, and K is presented in Fig. 5. In general, da/dt increases with K for a given specimen, but the correlation does not appear to be unique for two reasons. The first is the possible violation of the small-scale-creep condition in the test specimens. This can be examined further by comparing the test time with the transition time, t_T. Table 1 lists some typical test times along with the transition times based on the average crack length during the various tests. From these comparisons, it appears that significant creep deformation could have occurred during the tests and may have caused the lack of correlation between da/dt and K. However, the above transition time calculation is valid only for a stationary crack, and when moving crack considerations are taken into account, the extent of creep deformation can be significantly less in the test specimen than predicted by equation (10). The second reason for lack of correlation between da/dt and K is due to the non-uniqueness of the relationship between K and

Table 1. Total test times compared with the transition test times, t_T, for creep crack growth tests

Test time (hrs)	t_T *(hrs)*
2035	64 298
760	499
950	3124
4203	7118
4847	21 379
220	373

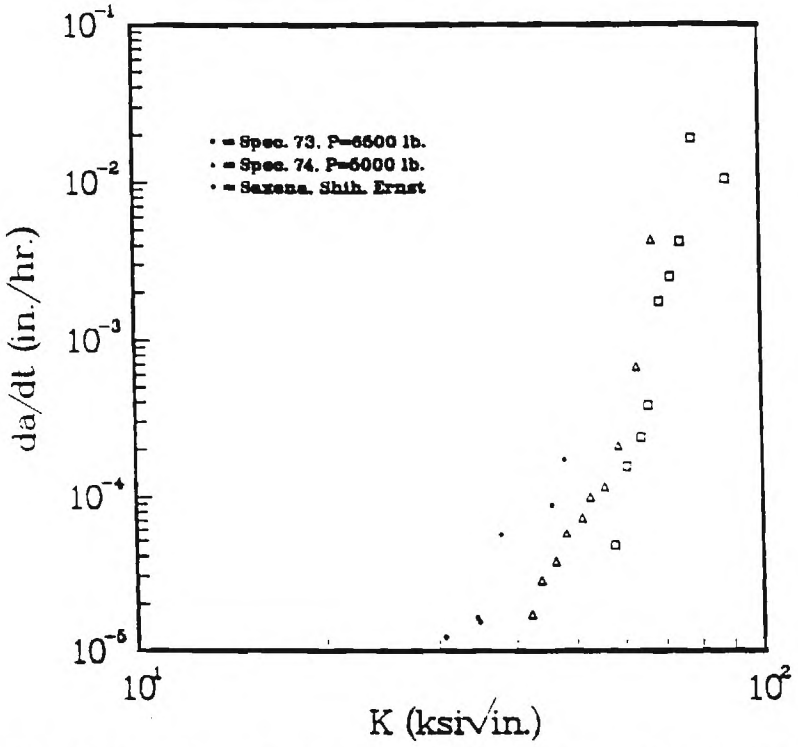

Fig. 5. Correlation between creep crack growth rate and the stress intensity parameter, K

the crack tip stress, even under SSC conditions. This is evident upon examination of equations (2) and (3). Under SSC conditions, the crack tip stress field characterized by $C(t)$ is clearly a function of K and time, t, and not just K. The creep zone size and its rate of expansion are similarly dependent on K and time under SSC conditions, equation (4). However, equations (2)–(4) are for stationary cracks and the conditions for moving cracks are different. A general and complete crack tip stress field solution for a growing crack under creep conditions is not available. Some early work of Hui and Riedel (28), recent work of Hawk and Bassani (29), and by Hui (30) may be used to make qualitative arguments on when a unique relationship between da/dt and K can be expected. This is further explained below.

We consider a moving Cartesian coordinate system attached to the crack tip with its x axis located along the crack plane and perpendicular to the crack front. Under SSC conditions, K controlled crack growth can occur only if $\partial\sigma(x, t)/\partial t = 0$, where, $\sigma(x, t)$ represents the crack tip stress. This is possible only if the creep zone is non-existent or its size remains constant with time. In other words, $\dot{r}_c = 0$. The numerical results of Hawk and Bassani (29) in Mode III (Fig. 6) show that such a condition is theoretically possible (at least in an approximate way). In Fig. 6, the creep zone size is normalized by a reference

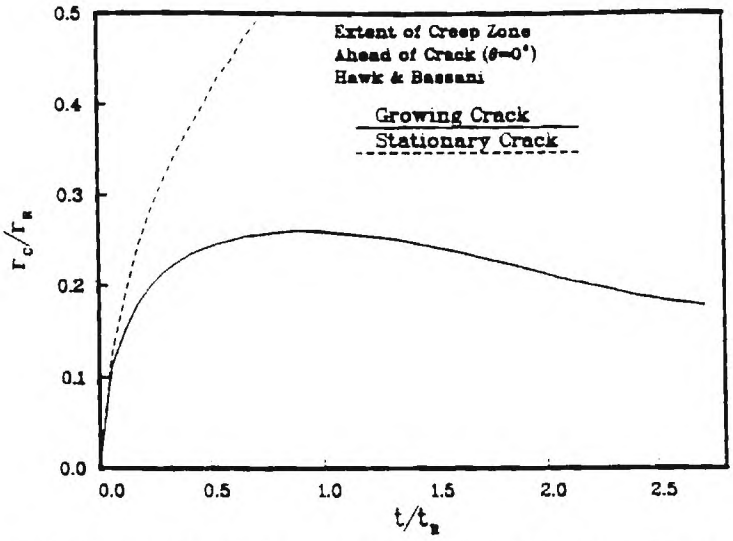

Fig. 6. Normalized creep zone size as a function of normalized time for a growing and stationary crack in Mode III (from Hawk and Bassani (29))

creep zone size, r_R, and is plotted as a function of time normalized by a reference time t_R. The creep zone size for a stationary crack is also shown for comparison. Up to a t/t_R value of 2.0, $\dot{r}_c$ is non zero, therefore steady-state relationship between da/dt and K is not expected. For $t/t_R > 2.0$, the creep zone size appears to be approaching a constant size and a unique da/dt vs K relationship may be obtained. The amount of crack extension prior to attainment of steady-state conditions is dependent on da/dt and the creep properties. It is expected that K-dominated conditions will be promoted for extremely creep brittle materials and at high da/dt values. More experimental work is needed in order to determine a quantitative criterion for K-controlled creep crack growth.

Another result which can be derived from Fig. 5 is that the creep zone size ahead of a moving crack is smaller than predicted from stationary crack considerations. Therefore, for growing cracks, the conditions of SSC prevail for longer periods than predicted by transition time, t_T, equation (10).

Correlation between da/dt *and* C^*

Figure 7 shows that the correlation between da/dt and C^* is not good. Since a significant portion of the various tests were in the SSC and TC regions where C^* is not valid as a crack tip parameter, this result is not surprising.

Correlation between da/dt *and* C(t)

The correlation between da/dt and $C(t)$ is shown in Fig. 8. A unique correlation appears to be lacking. The crack tip parameter $C(t)$ accounts for the stress relaxation at the crack tip due to creep in the SSC and the TC regions

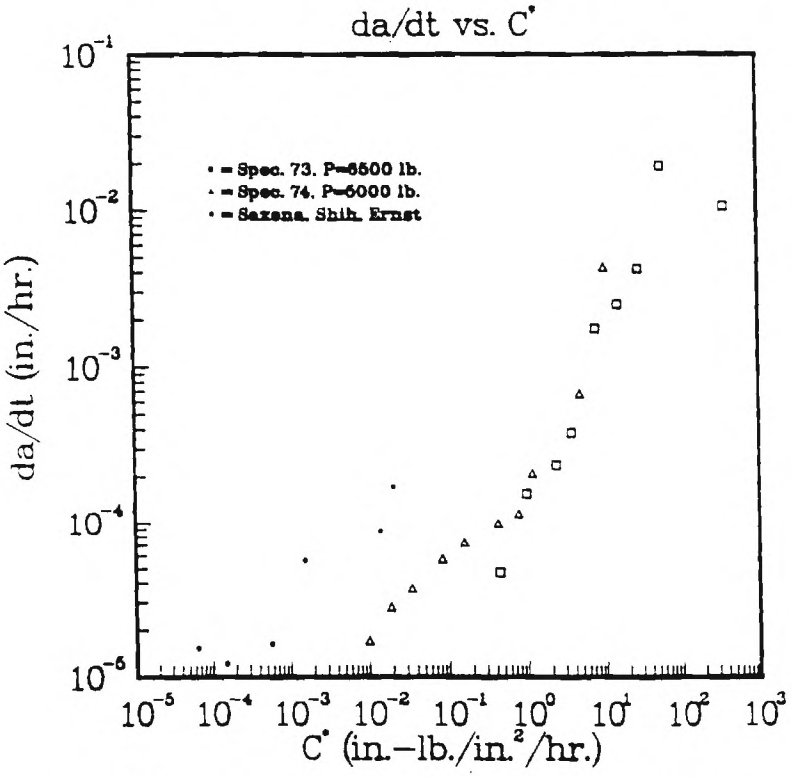

Fig. 7. Correlation between creep crack growth rate and the C^* integral

and characterizes the amplitude of the HRR fields for stationary cracks. However, when growing crack effects become significant over the creep zone, $C(t)$ loses its significance because, as shown by the finite element analysis of Hawk and Bassani (29), HRR type stress fields are annihilated. The new singularity which develops at the crack tip is not of HRR type (28). This explains the lack of correlation between da/dt and $C(t)$.

Correlation between da/dt and C_t

Figure 9 shows the same creep crack growth data which was plotted in Figs 5, 7, and 8 but correlated with the C_t parameter. There is an excellent correlation between da/dt and C_t. The two slashed points represent data from the very early portion of the test. The reason for why they do not fall in the general trend will be discussed later.

The C_t parameter is uniquely related to the rate of expansion of the creep zone size, equation (8), and the stress power release rate, equation (5) in the SSC regime. Neither of these definitions of C_t are affected by crack growth. In estimating C_t, the creep zone expansion rate should be determined from an appropriate analysis. When deflection rates are measured and used to estimate

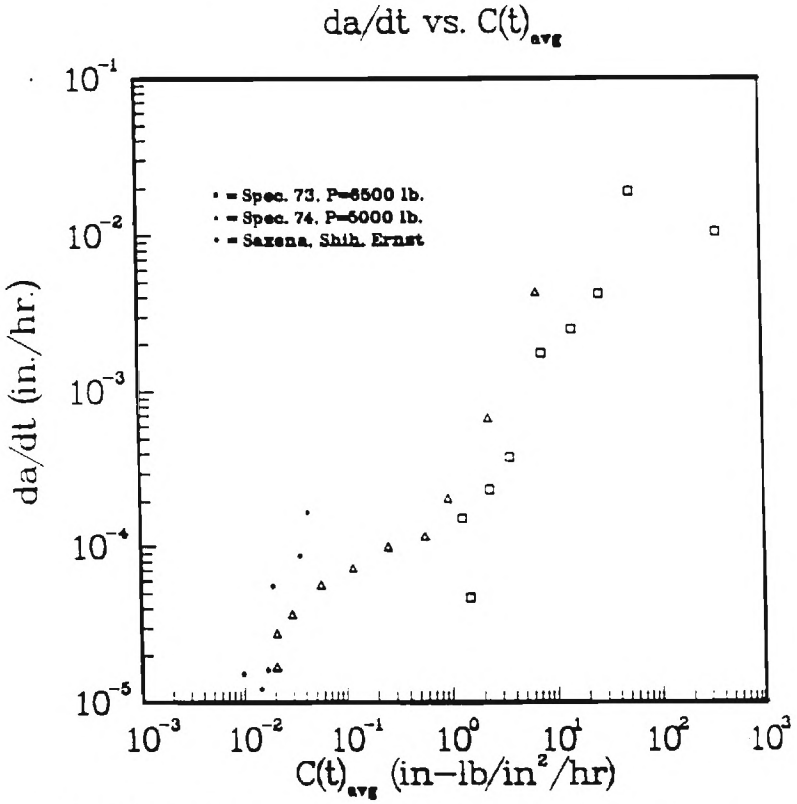

Fig. 8. Correlation between creep crack growth rate and the $C(t)$ parameter

C_t such as in equation (6), the influence of the growing crack on the crack tip stress field is automatically reflected in the measured value of the deflection rate due to creep. Similarly, the influence of primary and tertiary creep is also included in the measured deflection rates of specimens (31).

In the correlation between da/dt and C_t shown in Fig. 9, there are data which were obtained under a variety of conditions, ranging from SSC to extensive creep or SS conditions. The following parameter, τ, determines the extent to which transient conditions exist in the specimen. τ is defined by

$$\tau = \frac{C^*}{C_t} \tag{15}$$

For SSC conditions, $\tau \ll 1$. For extensive creep conditions $C_t = C^*$ therefore, $\tau = 1$. The values of τ ranged from 10^{-2} to essentially 1 for the various points included in Fig. 9. It is clear that the data span a wide variety of conditions ranging from SSC to SS. Recently, several other experimental studies have shown that creep crack growth rate over a wide range of conditions correlate

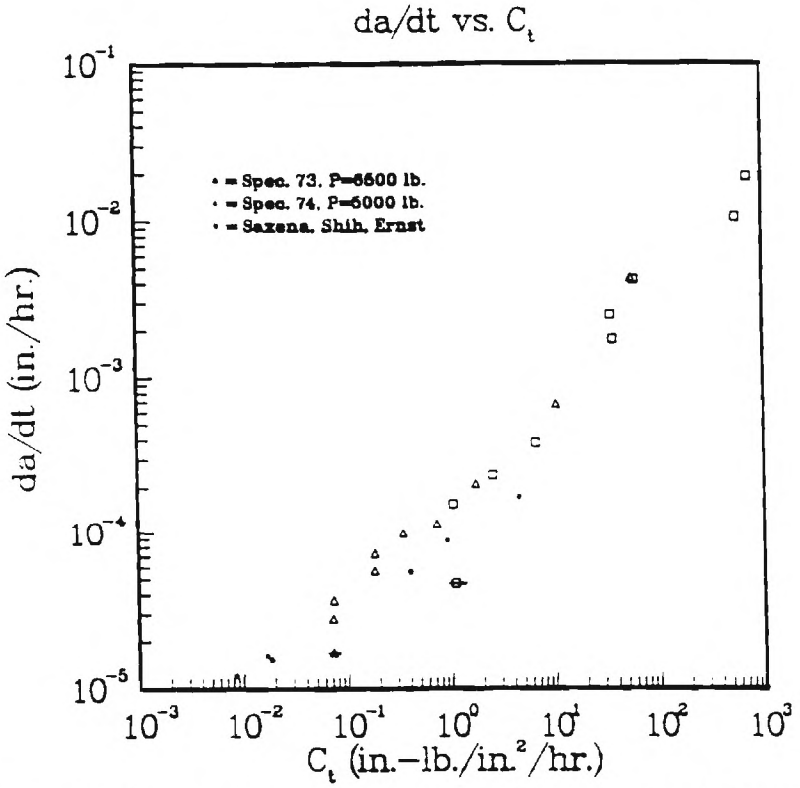

Fig. 9. Correlation between creep crack growth rate and the C_t parameter: slashed points represent data from the very early portion of the test

extremely well with C_t (32). Hence, it can be stated that C_t is able to account for the influence of deformation transients adequately.

The two slashed points from the very early portions of the test were in the region where crack growth transients operate. A rough estimate of this region is 0.25 mm. The analytical calculations show that the crack should advance by fifteen intercavity distances before steady-state crack growth rates can be established (4). If intercavity distance is on the order of 10 μm, the amount of crack extension required prior to establishment of steady-state is 0.15 mm. This compares favourably with the experimental findings.

Creep–fatigue crack growth data

Figure 10 shows the average time rate of crack growth (equation 15) during the hold time for hold times of 50 s, 30 minutes and 24 h. The data for each hold time are plotted with a different symbol and are correlated with the average C_t parameter estimated from equation (14). For comparison, the creep crack growth data are plotted in the same figure for comparison. There appears to be an excellent correlation between the creep–fatigue crack growth

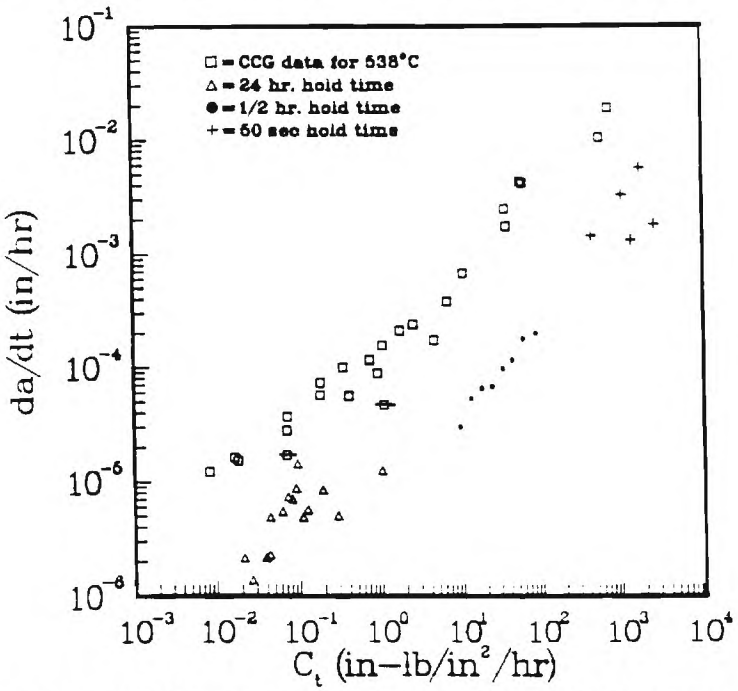

Fig. 10. Creep–fatigue crack growth rates as correlated with the C_t parameter

rates for various hold times when correlated with C_t. However, there is a significant difference between the crack growth rates under creep conditions and those under creep–fatigue conditions. This difference can be attributed to the crack growth transients introduced by unloading. Correlating the data with C_t does not account for these transients. On the other hand, the deformation transients from the expanding creep zone appear to be completely normalized when the crack growth rates are correlated with the C_t parameter.

The excellent correlation between da/dt and C_t during fatigue with hold time has several interesting implications. By inspecting equations (1) and (9) it is evident that, even for a given loading waveform and cycle time (constant t_h), the average C_t is not uniquely determined by K because of the additional crack size and geometry dependent term F'/F. However, in the past, fatigue crack growth data at elevated temperature have been routinely correlated with ΔK for constant loading waveforms and cycle times **(25)(26)(33)**. These correlations have been obtained with a simple specimen geometry, mostly CT specimens for which F'/F does not vary significantly over a wide range of crack length interval. Also, if the cycle times are small, the contribution of the time-dependent crack growth is small and the overall crack growth per cycle (da/dN) can be dominated by the cycle-dependent portion which correlates with K. Thus, it may be that the correlation between da/dN and ΔK observed in the past have been fortuitous. To the knowledge of the authors, there is no

elevated temperature crack growth data on the same material from two very different specimen geometries for long cycle times.

On the other hand, if da/dt were correlated with $C(t)$ for creep–fatigue crack growth, unique relationship between da/dN and ΔK for a constant cycle time and loading waveform is in fact implied. Figure 11 shows the same data correlated with the average $C(t)$ parameter, according to equation (12) with t_{i+1} taken as t_h and t_i taken as 1 s. The lack of correlation between the data for various hold times is clearly evident. Therefore $C(t)$ is unable to normalize the influence of deformation transients.

A significant difference between the da/dt values for creep and creep–fatigue crack growth exists for hold times of 24 h. If the hold time is increased further, this difference should gradually vanish. From these data it appears that the time needed for creep–fatigue interactions to vanish is much larger than 24 h at the load levels used during testing.

In correlating da/dt with C_t for creep–fatigue crack growth tests, the analytical expression, equation (9), was used to estimate C_t. For reducing the creep crack growth data the experimentally measured $\dot{V}_c$ values were utilized. A possibility exists that some difference between creep crack growth and creep–fatigue crack growth maybe due to differences in expression for estimating C_t.

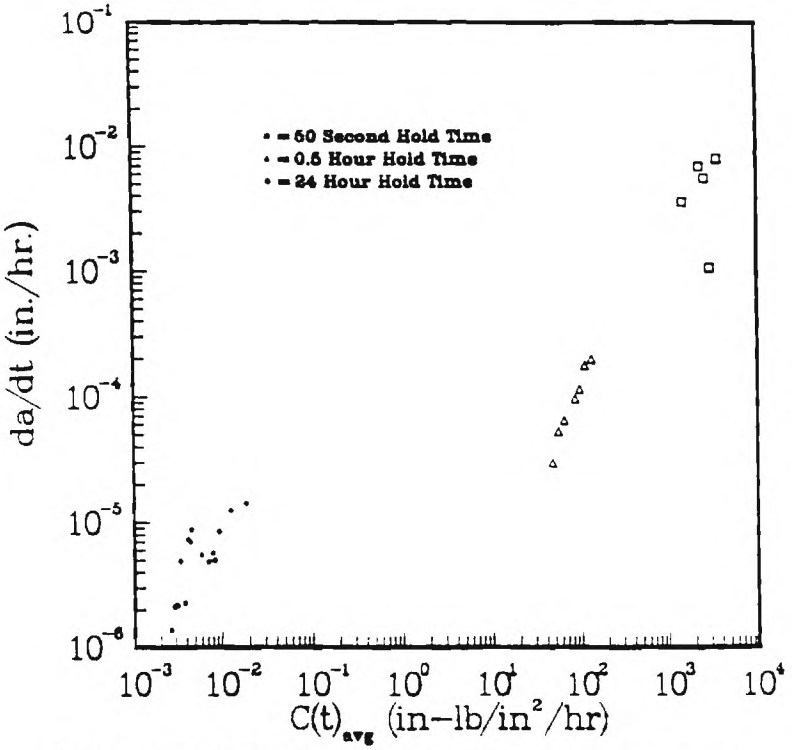

Fig. 11. Creep–fatigue crack growth data correlation with the $C(t)$ parameter

Specifically, the value of $\beta\tilde{r}_c(\theta)$ was chosen to be one because for CT specimens this value has been shown to give estimates of C_t (32) which agreed with experiments on 1.25Cr–0.5Mo steels. On the other hand, the finite element calculations yield a value of 0.13 for $\beta r_c(\theta)$ and the difference was thought to be due to the presence of primary creep. The extent of primary creep may be different for 1Cr–1Mo–0.25V steel used in this study as compared to the other steel. Therefore, the value of $\beta\tilde{r}_c(\theta)$ of one is not completely justified for this material and there is some uncertainty in the calculation of C_t for the creep–fatigue tests. However, the uncertainty factor is a constant; therefore, it does not influence the conclusions regarding the general trends. It is also unlikely that the discrepancy, if any, in the estimation of C_t is two orders of magnitude which is what it will take to collapse the creep–fatigue and creep crack growth into a single trend. Therefore, we feel that creep–fatigue interaction effects are strong. There is a need for developing models which will predict the extent of creep–fatigue interaction effects for making accurate life time predictions of elevated temperature components.

Summary and conclusions

In this paper, an effort was made to correlate creep crack growth rate data developed under conditions ranging from small scale to extensive creep on a 1Cr–1Mo–0.25V turbine rotor steel with several crack tip parameters. The data clearly show a lack of correlation with K, C^*, and the $C(t)$ parameters, but good correlation was obtained when the data were plotted with C_t. The creep–fatigue crack growth rates during hold times ranging from 50 s to 24 h and under small scale creep were also shown to correlate with C_t for the same material. The crack growth rate vs C_t relationship is significantly different for creep as compared with creep–fatigue conditions.

It was also shown that the transient crack growth characterized by non-unique da/dt vs C_t behaviour is observed early during creep crack growth tests. In reporting creep crack growth behaviour, it is recommended that the data developed over the first 0.25–0.5 mm of crack extension should be discarded to avoid the influence of such transients on the creep crack growth behaviour reported. Since such transient behaviour is important for component life times, it should be studied in greater depth.

Acknowledgements

The authors wish to acknowledge the financial support of the Department of Energy – Basic Energy Sciences Grant No. DE-FG05-86ER-45257 (Dr J. B. Darby, Project Manager) for conducting the research.

References

(1) WILKINSON, D. S. and VITEK, V. (1982) *Acta Met.*, **30**, 1723–1732.

(2) BASSANI, J. L. and VITEK, V. (1982) *Proceedings of the 9th National Congress of Applied Mechanics – Symposium on Non-Linear Fracture Mechanics* (Edited by L. B. Freund and C. F. Shih) pp. 127–133.

(3) RICE, J. R. (1981) *Acta Met.*, **29**, 657–681.
(4) HUI, C. Y. and BANTHIA, V. (1986) The Extension of Cracks at High Temperature by Growth and Coalescence of Voids, Cornell University, USA.
(5) JANI, S. and SAXENA, A. (1987) Influence of Thermal Aging on Creep Crack Growth Behavior, TMS-AIME Symposium, Denver, Colorado, USA.
(6) SAXENA, A. (1980) in *Fracture Mechanics: Twelfth Conference, ASTM STP 700*, pp. 131–151.
(7) SAXENA, A. (1986) in *Fracture Mechanics: Seventeenth Conference, ASTM STP 700*, pp. 185–201.
(8) OHJI, K., OGURA, K., and KUBO, S. (1979) *Japan Soc. Mech. Engrs*, No. 790–13, 18–20 (in Japanese).
(9) RIEDEL, H. and RICE, J. R. (1980) in *Fracture Mechanics: Twelfth Conference, ASTM STP 700*, pp. 131–151.
(10) BASSANI, J. L. and McCLINTOCK, F. A. (1981) *Int. J. Solids Structures*, **7**, 479–492.
(11) HUTCHINSON, J. W. (1968) *J. Mech. Phys. Solids*, **16**, 13–31.
(12) RICE, J. R. and ROSENGREN, G. F. (1968) *J. Mech. Phys Solids*, **16**, 1–12.
(13) SHIH, C. F. (1983) *Tables of Hutchinson–Rice–Rosengrem Singular Field Quantities*, Division of Engineering, Brown University, USA.
(14) EHLERS, R. and RIEDEL, H. (1981) in *Advances in Fracture Research*, ICF-5 (Edited by D. Francois) vol. 2, pp. 691–698.
(15) LANDES, J. D. and BEGLEY, J. A. (1976) in *Mechanics of Crack Growth, ASTM STP 590*, pp. 128–148.
(16) SMITH, D. J. and WEBSTER, G. A. (1983) in *Elastic–Plastic Fracture: Second Symposium, vol. I – Inelastic Crack Analysis, ASTM 803*, pp. 1654–1674.
(17) BASSANI, J. L., HAWK, D. E., and SAXENA, A. (1986) Evaluation of the C_t Parameter for Characterizing Creep Crack Growth Rate in the Transient Regime, *Third ASTM International Symposium on Nonlinear Fracture Mechanics* (in press).
(18) LEUNG, C., McDOWELL, D. L., and SAXENA, A. (1986) Evaluation of the C_t Parameter for Characterizing Creep Crack Growth Rate in the Transient Regime, *Third ASTM International Symposium on Nonlinear Fracture Mechanics* (in press).
(19) SAXENA, A., SHIH, T. T., and ERNST, H. A. (1984) in *Fracture Mechanics: Fifteenth Symposium, ASTM STP 833*, pp. 516–531.
(20) SCHWALBE, K. H. and HELLMAN, D. (1981) *J. Testing Evaluation*, **9**, 218–221.
(21) SRAWLEY, J. E. (1976) *Int. J. Fracture*, **12**, 475–476.
(22) KUMAR, V., GERMAN, M. D., and SHIH, C. F. (1981) An Engineering Approach to Elastic–Plastic Analysis, EPRI Report, NP 1931, Palo Alto, CA, USA.
(23) SAXENA, A., LANDES, J. D., and ERNST, H. A. (1983) *Int. J. Fracture*, **23**, 245–257.
(24) SAXENA, A. and LANDES, J. D. (1984) *Advances in Fracture Research*, ICF 84 (Edited by P. Rama Rao *et al.*) pp. 3977–3988.
(25) SAXENA, A., WILLIAMS, R. S., and SHIH, T. T. (1981) in *Fracture Mechanics: Thirteenth Conference, ASTM STP 743* (Edited by R. Roberts) pp. 86–99.
(26) SAXENA, A. and BASSANI, J. L. (1984) in *Fracture: Interactions of Microstructure, Mechanisms and Mechanics*, TMS-AIME, pp. 357–383.
(27) WILSON, W. K. (1982) unpublished research, Westinghouse R&D Center, Pittsburgh, PA, USA.
(28) HUI, C. Y. and RIEDEL, H. (1981) *Int. J. Fracture*, **17**, 409–425.
(29) HAWK, D. E. and BASSANI, J. L. (1986) *J. Mech. Phys Solids*, **34**, 191–212.
(30) HUI, C. Y. (1985) The Mechanics of Constantly Growing Crack in an Elastic Power-Law Creeping Material, Cornell University Report, USA.
(31) LEUNG, C., McDOWELL, D. L., and SAXENA, A. (1987) Primary Creep at Stationary Crack Tips – Implications to the C_t Parameter, *Int. J. Fracture*, submitted for publication.
(32) SAXENA, A. and LIAW, P. K. (1986) EPRI Contract Report CS 4688, Electric Power Research Institute, Palo Alto, CA, USA.
(33) JAMES, L. A. (1972) in *Stress Analysis and Growth of Cracks, ASTM STP 513*, pp. 218–229.

Fracture Mechanics: microstructure and micromechanisms

S.V. Nair, J.K. Tien, R.C. Bates, O. Buck

1989

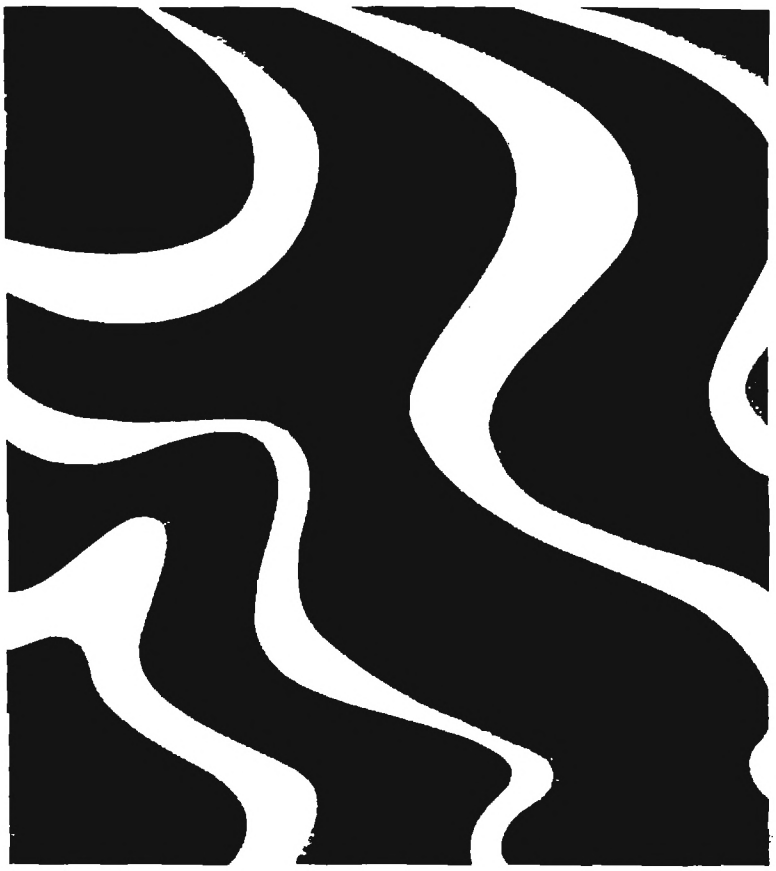

ASM INTERNATIONAL™

INTRODUCTION

ritical gas and steam turbine, power-plant boiler, and petrochemical ctor components that operate at elevated temperature tend to develop :ks during the early stages of service life. Some components contain ck-like defects even as they enter into service. These defects can grow l cause failures during service. Some examples of major failures in the ver industry involving elevated temperature components where creep s a major contributing factor are described in Ref 1 to 3. These failures ulted in millions of lost dollars in down-time and repair costs and, in some es, also loss of human lives.[2] Thus, crack growth under creep conditions a major industrial problem.

'urther impetus for studying creep crack growth comes from the need to ess the remaining life of components that have been in service and are proaching their originally predicted design life. More and more equip- nt operators such as the Air Force, Navy, utility companies, and rochemical companies are turning to a retirement-for-cause (RFC) ilosophy rather than rely on life predictions made several years ago that re based on concepts that are now out-dated.[4-7]

'ailures due to creep can be classified either as resulting from widespread bulk damage, or resulting from localized damage. Structural components at are vulnerable to bulk damage are subjected to uniform loading and iform temperature distribution during service, for example, thin-wall es. The life of such a component can be estimated from creep-rupture ta. On the other hand, components that are subjected to stress and nperature gradients (typical of thick section components) will not fail by ep rupture. It is more likely that, at the end of the predicted creep-rupture e, a crack develops at a critical location, which propagates and ultimate- causes failure. Figure 1 shows cracks in the interior of a steam header at had been in service for 24 years.[8] The cracks emanating from holes in- ated and propagated to some distance by thermal fatigue. However, the ntinued crack growth may have been due to creep from pressure stresses.

In this paper, the concepts of time-dependent fracture mechanics (TDFM) r characterizing creep crack growth behavior are reviewed. We start by rst describing the stresses in front of crack tips in creeping solids. This in- udes a discussion of the crack tip parameters for characterizing creep crack owth. The microscopic aspects of creep crack growth and the metallurgical riables affecting the creep crack growth behavior are discussed in the bsequent sections of this paper.

Fig. 1 Ligament cracks on the inside surface of the Mississippi Power and Light header used as test material in this study. (Courtesy of Babcock and Wilcox Co.)

Page missing from report

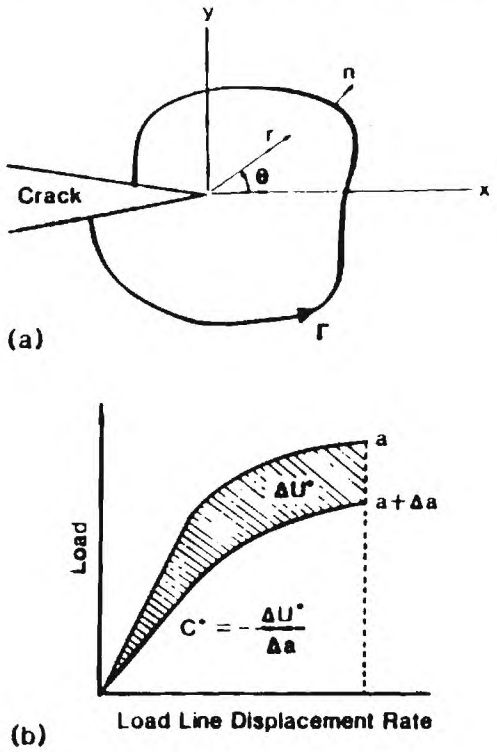

Fig. 3 (a) Crack tip coordinate system and arbitrary line integral contour. (b) Schematic illustration of the energy rate interpretation of C^*.

difference between two identically loaded bodies having incrementally differing crack lengths:

$$C^* = -\frac{1}{B}\frac{dU^*}{da} \tag{4}$$

where U^* is the power or energy rate defined for a load P and an associated load-line displacement rate, $\dot{V}$, as shown in Fig. 3(b); B is the thickness of the cracked body. The other property of C^* is its ability to uniquely characterize the stress distribution at the crack tip. For a power-law creep material, the crack tip stress is given by:[11]

$$\sigma_{ij} = \left| \frac{C^*}{AI_n r} \right|^{\frac{1}{1+n}} \tilde{\sigma}_{ij}(\theta,n) \tag{5}$$

where $\tilde{\sigma}_{ij}(\theta,n)$ is an angular function and I_n is a nondimensional constant

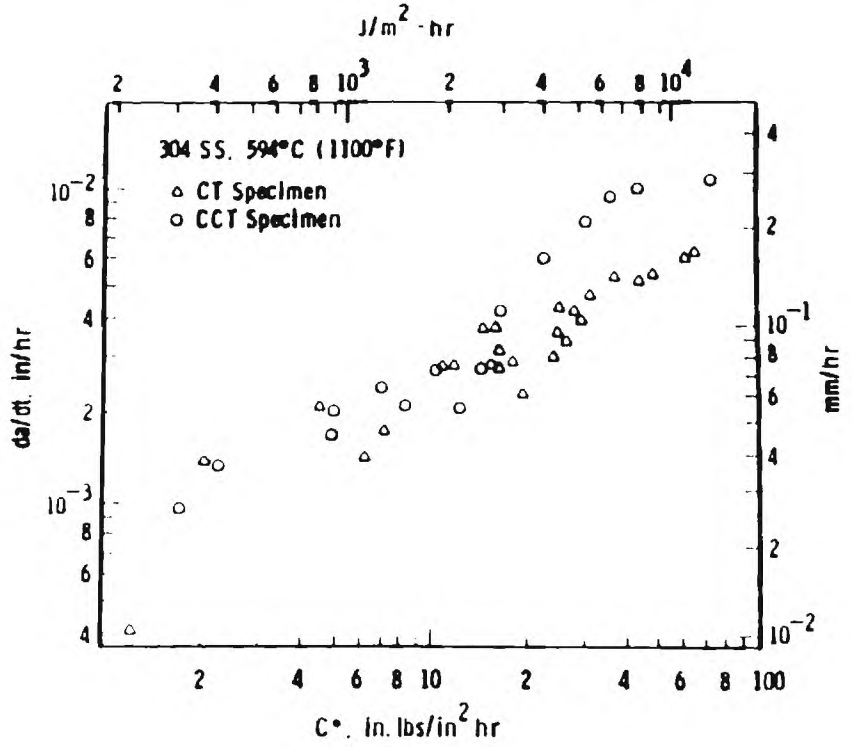

Fig. 4 Creep crack growth rate behavior of 304 stainless steel at 594 °C (1100 °F) as a function C^* for two specimen geometries.

with a value ranging between 3.8 and 6.3 for a range of n values. The numerical values of both are listed elsewhere.[12] Here, r is the distance from the crack tip.

Figure 4 shows a plot of creep crack growth rate, da/dt, as a function of the C^*-integral in 304 stainless steel obtained from specimens tested at 594 °C (1100 °F).[13] There is good agreement between data obtained from compact-type (CT) and the center-crack-tension (CCT) specimens. There is now considerable experimental evidence to show that under steady-state conditions C^* is able to characterize the creep crack growth rates.

In addition to calculating the value of the contour integral (Eq 2) or measuring it using Eq 4, there are two other methods of determining C^*. The first of these methods is suitable for determining C^* in test specimens where the load, the load-line deflection rates, and the crack size measurements are available. A number of investigators[14-16] have used this

Page missing from report

acked ligament length), the amplitude factor is given by the value of
h integral identical to C*, but defined very close to the crack tip where
p strains dominate the elastic strains.[20] In the extensive creep limit,
ame integral becomes path independent and is C*. In the SSC regime,
is also approximately given by Ref 19 to 22 for plane-strain conditions:

$$(C(t))_{ss} = \frac{(1 - \nu^2)K_I^2}{(n + 1)\,E\,t} \tag{13}$$

s defines the short-time behavior. For long times under constant applied
when extensive creep occurs everywhere in the specimen, C approaches
constant, steady-state value C*, which was discussed earlier. The tran-
on time t_1 between small-scale creep (SSC) and extensive creep is approx-
ted by setting the value of C(t) from Eq 9 equal to C*:[19,22]

$$t_1 = \frac{(1 - \nu^2)K_I^2}{(n + 1)\,E\,C^*} \tag{14}$$

equations for estimating K_I and C* are tabulated for several crack con-
urations in Ref 25 and 18, respectively. Ehlers and Riedel[21] have sug-
ted a convenient interpolation formula for approximately calculating
between SSC and extensive creep:

$$C(t) \equiv C^*(t_1/t + 1) \tag{15}$$

SSC, the creep zone is defined as the region around the crack tip where
creep strains exceed the elastic strains.[19] A measure of the creep zone
is denoted by r_c, which tends to grow in time; its radial extent around
crack tip as a function of K_I, t, and θ is:

$$r_c(\theta, t) = \frac{1}{2\pi}\left(\frac{K_I}{E}\right)^2 \left|\frac{(n + 1)AI_n tE^n}{2\pi(1 - \nu^2)}\right|^{\frac{2}{n-1}} \tilde{r}_c(\theta) \tag{16}$$

ere $\tilde{r}_c$ is a nondimensional function that can be approximated in terms
he $\tilde{f}_{ij}(\theta)$ and $\tilde{\sigma}_{ij}(\theta;n)$ functions, as plotted in Ref 19. Otherwise, $r_c(\theta,t)$ must
determined numerically. In the following, for plane-strain conditions
ause r_c is roughly maximum at $\theta = 90°$, we will refer to $r_c(\theta,t)$ as
$\theta = 90°,t)$. At $\theta = 90°$, $\tilde{r}_c(\theta) \approx 0.2$ to 0.5, depending on n.
C(t) can also be estimated by an integral that is evaluated locally in the
ack tip region, $r \to 0$.[20] The formulation of this integral is the same as
, except that it is not path independent in the transient regime. In the
ady-state regime C(t) = C*. Because C(t) is valid for the entire regime
tween small-scale creep and steady-state creep, it is an attractive can-
late crack tip parameter for characterizing creep crack growth.

The disadvantage of C(t) is that it cannot be measured in the transient regime. It can only be estimated from Eq 15. It also does not have the stress-power dissipation rate interpretation as C* does in the steady-state regime. However, as mentioned before, it does characterize the amplitude of the HRR field, which is a property it has in common with C*.

An alternate crack tip parameter, C_t, based on the stress-power dissipation rate was proposed by Saxena.[26] The magnitude of this parameter can be measured at the loading pins from small-scale creep to steady-state creep. Under steady-state conditions, $C_t \equiv C^* \equiv C(t)$. Recent work by Bassani *et al.*[27] has shown that C_t characterizes the rate of growth of the creep zone size and thus captures the history of deformation in the crack tip region. The definition of C_t is as follows.[26]

Based upon a partitioning of the load-line deflection, V, into a purely instantaneous part, V_e, and a part due to the growth of the crack tip creep zone or changes in creep strain rate after creep zone expansion, V_c, C_t is an extension of the C*-integral into the transient creep regime via its stress-power dissipation rate interpretation.[10] The growth of the creep zone and, therefore, V_c is intimately connected with the elastic strain rates that arise due to crack tip stress relaxation, as well as the creep strain rates.

To define the partitioning of load line displacements in small-scale creep (SSC), imagine a specimen with a crack of length, a, subjected to load P. The total load-line deflection is expressed as:

$$V = V_e + V_c \tag{17}$$

where $V_e(P, a)$ is the total deflection of an identical specimen that undergoes only the instantaneous *elastic* deformation, and V_c is the *remaining deflection* that accumulates with time for the actual specimen undergoing both *elastic and creep deformation*. The latter elastic deformation is caused by the redistribution of stresses at the crack tip. It is important to note that V_e and V_c are not compatible with the elastic and creep strains, respectively, of the specimen. In fact, because in SSC V_c is due to the growth of the crack tip creep zone, it is intimately connected with the crack tip stress relaxation and the associated elastic strain rates. It may be recalled that in the time-independent elastic-plastic case, Edmonds and Willis[28] have demonstrated that this partitioning is asymptotically exact (see Hutchinson[29] for an analogous discussion based on the Dugdale solution). Note that for a stationary crack under constant load, $\dot{V} = \dot{V}_c$.

C_t is defined as the instantaneous rate at which stress power is dissipated. Consider several identical pairs of cracked specimens. For each pair, one specimen has a crack length a and the other has a crack length a + Δa. The specimens of each pair are loaded to various load levels $P_1, P_2, P_3 \cdots P_i$, etc., at elevated temperature. It is assumed that no crack extension occurs in any of the specimens and that the instantaneous response is linear-elastic with

Page missing from report

onverted to K by the well-known relationship $K^2/E = (P^2/2B)(dC/da)$:

$$(C_t)_{ssc} = 2(1 - \nu^2)\frac{K^2}{EW}F'/F \cdot \beta\tilde{r}_c \tag{22}$$

lext, substituting for r_c from Eq 16 yields:

$$(C_t)_{ssc} = \frac{4\alpha\beta\tilde{r}_c(\theta)(1-\nu^2)}{E(n-1)}(EA)^{\frac{2}{n-1}}\frac{F'}{F}\frac{K^4}{W}\left(\frac{1}{t}\right)^{\frac{n}{n-1}} \tag{23}$$

here the geometric factors F and F′ are defined as follows:

$$F = (K/P)BW^{1/2} \text{ and } F' = dF/d(a/W) \tag{24}$$

$$\alpha = \tfrac{1}{2}\pi\left(\frac{n+1}{1.38n}\right)^{(n-1)} \text{ for } 3 \le n \le 13 \tag{25}$$

here W is the width of the specimen, and K is the elastic stress-intensity ictor as defined before. Equation 21 is very convenient for obtaining $(C_t)_{ssc}$ i test specimens when load and deflection rates are measured. It also rcumvents the problem of determining the values of β and $\tilde{r}(\theta)$. However, ie value of $\beta\tilde{r}_c(\theta)$ should be determined for estimating C_t in components. has been estimated to be approximately 1/7.5 by comparing C_t values from q 21 and 23 in a finite-element analysis.[27] In earlier work,[26] this value was iosen to be unity on the basis of experimental data. This discrepancy beveen the experiments and analysis results from primary creep deforma-on that was not considered in the analysis. This will be discussed further i the next section.

The expression for determining C_t over a wide range of creep deformation in be written as follows:

$$C_t = (C_t)_{ssc} + C^* \tag{26}$$

o calculate C_t in Eq 26, $(C_t)_{ssc}$ can be substituted from Eq 21 or 23, and C^*, hich was given in terms of a path-independent integral, can be obtained om solutions given in Ref 18. Combining Eq 23 with Eq 9 provides a conenient means for predicting C_t for components, and combining Eq 21 with q 6 yields a convenient method of obtaining C_t for laboratory specimens. In SSC, C_t is related to the rate of growth of the crack tip creep zone as evolves with time (Eq 22). Furthermore, note from Eq 13 and 22 that under mall-scale creep conditions:

$$(C_t)_{ssc} = \beta(1-\nu^2)\frac{n+1}{n-1}(F'/F)\frac{r_c}{W}(C(t))_{ssc} \tag{27}$$

Thus, $(C_t)_{ssc}$ is clearly not equal to $(C(t))_{ssc}$, which characterizes the amplitude of the HRR stress fields. In fact, the ratio of the two parameters is also not constant because of r_c on the right side of the equation, which is function of time (Eq 1b). However, in a specimen under constant load and crack size, the relationship between $(C_t)_{ssc}$ and $(C(t))_{ssc}$ is single valued, because for a given time, there can only be one r_c and one $(C(t))_{ssc}$. This observation, when combined with the observation that $C_t = C(t) = C^*$ in the extensive creep regime, has the following implication. The two parameters C_t and C(t) are not the same over a wide range of creep conditions; hence, both cannot correlate a wide range of creep crack growth data in a single trend. This is because C_t and C(t) are equal under extensive creep conditions, but have different time dependencies in the SSC regime. Thus, only one or neither of the two parameters are expected to correlate wide range creep crack growth data. Experimental studies have definitely shown that C_t correlates wide range creep crack growth data, as will be discussed in detail later in this section.

Recall that setting $(C(t))_{ssc}$ in Eq 13 equal to C^* yields an estimate for the transition time t_T given in Eq 14. Similarly, C_t in Eq 23 can be equated to C^* to give another estimate of the transition time $\hat{t}$, which must closely approximate t_T. Therefore, with $\hat{t} = t_T$, an interpolation formula for C_t from small-scale to extensive creep that is similar to Eq 15 for C(t) is:[27]

$$C_t = C^*[(t_T/t)^{\frac{n-3}{n-1}} + 1] \tag{27a}$$

C_t can be estimated in test specimens for conditions ranging from small-scale creep to extensive creep by substituting Eq 21 and 6 into Eq 26 and simplifying:[17]

$$C_t = \frac{P\dot{V}_c}{Bw}F'/F + C^*\left(\frac{F'/F}{\eta} - 1\right) \tag{28}$$

All terms in Eq 28 have been defined earlier. Figure 6 compares the estimated value of C_t from a finite-element analysis of a C_T specimen[27] using Eq 26, 27, and 28. The estimates of C_t from Eq 26 and 27 are indistinguishable and compare extremely well with those from Eq 28 (termed $C_t(P\dot{V})$) from SSC to extensive creep conditions. Figure 6 also compares the values of C_t with C(t). As expected, the two parameters diverge in the SSC regime and become equal in the extensive creep regime.

2.3 Consideration of Primary Creep

The assumption of elastic power-law creep is often not sufficient to describe the complex deformation behavior of several engineering materials at

Page missing from report

elds can be written in the HRR format as:[31]

$$\sigma_{ij}(r,\theta,t) = \left[\frac{C_h^*}{A_1(1+p)t^{\frac{1}{1+p}} I_{n_1} r} \right]^{\frac{1}{n_1+1}} \tilde{\sigma}_{ij}(\theta,n_1) \tag{31}$$

here all terms have been defined previously. It should be noted that by he correspondence principle, the stationary stress states for time-hardening rimary creep (first term in Eq 24) and secondary creep are the same.

When a steady-state creep zone is growing out of the primary creep zone uch that both terms on the right side of Eq 29 are comparable in magnitude omewhere in the cracked body, it cannot be shown rigorously that the *-integral in Eq 2 is path independent. This regime also corresponds to onditions of extensive creep. It is understood in discussion of primary creep ffects that the C*-integral in Eq 2 becomes time dependent, whereas the ore narrow definition of Ref 6 pertains to steady-state secondary creep conitions only. However, recent finite-element numerical calculations have hown that C* in this regime is in fact path independent to a good degree f approximation.[32] It thus follows that C_t is approximately equal to C* in his regime and that the HRR amplitude factor C(t) is also approximately qual to C*. Hence, $C_t \simeq C(t)$ in this regime of extensive creep conditions inolving both primary and secondary creep behavior. We can thus make use f the recent interpolation formula derived by Riedel and Detampel[33] for stimating C(t) in this regime to also estimate C_t:

$$C_t = C(t) = [(t_2/t)^{p/(p+1)} + 1]C^* \tag{32}$$

here C* represents the steady-state value at time $t \to \infty$ when secondary reep conditions dominate, and t_2 is a transition time obtained by the follow-ng expression:

$$t_2 = \left(\frac{C_h^*}{(1+p)C^*} \right)^{(1+p)/p} \tag{33}$$

C_h^* can be obtained[31] for various cracked geometries by substituting $A_1(1+p)^{1/1+p}$ for A and n_1 for n in Eq 9, which was originally derived for alculating C*. Thus, from the knowledge of the primary and steady-state reep constants, geometry, crack size, and applied stress (or load), C(t) (or C_t) can be completely calculated from handbook-type solutions.[18]

Next, we look at inclusion of primary creep when small-scale creep conitions exist. For small-scale primary creep alone, the HRR amplitude factor, (t), and the creep zone size has been estimated by Riedel.[31] Furthermore,

Riedel and Detampel[33] have recently modified Eq 32 to include only primary creep in the small-scale creep regime (Eq 34):

$$C(t) = [t_1/t + (t_2/t)^{p/(1+p)} + 1]C^* \tag{34}$$

where

$$t_1 = \left(\frac{K^2(1-\nu^2)}{E(n_1+1)C_h^*} \right)^{1+p} \cdot \frac{1}{1+n_1} \tag{35}$$

The value of C* in Eq 34 corresponds to the steady-state value of the C*-integral. The above equations also assume that, in the presence of significant primary creep, the transition to extensive creep conditions is dominated by the primary creep strains, as opposed to steady-state creep as in Eq 15. This assumption is realistic because the initial primary creep rates are significantly higher than the secondary creep rates. If primary creep is not relevant, $p = 0$, and the magnitude of $t_1 = t_T$. Therefore, the expression for C(t) becomes consistent with the earlier expression for C(t) for elastic materials deforming by elastic power-law creep (Eq 15).

In the definition of C_t for small-scale creep, there is a provision to include primary creep deformation. For example, Eq 22 is general and is valid for any type of creep deformation behavior. However, the expression for $\dot{r}_c$ must include the correct deformation law. Assuming that when primary creep is present the transition from SSC to extensive creep will be dominated by the spread of the primary creep deformation, the following expression for $\dot{r}_c$ can be derived[33] from Riedel's previous work:[31]

$$\dot{r}_c = \frac{K_I^2 \dot{r}_c(\theta)}{2\pi} \left| \frac{I_{n_1} E}{2\pi(1-\nu^2)} \right|^{\frac{2}{n_1+1}} \cdot [(n_1+1)(1+p)A_1]^{\frac{2}{(1+p)(n_1-1)}} \cdot \left| \frac{1}{1+p} \right| \left| \frac{2}{n_1-1} \right| t^{\left[\frac{2}{(1+p)(n_1-1)}-1\right]} \tag{36}$$

where all terms in Eq 36 have been defined before. Thus, substituting Eq 36 into Eq 22 gives the expression for $(C_t)_{ssc}$ in the presence of primary creep.

The wide range expression for C_t in the presence of primary creep can also be derived as:

$$C_t = (C_t)_{ssc} + [(t_2/t)^{p/(1+p)} + 1]C^* \tag{37}$$

where $(C_t)_{ssc}$ is derived as mentioned previously. Considerable numerical work has been performed recently to verify the validity of Eq 37.[32] For test specimens under creep conditions ranging from small-scale to extensive

Page missing from report

correlate data. A brief discussion of these parameters is included below. Under extensive creep conditions dominated by steady-rate creep, the ack-tip opening displacement rate and C^* are related to each other niquely much in the same way as the relationship between the J-integral id the crack-tip opening displacement derived by Shih.[43] The relationship as follows:

$$\dot{\delta}_t \propto \sigma_0 C^* = \sigma_0 C_t \tag{40}$$

here σ_0 is a constant on the order of the yield strength and the constant proportionality is on the order of one. Thus, for extensive creep conditions, and C^* (or C_t) can be considered as equivalent parameters.

Under small-scale creep conditions, we can show (see Appendix for derivation) that:

$$(C_t)_{ssc} = \left(\frac{2\pi\beta}{}\right)^{1/2}(F'/F)\left(\frac{Kr_c^{1/2}}{W}\right)\dot{\delta}_t \tag{41}$$

nd

$$(C(t))_{ssc} = \frac{n-1}{n+1}\frac{KW}{1-\nu^2}\left(\frac{2\pi}{2\beta}\right)^{1/2}\frac{K}{r_c^{1/2}}\dot{\delta}_t \tag{41a}$$

Whereas Eq 41 is valid for any general constitutive law, Eq 41(a) is only valid r elastic power-law creep behavior. From these equations, it is observed nat neither $(C_t)_{ssc}$ and $\dot{\delta}_t$ nor $(C(t))_{ssc}$ and $\dot{\delta}_t$ are related to each other by simle constants. However, within the realm of SSC only, the relationships beveen C_t and $\dot{\delta}_t$ and also $C(t)$ and $\dot{\delta}_t$ are single valued. As we had argued reviously when we examined the relationship between C_t and $C(t)$ (Eq 27), $_t$, $\dot{\delta}_t$, and $C(t)$ cannot all correlate with creep crack growth rate data over wide range of creep conditions, because their interrelationships are unique nly if either SSC or extensive creep conditions are assumed. Also, if one f these parameters correlates with creep crack growth behavior, it ecessarily implies that others cannot. A further difficulty with $\dot{\delta}_t$ is that s measurement is not practical. For this reason, there are not many experimental studies in which an attempt to correlate $\dot{\delta}_t$ and da/dt has been made. The C^*_{exp} parameter of Webster *et al.*[14,42] is determined as follows:[14]

$$C^*_{exp} = \frac{P\dot{V}_c}{BW}\eta(a/W,n) \tag{42}$$

Table 1. F'/F and η for CT and CCT Specimens

	CT specimen				CCT specimen			
		$\eta(a/W,n)$				$\eta(a/W,n)$		
a/W	F'/F	n = 3	n = 8	n = 10.1	F'/F	n = 3	n = 8	n = 10.1
0.20	2.976	1.966	2.37	2.431	2.755	0.312	0.486	0.512
0.30	2.590	2.307	2.766	2.835	2.0688	0.357	0.555	0.585
0.40	2.644	2.725	3.255	3.335	1.821	0.417	0.648	0.683
0.50	3.077	3.274	3.900	3.994	1.785	0.50	0.778	0.820
0.60	3.920	4.063	4.829	4.945	1.914	0.625	0.972	1.025
0.70	5.700	5.340	6.338	6.489	2.255	0.833	1.296	1.366
0.80	8.307	7.856	9.317	9.538	3.042	1.25	1.944	2.049

where η in Eq 42 is the same as in Eq 6. Thus, when extensive steady-state creep conditions prevail, $\dot{V}_c = \dot{V}_{ss}$ (see Eq 6 for the definition of $\dot{V}_{ss}$), and it is easy to see that $C_t = C^*_{exp}$. Under extensive primary creep, the η function changes slightly because a different value of n applies instead of the one describing the steady-state creep response of the material. However, this dependence is small and is not of much consequence when treating experimental data. It thus follows that C^*_{exp} and C_t are approximately equal in the extensive creep regime.

In the small-scale creep range, C^*_{exp} is not a viable parameter. Experimentally, it can still be determined by Eq 42 for test specimens. However, it must be remembered that η is derived from analogy to a limit-load-type analysis for fully plastic structures and thus assumes that the specimen is under extensive creep.[14] Therefore, the use of η derived from such analysis under small-scale creep is not justified. An interesting point is noted when we compare Eq 42 for determining C^*_{exp} to Eq 38 for determining C_t. We find that for geometries for which $F'/F = \eta$, $C^*_{exp} = C_t$.

In a previous study,[26] the author has compared the values of η and F'/F for the CT and CCT specimen geometries over a wide range of n and a/W values. These results are reproduced in Table 1. For CT specimens, η is within 15% of F'/F over a wide range of a/W and n values. Thus, for these specimens, $C^*_{exp} = C_t$. Much of the success of C^*_{exp} in correlating creep crack growth data may be due to the fact that a large amount of the data are obtained on CT specimen geometry for which it is an approximation for C_t. It may also be mentioned that the C_j parameter of Jaske[44] and an old version of C_t[38] are identical to C^*_{exp}.

Page missing from report

experimentally shown to correlate with CCGR behavior over a wide range creep conditions, it implies that a unique relationship between CCGR d the other two parameters cannot exist for the same conditions.

n this section, creep crack growth data in a recently concluded ASTM ogram[45] on a Cr-Mo-V steel at 594 °C (1100 °F) are analyzed using dif- ent crack tip parameters. (Fig. 8 to 11). These data were developed using mpact-type specimens that were 50.8 mm (2 in.) wide. The steady-state eep deformation behavior in this material is shown in Fig. 12. No further nsideration of δ_i is possible, because no systematic studies where it has en measured are available.

Figures 8 to 11 show plots of the creep crack growth rate, da/dt, as a func- on of K_{eff}, which is a plasticity-modified stress-intensity parameter, C^*, t), and C_t, respectively. Specimens 19 through 22 were 6.25 mm (0.25 in.) ick and specimens 11 and 12 were nominally 25.4 mm (1 in.) thick with 25% side groove.

As expected from the previous discussion, little correlation exists between ie data from different specimens when plotted with K_{eff}. Figure 9 shows similar lack of correlation with C^*, indicating that transient conditions revailed during these tests. C^* was calculated using Eq 9. A parameter τ defined to determine whether the test is in the transient or steady-state egime:

$$\tau = \frac{C^*}{C_t} \tag{43}$$

When steady-state conditions are reached, $C_t = C^*$ and τ approaches 1. When highly transient conditions exist, $\tau << 1$. The values of τ at the eginning and end of each test are listed in Table 2. Also listed are the tran- ition time t_T and the test duration, t_0. In several of the tests, the value of is considerably less than 1, thus confirming that the specimens were under ransient conditions at least for some time during each test.

A similar lack of correlation is also observed when da/dt values are plot- ed with C(t) as determined from Eq 15. However, when the same data are plotted with C_t, they correlate very well with each other. Some distinction can be made between data from the 25.4-mm-thick side-grooved specimens and the 6.25-mm-thick non-side-grooved specimens. This may be attributed to the state-of-stress effects. The side-grooved specimens are expected to be under plane-strain conditions, whereas the others are closer to plane-stress conditions. Riedel and Detampel[32] have also made a similar evaluation of C^*, C(t), and C_t on a 2.25Cr-Mo material tested at 540 °C and have reached the conclusion that better correlations are obtained when creep crack growth rates are plotted with C_t.

Table 2. Values of τ and Transition Time During Various Creep Crack Growth Tests

Specimen ID	a/W	τ	Test duration, h t_T	Test duration, h T_0	t_0/t_T
CT-19	0.557	0.300	26.3	266.7	10.1
	0.610	0.053	6.76	...	39.5
CT-20	0.561	0.125	16.2	108.3	6.7
	0.590	0.044	7.69	...	14.1
CT-21	0.520	0.5	15.3	187.1	12.2
	0.616	0.00646	1.34	...	139.6
CT-22	0.516	0.260	8.89	84.7	9.5
	0.593	0.0136	1.40	...	60.5
SG-11	0.550	1	3.86	53.6	13.9
	0.653	0.296	0.24	...	223.3
SG-12	0.551	0.90	2.25	29.2	13.0
	0.616	0.70	0.42	...	69.5

The data shown in Fig. 11 and from other studies[32] clearly show that C_t should be the crack tip parameter of choice for correlating creep crack growth rate data. However, it was surprising that the correlation between da/dt and C(t) is not better than the correlation with C^*. From examining the ratios t_0/t_T given in Table 2, it is expected that all tests should lie in the extensive creep regime, and the data should correlate just as well with C^* as with C(t) and C_t because all three are the same in this regime. This point merits further discussion.

The measured values of C_t are significantly higher than the values of C^*, indicating that transient conditions still existed at times significantly larger than t_T. It may be argued that the t_T estimate of transition time in Eq 14 is for stationary cracks, and it may not be an accurate representation of the transition time for growing cracks. However, these differences are too large for such a simplistic explanation. At this point, there is no rigorous explanation for this behavior. However, Bassani[46] has recently given an explanation that has considerable appeal and is discussed below.

In the remaining ligament of CT specimens, there is a point (neutral axis) where the stress fields change from tension to compression. The region along this point is subjected to low stresses. As crack advances in a creep crack growth test and the remaining ligament shrinks, the neutral axis also shifts. Thus, a previously undeformed region now undergoes creep deformation, which possibly increases the transition period. Such an effect will

Page missing from report

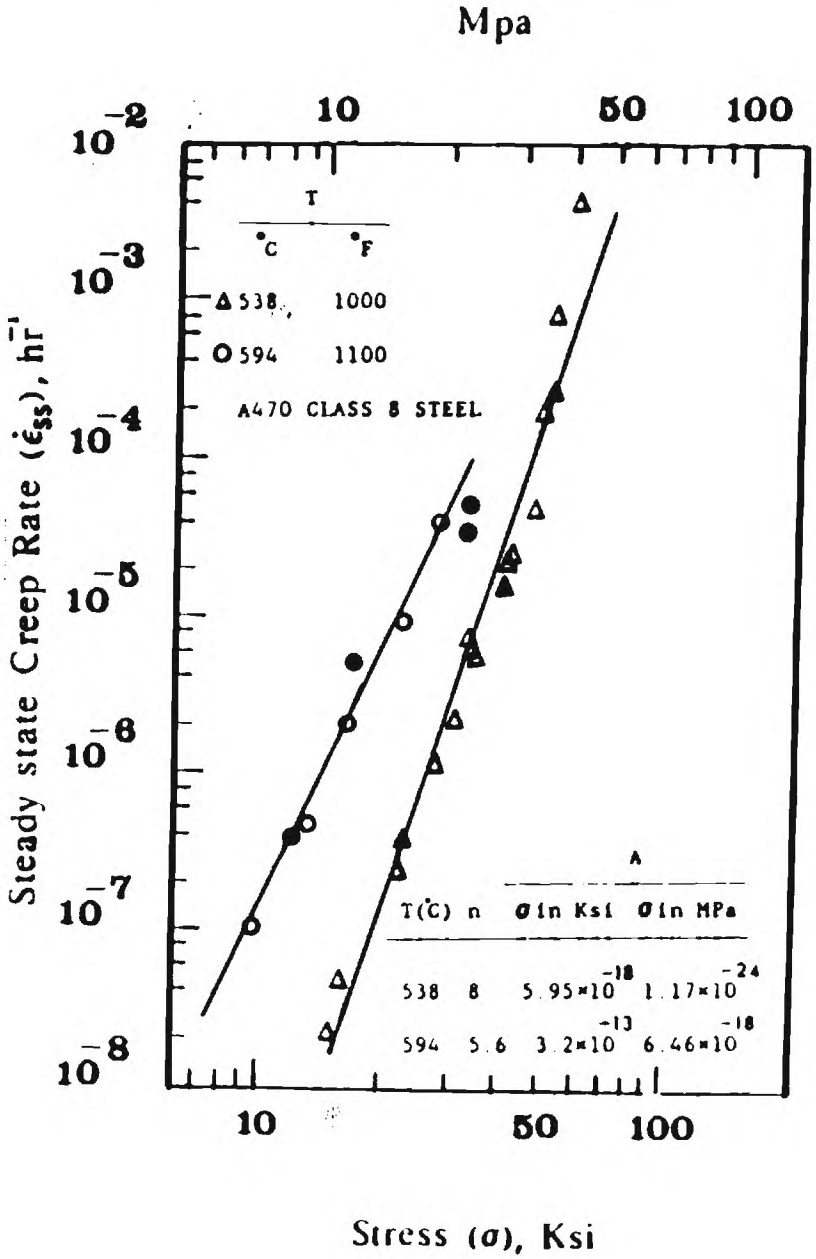

Fig. 12 Creep deformation behavior of A470 class 8 steel.

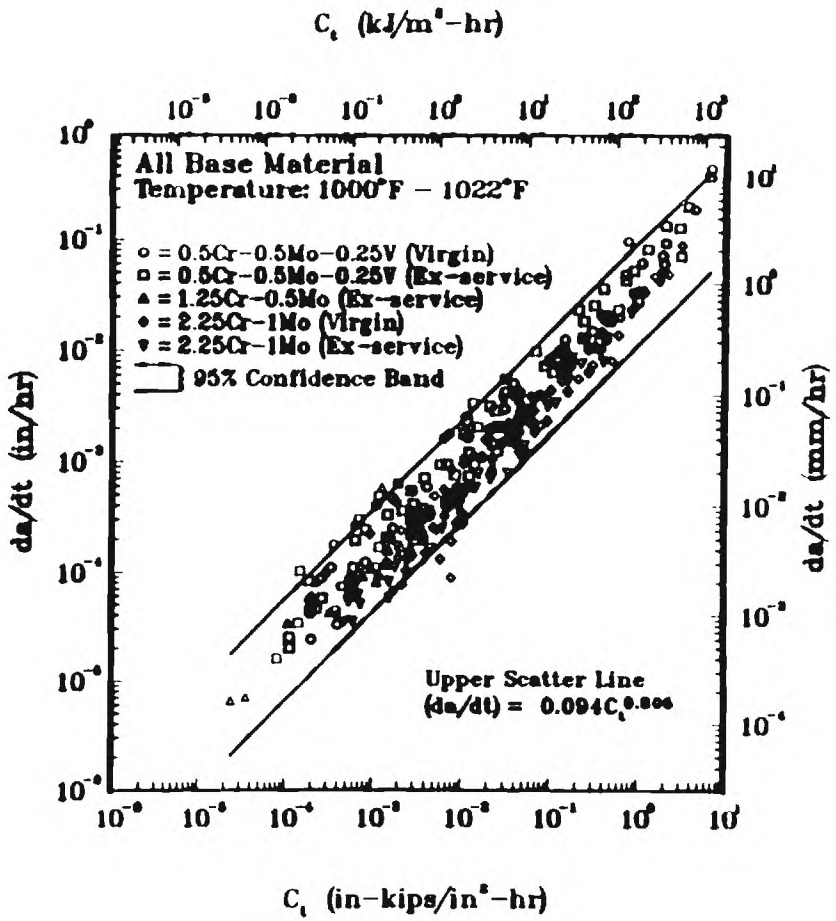

Fig. 13 Creep crack growth behavior of Cr-Mo and Cr-Mo-V base material. The data include all ex-service and new material data.

3. CREEP CRACK GROWTH TRENDS IN ELEVATED TEMPERATURE MATERIALS

In this section, the creep crack growth behavior of austenitic and ferritic steels used in elevated temperature applications is considered. Creep cracks in these materials grow by grain boundary cavitation, and the environmental effects are only secondary. In that sense, these materials are quite distinct

Page missing from report

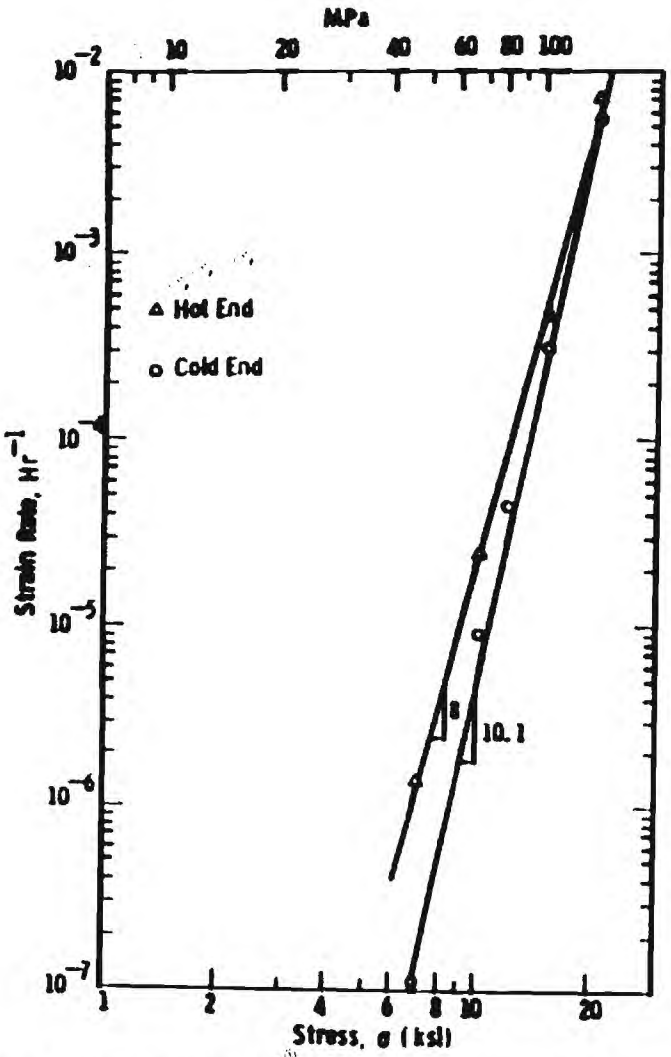

Fig. 16 Steady-state creep rate as a function of stress for 1.25Cr-0.5Mo steel.

2.25 Cr-1Mo, 1.25-0.5Mo, and 0.5Cr-0.5Mo-0.25V steels. Figure 13 also ludes data obtained on new (virgin) material, as well as on material ioved after several years of elevated temperature service. Despite the ying material compositions and the thermal histories of the material CCGR behaviors are very similar. The scatterband is about a factor of it for crack growth rate.

Figure 14 shows the influence of temperature on the CCGR behavior of 1Cr-1Mo-0.25V steel. Again, the behavior at 482 °C (900 °F) and 538 °C (1000 °F) is very comparable, even though the creep deformation rates at these temperatures for the material are very different (Fig. 12). The lack of strong material composition and temperature dependence of CCGR behavior requires further explanation.

Consider two identical cracked specimens of the same material loaded with identical loads, except that one is subjected to a temperature T_1 and the other to a temperature $T_2 > T_1$. To simplify matters, assume that both specimens are under steady-state conditions and that the creep crack growth rate correlates with C^*. To estimate C^*, either Eq 6 or 9 can be used. Because the applied load (or stress) is the same in the two specimens and n does not change significantly with temperature, the value of C^* from Eq 9 depends strongly on the value of A or on the value of $\dot{V}_c$ if Eq 9 is used. In either case, a higher value of C^* is predicted for the test at temperature T_2 compared to T_1. Thus, even if the da/dt versus C^* relationships at both temperatures were the same, the crack growth rate in the higher temperature specimen is expected to be much faster.

From the above argument, it appears that correlating creep crack growth rate with C^* (or C_t) provides a first-order normalization with respect to changes in temperature. The same argument can be applied to rationalize the similarity in the da/dt versus C_t relationship for materials with different compositions. However, these trends are expected to hold true only when there are no substantial changes in rupture ductilities due to changes in temperature, composition, or thermal history. When significant changes in creep ductilities occur, the da/dt versus C_t relationship in fact changes, as discussed below.

3.2 Influence of In-Service Aging

Figures 15 and 16 show the CCGR and the secondary-stage creep deformation rate behavior, respectively, of a 1.25Cr-0.5Mo steel[17] from a component in service for 24 years. The region marked "hot" was subjected to a temperature of 538 °C (1000 °F) and the region marked "cold" was subjected to a temperature of approximately 510 °C (950 °F). Both the CCGR and deformation rates in the hot region were significantly higher than the cold region. The corresponding microstructures of the regions at low and high magnification are shown in Fig. 17 and 18. The grain size and the microstructure at low magnification appear to be virtually indistinguishable between the two regions. There was also no evidence of creep cavitation at the grain boundaries in either material. However, at the high magnification, the difference in the grain boundary carbide morphology becomes evident. This was further confirmed by transmission electron

Page missing from report

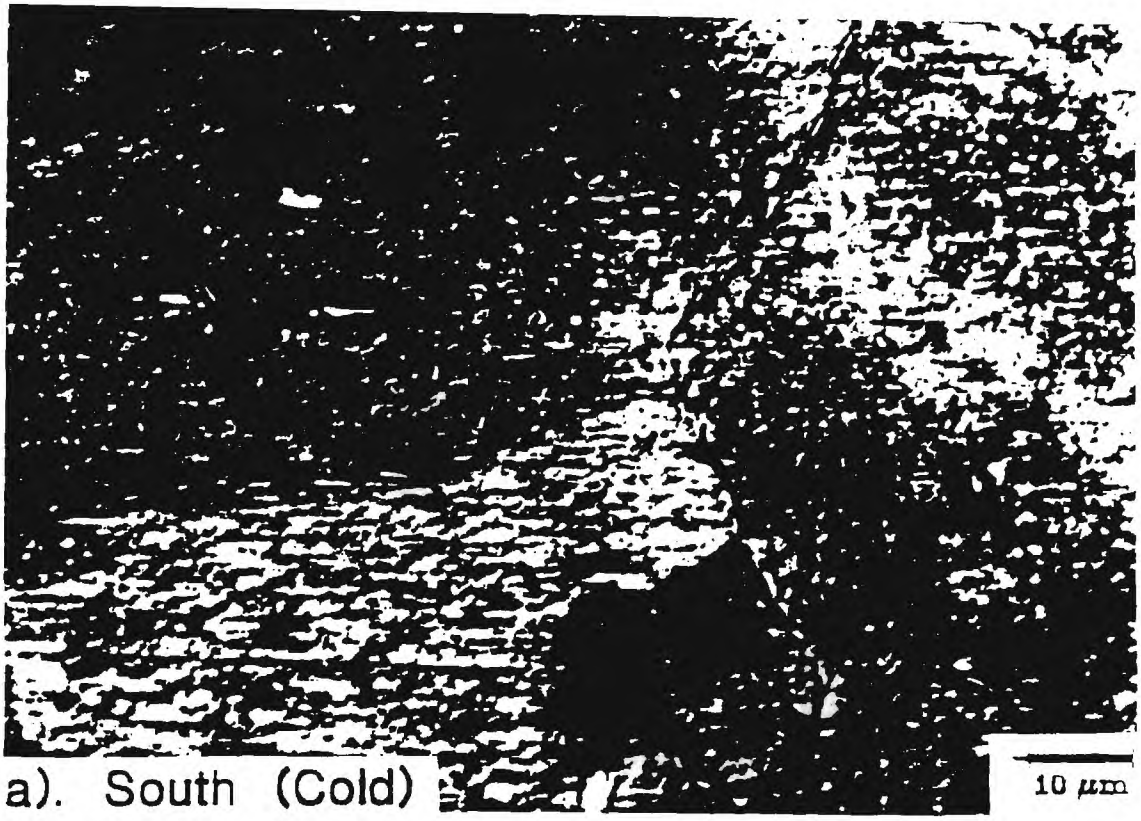

Fig. 18 (a) High-magnification micrograph of the cold end materials (Nital etch).

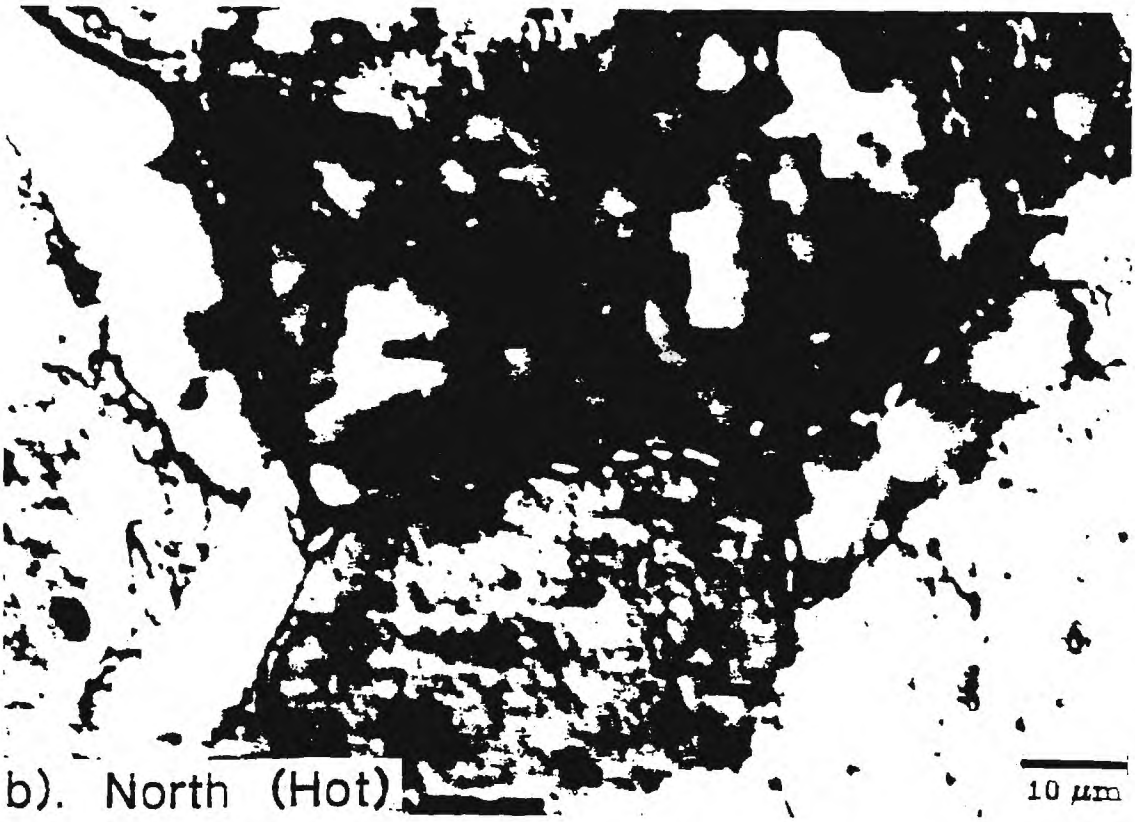

Fig. 18 (b) High-magnification micrograph of the hot end materials (Nital etch).

Page missing from report

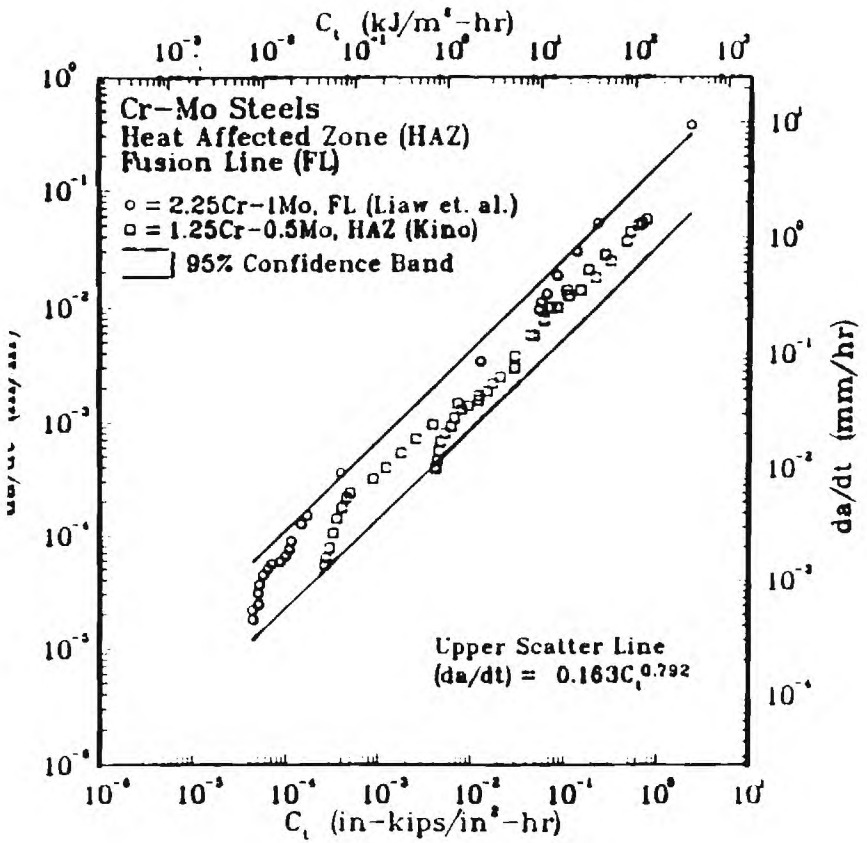

Fig. 21 Creep crack growth behavior of Cr-Mo HAZ/FL regions (Ref 51 and 52).

emperature and higher levels of impurity (S,P,As) content results in the orst CCGR behavior. These rates are as much as 50 times higher than the orst case behavior in the HAZ/FL data of Fig. 21.

The influence of impurities on the creep crack initiation and growth ehavior in 2.25Cr-1Mo steel was also investigated by Lewandowski *et l.*[54,55] Their data also show higher crack growth rates in materials with igher levels of impurities. Among the Konosu and Maeda[53] and Lewandowski *et al.*[54,55] studies, there is controversy over the role of sulfur in causng the embrittlement. The former investigators did not find any segregaon of sulfur on the fracture surface of the material that had a high amount f sulfur, whereas the latter investigators report considerable amounts of

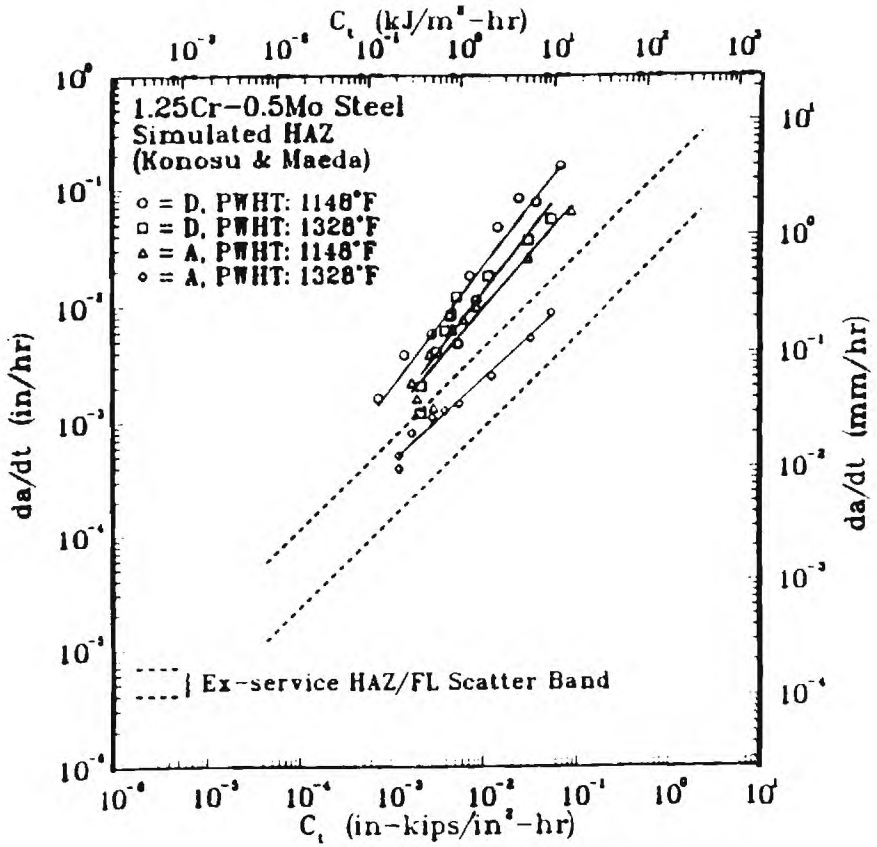

Fig. 22 Creep crack growth behavior of simulated HAZ 2.25Cr-1Mo steel. Steel A was a high-purity material, and steel D was a low-purity steel (Ref 53).

sulfur segregation. Despite the disagreement, both studies are quite revealing on the role of impurities in determining creep crack growth behavior. This appears to be an interesting area for further investigation.

4. MICROSCOPIC ASPECTS OF CREEP CRACK GROWTH

Figure 23 shows the cavitation damage ahead of a 1.25Cr-0.5Mo creep crack growth rate specimen.[49] The tested specimen was sectioned at midthickness and the area directly ahead of the creep crack growth was

Page missing from report

nplicity, only a one-dimensional array of cavities was considered, and the ıgular dependence of the stress field (which is a factor on the order of one) ıs dropped, because only qualitative trends are presently being considered. ıe crack is supposed to advance by a distance 2b when the cavity nearest the crack tip grows to a critical size, ρ_c. If this occurs over a time interval, ., the crack growth rate is:

$$\frac{da}{dt} = \frac{2b}{\Delta t} \tag{45}$$

ıuring the time interval Δt, the cavity with radius ρ_2 grows to a radius ρ_1, nd a new cavity of radius ρ_N nucleates at a distance 2bN from the crack p. In this manner, a steady-state crack growth process can be established, hich leads to the following set of N integral equations:

$$\Delta t = \int_{\rho_m}^{\rho_{m-1}} \frac{d\rho}{\dot{\rho}} \quad m = 0, 1, 2, \ldots N-1 \tag{46}$$

here $\rho_0 = \rho_c$. The solution of these N integral equations yields:

$$\frac{da}{dt} = \frac{(2b)^{\frac{1-\alpha_1}{n+1}}}{\psi_0 - \psi_N} \frac{1}{N \sum_{m=1} m^{\frac{\alpha_1}{n+1}}} \left(\frac{C^*}{I_n A}\right)^{\alpha_1/n+1} \tag{47}$$

/here

$$\psi = \int \frac{d\rho}{\phi(\rho,b)} \tag{48}$$

or constrained cavity growth, the function ϕ can be derived from previous vork by Rice[63] and subsequently used by Jani and Saxena:[49]

$$\phi = \frac{1}{2.5}\left(\frac{2b}{\rho}\right) d \cdot A \tag{49}$$

vhere d is the grain diameter, and A is the power-law creep coefficient. Therefore:

$$\psi = \int \frac{d\rho}{\phi(\rho,b)} = \frac{2.5\rho^3}{3(2b)^2}\, d \cdot A \tag{50}$$

ınd

$$\psi_0 - \psi_N = \frac{2.5}{3(2b)^2 d.A}(\rho_c^3 - \rho_N^3) \tag{51}$$

Substituting Eq 18 into Eq 14 yields:

$$\frac{da}{dt} = \frac{(2b)^{\frac{2n+3}{n+1}} \cdot 3d \cdot A^{\frac{1}{n+1}}}{2 \cdot 5\ (\rho_c^3 - \rho_N^3) \sum_{m=1}^{N-1} (m)^{\frac{n}{n+1}}} \left(\frac{C^*}{I_n}\right)^{n/n+1} \tag{52}$$

The following interpretations can be drawn from the model presented in Eq 52:

- The crack growth rate is not very sensitive to A for a constant value of n. For this reason, the crack growth rates are expected to be only weakly dependent on temperature, which has been observed for Cr-Mo steels.[48]
- Creep crack growth rate will be sensitive to the intercavity spacing (2b), the critical cavity size for coalescence ρ_c, and the cavity nucleation size ρ_N. If cavities nucleate at grain boundary carbides, then the carbide size can be considered to be ρ_N. Therefore, a coarsened grain boundary carbide structure will result in higher crack growth rates.

Although the model does qualitatively predict the trend observed in this study, which is encouraging, it is important to note its limitations. The model assumes an idealized cavitation behavior on a grain boundary along the plane of the crack. It also assumes that cavity growth occurs under steady-state stress fields characterized by the HRR singularity, which limits its application to steady-state conditions. Also, the critical cavity radius for coalescence is a constant value, which may be simplification. In reality, ρ_c must be stress dependent over a wide range of crack growth rates, and such dependence must be incorporated into the model. Also, under the more realistic transient creep conditions (SSC and TC), the stress fields ahead of the crack tip are relaxing with time, and the model must be modified to account for that and the stress fields must be modified to account for damage. The constant cavity spacing precludes simultaneous nucleation and growth of cavities. This is a major shortcoming of the model.

For the Cr-Mo material used in the study mentioned earlier,[48] it was observed that the largest cavities ahead of a crack tip were on the order of 70 μm, whereas the average carbide size ρ_N was on the order of a few microns. If the largest cavities can be taken as ρ_c, then the term $\rho_c^3 - \rho_N^3$ in the model is relatively insensitive to small changes in ρ_N, and the crack growth rate will be controlled by ρ_c. The possibility of embrittling species such as tin, antimony, sulfur, and phosphorus affecting the critical radius for cavity coalescence becomes relevant and needs to be addressed in the future.

Page missing from report

Detroit Edison Today, Detroit Edison, Detroit, MI 14(4), Feb 1986
J.A. Harris, D.L. Sims, and C.G. Annis, Concept Definition: Retirement for Cause of F100 Rotor Components, AFWAL Tr-80-4118, Wright Patterson Air Force Base, Sep 1980.
Proceedings of Electric Power Research Institute (EPRI) Conference on Life Extension and Assessment of Fossil Plants, Wasington DC, Jun 2-4, 1986. Pergamon Press, R. Visnanathan, Ed., 1988.
W.A. Logsdon, P.K. Liaw, A. Saxena, and V. Hulina, *Eng. Fract. Mechan., 25*, 1986, p 259-288.
A. Saxena, P.K. Liaw, W.A. Logsdon, and V. Hulina, *Eng. Fract. Mechan., 25*, 1986, p 290.
L. Sarver, Destructive Examination and Testing of Retired Secondary Superheater Outlet Header from RB-304, unpublished research, Babcock and Wilcox Co., Alliance, Ohio, May 1985.
J.D. Landes and J.A. Begley, in *Mechanics of Crack Growth, ASTM STP 590*, ASTM, Philadelphia, 1976, p 128-148.
K.M. Nikbin, G.A. Webster, and C.E. Turner, in *Cracks and Fracture, ASTM STP 601*, ASTM, Philadelphia, 1976, p 47-62.
N.L. Goldman and J.W. Hutchinson, *Int. J. Solids Struct., 11*, 1975, p 575-591.
C.F. Shih, Tables of Hutchinson-Rice-Rosengren Singular Field Quantities, Materials Research Laboratory, Brown University, MRL E-147, 1983.
A. Saxena, in *Fracture Mechanics: Twelfth Conference, ASTM STP 700*, ASTM, Philadelphia, 1980, p131-151.
D.J. Smith and G.A. Webster, in Elastic-Plastic Fracture, Vol I—*Inelastic Crack Analysis, ASTM STP 803*, ASTM, Philadelphia, 1983, p 654-674.
A. Saxena, H.A. Ernst, and J.D. Landes, *Int. J. Fract., 23*, 1983, p 245-257.
A. Saxena, T.T. Shih, and H.A. Ernst, in *Fracture Mechanics: Fifteenth Symposium, ASTM STP 833*, ASTM, Philadelphia, 1984, p 516-531.
A. Saxena and P.K. Liaw, Renaming Life Estimation of Boiler Pressure Parts—Crack Growth Studies, Electric Power Research Institute, Palo Alto, Contract Report CS-4688, Jul 1986.
V. Kumar, M.D. German, and C.F. Shih, An Engineering Approach to Elastic-Plastic Fracture Analysis, EPRI NP 1931, Electric Power Research Institute, Palo Alto, Jul 1981.
H. Riedel and J.R. Rice, in *Fracture Mechanics: Twelfth Conference, ASTM STP 700*, ASTM, Philadelphia, 1980, p 112-130.
J.L. Bassani and F.A. McClintock, *Int. J. Solids Struct., 7*, 1981, p 479-492.
R. Ehlers and H. Riedel, in *Advances in Fracture Research, Vol 2, ICF-5*, D. Francois et al., Ed., Pergamon Press, 1981, p 691-698.
K. Ohji, K. Ogura, and S. Kubo, *Jpn. Soc. Mechan. Eng.* 790-13, 1979, p 18-20 (in Japanese).
J.W. Hutchinson, *J. Mechan. Phys. Solid, 16*, 1968, p 13-31.
J.R. Rice and G.F. Rosengren, *J. Mechan. Phys. Solids, 16*, 1968, p 1-12.
H. Tada, P.C. Paris, and G.R. Irwin, *The Stress Analysis of Cracks Handbook*, Paris Productions Inc., St. Louis, 1985.
A. Saxena, in *Fracture Mechanics, ASTM STP 905*, Vol 17, ASTM, Philadelphia, 1986, p 185-201.
J.L. Bassani, D.E. Hawk, and A. Saxena, Evaluation of the C_t Parameter for Characterizing Creep Crack Growth Rate in the Transient Regime, Third ASTM International Symposium on Nonlinear Fracture Mechanics, Knoxville, TN Oct 6-8, 1986, to appear in related ASTM STP.

28. J. Edmonds and W. Willis, *J. Mechan. Phys. Solids, 24*, 1976, p 205-225.
29. J.W. Hutchinson, Nonlinear Fracture Mechanics, Technical University of Denmark Report, 1979.
30. C. Leung, D.L. McDowell, and A. Saxena, A Numerical Study of Nonsteady State Creep at Stationary Tips, Third International Symposium on Nonlinear Fracture Mechanics, Knoxville, TN, Oct 6-8, 1986, to appear in ASTM STP.
31. H. Riedel, *J. Mechan. Phys Solids, 29*, 1981, p 35-49.
32. H. Riedel and V. Detampel, *Int. J. Fract. 33*, 1987, p 239-262.
33. C. Leung, D.L. McDowell, and A. Saxena, unpublished results, Georgia Institute of Technology, Jan 1988.
34. C.Y. Hui and H. Riedel, *Int. J. Fract. 17*, 1981, p 409-425.
35. C.Y. Hui, in *Elastic-Plastic Fracture, Second Symposium, ASTM STP 803*, Vol I, 1983, p 573-593.
36. H. Riedel and W. Wagner, in *Advances in Fracture Research*, 5th International Conference on Fracture ICF-5, Cannes, Mar 1981, D. Francies, et. al. eds., Pergamon Press, 1982, p 683-690.
37. D.E. Hawk and J.L. Bassani, *J. Mechan. Phys. Solids, 34*, 1986, p 191-212.
38. A. Saxena and J.D. Landes, in *Advances in Fracture Research*, Proceedings of the 6th International Congress on Fracture (ICF-6), 1984, S.R. Valluri, et. al. eds., Pergamon Press, 1985, p 3977-3988.
39. K. Sadananda and P. Shahinian, *Metall. Trans. A, 8A*, Mar 1977, p 439-449.
40. A.J. McEvily and C.H. Wells, in *International Conference on Creep and Fatigue in Elevated Temperature Applications*, ASME, Philadelphia, 1973.
41. J.R. Haigh, *Mater. Sci. Eng., 20*, 1975, p 213-223.
42. G.A. Webster, in *Engineering Approaches to High Temperature Design*, B. Wilshire and D.R.J. Owen, Ed., 1983, p 1-55.
43. C.F. Shih, *J. Mechan. Phys. Solids, 29*, 1981, p 305-326.
44. C.E. Jaske, Long-Term-Creep and Creep-Crack-Growth Behavior of 9Cr-1Mo-V-Nb Steel, ASM Conference on Advances in Materials Technology, Sep 1-3, Chicago, 1987.
45. A. Saxena and J. Han, Evaluation of Crack Tip Parameters for Characterizing Crack Growth Behavior in Creeping Materials, ASTM Task Group Report, Georgia Institute of Technology, Sep 1986.
46. J.L. Bassani, private communication, Jul 1987.
47. R.C. Donath, T. Nicholas, and L.S. Fu, in *Fracture Mechanics: Thirteenth Conference, ASTM STP 743*, 1981, p 186-206.
48. A. Saxena, J. Han, and K. Banerji, *J. Press. Vessel Technol.*, Vol 110, 1988, p 137-146.
49. S. Jani and A. Saxena, in *Effects of Load and Thermal Histories on Mechanical Behavior of Materials*, P.K. Liaw and T. Nicholas, Ed., TMS Publication, 1987, p 201-220.
50. K. Banerji and A. Saxena, Creep and Creep-Fatigue Crack Growth Behavior in Cr-Mo-V Rotor Steels, EPRI Topical Report, Electronic Power Research Institute, Palo Alto, Jan 1988.
51. P.K. Liaw, A. Saxena, and J. Schaefer, *Eng. Fract. Mechan.*, to be published, 1988.
52. H. Kino, Elastic Potential Technique for Monitoring Crack Growth and Creep Crack Growth Behavior in Various Teels, Mitsubishi Heavy Industries, Dec 1985.
53. S. Konosu and K. Maeda, Creep Embrittlement Susceptibility and Creep Crack Growth Behavior in Low Alloy Steels, Third International Symposium on Nonlinear Fracture Mechanics, ASTM, Oct 1986.

Acta metall. mater. Vol. 00, No. 0, pp. 000–000, 1990
Printed in Great Britain.

0001-6160/90 $3.00 + 0.00

MECHANISMS OF CREEP CRACK GROWTH IN 1 wt% ANTIOMONY–COPPER: IMPLICATIONS FOR FRACTURE PARAMETERS

J. T. STALEY Jr[1] and A. SAXENA[2]

Mechanical Properties Research Laboratory, School of Materials Engineering, Georgia Institute of Technology, Atlanta, GA 30332-0245, U.S.A.

(*Received* 21 *April* 1989; *in revised form* 1 *December* 1989)

Abstract—A copper alloy with 1% (by weight) antimony was used as a model material and tested at 400°C to study the mechanisms of creep crack growth. At this temperature, the creep deformation in this material was dominated by secondary and tertiary creep. The expression for estimating C_t (a crack tip parameter for creep conditions) in a compact type specimen used for testing was modified to include tertiary creep deformation. Extensive damage characterization was conducted on tested creep crack growth specimens using optical metallography and scanning electron microscopy. The following observations were derived from the test results. The creep crack growth rates correlated with C_t only when intense cavitation damage was restricted to a region approximately 1.3 mm in size near the crack tip and no crack branching occurred. It was observed that the average diameter, areal density, and percent of grain boundary area cavitated decreased as function of distance from the crack tip. From these results it is argued that simultaneous nucleation and growth of cavities occur on grain boundary facets during the creep crack growth process. Percent grain boundary area cavitated is proposed as the most reasonable measure of creep damage. The critical amount of damage for crack extension appears to depend on the magnitude of the C_t parameter.

Résumé—

Zusammenfassung—

BACKGROUND

The development and use of materials for elevated temperature applications is of critical importance for many industries. Within the power generation and jet engine industry, there is a need for optimum utilization of elevated temperature components which is being accomplished by the implementation of retirement-for-cause criteria [1–4]. Components are no longer routinely retired at the end of their originally estimated design life. Thus, there is a need for developing accurate methods for predicting the

[1]Present address: Rockwell International, Rocketdyne Division, 6633 Canoga Avenue, Canoga Park, CA 91304, U.S.A.

[2]To whom all correspondence should be addressed.

remaining service life of these components for establishing appropriate inspection intervals and criteria.

At high temperatures, a prominent damage mechanism for metals and alloys which can ultimately cause rupture is intergranular cavitation which occurs in response to creep deformation [5]. However, several high temperature structures consist of thick sections which are designed to resist widespread creep deformation. These components do not completely fail by creep rupture. Instead, creep cracks initiate at the high stress and high temperature regions and then propagate to failure. A significant fraction of life of these components is spent in crack propagation. Cracks in components can often be introduced during fabrication such as in welded structures. In these components, the entire life of the component can be spent in crack propagation.

The phenomenon of crack extension due to creep deformation and damage in the crack tip region in response to sustained (or slowly varying) load is known as creep crack growth. Creep cracks often grow by nucleation, growth and coalescence of grain boundary cavities [6]. However, much more work is needed for developing a better understanding of the mechanisms of creep crack growth.

In this paper, the mechanisms of creep crack growth at 400°C ($\sim 0.5\ T_m$) in a Cu–1 wt% Sb alloy are investigated. Unlike most structural alloys, the simple copper system contains minimal secondary phases and artifacts and is known to cavitate on grain boundaries when subjected to creep deformation [7, 8]. By adding 1 wt% Sb to the Cu, it is possible to reveal cavitated grain boundaries by intergranular fracture at room temperature. Recent creep crack growth results on the same material by Nix *et al.* [8] showed that the size of the grain boundary cavities ahead of the crack tip was dependent on the distance from the crack tip. Therefore, this material was considered ideal for studying evolution of creep damage in specimens subjected to different load histories.

The objectives of this study were to (i) quantify grain boundary cavitation damage in this model material as function of the magnitude of the crack tip parameter, C_t [9], (ii) to compare crack tip damage in specimens subjected to the same levels of C_t but undergoing different levels of creep deformation vis á vis small-scale vs extensive creep and (iii) characterize the influence of the level of creep damage (constrained vs unconstrained) on the validity of the crack tip field parameters which are deformation based and do not explicitly account for cavitation damage. This work is a part of an ongoing study which in the near future will also consider crack tip damage under creep-fatigue conditions as affected by loading variables such as cycle time and waveform.

Fig. 1. Intergranular fracture at room temperature in 1% antimony–copper.

EXPERIMENTAL

Material preparation and characterization

The Cu–1 wt% Sb alloy used in this study was produced by Oak Ridge National Laboratory (ORNL). 99.99% pure OFHC copper and 99.999% pure antimony were induction melted in a ZrO_2 crucible at a vacuum of 10^{-4} torr and cast in the form of 126 mm (5 in.) diameter ingot. The ingot was homogenized at 950°C for 5 h and extruded into a rectangular bar of 38.1 × 75 mm (1.5" × 3") cross section at 700°C. Considerable antimony segregation to the grain boundary occurred during the extrusion process itself. This was confirmed by examining fracture surfaces of small charpy type specimens taken from the as-extruded material which showed 100% intergranular fracture at room temperature, Fig. 1. A piece of the extruded material was also given a further segregation treatment for 24 h at 675°C. The Auger analysis of this material compared well with that of the extruded material [10] implying that the antimony segregation was nearly complete in the as-extruded material itself. This also provided assurance that no further antimony segregation will occur during the creep tests which were conducted at 400°C. The material had an average grain diameter of 57 μm (Fig. 2) and was uniform on samples taken from all faces of the rectangular bar. Based on these results the as-extruded material was used for our studies. All bars were ultrasonically tested for defects. The defective material near the end of the bars was discarded to avoid taking any samples from those areas.

The chemical composition of the material is given in Table 1. Table 2 lists the short term tensile properties of the test material at 400°C which was the test temperature for all our subsequent work. The following equation describes the plastic strain (ϵ_p) vs applied stress, σ, behavior

$$\epsilon_p = 5.39 \times 10^{-3} (\sigma/\sigma_{YS})^{4.76} \qquad (1)$$

where, σ_{YS} = 0.2% yield strength given in Table 2.

Creep deformation tests

Cylindrical specimens of 12.6 mm (0.505") diameter were tested at 400°C in air under constant load using SATEC lever type, dead weight creep machines.

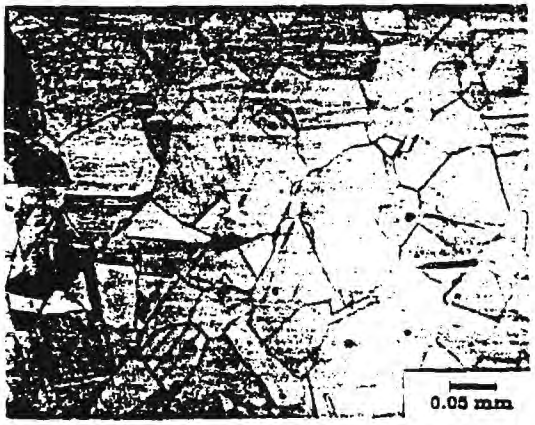

Fig. 2. Microstructure of the as extruded test material.

Testing standards and procedures were in accordance with American Society for Testing and Materials (ASTM) specification E139-79 [11]. Four specimens were subjected to stress levels ranging from 24.1 to 55.1 MPa (3.5 to 8 Ksi). Continuous measurement of strain in the gage length was made to characterize the full creep curve. Figure 3 shows typical creep curves from specimens tested at various stress levels. The creep curves exhibited mostly secondary and tertiary creep deformation. The primary creep region seemed to be absent in this material. The data were fit to the following equation

$$\dot{\epsilon} = A\sigma^n + A_3\sigma^{n_3}(\epsilon - A\sigma^n t)^{p_3} \qquad (2)$$

where, A, n, A_3, n_3 and p_3 are regression constants derived from the creep data. The values of these constants are listed in Table 3 for 400°C. Figure 3 shows the comparison between the measured creep rates and those predicted from equation (2) at various stress levels. Equation (2) appears to describe the creep deformation accurately. The steady-state creep rate as a function of stress is compared with other data in the literature [7, 12] for Cu and antimony–copper. Fig. 4. Creep rates generally appear to decrease with increase in the grain size of the material.

Creep crack growth tests

Creep crack growth testing was conducted at 400°C in air under constant load also using lever type, dead weight creep machines. Five standard compact type (CT) specimens [13] which were 50.8 mm (2 in.) wide and nominally 15.24 mm (0.6 in.) thick were fatigue-precracked at room temperature prior to testing. A MTS servo-hydraulic test system under load control conditions was used. Subsequently, these specimens were mounted on a creep machine. The load-line deflection as a function of time was measured using a LVDT system and the crack size was continuously monitored using an electric potential system. The details of the test method are described elsewhere [14, 15]. Each test was terminated prior to fracture to allow crack tip metallography to be performed for characterizing damage in the tested specimens.

Table 1. Chemical composition of the test material (wt%)

Ag	Si	S	Sb	Cr	Cu
0.01	0.06	0.01	0.98	0.02	Balance

Damage characterization in crack growth specimens

All creep crack growth specimens were sectioned through mid-thickness and the crack tip region of one-half of the specimen was mounted for metallography. Thus, a complete two-dimensional view of the creep cavitation surrounding the crack tip could be observed. The second half of the compact type specimens CT-2 and CT-5 were fractured to reveal the creep crack fracture surface and also the cavitated grain boundary facets ahead of the crack tip. These fracture surfaces were examined at a high magnification in a scanning electron microscope (SEM).

The SEM micrographs obtained at various distances (0.2, 0.6, 1, 1.3, 5.5 and 8.3 mm) from the crack tip for the two specimens were analyzed for cavity sizes and distribution using quantitative metallography procedures [16] briefly described below. The magnifications of the pictures analyzed were 330 to 400×.

A system of grids with a known total length was placed on the pictures. The total length sampled in a single field of view (FOV) was 5.091 mm. In all eight fields of view were analyzed at each of the various distances from the crack tip. The total numbers of cavities which intersected the grid lines were counted and a linear density of cavities, N_L, per mm of length was determined. The total number of cavities in all fields of view were determined and divided by the area to determine the areal density of cavities, N_A. The average diameter is then computed from the following relationship [16]

$$D_{avg} = 2.\left[\frac{2N_L}{\pi N_A}\right]. \qquad (3)$$

The fraction of projected grain boundary cavitated, A_c, is then approximately obtained by [16]

$$A_c = \frac{\pi}{4} N_A \cdot D_{avg}^2. \qquad (4)$$

The D_{avg}, N_A and A_c were related to the distance ahead of the crack tip.

Table 2. Tensile properties of the test material (400°C)

E (MPa)	σ_{YS}(0.2%) (MPa)	σ_{UTS} (MPa)	% Elongation (25.4 mm gage length)	$D^{(a)}$ $(MPa)^{-m}$	$m^{(a)}$
103.4×10^3	64.1	102.7	7	5.93×10^{-3}	4.76

(a) $\epsilon_p = D(\sigma/\sigma_{YS})^m$.

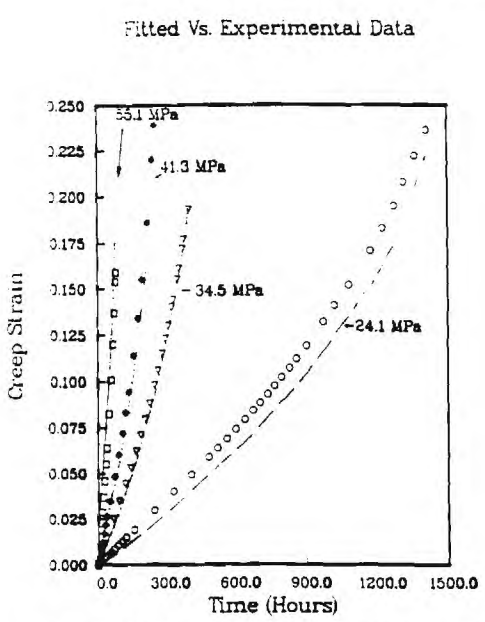

Fig. 3. Comparison between measured creep strains as a function of time for Sb–Cu at 400°C with those predicted from equation (2). The points designate measured strains and the curves designate the respective fitted trends.

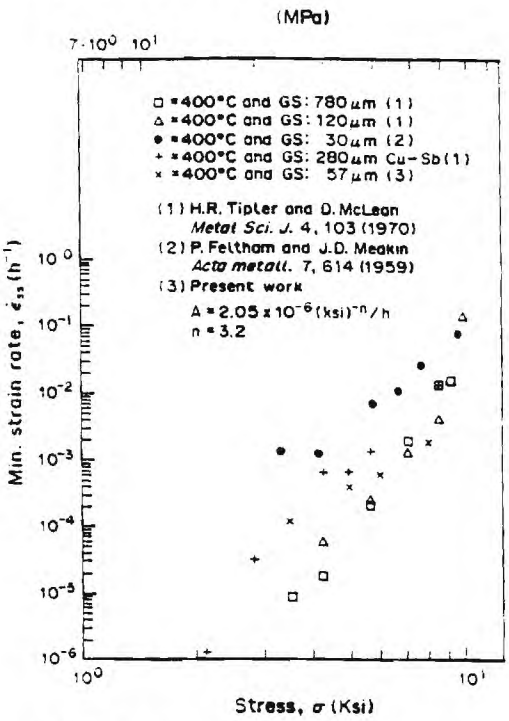

Fig. 4. Minimum (or steady-state) strain rate vs stress compared with other data on Cu and Cu–Sb.

THE C_t PARAMETER

The definition of C_t is as follows [9]. Consider several identical pairs of cracked specimens. Within each pair, one specimen has a crack length, a, and the other has an incrementally differing crack length, $a + \Delta a$. The specimens of each pair are loaded to various load levels P_1, P_2, $P_3 \ldots P_t$—etc., at elevated temperatures, and the load–line deflection as a function of time is recorded, Fig. 5(a). The load–line deflection due to creep is V_c and its time rate is given by $\dot{V}_c$. It is assumed that no crack extension occurs in any of the specimens, and the instantaneous response is linear-elastic. Consider the behavior at a fixed time, t, in the transient region where $\dot{V}_c$ is continuously changing due to the presence of small-scale creep conditions or due to transient creep resulting from primary and/or tertiary creep strains. The load vs creep deflection rate behavior is plotted for all specimens. A schematic of the expected behavior is shown in Fig. 5(b). Several such plots can be generated from the above tests by varying time.

The area between the P–$\dot{V}_c$ curves for specimens of crack lengths, a and $a + \Delta a$, is called ΔU_t^*. Physically, ΔU_t^* (the subscript denotes that this value is at a fixed time t) represents the difference in the energy rates (or power) supplied for deforming the two crack bodies with identical creep deformation histories as they are loaded to different load or deflection-rate levels. The C_t parameter is given by the following equation

$$C_t = \lim_{\Delta a \to 0} -\frac{1}{B}\frac{\Delta U_t^*}{\Delta a} = -\frac{\partial U_t^*}{B \partial a} \qquad (5)$$

where B = specimen thickness. Under small-scale-creep (SSC) conditions C_t uniquely characterizes the rate of expansion of the creep zone size [18, 19] irrespective of the type of creep deformation, vis á vis primary, secondary or tertiary creep. Under extensive creep conditions, C_t uniquely characterizes the Hutchinson, Rice and Rosengren (HRR) [20, 21] crack tip stress fields if either primary or secondary or tertiary creep dominate the deformation behavior. If a combination of more than one of the three creep deformation stages exist under extensive creep conditions, C_t still approximately characterizes the HRR field [17]. Under the special condition of extensive secondary-stage creep deformation, C_t by definition is equal to the C^*-integral of Landes and Begley [22].

A general expression for estimating C_t in test specimens has been derived [2, 9, 17]

$$C_t = \frac{P\dot{V}_c}{BW}\frac{F'}{F} - C^*(t)\left[\frac{F'/F}{\eta} - 1\right] \qquad (6)$$

where

F = K-calibration factor given by $F = (K/P)BW^{1/2}$
P = applied load
W = width of a specimen
K = applied stress intensity parameter at the time of the loading

Table 3. Creep deformation constants for the test material at 400°C. See equation (12) for a description of the A^* constants

A $(MPa)^{-n}h^{-1}$	n	A_1 $(MPa)^{-n_1}h^{-1}$	n_1	p_1
5.52×10^{-4}	3.135	4.87×10^{-4}	3.236	0.75

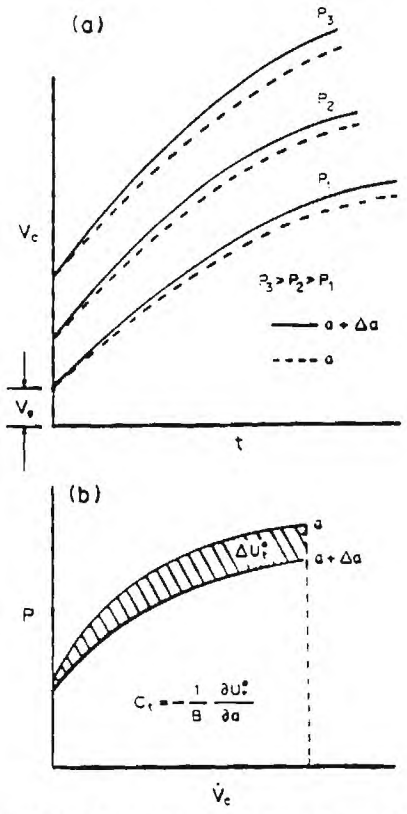

Fig. 5. (a) Load–line deflection, $\dot{V}_c$, as a function of time for bodies of crack lengths a and $a + \Delta a$ at various load levels and (b) the definition of C_t parameter.

$F' = dF/d(a/W)$

a = crack size

η = calibration factor dependent on the creep exponent, n or n_3, and crack size [17, 13].

$C^*(t)$ for materials whose creep deformation behavior is dominated by a combination of secondary and tertiary creep, such as our test material, can be derived by following the procedure of Refs [17] and [23] as follows

$$C^*(t) = C_{ss}^*[1 + (t/t_3)^{p_3/(1-p_3)}] \tag{7}$$

where, C_{ss}^* is steady-state value of $C^*(t)$ when secondary stage creep dominates and is given by the following equation for CT specimens under plane strain

$$C_{ss}^* = (W-a)A\,h_1\left[\left(\frac{P}{W-a}\right)\frac{1}{1.455\alpha B}\right]^{n+1} \tag{8}$$

where, h_1 is a calibration function listed in a handbook [25] and

$$\alpha = \left[\left(\frac{2a}{W-a}\right)^2 + 2\left(\frac{2a}{W-a}\right) + 2\right]^{1/2} - \frac{2a}{W-a} - 1. \tag{9}$$

t_3 in equation (7) is a transition time for the specimen to go from extensive secondary creep conditions to extensive tertiary creep conditions and is given by [24]

$$t_3 = \left[\frac{(1-p_3)C_{ss}^*}{C_h^*}\right]^{1-p_3/p_3} \tag{10}$$

where, C_h^* can be obtained from a simple modification of equation (8) which involves substituting $[A_3(1-p_3)]^{1/(1-p_3)}$ for A and $n_3/(1-p_3)$ for n [23]. $\dot{V}_c$ in equation (6) can be estimated from the measured deflection rate, $\dot{V}$, by the following equation [26]

$$\dot{V}_c = \dot{V} - \frac{\dot{a}B}{P}\left(\frac{2K^2}{E}\right) \tag{11}$$

where, E = elastic modulus. For slowly growing cracks, the second term in equation (11) is negligible in comparison to $\dot{V}$ and $\dot{V}_c \simeq \dot{V}$. Since the definition of C_t is based on stationary cracks, it is important that the condition of slowly growing cracks be met. This can be checked by assuring that the second term on the right hand side of equation (11) is less than 10% of the measured value of $\dot{V}$.

Creep crack growth rate, da/dt at any given point in the test was estimated by the secant method in which an increment in crack extension, Δa, was divided by the corresponding increment in time, Δt. Thus, da/dt and the corresponding C_t values were determined. These results are discussed in the next section.

RESULTS AND DISCUSSION

da/dt vs C_t *correlation*

Figure 6 shows the creep crack growth rate, da/dt, plotted as a function of C_t at 400°C for all five compact specimens. The data from the various tests do not correlate with C_t which was, at first, a surprising result. However, a possible explanation of this trend is as follows. Since this material cavitates extensively with large cavity sizes, it is suspected that the lack of correlation may be due to the development of large scale cavitation damage at the crack tip. C_t

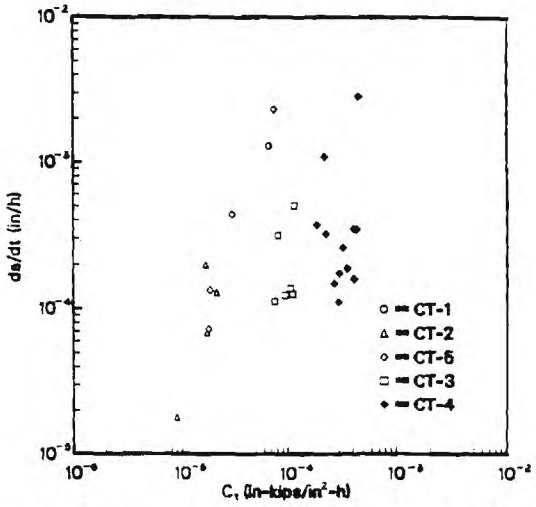

Fig. 6. Creep crack growth rate as a function of the C_t parameter.

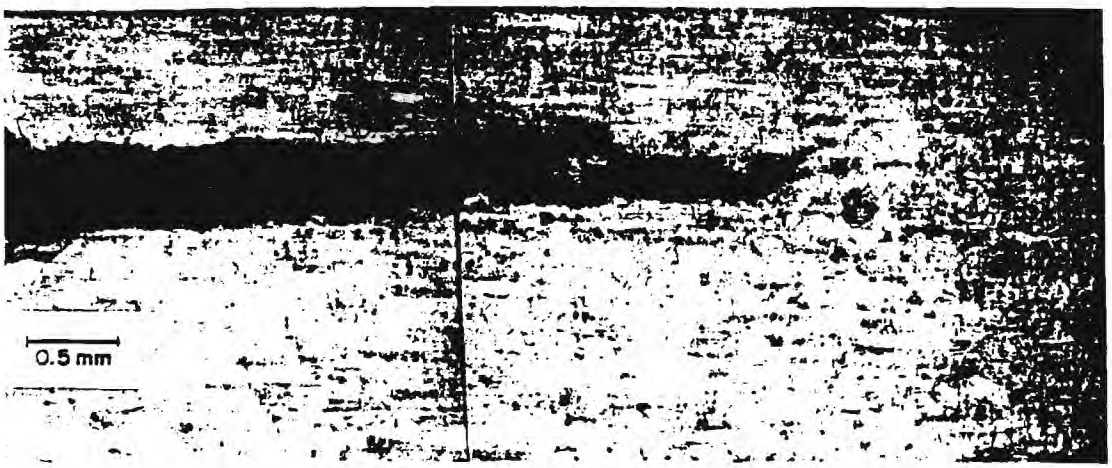

Fig. 7. Crack tip region of tested specimen CT-2.

is a deformation based global parameter much like the J-integral [27]. Therefore, the relationship between C_t and the creep zone expansion rate in small scale creep regime [18] as well as the relationship between C_t and the crack tip stress in extensive creep regime [17, 19] are based on the assumption that the damaged region containing cavities or micro-cracks is small in comparison to the crack size and the remaining ligament size of the specimen (or component). This explanation was further explored by characterizing the extent of damage ahead of the crack tip in the various creep crack growth specimens using metallography and scanning electron microscopy (SEM).

Figures 7 to 10 show photo-micrographs from the crack tip regions of specimens CT-2 through CT-5, respectively. Specimens CT-2 and CT-5 show isolated grain boundary cavities while as the micrographs from specimens CT-3 and CT-4 show extensive microcracking and crack branching at their respective crack tips. In fact, the damage in these latter specimens was present over a large region ahead of the main crack. In specimen CT-4, crack branching occurs almost from the tip of the deformed precrack indicating that very little, if any, of the crack growth occurred as growth of a single dominant flaw. Since fracture mechanics concepts are limited to the characterization of the growth of single flaws, the lack of correlation between da/dt and C_t is understandable.

In view of the above findings, the creep crack growth rate data obtained on specimens CT-1, CT-2 and CT-5 (the behavior of CT-1 was similar to CT-2 and CT-5) are plotted on a separate plot shown in Fig. 11. A good correlation between da/dt and C_t in these set of data was in fact obtained which further supports the argument that the lack of correlation between creep crack growth rate and C_t in Fig. 6 was

Fig. 8. Same as Fig. 7 except for specimen CT-3.

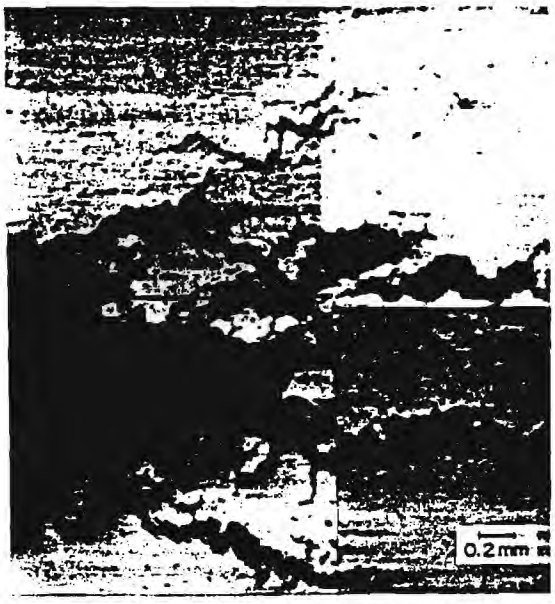

Fig. 9. Same as Fig. 6 except for specimen CT-4.

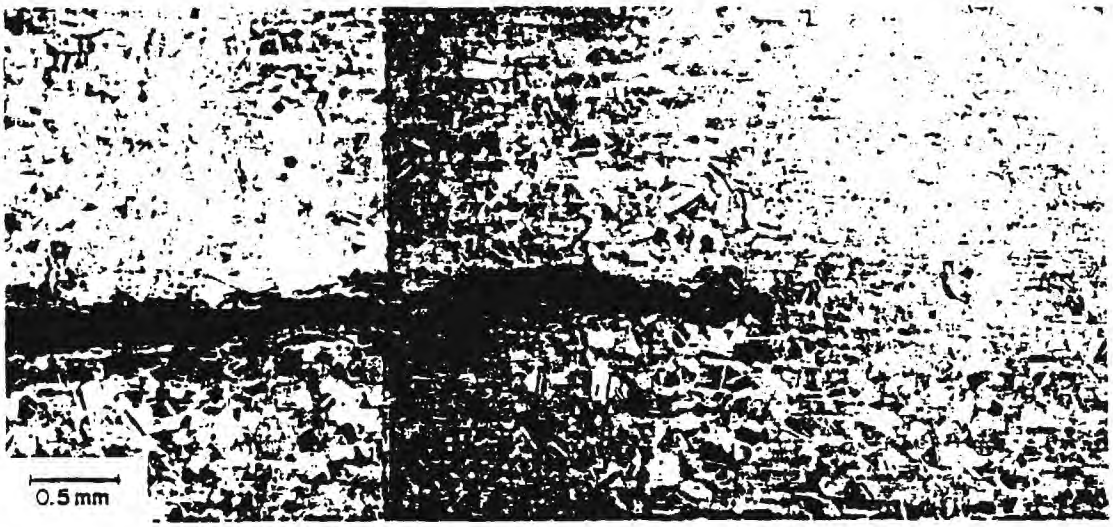

Fig. 10. Same as Fig. 6 except for specimen CT-5.

due to development of large scale damage in some of the specimens tested. The specimens in which the problem of large scale damage was encountered were the ones in which the initially applied K levels were higher (factor of 2 higher than the specimens from which consistent data were obtained). The high initial K levels may have led to nucleation of large amounts of cavities and subsequently a high rate of growth over a substantial portion of the ligament. The cavities can then coalesce to form microcracks and branched cracks. At lower initial K levels, cavitation may have been isolated as well as restricted to the near crack tip process zone with less opportunity to form microcracks. This facilitated the growth of a single dominant crack in these specimens.

Since the onset of tertiary creep is often associated with significant cavitation, it is interesting to see if crack branching occurs in specimens in which significant tertiary creep deformation occurs also. One measure of the extent of tertiary creep in specimens is obtained when the test time is compared with t_3, the transition time for significant tertiary creep to develop from extensive secondary creep conditions. Thus, the transition time, t_3, was calculated for the various test specimens for plane strain and plane stress conditions using equation (10) and are listed in Table 4. Also reported in Table 4 is the transition time, t_T, for extensive steady-state creep conditions to develop from small-scale creep conditions. t_T is given by the following equation [28, 29] .

$$t_T = \frac{[K^2(1-\nu^2)]}{E(n+1)C_t^*}. \tag{12}$$

All terms in equation (12) have been defined previously. It is observed that t_T for all tests are considerably smaller than the corresponding test durations. Thus, for practical purposes, all tests can be considered to have been in extensive creep conditions for the entire duration. We now turn our attention to the transition from extensive secondary creep to extensive tertiary creep given by t_3. Since plane stress estimates of t_3 are considerably shorter than the plane strain estimates, the former are used for comparison with the test duration. The appropriateness of this assumption is further discussed later in this section.

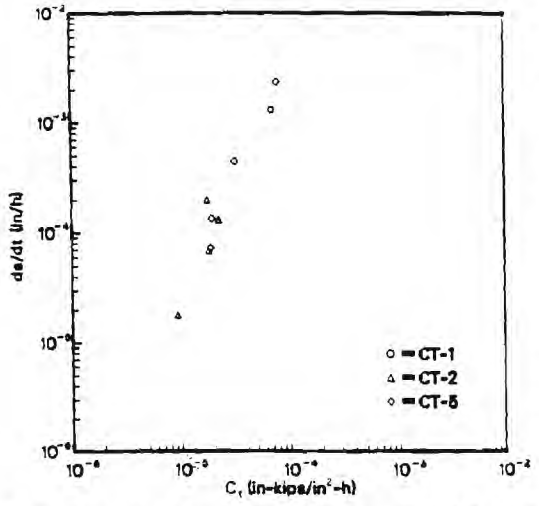

Fig. 11. Creep crack growth data as a function of C_t from three specimens which did not show unconstrained damage and crack branching.

For specimens CT-2 and CT-5 which exhibited singular crack growth, t_3 is approximately two orders of magnitude higher than the operating time. Hence, tertiary creep conditions in these specimens are expected to be restricted only to a small region ahead of the crack tip. This is also in agreement with the earlier observations from crack tip metallography. On the other hand the test duration is 16 and 40% of t_3 for specimens CT-3 and CT-4, respectively. These specimens did not exhibit singular crack growth and the creep crack growth rate data obtained from these specimens did not correlate with C_t. Therefore, in order to maintain constrained cavity

Table 4. Transition times t_T and t_1 for the creep crack growth specimens tested

Specimen No.	Crack size a(mm)	Initial K (MPa$\sqrt{}$m)	t_T (h)	t_1(h) pl strain	t_1(h) pl stress	Test duration (h)
CT-2	15.24	1.63	22.6	2.56×10^5	8.4×10^4	1217
CT-3	15.24	3.71	3.68	1.83×10^4	4.93×10^3	772
CT-4	21.59	4.07	2.55	1.05×10^4	1.75×10^3	720
CT-5	15.24	1.63	22.5	2.59×10^5	8.19×10^4	210.5

growth in the crack tip region, it appears necessary to restrict test time to a small fraction of t_1.

We now return to the question of the appropriateness of the plane stress vs plane strain assumption. Plane strain conditions are expected to prevail in the near crack tip region in test specimens. Therefore, when the specimen is in small scale creep where the creep deformation is restricted to the crack tip region, plane strain conditions are the appropriate condition. This will be the case in the beginning of the test. On the other hand, as the test progresses and the creep deformation becomes more wide spread, plane stress conditions which exist away from the crack tip region will contribute significantly to the overall deformation behavior of the specimen. Therefore, under extensive creep conditions, perhaps the plane stress estimates are more appropriate.

Another aspect of the above discussion deals with side grooving of specimens which promotes plane strain conditions. From the above discussion it follows that side grooving will have the effect of increasing t_1 and forcing constrained cavitation in a regime where unconstrained cavity growth is expected without the side grooves. Therefore, side grooves may help in extending the regime over which valid crack growth rate measurements can be obtained.

Damage zone growth

From the previous discussion it is evident that creep cracks in antimony–copper grow due to cavitation damage ahead of the crack tip. As discussed earlier, C_t is a deformation based parameter and can only correlate creep crack growth data if the damage zone is completely constrained by a significantly larger deformation zone in which the crack tip fields apply. It is thus interesting to explore the relationship between the characteristics of cavitation with the damage zone and the applied C_t levels.

The terminal C_t levels for specimens CT-2 and CT-5 were 1.63 and 3.29 J/m²h, respectively. The corresponding average crack growth rates were 2.36×10^{-4} and 1.84×10^{-3} mm/h, respectively. Figures 12 and 13 show the cavitation damage ahead of the crack tip in the mid-thickness region of specimens CT-2 and CT-5, respectively. The cavity sizes and numbers as a function of distance ahead of the crack tip were quantitatively measured in these specimens following the procedure described in an earlier section. Figures 14a and 14b show the linear density and Fig. 14(c) and (d) show the areal density respectively, of cavities as a function of distance ahead of the crack tip in specimens CT-2 and CT-5. The average cavity diameter [calculated using equation (3)] as a function of distance from the crack tip is plotted in Fig. 15 for the two specimens. The percent grain boundary area cavitated [calculated using equation (4)] as a function of distance from the crack tip is also plotted, Fig. 16. There are several interesting implications of these results which merit further discussion.

It is observed that the areal density, diameter and the fraction of grain boundary area cavitated (A_c) increase significantly as the crack tip is approached. Cavities were found to exist as far as 8 mm ahead of the crack tip, however, the diameter, density and A_c decreased at a rapid rate up to a distance of 1.3 mm and changed only marginally for larger distances. Therefore, it can be argued that the zone of intense damage extends up to approximately 1.3 mm from the crack tip. The remaining ligament size was about 34 mm which was more than 25 times of the damage zone. Therefore, the condition that the damage be contained in a small region near the crack tip for C_t to be applicable appears to have been met in these specimens.

Fig. 12. SEM photomicrograph showing creep cavities on the fracture surface of specimen CT-2.

Fig. 13. Same as Fig. 12 except for specimen CT-5.

The C_t level of specimen CT-5 was twice that of CT-2. The cavity diameter as a function of distance from the crack tip shows an opposite trend. In other words, the cavity diameters in speciment CT-2 appear to be consistently larger than in specimen CT-5 (Fig. 15). However, the areal density of cavities was higher in specimen CT-5 (Fig. 14) and the percent grain boundary area cavitated also appears to be somewhat higher in specimen CT-2, Fig. 16. From these observations, the following interpretations can be made regarding the damage accumulation during the creep crack growth process.

The smallest stable cavities which were detected in the crack tip region were approximately 3 μm in diameter and the largest were approximately 15 μm in diameter. Hence, considerable cavity growth must occur due to creep deformation in the crack tip region as a fixed point in the material ahead of the crack tip is being approached by the growing crack. The cavity growth can occur by a Hull–Rimmer type [30] atomic diffusion process which in all likelihood in the crack tip region is constrained by deformation in the surrounding grains. Simultaneously, cavity growth can also occur by a process in which the larger cavities grow by consuming the smaller ones in its neighborhood. This will generally lead to a reduction in areal density of cavities. It was observed [31] that in uniformly and uniaxially loaded creep specimens of this material which were interrupted at various life fractions that the cavity density (number of cavities/unit area) decreased with increasing life fraction (or creep strain). Therefore, the latter mechanism of cavity growth at the crack tip is in fact supported by experimental observations.

The data also clearly show that fresh cavities must continuously nucleate at fixed points as they are approached by the moving crack tip. This is apparent from Fig. 14(b) which shows an increasing density of cavities with decreasing distance from the crack tip. This is not surprising in view of the high stresses (or strains) encountered as the distance to the crack tip decreases thus causing new cavities to nucleate. Some of these cavities coalesce with the larger ones and contribute to their growth as discussed in the preceding paragraph while others grow to larger sizes by themselves. It appears that the nucleation rate of cavities increases with C_t [Fig. 14(c, d)].

The accumulated creep damage in the crack tip region is a complex function of the rate at which cavities nucleate and subsequently grow by one or more of the operative mechanisms. A suitable measure of overall creep damage is A_c as shown in Fig. 16. This measure of damage includes the contributions from the different cavity nucleation and growth processes operating in the crack tip region. It appears that the damage levels are consistently higher for specimens with the lower crack growth rate. This trend is discussed later in this section.

In view of the experimental results, it is worthwhile to examine the various criteria for crack extension due to damage for cavitating materials. Previous researchers [32, 33] have used the attainment of a critical cavity size as a condition for coalescence with the crack tip. When this condition is met, the crack is postulated to extend by a distance equal to the average cavity spacing. For cavity growth mechanisms which are constrained by deformation, this is equivalent to a critical strain criterion. This criterion appears to be reasonable if cavity nucleation is not continuous. In other words, once cavity nucleation has taken place at a certain distance in front of the crack tip, no new cavities form at that location as it approaches the moving crack tip. The criterion applies well to materials in which cavity nucleation occurs only at second phase particles [6] where the areal density of cavities remains constant with respect to distance from the crack tip. For this condition, the fraction of grain boundary area cavitated, A_c,

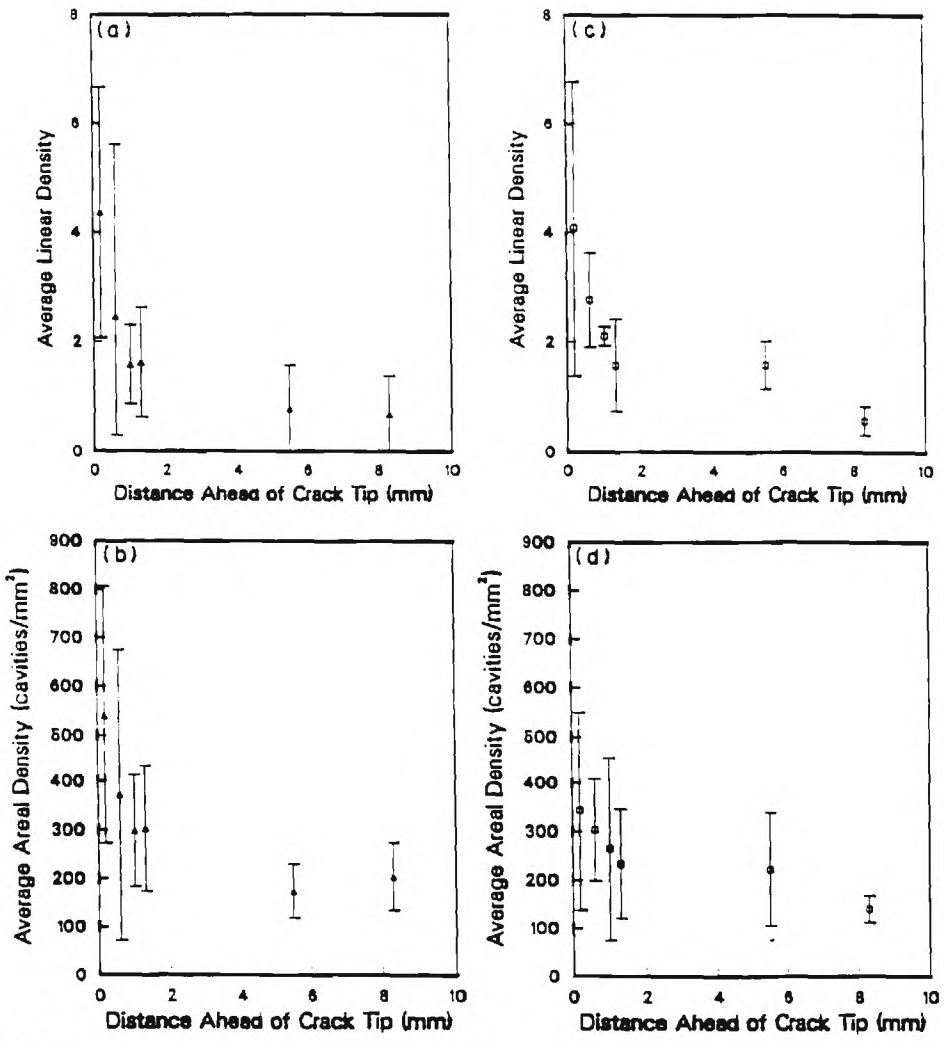

Fig. 14. (a,b) Average linear density of cavities as a function of distance from the crack tip for specimens CT-5 and CT-2, respectively. (c,d) Average areal density of cavities as a function of distance from the crack tip for specimens CT-5 and CT-2, respectively.

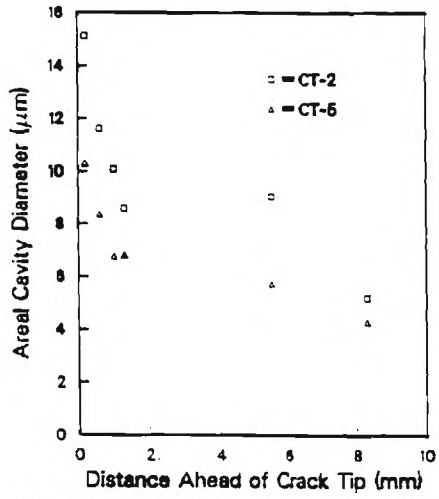

Fig. 15. Average cavity diameter vs distance ahead of the crack tip in CT-2 and CT-5.

depends uniquely on the cavity size [equation (4)]. Hence, there is no difference between using critical A_c or critical cavity diameter as a condition for coalescence. On the other hand, in the presence of continuous nucleation, A_c continues to be relevant while the critical cavity diameter no longer remains a valid crack extension criterion.

The other commonly used crack extension criterion is the Kachanov–Rabotnov ω which is an internal variable with a value of zero in undamaged condition and one in the critically damaged condition [34, 35]. In variations of this approach, the critical value of ω, ω_c, is assumed to be a constant which is less than one. A direct relationship between ω and A_c has also been suggested. Thus, the use of A_c also appears to be consistent with this approach.

In the current approaches [32–34], ω_c and the critical cavity sizes are treated as constants independent of stress. However, our data from the two specimens examined show that the value of A_c in the immediate vicinity of the crack tip varies inversely

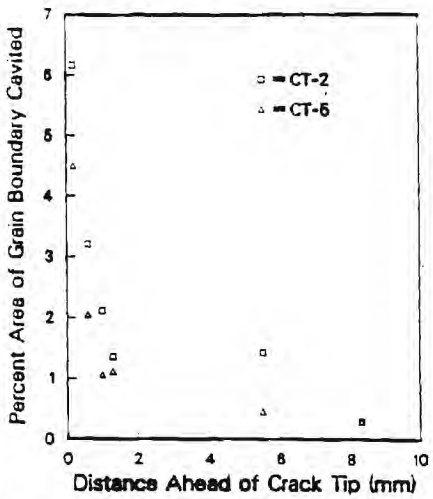

Fig. 16. Fraction of grain boundary area cavitated as a function of distance from the crack tip for specimens CT-2 and CT-5.

with crack growth rate or with C_t. These values of A_c represent the critical values of A_c for crack extension in these specimens. This trend will be confirmed by additional testing.

Another point of interest from the data of Fig. 16 is the distribution of damage as a function of distance from the crack tip and its relationship with the crack tip parameters such as C_t and C^*. Specifically, it is of interest to determine if the extent of the region of intense damage varies significantly and uniquely with the magnitude of C_t. Before discussing these trends, it is necessary to examine some governing equations for evolution of damage in front of the crack tip. For simplicity, we will consider damage distribution along the crack plane only.

Consider a crack moving at a velocity $\dot{a}$ (da/dt) and a fixed rectangular coordinate system with the x-axis located along the crack plane and the origin located at the original crack position. The crack growth rate varies with time in a transient problem. Damage at a point along the x-axis is modelled as a function of both position and time, t, and is represented by $A_c(x, t)$ or $D(x, t)$. Thus, the rate of damage accumulation, dD/dt, will be given by (recognizing that $dx/dt = -\dot{a}$)

$$\frac{dD}{dt} = \frac{dA_c}{dt} = \left[\frac{\partial A_c}{\partial t}\right]_x - \dot{a}\left[\frac{\partial A_c}{\partial x}\right]_t. \qquad (13)$$

During the initial incubation period following loading, $\dot{a}$ is nearly zero and dD/dt is expected to be dominated by the $(\partial A_c/\partial t)_x$ term. However, $(\partial A_c/\partial t)_x$ will decrease with time and will nearly become zero when the crack tip stresses are completely relaxed and attain a stationary stress state. The rate of damage accumulation at this point will be given completely by the $(\partial A_c/\partial x)_t$ term. With respect to a coordinate system which moves the crack tip, dD/dt will then be zero. In order to determine the damage function $D(x, t)$, it is necessary to integrate equation (13) with knowledge of the functional forms of $(\partial A_c/\partial t)_x$ and $(\partial A_c/\partial x)_t$. At present, sufficient information is not available to derive the complete damage distribution function. However, it seems reasonable to expect from equation (13) that a high value of $\dot{a}$ will lead to a lower accumulated damage ahead of the crack tip.

SUMMARY AND CONCLUSIONS

Tensile, creep deformation and creep crack growth tests were conducted on a model 1% antimony–copper alloy at 400°C. The mechanical tests were followed by extensive characterization of grain boundary cavitation damage in the creep crack growth specimens by optical metallography and scanning electron microscopy (SEM). The following observations and conclusions can be made from the results of these experiments.

1. Creep deformation behavior in this model alloy at 400°C is dominated by secondary and tertiary creep deformation. It is, therefore, important to account for tertiary creep in estimating the magnitude of C_t, a crack tip parameter for creep conditions.

2. The creep crack growth rate correlates with C_t provided the cavitation damage is contained and therefore restricted to a small region near the crack tip. Further, no crack branching should also occur.

3. It is shown that creep cracks propagate by simultaneous nucleation, growth and coalescence of grain boundary cavities. The cavity diameter, areal cavity density and percent fraction of grain boundary area cavitated decrease with distance from the crack tip.

4. The most suitable index of crack tip damage appears to be the percent grain boundary area cavitated. The extent of damage is a complex function of position and time. The critical damage for crack extension appears to vary inversely with the applied value of C_t. Further tests are recommended for completely mapping the complex damage function and determining whether a unique relationship exists between the distribution of damage and the applied value of C_t.

Acknowledgements—The authors are indebted to the Basic Energy Sciences Division of the U.S. Department of Energy (DOE) for the financial support of this work under Research Grant DE-FG05-86ER-45257 with Dr J. B. Darby as the contract monitor. The assistance of Dr V. K. Sikka of Martin Marietta Energy Systems, Oak Ridge National Laboratory in producing and processing the antimony–copper alloy is also appreciated. Useful technical discussions with Professors S. R. Stock, A. M. Gokhale and D. L. McDowell are gratefully acknowledged and so is the considerable assistance of R. C. Brown, B. Gieseke, Richard Norris and K. Banerji in various experimental aspects of the program.

REFERENCES

1. A. Saxena, P. K. Liaw, W. A. Logsdon and V. E. Hulina, *Engng Fract. Mech.* **25**, 289 (1986).
2. A. Saxena and P. K. Liaw, CS-4688, Project 2253-7, Electric Power Res. Inst., Palo Alto, Calif. (1986).

3. *Life Assessment and Improvement of Turbo-Generator Rotors for Fossil Plants* (edited by R. Viswanathan). Pergamon Press, Oxford (1985).
4. J. A. Harris, D. L. Sims and C. A. Annis, Tech. Rep. AFWAL-TR-80-4118 (1980).
5. H. Riedel, *Fracture at High Temperatures*. Springer, Berlin (1987).
6. S. Janis and A. Saxena, in *Effects of load and Thermal Histories* (edited by P. I. Liaw and T. Nicholas), pp. 201–220. T.M.S.-A.I.M.E., New York (1987)
7. H. R. Tipler and D. McLean, *Metals Sci. J.* **4**, 103 (1970).
8. J. C. Earthman, J. C. Gibeling and W. D. Nix, *Acta metall.* **33**, 805 (1985).
9. A. Saxena, in *Fracture Mechanics: Seventeenth Volume* (edited by J. Underwood *et al.*), ASTM STP 905, pp. 185–201. Am. Soc. Test. Mater., Philadelphia, Pa.
10. J. T. Staley Jr, M.S. thesis, Georgia Inst. of Technology (1988).
11. ASTM Standard E139-79, *ASTM Book of Standards*, Part 10, pp. 332–347 (1980).
12. P. Feltham and D. Meakin, *Acta metall.* **7**, 614 (1959).
13. ASTM Standard No. 813-81, *ASTM Book of Standards*, Part 10, pp. 822–840 (1982).
14. A. Saxena, in *Fracture Mechanics: Twelfth Conference*, ASTM STP 700, pp. 131–151. Am. Soc. Test. Mater., Philadelphia, Pa.
15. A. Saxena, T. T. Shih and H. A. Ernest, in *Fracture Mechanics: Fifteenth Symposium*, ASTM STP 833, pp. 516–531. Am. Soc. Test. Mater., Philadelphia, Pa (1984).
16. E. E. Underwood, *Quantitative Stereology*. Addison-Wesley, Reading, Mass. (1970).
17. C. P. Leung, D. L. McDowell and A. Saxena, Topical Report on Contract 2253-10, Electric Power Research Inst., Palo Alto, Calif. (1988).
18. J. L. Bassani, D. E. Hawk and A. Saxena, *Third Int. Symp. Nonlinear Fracture Mechanics*, Knoxville, ASTM STP 905 (1986). In press.
19. A. Saxena, *ASM Mater. Sci. Seminar on Fracture Mechanics, Microstructure and Micromechanisms*, 1987. In press.
20. J. W. Hutchinson, *J. Mech. Phys. Solids* **16**, 13 (1968).
21. J. R. Rice and G. F. Rosengren, *J. Mech. Phys. Solids* **16**, 1 (1968).
22. J. D. Landes and J. A. Begley, in *Mechanics of Crack Growth*, ASTM STP 590, pp. 128–148. Am. Soc. Test Mater., Philadelphia, Pa (1976).
23. H. Riedel and V. Detampel, *Int. J. Fract.* **24**, 239 (1987).
24. H. Riedel, *J. Mech. Phys. Solids* **29**, 35 (1981).
25. V. Kumar, M. D. German and C. F. Shih, EPRI NP-1931, Palo Alto, Calif. (1981).
26. A. Saxena and J. D. Landes, in *Advances in Fracture Research*, ICF-6 (edited by S. R. Valluri *et al.*), pp. 3977–3988. Pergamon Press, Oxford (1984).
27. J. R. Rice, *Trans. ASME, J. appl. Mech.* **35**, 79 (1968).
28. H. Riedel and J. R. Rice, in *Fracture Mechanics: Twelfth Conference, ASTM* STP 700, pp. 112–130. Am. Soc. Test. Mater., Philadelphia, Pa (1980).
29. K. Ohji, K. Ogura and S. Kubo, *Trans. Japan Soc. Mech. Engng*, No. 790-13, pp. 18–20 (1979).
30. D. Hull and D. E. Rimmer, *Phil. Mag.* **4**, 673–687 (1959).
31. S. R. Stock, Y. Lee, J. T. Staley and A. Saxena, To be published.
32. D. A. Wilkinson and V. Vitek, *Acta metall.* **30**, 1723 (1982).
33. F. H. Wu, J. L. Bassani and V. Vitek, *J. Mech. Phys. Solids*, pp. 455–475 (1986).
34. H. Riedel, Recent advances in modelling creep crack growth, *Proc. Seventh Int. Conf. on Fracture* (ICF7) Houston, Texas (1989).
35. J. L. Bassani and D. E. Hawk, in *Proc. Mecamat Int. Seminar on High Temperature Fracture Mechanisms and Mechanics*, Dourdan, France (edited by P. Bensussan *et al.*), pp. 19–40. Moissy-Cramayet (1987).

Reprinted from

Advances in Fracture Research

PROCEEDINGS OF THE 7th INTERNATIONAL CONFERENCE ON FRACTURE (ICF7), HOUSTON, TEXAS, 20–24 MARCH 1989

Editors

K. SALAMA, K. RAVI-CHANDAR
D. M. R. TAPLIN, P. RAMA RAO

Sponsored by

THE INTERNATIONAL CONGRESS ON FRACTURE (ICF)

Organized by

THE UNIVERSITY OF HOUSTON

PERGAMON PRESS

OXFORD · NEW YORK · BEIJING · FRANKFURT
SÃO PAULO · SYDNEY · TOKYO · TORONTO

Recent Advances in Elevated Temperature Crack Growth and Models for Life Prediction

ASHOK SAXENA

Professor, Mechanical Properties Research Laboratory, School of Materials Engineering, Georgia Institute of Technology, Atlanta, Georgia 30332-0245, USA

ABSTRACT

This paper summarizes the recent developments in the field of time-dependent fracture mechanics over the past few years. The state of understanding in this area is now at the same level as elastic-plastic fracture mechanics. The important developments and their applications are described in this paper.

KEYWORDS

Creep, Cracks, J-Integral, C^*-Integral, C_t, Fatigue

INTRODUCTION

Critical gas and steam turbine, power-plant boiler and petro-chemical reactor components which operate at elevated temperature tend to develop cracks during the service life. Some components have crack like defects even at the time they go into service which can grow and cause failure. Some examples of major failures in the power industry involving elevated temperature components where creep was a major contributing factor include turbine rotors (Kramer and Randolph, 1976) and steam pipes. These failures resulted in millions of lost dollars in down time and repair costs and, in some cases, also loss of human lives. Thus, crack growth under elevated temperature creep conditions is a major industrial problem.

Further impetus for studying elevated temperature crack growth comes from the need to assess the remaining life of components which have been in service and are approaching their originally predicted design life. More and more operators of equipment are turning to a retirement-for-cause (RFC) philosophy rather than to rely on life predictions made several years ago with concepts which are now out-dated (Harris et al., 1980; Saxena et al. 1986).

Failures due to creep can be classified either as resulting from widespread or bulk damage, or resulting from localized damage. The structural components which are vulnerable to bulk damage are subjected to uniform loading and uniform temperature distribution during service, for example, thin wall pipes. The thin life of such a component can be estimated from creep rupture data. On the other hand, components which are subjected to stress and temperature gradients (typical of thick section components) will not fail by creep rupture. It is more likely that at the end of the predicted creep rupture life, a crack develops at the critical location which propagates and ultimately causes failure. Thus, crack growth is an important part of a component's overall life.

In this paper, the concepts of time dependent fracture mechanics (TDFM) for characterizing elevated temperature crack growth behavior and their role in life prediction are briefly reviewed. No attempt is made to summarize developments in the methods for predicting creep rupture which is broad enough by itself to warrant a separate review.

ADVANCES IN TIME-DEPENDENT FRACTURE MECHANICS (TDFM) CONCEPTS

Crack Tip Stress Analysis

The difference between the crack tip stress and strain fields of bodies loaded in the creep and subcreep temperature regime occurs due to the presence of time dependent strains in the creep regime. The accumulated strain in front of a stationary crack tip changes continuously and the crack tip stress can also vary with time depending on whether or not steady-state conditions have been reached.

The levels of creep deformation under which creep crack growth can occur include the small-scale-creep (SSC) region, the tran-sition creep region and the extensive creep region. Under SSC, the creep zone is small in comparison to the size of the body and the crack size and its growth is constrained by the surrounding elastic material. Under extensive creep conditions, the creep zone enguifs the entire ligament. The transition creep region is the intermediate condition. These regions are analogous to the small-scale-yielding, the elastic-plastic and fully plastic conditions, respectively, encountered in the sub-creep temperature regimes. In addition to the above, the picture at elevated temperature is further complicated when primary and tertiary creep deformations occur either by themselves or in conjunction with elastic and/or secondary creep deformations. Fortunately, following the pioneering work of Landes and Begley (1976) which led to the discovery of C^*, the crack tip stress fields for a variety of creep deformation laws have been worked out (Riedel and Rice, 1980; Riedel, 1981, Riedel and Detempel, 1987; Ehlers and Riedel, 1981, Ohji et al, 1979). In general, we can express the amplitude of the Hutchinson, Rice and Rosengren (HRR) (Hutchinson, 1968; Rice and Rosengren, 1968) crack tip stress fields by the following equation.

$$\sigma_{ij} = \left[\frac{C(t)}{BI_\gamma r} \right]^{\frac{1}{1+\gamma}} \tilde{\sigma}_{ij}(\theta,\gamma) \qquad (1)$$

Here, B and γ are treated as generic material constants whose values depend on the dominant mechanism of creep deformation operating in the crack tip region. For example, for power-law creep B=A and γ=n; for primary creep $B=A_1/(1+p)$ and $\gamma=n_1$.A, n, p, A_1 n_1 are material constants in the respective creep deformation equations given in Table 1. I_γ is a nondimensional constant which depends on γ and ranges between 3.8 and 6.3 for a range of γ values (Shih, 1983). $\tilde{\sigma}_{ij}(\theta,\gamma)$ is an angular function and r=distance from the crack tip. The expressions for extimating C(t) for several creep deformation laws are given in Table 1. Note that for extensive power-law creep $C(t)=C^*$. There is an abundance of experimental data which show that under these conditions C^* characterizes the creep crack growth behavior (Saxena, 1980).

Since C(t) uniquely relates to the amplitude of the crack tip stress fields for a variety of creep deformation laws, it is an attractive candidate crack tip parameter for characterizing creep crack growth for other than just the conditions for which it is equal to C^*. However, there are two major shortcomings of this approach. First, C(t) cannot be measured at the loading pins of the test specimens except for the two very special conditions of extensive power-law creep and the extensive primary creep shown in Table 1 (Saxena, 1988). Under these conditions, C(t) is also equal to the stress-power dissipation rate (U^*) in the cracked body. For extensive power-law creep, this relationship is given by (Landes and Begley, 1976)

$$C(t) = C^* = -\frac{1}{B}\frac{dU^*}{da} \qquad (2)$$

where, B = thickness of the specimen. However, under small-scale and transition creep conditions $C(t) \neq -1/B\,(dU^*/da)$.

The second shortcoming results from the question about the dominance of the HRR fields for growing cracks. It has been experimentally (Saxena et al., 1984) and numerically (Hawk and Bassani, 1986) shown that this limitation is not important in the extensive creep regime when crack velocities are low and the HRR fields essentially dominate over large distances ahead of the crack tip. Recent numerical results (Hawk and Bassani, 1986), reproduced in Fig. 1, have shown that in SSC, the region of influence of growing cracks (known as the Hui-Riedel (or HR) field (Hui and Riedel, 1981; Hui, 1983) can in fact be significant in comparison to the HRR fields. Under these circumstances the use of C(t) as a crack tip parameter is invalid. Other approaches must be considered.

C_t - Parameter

The C_t parameter (Saxena, 1986) is an extension of the stress-power dissipation rate interpretation of C^* into the transient regime. It also

Deformation Law	Expressions for Estimating the Amplitude of the HRR Field, C(t)		Reference
1. Power-law creep	C^*	---A	Landes and Begley (1975)
$\dot{\varepsilon} = A\sigma^n$			Goldman and Hutchinson (1975)
2. Elastic + power-law creep			
$\dot{\varepsilon}=\dot{\sigma}/E+A\sigma^n$			Riedel and Rice (1980)
a. SSC condition	$\frac{(1-\nu^2)\,K^2}{(n+1)Et}$	---B	Ohji, Ogura and Kubo (1978)
b. Transition creep condition	A + B		Ehlers and Riedel (1981)
3. Primary creep			
$\dot{\varepsilon}=A_1[\sigma(t)]^{-p}\sigma^{n_1(1+p)}$	$\frac{C_h^*}{A_1(1+p)c^{1/(1+p)}}$	---C	Riedel (1981)
4. Elastic + primary creep			
$\dot{\varepsilon}=\dot{\sigma}/E+A_1[\sigma(t)]^{-p}\sigma^{n_1(1+p)}$			
a. SSC condition	$\left(\frac{K^2(1-\nu^2)}{Et}\right)^{\frac{1+p}{1+n_1}}\frac{1}{1+n_1}$	---D	Riedel (1981)
b. Transition creep	C + D		Riedel and Detampel (1987)
5. Elastic + primary + secondary creep			
$\dot{\varepsilon}=\dot{\sigma}/E+A_1[\sigma(t)]^{-p}\sigma^{n_1(1+p)}+A\sigma^n$	A + C + D		Riedel and Detampel (1987)

A, n, p, n_1, A_1 are material constants derived from creep deformation tests at several stress levels. E = elastic modulus, t = time elapsed. C^* and C_h^* are path-independent integrals, K = stress intensity parameter.

Table 1. Summary of major crack tip stress analysis results in creeping bodies.

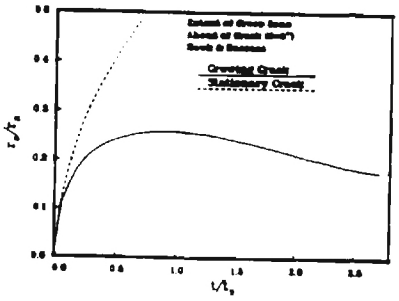

Fig. 1. Normalized creep zone size as a function of normalized time for a growing and stationary crack in Mode III. Hawk and Bassani (1986).

alleviates the two primary shortcomings of the C(t) approach as will be explained in this section. C_t is defined as the instantaneous stress-power dissipation rate as follows:

$$C_t = -\frac{1}{B}\frac{\partial U_t^*}{\partial a} \tag{3}$$

where, U_t^* represents an instantaneous value at time, t, after application of the load. The parameter is defined for a stationary crack and the implications for the growing crack will be considered later in this section. Under the conditions of extensive steady-state creep it is obvious from the respective definitions that $C_t = C^*$. Therefore, under these conditions and for extensive primary creep conditions, $C_t = C(t)$ and hence it also characterizes the amplitude of the HRR field. Under conditions of small-scale and transition creep $C_t \neq C(t)$ as shown clearly in the numerical results (Bassani et al., 1986) and reproduced in Fig. 2.

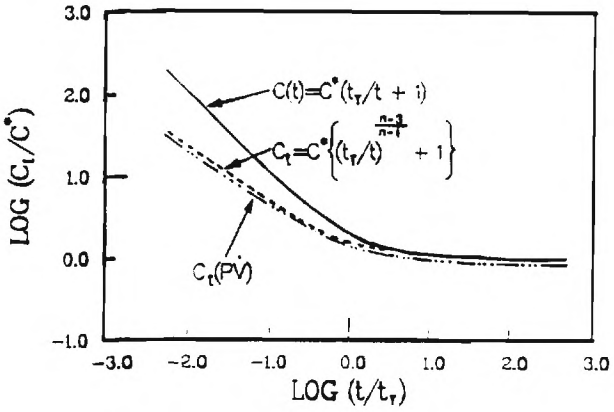

Fig. 2. Results of the stationary crack analysis of the CT Specimen, Bassani et al. (1986).

In small-scale-creep regime, a general expression for estimating C_t is derived as follows (Saxena, 1986)

$$C_t = \frac{P\dot{V}_c}{BW}\, F'/F \tag{4}$$

where, W = width of the specimen, P = applied load, $F = (K/P)BW^{1/2}$, K-calibration factor, $F' = dF/d(a/W)$, $\dot{V}_c$ = rate of deflection at the load-line due to creep deformation. Equation (3) is equally valid for power-law or primary creep law provided small-scale-creep conditions are met. In a test specimen, if $\dot{V}_c$ is measured, the magnitude of C_t is readily obtained irrespective of the prevailing creep deformation law. In components, where $\dot{V}_c$ cannot be measured, it can be estimated under small-scale-creep conditions by (Bassani et al. 1986).

$$\dot{V}_c = \frac{2B}{E}\frac{K^2}{P}\beta \dot{r}_c (1-\nu)^2 \qquad (5)$$

where $\dot{r}_c$ = rate of expansion of the creep zone size and β is a scaling factor and is approximately equal to 1/3 as determined from finite element analyses (Bassani et al., 1986). The value of $\dot{r}_c$ is dependent on the prevailing creep deformation law. For power-law creep and primary creep it can be obtained from the following relationship.

For power-law creep (Riedel and Rice, 1980):

$$\dot{r}_c = \frac{1}{2\pi}\left(\frac{K}{E}\right)^2\left[\frac{(n+1)AI_nE^n}{2\pi(1-\upsilon^2)}\right]^{\frac{2}{n-1}} \tilde{r}_c(\theta)\cdot t^{-\frac{n-3}{n-1}} \qquad (6)$$

For primary creep (Riedel, 1981):

$$\dot{r}_c = \frac{K^2\tilde{r}_c(\theta)}{2\pi}\left[\frac{I_{n_1}E}{2\pi(1-\upsilon)}\right]^{\frac{2}{n_1-1}}\left[(n_1+1)(1+p)A_1\right]^{\frac{2}{(1+p)(n_1-1)}} \cdot \left[\frac{1}{1+p}\right]\left[\frac{2}{n_1-1}\right]^{t^{\left[\frac{2}{(1+p)(n_1-1)}\right]-1}} \qquad (7)$$

It should be pointed out that both Eqs (6) and (7) are strictly valid for stationary cracks only. However, they may be used for slowly growing cracks defined by the condition $\dot{a} \ll \dot{r}_c$. Expressions for estimating $\dot{r}_c$ which account for growing crack effects are currently not available. Hence, even though there is no fundamental difficulty in the use of C_t for situations where crack growth effects significantly influence $\dot{r}_c$, there are practical limitations due to lack of adequate analyses. However, this is not a problem in test specimens where $\dot{V}_c$ is easily obtained from the measured deflection rates following the deflection rate partitioning method (Saxena et al., 1984). By combining Eqs 6 and 6, the relationship between C_t and the crack tip creep zone size is easily derived. This relationship is unique for a fixed applied value of K. Thus, C_t can relate the load and deflection rate measurements made at the load-point which is remote from the crack tip to the crack tip creep zone expansion rate. The following equations relates C_t to C(t) under the small-scale-creep condition (Saxena, 1981).

$$(C_t)_{ssc} = \beta(1-\upsilon^2)\frac{n+1}{n-1}(F'/F)\frac{r_c}{W}(C(t))_{ssc} \qquad (8)$$

Since r_c is a function of applied K and time, t, the relationship between $(C_t)_{ssc}$ and $(C(t))_{ssc}$ is not unique. Often, creep crack growth data are correlated with crack tip opening displacement (CTOD) rate, $\dot{\delta}_t$. The following relationships can be derived between C_t and C(t) and $\dot{\delta}_t$ in the small-scale-creep regime (Saxena, 1988):

$$(C_t)_{ssc} = (2\pi\beta)^{1/2}\,(F'/F)\,\left(\frac{Kr_c^{1/2}}{W}\right)\dot{\delta}_t \qquad (9)$$

$$(C(t))_{ssc} = \frac{n-1}{n+1}\,\frac{1}{1-\upsilon^2}\left(\frac{2\pi}{\beta}\right)^{1/2}\frac{K}{r_c^{1/2}}\,\dot{\delta}_t \qquad (10)$$

Neither of the two parameters are uniquely related to δ_t in the small-scale-creep region. In the extensive creep region, δ_t and C^* are uniquely related.

Over a wide range of creep deformation conditions ranging from small-scale to extensive creep, it was shown in the above discussion that neither parameters, C(t), C_t or δ_t are uniquely related to each other. However, in the extensive creep region the relationship is infact unique. In correlating wide range creep deformation data a good correlation with one of these parameters necessarily implies no unique correlation with the others. Figures 3 and 4 show the creep crack growth data correlations with C_t and C(t). From these results it is concluded that C_t parameter is most appropriate for correlating wide range creep crack growth data.

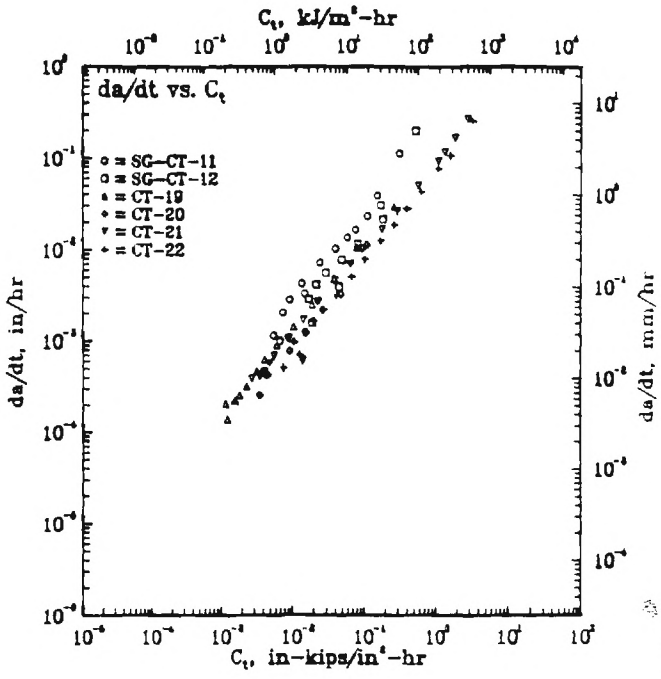

Fig. 3. Creep crack growth rate as a function of C_t in a Cr-Mo-V steel at 594°C.

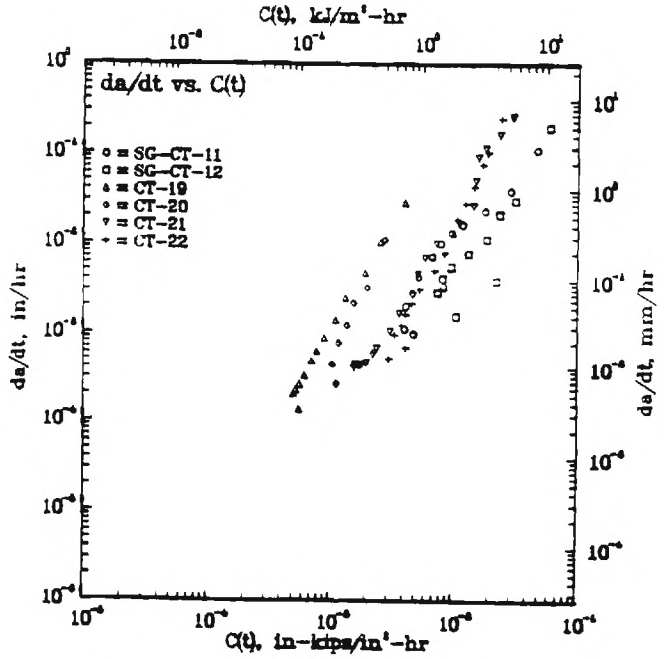

Fig. 4. Creep Crack growth rate as a function of the C(t) in a CrMoV steel at 594°C.

APPLICATION OF TDFM IN LIFE PREDICTION

As mentioned earlier in this paper, there are several potential applications of TDFM concepts in life prediction analyses of elevated temperature components. In this section a methodology for predicting creep crack growth life is described. Subsequently, the methods for predicting creep-fatigue crack growth life are also briefly discussed. Some areas which need further development to achieve greater accuracy in life prediction are outlined at the end of this section.

Prediction of Creep Crack Growth Life

Figure 5 shows a general methodology for predicting the remaining creep crack growth life of an elevated temperature component (Saxena and Liaw, 1985). The top of the figure shows the type of specimens used in material testing, and the data obtained from these tests. Material data needed are fracture toughness (to establish the crack size which will cause rupture), creep deformation properties, the tensile stress-strain properties and the creep crack growth rate behavior. Crack growth rates in structural components are predicted using the calculated value of C_t. These rates are integrated to develop the crack size versus time curve or the remaining life

versus crack size curve. The procedure outlined above is similar to the procedure used for predicting fatigue crack growth life except, fatigue cycles are replaced with time and ΔK (cyclic stress intensity parameter) is replaced by C_t.

Most components such as steam pipes or gas turbine disks are periodically shut down. This has a very significant influence on the estimated value of C_t. As time elapses the relative contribution of the transient term in estimating C_t decreases as steady-state conditions dominated by C^* are approached. When load interruptions occur, the stress relaxation process is also interrupted. Upon re-start the stress relaxation process is reinitiated independent of the relaxation in the previous cycle if small-scale-creep conditions dominate. This is schematically illustrated in Fig. 6 where a step increase in C_t value is shown following each start-up.

Since the methods of TDFM are complex and the remaining life is affected by so many factors, it is desirable to conduct the analyses with the help of a computer. Several personal computer based (Saxena, 1987; Wells, 1986) computer programs are now available for predicting creep crack growth life in specialized components. Figure 7 shows results from example calculations of creep crack growth life of a high temperature steam pipe (solid lines) containing surface defects in the radial-axial plane for several operating pressures. The dotted lines show the coresponding maximum allowable half crack lengths for assuring a leak-before-break situation. These calculations were performed using the PCPIPE computer code.

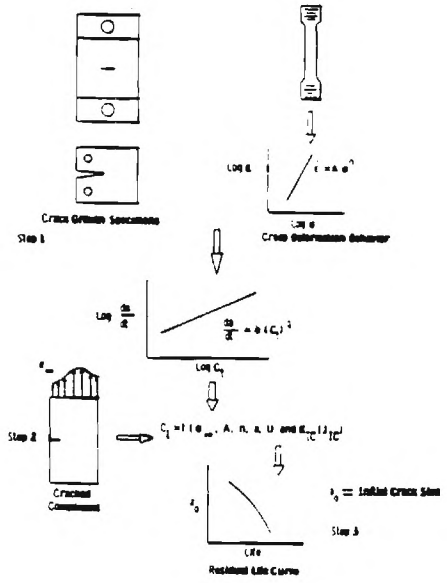

Fig. 5. Methodology for predicting crack propagation life using time-dependent fracture mechanics (TDPM) concepts.

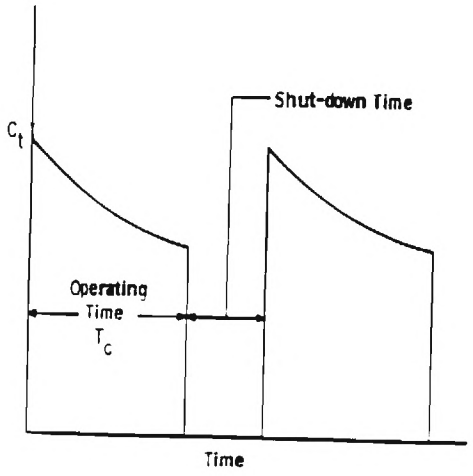

Fig. 6. C_t as a function of time operation.

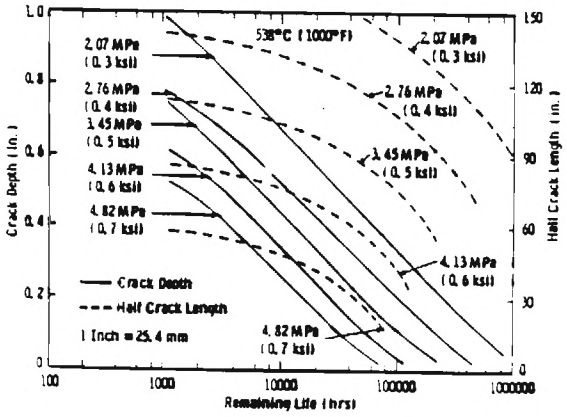

Fig. 7. Influence of steam pressure remaining crack growth life of steam pipes containing surface defects and operating at 538°C.

Crack Growth Due to Creep-Fatigue

The approach which has been most widely used to characterize creep-fatigue crack growth is to sum the cycle-dependent ($(da/dN)_c$) and time-dependent contributions to crack growth to obtain an overall crack growth rate (da/dN) for the cycle (Saxena et al., 1981). The governing equation for such an approach is:

$$\frac{da}{dN} = (da/dN)_c + \int_0^{t_c} (da/dt)dt \qquad (11)$$

where, t_c = cycle time and da/dt is the average time dependent crack growth rate. Within this general approach there are some variations between researchers. Nikbin and Webster (1988) estimate da/dt from creep crack growth tests to calculate the time-dependent contribution. This implies that there is no creep-fatigue interaction which influences the time-

dependent crack growth behavior. Our approach (Saxena and Gieseke, 1987) obtains da/dt from creep-fatigue tests which implies that creep-fatigue interactions cannot be ruled out as a general rule. For materials which do not show creep-fatigue interactions, both approaches are identical.

There are also apparent variations in the crack driving force used to characterize da/dt among the two approaches. Webster and co-workers use C^* to characterize da/dt in a cyclic situation where small-scale-creep is expected to dominate during one cycle. Our approach uses the $(C_t)_{avg}$ parameter which is the average value of C_t during the cycle to characterize da/dt. Figure 8 shows the correlation between da/dt and $(C_t)_{avg}$ in a 1Cr-1MO-0.25V steel (Banerji and Saxena, 1988) at 427°C and 538°C for a trapezoidal loading waveform with hold times ranging from a few seconds to twenty-four hours. A single plot is obtained for different hold times and also for different temperature. Such collapsing of data into a single trend for widely varying conditions is valuable for life prediction schemes.

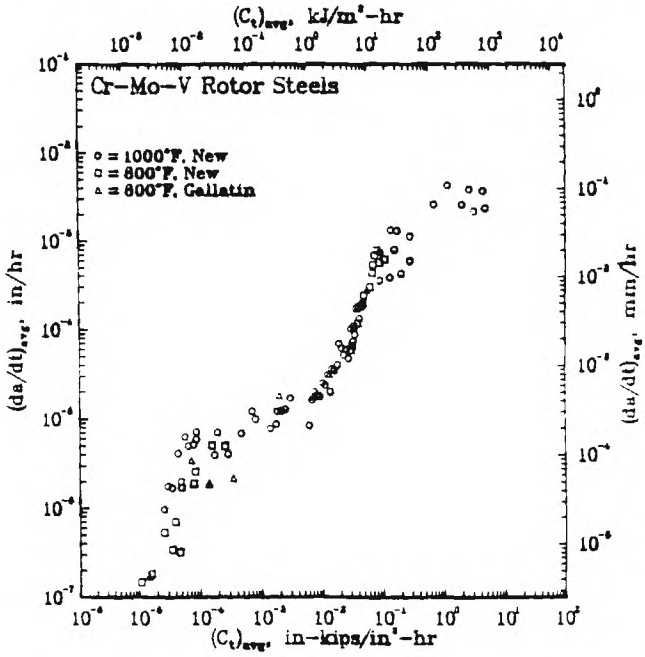

Fig. 8. Creep-fatigue crack growth rate data in Cr-Mo-V steel for trapezoidal waveforms with hold times ranging from 50 seconds to 24 hours and at temperatures of 427°C (800°F) and 538°C (1000°F).

Other approaches used for characterizing creep-fatigue crack growth (Ohji and Kubo, 1988) sum driving forces according to cycle and time-dependent parts. This gives rise to a combined ΔJ_c parameter which is the sum of ΔJ_ϵ, the time-independent cyclic J-integral and the integral of C^* over the cycle period. The relationship between ΔJ_c and the crack tip stress, strain or a related quantity is not clear. For a detailed discussion of these

approaches, the readers are referred to another paper (Gieseke and Saxena, 1989).

Recommendations for Future Work

Several problems of cracking in elevated temperature components result from thermal-mechanical stresses. As yet, there are no accepted approaches for predicting crack growth due to thermal-mechanical loading. Little work has been done in the area of transition from slow creep crack growth to fast fracture which may hold the key to accurate predictions of leak-before-break conditions. Additional work in the area of predicting time-dependent crack growth for long cycle times from laboratory tests conducted over short cycle periods is needed. On the analytical side, accurate methods are still needed for estimating C_t for complex material constitutive laws which properly account for effects due to primary creep, cyclic loading and crack growth. The solutions for estimating C^* are limited to only a few geometries and almost exclusively to 2-dimensional crack cases. This area also needs attention in the future.

SUMMARY AND CONCLUSIONS

This paper summarizes the recent developments in time-dependent fracture mechanics (TDFM) over the past few years. The applications of TDFM concepts have also kept pace with the new developments. The following conclusions can be drawn at this time about the status of the field.

1. It is now widely accepted that under the conditions of extensive steady-state creep, the creep crack growth rate is characterized by C^*.

2. Significant progress has occurred in the understanding of creep crack growth behavior under transient conditions to includes the effects due to small-scale-creep, primary creep and cyclic loading. C_t appears to be a promising candidate parameter for unifying the crack growth during the transient conditions with those during the steady-state conditions.

3. Applications of TDFM have kept pace with the concept developments largely because of the timely appearance of user-friendly computer codes.

4. Areas needing further development include crack growth due to thermal-fatigue, extension of the available C^* and C_t solutions and accurate models for predicting crack growth due to creep-fatigue.

ACKNOWLEDGEMENTS

The financial support for preparing the manuscript of this paper came from a Department of Energy, Basic Energy Sciences Grant No. DE-FGOS-86ER-45257

(Dr. J. B. Darby, Project Manager). This support is gratefully acknowledged.

REFERENCES

Banerji, K. and Saxena, A. (1988). Creep and Creep-Fatigue Crack Growth in Steam Turbine Rotor Steels. Unpublished research, Georgia Institute of Technology.

Bassani, J. L. and McClintock, F. A. (1981). International Journal of Solids and Structures, 7, 479-492.

Bassani, J. L., Hawk, D. E. and Saxena, A. (1986). Evaluation of the C_t Parameter for Characterizing Creep Crack Growth Rate in the Transient Regime. Third ASTM International Symposium on Nonlinear Fracture Mechanics, Knoxville, TN to appear in ASTM STP 995.

Ehlers, R. and Riedel, H. (1981). In Advances in Fracture Research, ICF-5. (D. Francois et al. Eds) Pergamon Press, 2, 691-698.

Gieseke, B. and Saxena, A. (1989). Correlation of Creep-Fatigue Crack growth Rates Using Crack Tip Parameters. Paper submitted for publication in the Proceedings of the Seventh International Conference on Fracture, ICF-7, Houston, TX.

Harris, J. A., Sims, D. L. and Annis, C. G. (1980). Concept Definition: Retirement for Cause of F100 Rotor Components. AFWAL-Tr-80-4118, Wright Patterson Airforce Base, Ohio.

Hawk, D. E. and Bassani, J. L. (1986). Journal of Mechanics and Physics of Solids, 34, 191-212.

Hui, C. Y. and Riedel, H. (1981). International Journal of Fracture, 17, 409-425.

Hui, C. Y. (1983). In Elastic-Plastic Fracture, Second Symposium, 1 ASTM STP 803, 1573-593.

Hutchinson, J. W. (1968). Journal of Mechanics and Physics of Solid, 16, 13-31.

Kramer, L. D. and Randolph, D. D. (1970). Analysis of the Tennessee Valley Authority Gallatin No. 2 Unit Turbine Rotor Burst, Part I-Metallurgical Examinations. AMSM-MPC Symposium Proceedings, pp. 1-24.

Landes, J. D. and Begley, J. A. (1976). In Mechanics of Crack Growth, ASTM STP 590, American Soceity for Testing and Materials, pp. 128-148.

Nikbin, K. M. and Webster, G. A. (1988). In Low Cycle Fatigue, ASTM STP 942, American Soceity for Testing and Materials, pp. 281-292.

Ohji, K., Ogura, K. and Kubo, S. (1979). Japan Society of Mechanical Engineers, No. 790-13, pp. 18-20 (in Japanese).

Ohji, K. and Kubo, S. (1988). In High Temperature Creep-Fatigue, (R. Ohtani et al. Eds), Elsevier Applied Sci., pp. 91-113.

Rice, J. R. and Rosengren, G. F. (1968). Journal of Mechanics and Physics of Solids, 16, 1-12.

Riedel, H. and Rice, J. R. (1980). In Fracture Mechanics: Twelfth Conference, ASTM STP 700, American Society for Testing and Materials, pp. 112-130.

Riedel, H. (1981). Journal of Mechanics and Physics of Solids, 29, 35-49.

Riedel, H and Detampel, V. (1987). International Journal of Fracture, 33, 239-262.

Saxena, A. (1980). In Fracture Mechanics: Twelfth Conference, ASTM STP 700, American Soceity for Testing and Materials, pp. 131-151.

Saxena, A. (1986). In Fracture Mechanics: Seventeenth Conference. ASTM STP 905. American Soceity for Testing and Materials, pp. 185-201.

Saxena, A. (1988). Mechanics and Mechanisms of Creep Crack Growth. In Fracture Mechanics, Microstructure and Micro-mechanism, (S. Nair et al, Eds), ASM, Metals Park, Ohio (in press).

Saxena, A., Williams, R. S. and Shih, T. T. (1981). In Fracture Mechanics: Thirteenth Conference, ASTM STP 743, American Soceity for Testing and Materials, pp. 86-99.

Saxena, A., Ernst, H. A. and Landes, J. D. (1983). International Journal of Fracture, 23, 245-257.

Saxena, A. and Landes, J. D. (1984). In Advances in Fracture Research, Proceedings of the 6th International Congress on Fracture (ICF-6), pp. 3977-3988.

Saxena, A., Shih, T. T. and Ernst, H. A. (1984). In Fracture Mechanics: Fifteenth Symposium, ASTM STP 833, American Society for Testing and Materials, pp. 516-531.

Saxena, A. and Liaw, P. K. (1986). Renaming Life Estimation of Boiler Pressure Parts - Crack Growth Studies. EPRI - Contract Report CS-4688.

Saxena, A., Liaw, P. K., Logsdon, W. A. and Hulina, V. (1986). Engineering Fracture Mechanics, 25, 290-300.

Saxena, A. and Gieseke, B. (1987). Transients in Elevated Temperature Crack Growth. Seminar Proceedings of MECAMAT, International Seminar on High Temperature Fracture Mechanisms and Mechanics, Dourdan, France, p III/19-III/36.

Saxena, A. and Saxena, M. (1987). PCPIPE - A Computer Code for Integrity Analysis of Elevated Temperature Steam Pipe. Structural Integrity Associates, San Jose, CA.

Shih, C. F. (1983). Tables of Hutchinson-Rice-Rosengren Singular Field Quantities. Materials Research Laboratory, Brown University, MRL E-147.

Wells, C. A. (1986). On Life Analysis of Longitudinal Seam Welds in Hot Reheat Piping. RTI Report, Palo Alto, CA.

ICF7

ADVANCES IN FRACTURE RESEARCH

Editors:

K. Salama, K. Ravi-Chandar
D. M. R. Taplin, P. Rama Rao

VOLUME 1

BRITTLE FRACTURE
DUCTILE FRACTURE
DYNAMIC FRACTURE

SEVENTH INTERNATIONAL CONFERENCE ON FRACTURE
UNIVERSITY OF HOUSTON
HOUSTON, TEXAS MARCH 20-24, 1989

Correlation of Creep-fatigue Crack Growth Rates Using Crack-tip Parameters

BRIAN GIESEKE* and ASHOK SAXENA**

*Graduate Student and **Professor, Mechanical Properties Research Laboratory, School of Materials Engineering, Georgia Institute of Technology, Atlanta, Georgia 30332-0245, USA*

ABSTRACT

Several approaches for correlating creep-fatigue crack growth (CFCG) rates are reviewed which incorporate time-dependent fracture parameters. The parameters C(t), C^*, and C_t have been evaluated for correlating CFCG rates by partitioning the overall growth rates into cycle- and time-dependent contributions. It is shown that the use of C_t is the most appropriate for describing the time-dependent contribution. Further, an additional crack length and geometry dependent factor is introduced by the presence of creep at the crack tip. This factor is not included in correlations with ΔK. Considerable creep-fatigue data from various sources are used to support these conclusions.

KEYWORDS

Creep; Fatigue; Creep-fatigue; Crack Growth; C_t; C^*

INTRODUCTION AND BACKGROUND

Since the early work of James (1972), high temperature fatigue crack growth rates have routinely been correlated using ΔK with full recognition of the fact that creep deformation occurs at the crack tip below certain frequencies. It is now well established that the crack-tip stress fields are affected by creep (Riedel, 1983; Saxena *et al.*,1986), and a fresh look at the validity of using ΔK for characterizing creep-fatigue crack growth (CFCG) rates is needed. In the past few years, the concepts in time-dependent fracture mechanics have evolved yielding several parameters such as C^*, C(t), and C_t which may be used to correlate crack growth under static loading, in other words, creep crack growth (Landes *et al.*, 1976; Riedel *et al.*, 1980; Saxena, 1986). Recently, attempts have also been made to use these parameters for correlating CFCG rates in combination with ΔJ or ΔK (Saxena, 1980; Okazaki *et al.*, 1983; Saxena *et al.*, 1987; Dimopulos *et al.*, 1988; Nikbin *et al.*, 1988; Ohji *et al.*, 1988). Of the various fracture mechanics parameters, C_t appears to show the most promise (Saxena *et al.*, 1987). The various crack-tip parameters which can

account for creep deformation are first briefly described with emphasis on their attributes and limitations in regard to correlation of creep-fatigue crack growth behavior. General methodologies for modeling creep-fatigue crack growth behavior are then described. Subsequently, data correlations are presented with the objective of evaluating the various parameters.

Candidate Time-Dependent Fracture Mechanics Parameters

Under static loading, the stress fields near a crack tip in a material undergoing elastic, power-law creep deformation are of the Hutchinson, Rice and Rosengren (HRR) type, the magnitude of which is denoted by C(t) (Riedel *et al.*, 1980; Bassani *et al.*, 1981). C(t) is approximately given by (Ehlers *et al.*, 1981):

$$C(t) = \frac{K^2(1-\nu^2)}{E(n+1)t} + C^* \qquad (1)$$

where E is Young's modulus, n is the creep exponent in Norton's creep law, t is time, ν is Poisson's ratio and C^* is a path-independent integral first introduced by Landes *et al.* (1976). For small scale creep conditions (SSC), which are analogous to small scale yielding, the first term in Eq. (1) dominates (Riedel *et al.*, 1980). When extensive creep (SS) conditions exist, $C(t) = C^*$ (Goldman *et al.*, 1975). A useful method for determining when extensive creep conditions exist is to compare the Riedel-Rice transition time, t_1 (the time at which the first term in Eq. (1) equals C^*), with the cycle time, t_c (Riedel, 1983; Saxena, 1988). SSC conditions exist when $t_c \ll t_1$ and extensive creep conditions exist when $t_c \gg t_1$. C^*, in Eq. (1), has also been interpreted as the stress-power dissipation rate in cracked bodies (Landes *et al.*, 1976). This interpretation (or definition) can be used to measure the value of C^* at the loading pins for bodies undergoing dominantly steady-state creep deformation.

The C_t parameter is an extension of the stress-power dissipation rate definition of C^* into the SSC regime (Saxena, 1986). It has been proposed for correlating creep crack growth for a wide range of conditions ranging from small-scale to extensive creep. C_t is also uniquely related to the rate of expansion of the crack-tip creep zone under SSC conditions (Bassani *et al.*, 1986; Leung *et al.*, 1988), and $C_t = C^*$ when extensive creep conditions exist. C_t can be measured at the loading pins for all deformation conditions including those involving primary creep (Leung *et al.*, 1988). There is also considerable evidence that C_t can correlate creep crack growth data for conditions ranging from small-scale to extensive creep (Saxena, 1986).

The crack-tip stress fields in creep-fatigue are more complicated than in creep. However, Riedel (1983) has numerically investigated the crack-tip stress fields for a few simple loading waveforms and his results are of interest here. He has shown that if rapid load variations occur within otherwise slow cycles, crack-tip stress peaks follow the peaks of the load variations. On the other hand, for waveforms with hold times and a rise time of approximately one half t_1, he has shown that the stress peak can be as much as 75% higher than the steady-state value. For waveforms with hold times, the stresses decay with time according to Eq. (1) and C^* does not characterize the stress fields except for very long hold times ($t_h \gg t_1$). Hence, C^* is not a valid parameter for characterizing the crack growth rates for short hold times. On the other hand, both C(t) and C_t are valid in the transient regime and can be considered as candidate parameters.

Methodologies for Modeling Creep-Fatigue Crack Growth

Creep-fatigue crack growth rates as a function of frequency, for a fixed ΔK range and waveform, show three regimes of behavior. At high frequencies, a cycle-dependent region exists where crack growth is controlled by fatigue processes. At very low frequencies, crack growth is entirely controlled by time-dependent processes. The crack growth rates in each regime are characterized by a different crack driving force. In the intermediate frequency regime, where the creep-fatigue interactions occur, two approaches have emerged to model crack growth rates.

Partitioning of Crack Growth Rates. Time-dependent fracture mechanics parameters are typically incorporated into creep-fatigue analysis by decomposing the CFCG rates into cycle-dependent and time-dependent contributions and using superposition to determine the overall rate, ie. (Saxena, 1980; Okazaki *et al.*, 1983; Saxena *et al.*, 1984; Saxena *et al.*, 1987; Dimopulos *et al.*, 1988; Nikbin *et al.*, 1988; Ohji *et al.*, 1988):

$$da/dN = (da/dN)_f + (da/dN)_t \tag{2}$$

where $(da/dN)_f$ and $(da/dN)_t$ are the fatigue and time-dependent components, respectively. $(da/dN)_f$ is uniquely characterized by either ΔK_{eff} (Dimopulos *et al.*, 1988) or ΔJ (Ohji *et al.*, 1988) depending upon the amount of instantaneous plasticity. Here ΔK_{eff} is the effective stress intensity factor range and ΔJ is the cyclic J-integral of Dowling *et al.* (1976). Thus $(da/dN)_f$ is given by:

$$(da/dN)_f = C(\Delta K_{eff})^m \tag{3a}$$

or by:

$$(da/dN)_f = C_0(\Delta J)^{m_0} \tag{3b}$$

where C, C_0, m and m_0 are material constants of which only two are independent. For example, $m = 2m_0$. For estimating $(da/dN)_t$, the time rate of crack growth is first estimated using:

$$da/dt = D(A)^\phi \tag{4}$$

where A is a time-dependent fracture parameter. This has been chosen as $C(t)$ by some researchers (Saxena, 1980; Saxena *et al.*, 1981; Saxena *et al.*, 1984; Saxena, 1988), as C^* by others (Dimopulos *et al.*, 1988; Nikbin *et al.*, 1988; Ohji *et al.*, 1988), and finally as C_t by Saxena *et al.* (1987). The time rate of crack growth can be converted to a growth rate per cycle by a simple integration over the cycle time.

Partitioning of Crack Driving Forces. An alternate approach to that of partitioning the crack growth rates has been to partition the crack driving force into cycle-dependent and time-dependent contributions (Taira *et al.*, 1979; Ohji *et al.*, 1988). For elastic-plastic-creep conditions, this has resulted in the so-called "total J-integral", ΔJ_T, which is defined as (Taira *et al.*, 1979):

$$\Delta J_T = \Delta J_f + \Delta J_c \tag{5}$$

ΔJ_f applies to fatigue only and ΔJ_c is the time-integral of C^* over one stress cycle. Crack growth rates are then correlated using Eq. (3b) with the substitution of ΔJ_T for ΔJ. The combined ΔJ_T parameter does not currently have a mechanics interpretation because it is not related to crack-tip stress, strain, or any other related crack-tip quantity.

DATA CORRELATIONS

Correlations Using C^* and ΔJ_t

In the time-dependent regime, under cyclic loading, Dimopulos *et al.* (1988) and Nikbin *et al.* (1988) have shown that CFCG rates fall on the same trend as creep crack growth data when converted to time rates of crack growth, da/dt, and plotted versus an experimentally measured value of C^*. They have observed this behavior in a nickel-base superalloy, a creep-brittle steel, and creep-ductile steel using a square loading waveform. An example of the correlation for a 2.25 Cr-Mo steel is shown in Fig. 1a. Their version of Eq. (2) is as follows (Dimopulos *et al.*, 1988):

$$da/dN = C\Delta K^{n}_{eff} + D(C^*)^{\phi}/(3600\nu) \qquad (6)$$

where C^* is experimentally determined at the maximum load in the trapezoidal cycle. Figure 1b shows an example of the experimental and predicted CFCG rates determined via Eq. (6) for one material (Dimopulos *et al.*,1988).

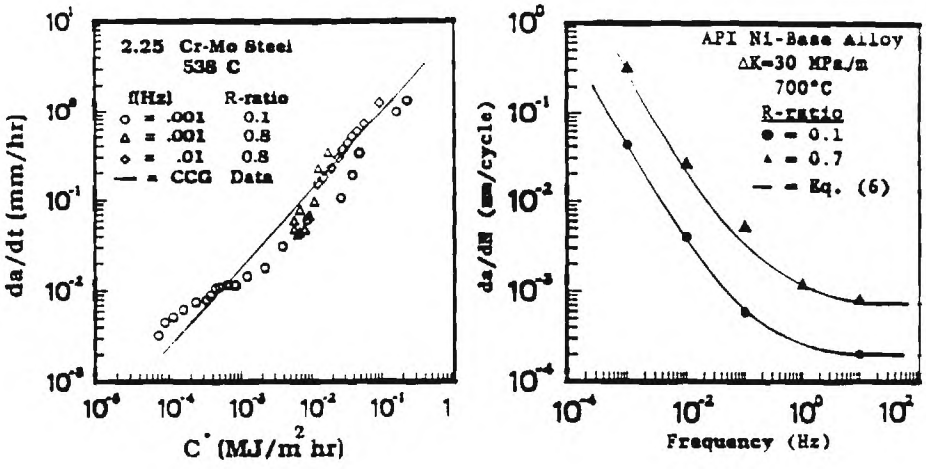

(a.) (b.)

Fig. 1. (a) Dependence of crack growth/cycle on frequency. (b) Low frequency crack growth rates as a function of C^*. (Dimopulos *et al.*, 1988)

There is in fact a good correlation which has led Dimopulos *et al.* (1988) to conclude that the crack growth rates for creep-fatigue loading can be determined from tests carried out under static loading and high frequency fatigue conditions to determine the time- and cycle-dependent components of crack growth. It should be noted that the Riedel-Rice transition times in many of these tests were on the order of one hour (Nikbin *et al.*, 1988). Since the longest reported cycle times were only 1000 seconds, SS conditions could not have developed during each cycle. The use of C^* can then be questioned. However, experimentally measured values of C^* for CT specimens are nearly equal to the values of C_t for a wide range of crack sizes (Saxena,

1986). Therefore, these data support the use of C_t as the time-dependent crack-tip parameter instead of C^*. The data correlations with C_t will be discussed later.

Creep-fatigue crack growth in 304 stainless was approached differently by Ohji *et al.* (1988). In their method, the term $(da/dN)_c$ in Eq. (2) is given by:

$$(da/dN)_c = AC^*/\nu = A\Delta J_c \tag{7}$$

where A is a material constant. In these studies also, C^* also was experimentally measured. The overall fatigue crack growth rate was given by:

$$da/dN = A(\Delta J_e + B\Delta J_f) \tag{8}$$

where A and B are experimentally determined constants. Using this relationship, they have obtained good correlation of fatigue data on 304 stainless tested using sinusoidal waveforms. Equation (8) is in fact a special case of Eq. (2) with constants m_o and ϕ in Eqs. (3b) and (4) being one.

Okazaki *et al.* (1983) have used the total J-integral approach in correlating data generated using balanced and unbalanced triangular, strain-controlled waveforms on 304 stainless at 600 and 700°C. Fatigue data plotted versus ΔJ_T collapsed into a band that lies between cyclic- and time-dependent data. However, a unique relationship between da/dN and ΔJ_T was not observed for all waveforms. Because of this non-unique relationship between da/dN and ΔJ_T, these researchers have suggested that ΔJ_f and ΔJ_c cannot be added linearly. As a result they have proposed a somewhat modified form of the ΔJ_T approach which does differentiate somewhat between waveforms. However, discussion of this technique is beyond the scope of this short paper.

Correlations Using C_t and C(t)

Saxena and co-authors (Saxena, 1980; Saxena *et al.*, 1981; Saxena *et al.*, 1984; Saxena, 1988) have used C(t) to correlate the time-dependent contribution to CFCG rates. Initially Saxena (1980) noted that the stress and strain fields at the crack tip, and therefore the crack growth rates, were dependent upon K^2/t, which is proportional to C(t), for SSC. Thus in Eq. (2), the time-dependent crack growth could be described by:

$$da/dt = b(K^2/t)^n = b_1[C(t)]^n \tag{9}$$

Equation (9) can be integrated over the fatigue cycle and the result can be expressed in the form which relates $(da/dN)_c$ to ΔK by a power-law relationship including terms which relate to cyclic frequency. Reasonable correlations were obtained by this approach.

Recently Saxena *et al.* (1987) evaluated whether time-dependent contributions to CFCG rates can be better correlated with C_t instead of C(t) in Eq. (9). Creep-fatigue data from hold time tests on a 1.0Cr-1.0Mo-.25V rotor steel were re-evaluated using the C_t and C(t) parameters. In these tests, the hold times were much shorter than the smallest calculated transition time, t_1, which was 585 hours. Thus these tests were conducted in a dominantly small scale creep regime.

The term $(da/dN)_c$, from Eq. (2), was taken to be the additional crack growth per cycle due to the hold time. This was converted to an average crack growth rate during the hold time, $(da/dt)_{avg}$, as follows:

$$(da/dt)_{avg} = [da/dN - (da/dN)_f]/t_h \qquad (10)$$

where da/dN is the overall crack growth rate, t_h is the hold time, and $(da/dN)_f$ is the crack growth rate per cycle associated with tests having zero hold time.

The average C_t parameter was calculated by integrating the analytical expression for estimating C_t and dividing it by the hold time. The expression for C_t in the small-scale-creep regime assumes elastic, power-law creep deformation and SSC conditions and is given by (Bassani *et al.*, 1988):

$$(C_t)_{ssc} = \frac{4q\beta K^4}{E(n-1)W}(1-\nu^2)\frac{F'}{F}(EA)^{2/(n-1)}\, t^{-(n-3/n-1)}\, \bar{r}_c(\theta) \qquad (11)$$

In Eq. (11), E is Young's modulus, F is the K-calibration function for the cracked body of interest, F'=dF/d(a/W) where W is the body width, a is the crack length, and the other symbols are described elsewhere (Saxena, 1986).

$(da/dt)_{avg}$ was plotted versus $(C(t))_{avg}$ in Fig. 2a and versus $(C_t)_{avg}$ in Fig. 2b. The correlation with $(C_t)_{avg}$ is considerably better than the correlation with $(C(t))_{avg}$. In Fig. 2b, creep crack growth data are also plotted for

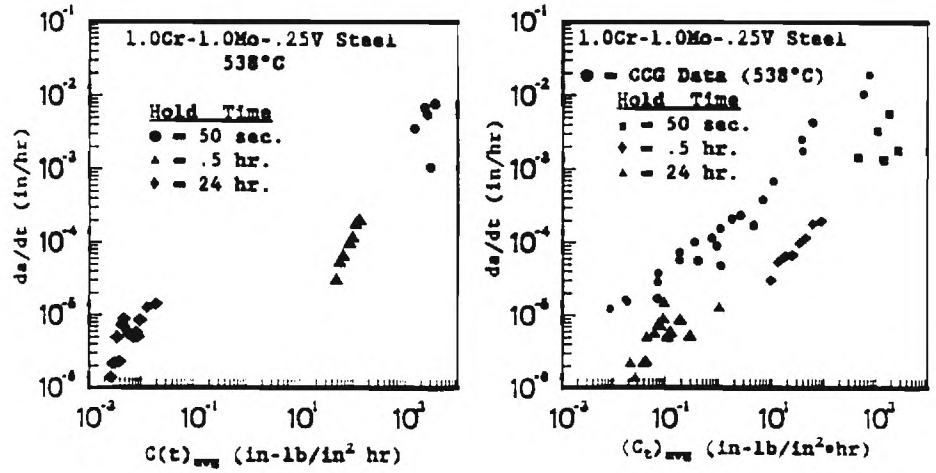

(a.) (b.)

Fig. 2. Average crack growth rate versus a.) $C(t)_{avg}$. and b.) $(C_t)_{avg}$. (Saxena *et al.*, 1987)

comparison. It is noted that the periodic loading/unloading events of fatigue have reduced the crack growth rates during the hold time. Excellent correlation between $(da/dt)_{avg}$ and $(C_t)_{avg}$ has also been observed in a 1.25Cr-0.5Mo steel waveforms with hold times of 10, 98, and 600 seconds preceded by an initial 100 percent overload (Yoon *et al.*, 1988). In this case, however, $(da/dt)_{avg}$ vs. $(C_t)_{avg}$ followed a trend similar to the creep crack growth data.

The correlation between $(da/dt)_t$ and $(C_t)_{avg}$ during the fatigue hold time in the approach described above has several interesting implications. First, it is evident from Eq. (11) that for a given waveform and cycle time (constant t_h),

the average C_t is not uniquely determined by K because of the additional crack size and geometry dependent term F'/F. However, in the past, fatigue crack growth data have been routinely correlated with ΔK for constant loading waveforms and cycle times (James, 1972; Saxena, 1980; Saxena *et al.*, 1981; Saxena *et al.*, 1984). This represents an apparent contradiction which is resolved as follows. It is noted that these correlations were obtained usually with a single specimen geometry, mostly CT specimens, for which F'/F does not vary significantly over a wide range of crack sizes (Saxena, 1986). In this case, $(C_t)_{avg}$ is approximately related to K for a constant waveshape and frequency. Also for short cycle times, the contribution of the time-dependent crack growth is small and the overall crack growth per cycle (da/dN) can be dominated by the cycle-dependent portion which correlates uniquely with ΔK. Hence the observed correlations with ΔK are not surprising, but at the same time should be viewed with caution especially for geometries other than the compact type.

Correlations of crack growth rates for waveforms other than trapezoidal have not yet been satisfactorily addressed. This is an area of future study.

SUMMARY AND CONCLUSIONS

Several approaches for correlating creep-fatigue crack growth rates have been reviewed in this paper. Time-dependent fracture parameters have been incorporated into the correlation of CFCG rates under elastic-creep and elastic-plastic-creep conditions with reasonable success. The presence of time-dependent creep deformation at the crack tip during cyclic loading at elevated temperatures introduces an additional crack length and geometry dependent factor which is not included in crack growth rate correlations with ΔK even for constant loading frequency and waveform. The implication is that a non-unique relationship is expected between da/dN and ΔK at elevated temperatures at loading frequencies where creep occurs. It is shown that the use of C_t is most appropriate parameter for describing the time-dependent contribution to the overall crack growth rates. Considerable creep-fatigue crack growth data from several sources are used to support these arguments.

ACKNOWLEDGEMENTS

Financial support for preparing the manuscript of this paper came from a Department of Energy, Basic Energy Sciences Grant No. DE-FGOS-86R-45257 (Dr. J.B. Darby, Project Manager). The authors are grateful for this support.

REFERENCES

Bassani, J. L. and F.A. McClintock (1981). Creep Relaxation of Stress Around a Crack Tip. *Int. J. of Solids Structures*, 17, 479-492.

Bassani, J.L., D.E. Hawk and A. Saxena (1988). Evaluation of the C_t Parameter for Characterizing Creep Crack Growth Rate in the Transient Regime. Third ASTM International Symposium on Nonlinear Fracture Mechanics 1986, ASTM STP (in press).

Dimopulos, V., K. Nikbin, and G. Webster (1988). Influence of Cyclic to Mean Load Ratio on Creep/Fatigue Crack Growth. *Met. Trans.*, 19A, 873-880.

Dowling, N. E. and J.A. Begley (1976). In: *Mechanics of Crack Growth, ASTM STP 590*, pp. 82-103. Am. Society for Testing and Materials, Philadelphia.

Ehlers, R. and H. Riedel (1981). A finite element analysis of creep deformation in a specimen macroscopic crack. In: *Advances in Fracture*

Research ICF-5 (D. Francois and C. Bathias, eds.), Vol. 2, pp. 691-698. Pergamon Press.

Goldman, N.L. and J.W. Hutchinson (1975). Fully Plastic Crack Problems: The Center-Cracked Strip Under Plane Strain. *Int. J. of Solids and Structures*, 11, 575-591.

James, L. A. (1972). The Effect of Frequency upon Fatigue Crack Growth of Type 304 Stainless Steel at 1000 F. In: *Stress Analysis and Growth of Cracks, Part I, ASTM STP 513*, pp. 218-229. Am. Society for Testing and Materials, Philadelphia.

Landes, J. D. and J.A. Begley (1976). A Fracture Mechanics Approach to Creep Crack Growth. In: *Mechanics of Crack Growth, ASTM STP 590*, pp.128-148. American Society for Testing and Materials, Philadelphia.

Leung, C-P., D.L. McDowell, and A. Saxena (1988). Consideration of Primary Creep at Stationary Crack Tips: Implications for the C_t Parameter. *Int. J. of Fracture*, 36, No. 4, 275-289.

Nikbin, K. M. and G.A. Webster (1988). Prediction of Crack Growth under Creep-Fatigue Loading Conditions. In: *Low Cycle Fatigue, ASTM STP 942*, (H.D. Solomon, G. Halford, L. Kaisand, and B.N. Leis, eds.), pp. 281-292. American Society for Testing and Materials, Philadelphia.

Ohji, K. and S. Kubo (1988). In: *High Temperature Creep-Fatigue* (R. Ohtani et al, eds.), pp. 91-113. Elsevier Applied Sci.

Okazaki, M., I. Hattori, F. Shiraiwa, and T. Koizumi (1983). Effect of Strain Wave Shape on Low-Cycle Fatigue Crack Propagation of 304 Stainless Steel at Elevated Temperatures. *Met. Trans.*, 14A, 1649-1659.

Riedel, H. and J.R. Rice (1980). Tensile Cracks in Creeping Solids. In: *Fracture Mechanics: Twelfth Conference, ASTM STP 700*, pp. 112-130. American Society for Testing and Materials, Philadelphia.

Riedel, H. (1983). Crack-Tip Stress Fields And Crack Growth Under Creep-Fatigue Conditions. In: *Elastic-Plastic Fracture: Second Symposium, Volume I-Inelastic Crack Analysis, ASTM STP 803* (C.F. Shih and J.P. Gudas, eds.), pp. I-505 to I-520. Am. Society for Testing and Materials, Phil.

Saxena, A. (1980). A Model For Predicting The Effect Of Frequency On Fatigue Crack Growth At Elevated Temperature. *Fatigue of Eng. Mat. and Structures*, 3, 247-255.

Saxena, A., R.S. Williams, and T.T. Shih (1981). In: *Fracture Mechanics: Thirteenth Conference, ASTM STP 743* (R. Roberts, ed.), pp. 86-99. American Society for Testing and Materials, Philadelphia.

Saxena, A. and J.L. Bassani (1984). Time-Dependent Fatigue Crack Growth Behavior At Elevated Temperature. In: *Fracture: Interactions of Microstructure, Mechanisms and Mechanics* (J.M. Wells and J.D. Landes, eds.), pp. 357-383. TMS-AIME.

Saxena, A. (1986). In: *Fracture Mechanics: Seventeenth Volume, ASTM STP 905* (J.H. Underwood *et al.*, eds.), pp. 185-201. American Society for Testing and Materials, Philadelphia.

Saxena, A. and B. Gieseke (1987). Transients in Elevated Temperature Crack Growth. In: *Seminar Proceedings of MECAMAT, Inter. Seminar on High Temperature Fracture Mechanisms and Mechanics*, Dourdan, pp. III/19-III/36.

Saxena, A. (1988). Limits of Linear Elastic Fracture Mechanics in the Characterization of High-Temperature Fatigue Crack Growth. In: *Basic Questions in Fatigue: Volume II, ASTM STP 924*, (R.P. Wei and R.P. Gangloff, eds.), pp. 27-40. Am. Society for Testing and Materials, Philadelphia.

Taira, S. *et al.* (1979). *Trans. Japan Mat. Sci.*, 28, 427-33.

Yoon, K. B. and A. Saxena, (1988). Unpublished research, Georgia Inst. of Technology.